

Testing theories on fisheries recruitment

Matteo Sinerchia

PhD Thesis

University of London

Imperial College London

Department of Earth Science and Engineering

September 2007

ABSTRACT

A new ecosystem model, the Lagrangian Ensemble Recruitment Model, LERM, is presented, representing a food chain composed of phytoplankton, zooplankton and squid, which are all modeled explicitly. It was built using the Virtual Ecology Workbench and based on the Lagrangian Ensemble metamodel, which treats plankton as individuals obeying primitive phenotypic equations. These equations, describing the behaviour and physiology of individuals, are taken from an extensive literature, and are based on reproducible laboratory experiments.

The LERM is used to test fisheries theories, in particular Cushing's match-mismatch hypothesis that seeks to explain the variability of fish recruitment. The LERM ecosystem is sited at a location in the Azores where the annual surface heat budget is zero. It is shown to be stable in the sense that after a few years, it adjusted to a stable attractor, in which the inter-annual variation is small compared to the multi-year mean.

The sensitivity of the ecosystem to various changes in exogenous factors is explored. In particular, analysis of the causes for recruitment variability in squid cohort spawning on different dates showed that the availability of food at the time of hatching was only one factor affecting recruitment. Annual recruitment emerged from a combination of food availability and composition, predation, infra- and intra-population competition, and speed of growth.

The thesis provides a proof of concept. It shows that LERM can be used to create a virtual ecosystem in which fisheries recruitment is an emergent property that is rationally dependent on exogenous properties.

The LERM provides a sound basis for further research into fisheries recruitment, but needs to be enhanced before it can usefully contribute to fisheries management. A number of suggestions for future work, with this long-term objective in mind, are also presented.

ACKNOWLEDGMENTS

This project has benefited from the guidance and passion of many.

Firstly, I would like to express my gratitude to the Department of Earth Sciences & Engineering Research for providing three and a half years of bursary to support this project.

I would like to thank Prof. John Woods for providing me with first rate research training, for sharing his experience, proposing the project theme and guiding its development and also for financing my student fees and attendance at conferences and workshop.

Thanks also to Dr. Tony Field, for his supervision, help in writing this thesis, encouragement throughout this project, especially during the hard times, and for his financial support in the final stages of this project. He is a real “*Saint*”.

Massive thanks to Dr. Wes Hinsley, for building and doing all the coding of VEW3.1, making this project technically possible. His support, encouragement and friendship have never lacked throughout this project. Thanks also for his helpful suggestions and proof-reading of this thesis.

Thanks also to Prof. Roger Wiley for his encouragement, wisdom and sharpness, from which I benefited especially for the ergodicity experiments. His good and reassuring character make him a joy to be around.

Thanks to Dr. Silvana Vallerga for her hospitality in her home in Italy. This provided a beautiful and stimulating environment for scientific discussion with her and Prof. Woods. Thanks also to Adrian Rogers, Mohammad Raza for their various contributions to the project and VEW development in general.

Last, but not least, I would like to express my love and gratitude to Flavia and my family for always being my “*Curva Sud*”.

TABLE OF CONTENTS

ABSTRACT	i
ACKNOWLEDGEMENTS	ii
TABLE OF CONTENTS	iii
CHAPTER 1 - INTRODUCTION	1
1.1 The decline of fisheries	1
1.2 Ecosystem-based management of fisheries	2
1.2.1 Ecosystem modeling	2
1.3 This thesis	3
1.3.1 The Virtual Ecology Workbench	3
1.4 Contributions	4
CHAPTER 2 - REVIEW	6
2.1 The fisheries problem	6
2.1.1 The recruitment problem	8
2.1.2 Cephalopods	9
2.1.3 Squid recruitment variability	12
2.2 Ecosystem modeling methods	15
2.2.1 Modeling complexity	16
2.2.2 Population-based modeling (PBM)	17
2.2.3 Individual-based modeling (IBM)	18
2.2.4 Lagrangian Ensemble metamodel (LEM)	20
2.2.5 Virtual Ecology Workbench, VEW	22
CHAPTER 3 - LERM-PS	24
3.1 Phytoplankton	24
3.1.1 Stoichiometry	24
3.1.2 Processes	26
3.1.2.1 Photoadaptation	27
3.1.2.2 Photosynthesis	27
3.1.2.3 Nutrients uptake	28
3.1.2.4 Chlorophyll synthesis	29
3.1.2.5 Respiration	30
3.1.2.6 Cell division	30
3.1.2.7 Motion	30
3.1.2.8 Mortality	31
3.2 Zooplankton	31

3.2.1	Stoichiometry	31
3.2.2	Processes	32
3.2.2.1	Molting	32
3.2.2.2	Ingestion	32
3.2.2.3	Gut processes	34
3.2.2.4	Faecal pellets production	34
3.2.2.5	Allocation of assimilated carbon	35
3.2.2.6	Respiration	35
3.2.2.7	Excretion	36
3.2.2.8	Maximum swimming speed	36
3.2.2.9	Diel migration	36
3.2.2.10	Foraging	37
3.2.2.11	Over-wintering	37
3.2.2.12	Reproduction	38
3.2.2.13	Mortality	38
3.3	Top predators	38
3.3.1	Visual top predators	39
3.3.1.1	Exogenous equations (top predator demography)	39
3.3.1.2	Endogenous equations	40
3.3.2	Basal top predator	41
3.3.2.1	Exogenous equations (top predator demography)	41
3.3.2.2	Endogenous equations	41
3.4	Particle management	42
3.4.1	Phyoplankton	42
3.4.2	Zooplankton	42
3.4.3	Top predators	43
CHAPTER 4 – LERM-ES		44
4.1	Squid	44
4.1.1	Stoichiometry	45
4.1.2	Stages	46
4.1.2.1	Spawning	47
4.1.2.2	Egg stage	47
4.1.2.2.1	Embryogenesis	47
4.1.2.3	Hatching	48
4.1.2.4	Paralarva stages	48
4.1.2.4.1	Yolk absorption rate	48
4.1.2.4.2	Motion	48
4.1.2.4.3	Ingestion	49
4.1.2.4.4	Gut processes	50

4.1.2.4.5	Respiration	52
4.1.2.4.6	Energetics	52
4.1.2.4.7	Recruitment	52
4.1.2.4.8	Starvation	52
4.1.2.4.9	Excretion	53
4.1.2.4.10	Egestion	53
4.2	Visual top predator	53
4.2.1	Exogenous equations	53
4.2.2	Endogenous equations	53
4.3	Particle management	54
4.3.1	Squid	54
4.3.2	Visual top predator	54
CHAPTER 5 – NUMERICAL EXPERIMENTS		55
5.1	Stability experiments	56
	Stage 1 – Does LERM-ES at the Azores have a VE that is on attractor after 15 years?	56
5.1.1	Stage 2 – Testing the ergodicity of the virtual Ecosystem	60
5.2	Sensitivity experiments	60
5.2.1	Stage 1 – Sensitivity of recruitment to a change in mesocosm dissolved silicate and nitrogen load	60
5.2.2	Stage 2 - Sensitivity of recruitment to abundance of basal predator	61
5.2.3	Stage 3 - Sensitivity of recruitment to predation	62
5.2.4	Stage 4 - Sensitivity of recruitment to spawning magnitude	62
5.2.5	Stage 5 - Sensitivity of recruitment to spawning date	63
CHAPTER 6 – RESULTS		65
6.1	Base run	65
6.1.1	Adjustment to the attractor	65
	6.1.1.1 Poincaré plots of vertically integrated biomasses	66
	6.1.1.2 Poincaré plots of vertically integrated concentrations	69
	6.1.1.3 Error distribution around the mean	72
6.1.2	On attractor (last 10 years)	74
	6.1.2.1 Demography	74
	6.1.2.2 Plankton biomass	82
	6.1.2.3 Number of agents	89
	6.1.2.4 Physical environment	91
	6.1.2.5 Chemical environment	92
6.2	Ergodicity	96

6.3	Sensitivity of stability	99
6.3.1	Doubling the 1 st Jan dissolved silicate concentration	99
6.3.1.1	Vertically integrated concentration of plankton	99
6.3.1.2	Causes of mortality	101
6.3.1.3	Vertically integrated biomass of plankton	103
6.3.1.4	Number of agents	107
6.3.1.5	Physical environment	108
6.3.1.6	Chemical environment	109
6.3.1.7	Causes of high recruitment event in year 16 (2020)	111
6.3.2	Increasing the competition for food	122
6.3.2.1	Vertically integrated concentration of plankton	122
6.3.2.2	Causes of mortality	124
6.3.2.3	Vertically integrated biomass of plankton	126
6.3.2.4	Number of agents	130
6.3.2.5	Physical environment	131
6.3.2.6	Chemical environment	132
6.3.3	Increasing predation pressure	134
6.3.3.1	Vertically integrated concentration of plankton	134
6.3.3.2	Causes of mortality	136
6.3.3.3	Vertically integrated biomass of plankton	138
6.3.3.4	Comparison between 1 st Jan vertically integrated biomass of diatom and copepod with base run	141
6.3.3.5	Number of agents	142
6.3.3.6	Physical environment	144
6.3.3.7	Chemical environment	144
6.4	Sensitivity of recruitment to spawning	146
6.4.1	Variation in spawning stock	146
6.4.1.1	Causes of mortality	146
6.4.1.2	Food availability and ingestion	147
6.4.1.3	Time spent in each stage	148
6.4.2	Variation in squid spawning date	149
6.4.2.1	Causes of mortality	150
6.4.2.2	Causes of recruitment variability	151
6.4.2.3	Predation	152
6.4.2.4	Competition for food	153
6.4.2.5	Food availability	154
6.4.2.6	Copepod protein availability	154
6.4.2.7	Squid protein ingestion	155
6.4.2.8	Prey composition	156
6.4.2.9	Recruitment	156

6.4.2.10 Squid audit trails	157
6.5 Preliminary results on the effect of temperature on recruitment	160
CHAPTER 7 - DISCUSSION	161
7.1 Stability	161
7.1.1 Ergodicity	163
7.1.2 Sensitivity	164
7.1.2.1 Variation in nutrients load	164
7.1.2.2 Variation in top predators abundance	166
7.1.2.3 Variation in spawning stock	167
7.1.2.4 The effect of temperature on recruitment	168
7.2 Causes of recruitment variability	169
7.2.1 Competition	169
7.2.1.1 Intra-population competition for food	170
7.2.1.2 Inter-population competition	171
7.2.2 Predation	172
7.2.3 Ingestion and prey composition	172
7.3 Cushing's match-mismatch	173
7.4 Verification	175
7.4.1 The formation of deep chlorophyll maximum	176
7.4.2 Observations of squid physiology and behaviour	177
CHAPTER 8 - CONCLUSIONS AND FUTURE WORK	178
8.1 Conclusions	178
8.1.1 LERM	178
8.1.2 The VEW	179
8.2 Future work	180
8.2.1 Using weather data provided by ERA-40	180
8.2.2 Coupling LERM with a 3D circulation model	181
8.2.3 Sensitivity of recruitment to a wider range of variation in exogenous factors	181
8.2.4 Method for testing the effect of temperature on squid recruitment	181
8.2.5 Modification of chemical budgeting	182
8.2.6 Lunar phase	182
8.2.7 VEW performance	182
8.2.8 Analysis of all dates of the timing of spawning experiment	182
8.2.9 Passage from food chain to food web	183
8.2.10 Copepod	183
8.2.11 Squid	183
8.2.12 Changing geographical location	184
8.2.13 Other fisheries recruitment theories	184

REFERENCES	185
APPENDICES	202
I Diatom model	203
II Copepod model	221
III Squid model	241
IV Top predators	263
V Contributions to the VEW.	276

CHAPTER 1 - INTRODUCTION

Fish represent the most important source of high-quality protein for human consumption, providing 16% of the annual protein consumed by the world's population and are particularly important in developing countries, where the livestock resources are scarce (FAO, 1997). Fish provide a little under 10% of the animal protein consumed in North America and Europe, 17% in Africa, 26% in Asia and 22% in China (FAO, 2000). One billion people rely on fish as their primary source of animal protein (FAO, 2000). The value of fish traded internationally was estimated to be 51 billion US\$ per annum (FAO, 2000), with 36 million people working directly in fishing and aquaculture industries (FAO, 2000) and about 200 million getting income from fish (Garcia and Newton, 1995). World demand for food fish has been increasing constantly: consumption has risen from 40 million tonnes in 1970 to 86 million tonnes in 1998, and is expected to reach 110 million tonnes by 2010 (FAO, 1999). The principal cause for this increase in demand can be attributed to the growing world population, especially in Africa, Asia and South America, as the per-capita consumption during this period has not significantly increased (Tidwell and Allan, 2001).

1.1 The decline of fisheries

Four hundred years ago Hugo Grotius (1609) wrote: “For everyone admits that if a great many persons hunt on the land or fish in a river, the forest is easily exhausted of wild animals and the river of fish, but such a contingency is impossible in the case of the sea”.

Four hundred years later, people read in newspapers: “Only 50 years left for sea fish. There will be virtually nothing left to fish from the seas by the middle of the century if current trends continue, according to a major scientific study” (BBC news, 2006). The reality is that a combination of over-fishing, bad management of fisheries, pollution and habitat loss are contributing to the decline of most commercially important species. About three quarters of monitored fish stocks are now fully exploited, overexploited or even depleted (Garcia and Newton, 1995), and in need of urgent management (FAO, 1997).

1.2 Ecosystem-based management of fisheries

Over-fishing of many fish stocks on a global scale associated with the degradation of marine ecosystems have progressively made evident the limits of current fisheries management. The Reykjavik Declaration of October (FAO, 2002) encourages governments to make fishing policies using an ecosystem approach.

The Ecosystem Approach to Fisheries (EAF), particularly recommended by FAO, calls for modifying the perception of fisheries management in an ecosystem context. EAF should consider the interactions between physical, biological, chemical and human components of the ecosystem, while ensuring the overall health of each component, including the sustainability of managed species (FAO, 2003). EAF aims to reconcile sustainable exploitation of fisheries resources and conservation, by quantifying the effects of fishing and by improving our understanding of population and dynamics of the marine ecosystem, including the interdependencies between different the trophic levels that compose it.

1.2.1 Ecosystem modeling

Undersampling of both the environment and populations is the biggest constraint to understanding the dynamics of the upper ocean ecosystem. Diagnosis from observations made at sea is an unrealistic target, considering the vastness of the oceans and the costs involved. As a result of this, most of the knowledge about the marine ecosystem is based on *theories*. Modeling is sought as one solution to improve the understanding of the processes driving the marine ecosystems and overcome the lack of reliable and long term observations. This is a technique used to predict the development of a system by formalising the key processes mathematically and by evolving a simulated ecosystem over time in accordance with the associated mathematical equations.

The key to success is to ensure that the model equations are based on sound scientific principles. In an ecosystem model, the physics (and chemistry) should adhere to known laws and the biological equations should be derived from reproducible laboratory experiments. This requires biologists and modellers to work closely together. Modeling can guide biologists to concentrate on processes that are

critical and poorly understood. On the other hand, biologists can help modellers in producing credible models based on sound biology.

1.3 This thesis

The objective of this thesis is to build an individual based plankton ecosystem model (Lagrangian Ensemble Recruitment Model, LERM), using the Lagrangian Ensemble metamodel (Woods, 2005) to couple the biology of individuals to their environment with a view to predicting recruitment variability in squid populations. Squid provides an interesting test case for modeling recruitment, as after spawning, adults die and the population is composed exclusively by their offspring. Understanding recruitment variability is thus a key to successful management of their fisheries, and should be based on a full understanding of the life cycle biology, in particular the early life phase, from egg to post planktonic juvenile (Rodhouse, 2001). In order to address this challenge LERM was built including three explicit trophic levels, the biology (physiology and behaviour) of which is described by equations derived by reproducible laboratory experiments. The interactions between individuals in different trophic levels (i.e. predator-prey interactions, carbon transfer to higher trophic levels, etc.) are modelled explicitly. LERM is used to investigate the adaptation and emergent properties of the virtual ecosystem (demography, biomass, etc.) under different conditions, which are considered significant in driving recruitment variability in squid (e.g. food availability, inter and intra-population competition for food, predation, etc.). It provides a simple, but biologically robust, tool for testing fisheries recruitment hypotheses, which can be adapted and used as a base for the investigation of different hypotheses.

1.3.1 The Virtual Ecology Workbench

The main obstacle to the widespread use of ecosystem models lies in its intrinsic complexity, relying on expert computer programmers to build them. This problem was addressed by the development of the Virtual Ecology Workbench, VEW (Hinsley, 2005), which is a user-friendly software tool, that allows users with no programming experience to create ecosystem models under the Lagrangian

Ensemble metamodel (Woods, 2005). The “language” of the VEW consists of mathematical equations familiar to biologists. The aim of the VEW is to help the user through the processes of creating and analysing a Virtual Plankton Ecosystem (Woods, 2005).

The VEW is the tool used to achieve the objectives of the thesis. However, at the beginning of the project, the VEW was still in the early stages of development. Development of the LERM model¹ exposed a number of limitations with the VEW that existed at that time. An additional objective of this thesis was to evaluate the usefulness of the VEW and to prescribe a series of modifications to enhance its functionality, when necessary. This gave an advantage to the development of the VEW, since LERM provided an immediate application that the software could be specified towards. It also gave advantages to the creation of LERM models, since the development process of the VEW could specifically include the features required for building LERM.

1.4 Contributions

The main contributions of this thesis are as follows:

- A model of recruitment in an explicit population of squid in an ecosystem model is presented. It includes explicit modeling of the prey field (zooplankton) and its variation in different scenarios (more nutrients, increased competitors for food, increased predation, etc.). An extensive set of results are presented in Chapter 6;
- As a first step to test squid recruitment, a basic food chain model, labelled LERM-PS (Parametrised Squid), has been created comprising nutrients, phytoplankton, zooplankton and parameterised top predators to provide trophic closure. A summary of its functionalities is provided in Chapter 3. A more detailed description of its biological components is given in Appendices I-IV.

¹ All VEW developments were performed by Dr. Hinsley.

- An explicit model of squid paralarvae is developed and this is used to replace the parameterised top predator in LERM-PS. The resulting model is labelled LERM-ES (Explicit Squid) and is summarised in Chapter 4.
- The description of physiology and behaviour of the individuals of each population in the model is developed using equations taken from an extensive literature, each derived from laboratory experiments, and described in Appendices I-IV;
- LERM-ES is shown to be stable in the sense that the inter-annual variability of the ecosystem emergent properties is small compared with the multi-year average. An extensive set of results are presented in Chapter 6. This provides the prerequisite for testing squid recruitment;
- A detailed analysis of the virtual ecosystems generated using LERM-ES is presented including analysis of the sensitivity of the ecosystem to various changes in the scenarios. Results are presented in Chapter 6 and discussed in Chapter 7;
- The LERM-ES model was used to investigate Cushing's match-mismatch hypothesis for squid recruitment as a function of varying the timing of spawning. It was also used to test density-dependent effects on squid recruitment as a function of varying the magnitude of spawning. Results are presented in Chapter 6 and discussed in Chapter 7;
- A summary of the enhancements made to the VEW in order to complete this investigation is presented in Appendix V. These include in particular zooplankton staged growth, an upgraded ingestion specification in the kernel to allow for predation between two migrating populations, etc.

CHAPTER 2 - REVIEW

2.1 The fisheries problem

Developments in world fisheries and aquaculture during recent years have continued to follow the trends that were already becoming apparent at the end of the 1990s (fig.2.1): capture fisheries production is stagnant and aquaculture output is expanding faster than any other animal-based food sector (FAO, 2000).

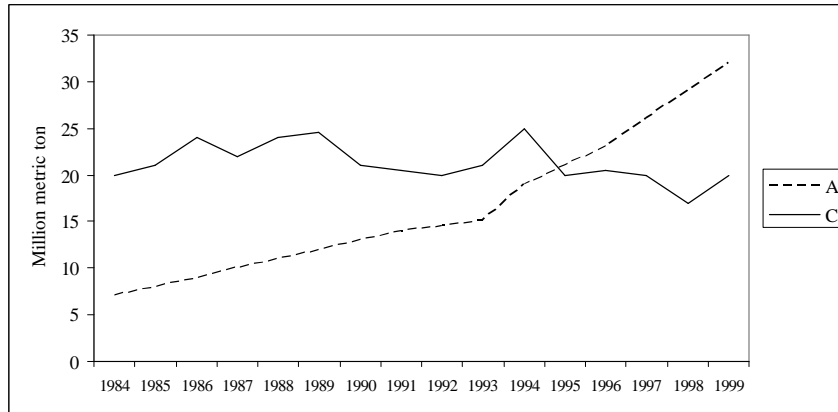


Fig. 2.1 – Aquaculture production (A) and pelagic fish landings (C), (FAO, 2000)

As a result, capture fisheries is not managing to keep up with increasing demand. There are growing concerns with regard to safeguarding the livelihoods of fishermen as well as the sustainability of the aquatic ecosystem.

From 1970 to 1992, the catch of the four major demersal species (silver hake, haddock, Cape hake and Atlantic cod) decreased by about 67% from 5.0 to 1.6 million tonnes. Atlantic cod was the second most important species in 1970 (after anchoveta) with 3.1 million tonnes. It was only the sixth most important species in 1989 (after Alaskan pollock, anchoveta, Japanese and South American pilchards and Chilean jack mackerel), with landings of 1.8 million tonnes and the tenth most important species in 1992, falling below capelin, Atlantic herring, skipjack tuna and European pilchard, with landings of 1.2 million tonnes (Garcia and Newton, 1995). The world fish supply is increasingly relying on low value species, characterised by large fluctuations in productivity, concealing the slow but steady degradation of the demersal high value resources (Garcia and Newton, 1995). As fisheries get depleted and fish harder to catch, fishermen and governments invest more money in

equipment and technology to fish longer, harder and farther away from their home ports. As a result, fishing fleets are so big and well equipped, that even newly discovered less valuable populations can be put under severe stress before regulators obtaining the relevant biological data can impose limitations (Tidwell and Allan, 2001).

This increase in fishing effort, in the attempt to satisfy demand, has been making fishing unprofitable. This approach not only pushes fishermen out of business, but ultimately puts an immense pressure on fish stocks already overexploited, making their recovery a slow and uncertain process. A significant example of the combined effect of inadequate management and over-fishing is that which led to the collapse of the once fertile Newfoundland cod stock.

Since 1977, the Government of Canada, through the Department of Fisheries and Oceans (DFO), has taken over the management of the fisheries. Instead of fish being a resource available to anyone with the means to catch them, they became state property, the rights to which were delegated in the management plans. Therefore, the management policy of the Canadian state has become a major factor in the condition of the industry since this time (Sinclair, 1992). The government controlled the number of fishermen through licensing systems, set quotas for different types of vessels, and, acting upon information from its own scientists, setting a Total Allowable Catch (TAC) for the industry each year (Palmer & Sinclair, 1997). Acting upon faulty data and the assumption that catch rate was a good indicator of stock size, the DFO licensed too many fishermen and set TACs that were too high. On July 2, 1992, the Canadian Federal Minister of Fisheries and Oceans at the time, the Honourable John Crosbie, announced a moratorium on fishing for northern cod in the waters surrounding the province of Newfoundland. This moratorium should have represented a “short-term” solution, but it still applies. Almost 20,000 people working in the industry were directly affected and up to 20,000 other jobs were lost (Steele, Andersen and Green, 1992). For rural Newfoundland, it meant breaking the economic backbone of hundreds of communities where the fishery was the only large employer (Mason, 2002).

2.1.1 The recruitment problem

The fluctuating nature of fish populations is evident from the earliest fishing records. However not all of these fluctuations are attributable to overfishing (Cushing, 1982). The magnitude of the spawning stock can influence the potential of a population to replenish itself, and stock-recruitment models of fisheries management are based upon this principle (Ricker, 1954; Beverton and Holt, 1957, Cushing, 1971; Shepherd, 1982). In an ideal fishery, put under moderate exploitation, the variation in quotas would be low and the danger of recruitment overfishing would be remote (Cushing, 1996). However, at present most commercially important species are not managed ideally. Over-exploitation has caused stocks to be composed by increasingly smaller year classes, limiting enormously their spawning potential and leading to recruitment overfishing (Shepherd, 1990; Cushing, 1996). This causes huge variability in annual recruitment to the adult fish stocks, as observed for Arctic cod and North Sea haddock, which cannot be explained exclusively by the number of eggs spawned each year (Shepherd, 1990). Recruitment variability is typically determined sometime between the egg and juvenile stage, and may vary by a factor of between three to more than one hundred, as it is controlled by a number of processes (Cushing, 1996). It is considered the single most important natural process causing fish population to fluctuate (Hjort, 1914; Cushing, 1975, Heath, 1992) and deserves careful consideration within planning fisheries management policies (Shepherd, 1990; Heath, 1992; Cushing, 1996). Exactly which factors determine recruitment and when they occur is the subject of considerable debate.

The significance of the larval stage in the regulation of fish populations was formally recognised at the start of the 20th century (Hjort, 1914, 1926). Prior to this time, migratory patterns of adult fish were thought largely responsible for fluctuating fisheries catches. In 1902, the international council for the Exploration of the Sea (ICES) was established as a multi-national, multi-disciplinary effort directed at understanding fish and their environment. Johan Hjort was appointed chairman of the migratory committee, the aim of which was to improve the understanding of variability in fish abundances, particularly Atlantic cod and herring

(Solemdal and Sinclair, 1989). Hjort eventually came to reject the concept of adult, migration-driven fisheries fluctuations in favour of several hypotheses emphasising mortality during the larval stage and the concept of fluctuating year class strength. He notes that “the numerical value of a year class is apparently determined at a very early stage...” (Hjort, 1914, pp.203) and suggested two possible reasons for this: “the conditions as regards nourishment to which the fish were subject at this stage, and the passive movement of the same stages under the influence of the currents” (Hjort, 1914, pp.204). Hjort’s first hypothesis, emphasising the adequate provision of food to larvae shortly after hatching, became known as the “critical period” hypothesis, and has ignited much fisheries research ever since.

The match-mismatch hypothesis (Cushing, 1972, 1990) generalised the “critical period” concept to suggest that food limitation causing high mortality of fish larvae may be related to the timing of fish spawning compared to that of high plankton abundance. If a fish spawning event matches in time and space a peak in zooplankton abundance, this would result in a successful year-class with increased chances of survival. Otherwise, if fish spawning occurs too early there could be insufficient food available, or if it occurs too late, zooplankton would have grown too big for the larvae to feed on. In either case, a mismatch would produce slow-growing larvae, which would either starve or get predated.

2.1.2 Cephalopods

Cephalopods have been fished artisanally for thousands of years, and have always been regarded as a food of high value in Mediterranean and Asian countries. However, large scale cephalopod fisheries of the world have developed since 1960, when Japan expanded its fishing effort worldwide (Rathjen and Voss, 1987). Their exploitation has steadily increased in significance since then. Since the early 60’s the world cephalopods catch has increased from around 0.5 million tons to almost 4 million tons in 2004, with squid making up about 75% of the catch (FAO, 2006). In a world fishery marked by overfishing and decline of many finfish, it seems that cephalopods are one of the few remaining marine groups of resource, where some

species in some areas are still experiencing increases in landings (fig.2.2-2.4; FAO, 2006).

World catches of squid and cuttlefish increased by 57% and 84% respectively, between 1970 and 1980, while the total increase of all other fisheries products was only 8% (Roper *et al.*, 1984).

In the English Channel, total catches of finfish in 2003 were 25% lower than in 1983, but catches of cephalopods increased by almost 300% from 8,000 to 23,000 t over the same period (ICES data).

This rapid increase in cephalopod catches has arisen partly by the global expansion of its fisheries into new ocean areas, partly because increased market demand has led to increased utilisation of cephalopod catches for human consumption rather than as bait for other fisheries, and partly because the abundance of cephalopods in some areas has apparently increased relative to fish (Boyle and Rodhouse, 2005).

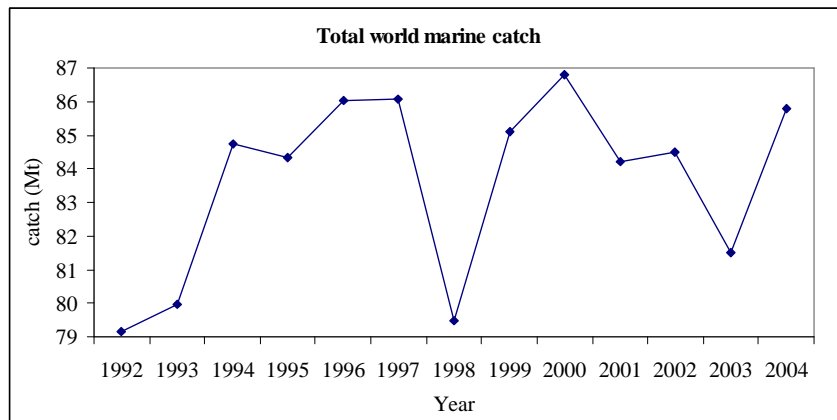


Fig.2.2 – Total world marine catch (FAO, 1999, 2006)

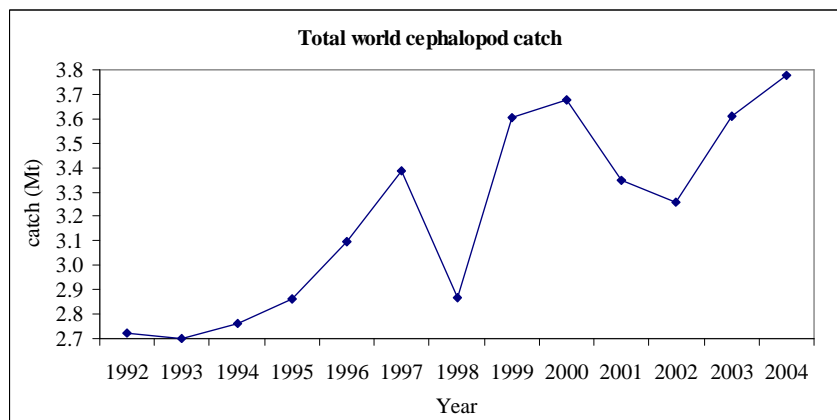


Fig.2.3 – Total cephalopods catch (FAO, 1999, 2006)

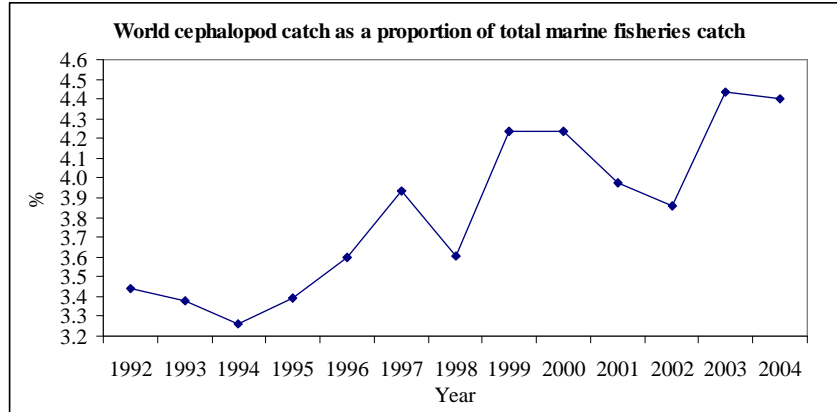


Fig.2.4 – World cephalopod catch as a proportion of total marine fisheries catch (FAO, 1999, 2006)

This has led to some speculation as to whether ecosystem perturbations caused by intensive fishing generally are leading to changes in the trophic structure in favour of this short-lived opportunistic species. Cephalopods, and especially squid, have a short life cycle, characterised by very fast growth rates leading to a rapid turnover and lower standing stock than longer-lived finfish species (Boyle and Rodhouse, 2005). Under high fishing pressure, groundfish are probably poor competitors, having less opportunity for spawning and replacement (Caddy and Rodhouse, 1998). Cephalopods, especially squid, are at the centre of a complex trophic web (fig.2.5). They are largely consumed by seabirds, seals, whales and larger fishes (Boyle and Rodhouse, 2005).

When a strong cohort of cephalopods passes through a system this will lead to a substantial energy and nutrient flux to higher trophic levels as well as increased catch rates in the fisheries (Boyle and Rodhouse, 2005). Overfishing of finfish always results in reductions in the size of older cohorts, which tend to be those preying on adult cephalopods (Smale, 1996). In some cases, such as the heavily exploited North Atlantic cod, stocks and mean age/size have been so reduced that predation on larger preys, such as cephalopods, is probably much reduced (Caddy and Rodhouse, 1998). The catch of sperm whales at whaling stations in the Azores, which was well documented in the years 1935-49, could have taken a total weight of 373,000 tonnes of cephalopods annually during their two months residence in Azorean waters, which is a significant figure considering that the total annual human catch of all fish species in the Azores is about 14,000 tonnes (Clarke, 1996).

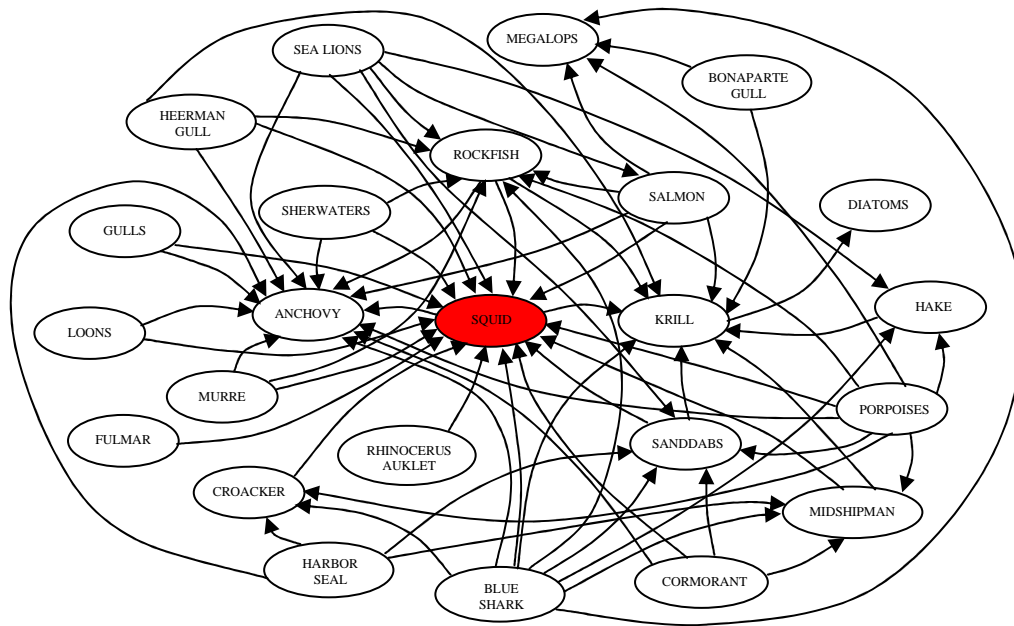


Fig.2.5 – Food-web centred on squid (adapted from Morejohn *et al.*, 1978)

When the relative failure of a cephalopod population occurs, reduced breeding success in predators may follow until the population recovers (Xavier *et al.*, 2003). The modeling and management of fishing on cephalopods is at an early stage. The methods available were mainly adapted from those used for finfish and most of them involve assumptions that are not completely appropriate to cephalopods (Boyle and Rodhouse, 2005). An unresolved issue is whether cephalopods (especially squid) may be treated in the same way as fish for assessment purposes and thus become subject to the range of methods traditionally applied to finfish.

2.1.3 Squid recruitment variability

Squid are short-lived ecological opportunists. There is evidence that while the abundance of fish stocks has been decreasing through over-fishing, stocks of squid have been increasing due to reduced predation pressure from fish and relaxed competition for food (Caddy and Rodhouse, 1998). Squid fisheries are therefore becoming increasingly important as a source of high quality protein for human

consumption and because of their possible role as an indicator of global ecological change driven by fishery exploitation in the oceans (Rodhouse, 2001).

Despite the increased importance of squid stocks, their assessment and management remain difficult. Populations of short-lived, semelparous (reproduces once then dies), opportunistic species, such as squid, are typically unstable, responding rapidly to changes in environmental conditions (Rodhouse, 2001). This constitutes a big challenge for managers, who are concerned with maintaining a stable recruitment (through the preservation of an adequate spawning stock biomass, SSB, known as “reproductive escapement”), while achieving optimal catch rates. For squid, the exploited stock is usually composed almost entirely of recently recruited animals of a similar age (Agnew *et al.*, 2002). So, knowledge of recruitment variability is highly desirable for management purposes. Squid populations display high recruitment variability: although they do not have strong stock-recruit relationships, they are believed to be vulnerable to over-exploitation because the stock is composed entirely of recruits (Beddington *et al.*, 1990). A study performed on *Todarodes pacificus* in the Sea of Japan, measured paralarval density index (PDI) as the number of paralarvae per 1000 m³ of water filtered in oblique tows of an 80 cm diameter plankton net from 75 m depth to the surface (Sakurai *et al.*, 2000). In the period 1976-1996 PDI ranged from about 2 to 90 per 1000 m³ of water (Sakurai *et al.*, 2000). Catches of the short-finned squid *Illex illecebrosus* in the NW Atlantic varied greatly from about 90,000 t in 1977 to about 1,000 t the following years (Dawe *et al.*, 2000). For many squid species, recruitment variability can be partly explained by environmental variability derived from synoptic oceanographic data (Robin and Denis, 1999; Agnew *et al.*, 2000; Waluda *et al.*, 2002). In the E. Pacific coastal upwelling system a fishery for *Dosidicus gigas* has grown rapidly during the last decade and abundance and catch rates seem to be linked to the El Niño Southern Oscillation (ENSO) (Waluda and Rodhouse, 2006). Variability in *Loligo vulgaris* in the English Channel has been shown to be correlated with inter-annual changes in Sea Surface Temperature, SST (Robin and Denis, 1999). In the Monterey Bay area, warmer than normal water temperatures appear to have a positive effect on catches 18 months later. ENSO events seem to have the opposite effect (Vojkovich, 1998).

For *Loligo gahi* in the SW Atlantic, 66% of the variance in recruitment strength (tab.2.1) could be explained by SST six months prior to recruitment, and a combination of SST and Spawning Stock Biomass, SSB, could explain 77% of recruitment variability (Agnew *et al.*, 2000). However, the exact causes of this relationship are unknown. The authors of the study suggested that the most likely explanations are that recruitment is affected by the abundance of plankton, the strength of which is indicated by SST (as a proxy for food abundance), and the growth rate (energy demand) of paralarvae, which is known to be strongly influenced by temperature (Agnew *et al.*, 2000).

Year	1 st Cohort	2 nd Cohort	Pooled	Ave
1987	2,471	4,745	7,216	3,608.0
1988	2,802	777	3,579	1,789.5
1989	6,837	1,062	7,899	3,949.5
1990	5,566	3,407	8,973	4,486.5
1991	1,392	3,811	5,203	2,601.5
1992	3,233	7,336	10,569	5,284.5
1993	1,163	1,682	2,845	1,422.5
1994	1,702	2,377	4,079	2,039.5
1995	4,534	2,422	6,956	3,478.0
1996	2,280	1,950	4,230	2,115.0
1997	975	2,124	3,099	1,549.5
1998	1,991	2,170	4,161	2,080.5
1999	1,556	1,213	2,769	1,384.5
2000	2,263	3,227	5,490	2,745.0
2001	872	3,373	4,245	2,122.5
2003	919	2,967	1,778	1,943.0
2004	268	1,510	5,071	889.0
2005	2,767	2,304	3,389	2,535.5
2006	1,862	1,527	5,023	1,694.5
Ave	2,392.3	2,630.7	5,086.2	2,556.9
SD	1,676.6	1,528.5	2,364.4	1,173.1
%err	70.1	58.1	46.5	45.9

Tab.2.1 –*L. gahi* recruitment (millions) around the Falklands – Years 1987-1999 from Agnew *et al.*, 2000; Years 2000-2006 from Agnew (personal communication) Year 2002 N/A.

The same study also found that very high SSB leads to a reduction in recruitment strength, suggesting a density dependent effect (Agnew *et al.*, 2000). The reduction of recruitment strength with increasing SSB seems a paradox as density-dependent effects in fish stocks are caused by cannibalism (Ricker, 1954). However, in squid such as *Loligo gahi*, the parent stock dies soon after spawning and is therefore not present to cannibalise the next generation when it starts to grow. So, the proposed density-dependent mechanism must presumably be different (Rodhouse, 2001). It would be possible that this density-dependent mechanism is food limitation (Cushing's match mismatch).

Bakun and Csirke, 1998 have proposed a set of hypotheses about how variability in ocean ecosystems might cause inter-annual variability in squid stocks. They proposed that recruitment may be dependent on one or more of:

1. Wind effects with onshore, wind driven Ekman transport being favourable to both onshore transport of surface dwelling larvae and offshore migration of pre-adults.
2. Fluctuations in prey abundance
3. Match-mismatch effects driven by temperature, as proposed for fish (Cushing, 1975)
4. Variation in predator pressure
5. Disease

2.2 Ecosystem modeling methods

There are two main branches concerned with modelling complex systems:

- Complex non-adaptive systems, obeying the laws of physics (e.g. weather).
- Complex adaptive systems based on equations, responding to behavioural changes of the modelled agent, due to learning behaviour (e.g. adult fish or people).

Complex adaptive systems are difficult to model. They, at best, have “strange” attractors with poor predictability (Woods, 2003). On the other hand, plankton are microscopic organisms, which are so simple that they cannot learn new tricks or change their behaviour. Their behaviour is governed directly by their genes, rather than by their decisions, thus, responding directly to variations to their environment. It is possible to derive equations describing the behaviour and physiology of planktonic organisms under laboratory conditions. Plankton ecosystems exhibit ordinary attractors and offer useful predictability (Woods et al., 2005). The limits of the predictability are set not by the biology, but by the chaotic fluctuations in the exogenous factors, notably the weather and the ocean circulation. Thus, for plankton modeling, the limits to predictability arise not from the biology, but from the physics.

2.2.1 Modeling complexity

Starting with the premise that realistic predictions can only be expected if the key processes associated with a system feedback are represented correctly (Doney, 1999), the modeller is faced with the decision on which strategy (method) is best suited for representing such processes.

The level of complexity required in a model ultimately depends on the finality of the investigation. Oversimplification of processes risks reaching the right answer for the wrong reasons. On the other hand increasing the complexity of a model by including more and more processes, species, chemicals and so on has the risk of accumulating the errors deriving from the uncertainties linked with the representation of such processes and interaction (Flynn, 2005). Apart from the technological constraints in computing power, trying to include any process occurring in nature is neither a good nor achievable modelling approach.

The problem is then to understand where to stop. A good model has to capture the processes that drive the system and represent them in an accurate, realistic and possibly simple way. Ideally, a model should pursue the best balance between accuracy and performance.

At this point in time, with computing power still constraining the performance of a model, an ideal model would be capable of adapting its complexity to the level of complexity and detail required by a specific investigation.

Two main schools of thought have developed to answer these questions and two branches of ecosystem modelling have generated from them: Eulerian or population based modelling (PBM) and Lagrangian or individual based modeling (IBM).

Both of them have virtues and caveats, but they are both aiming to solve the same problem.

2.2.2 Population-based modeling (PBM)

Eulerian integration is the classic method for modeling plankton ecosystems. It treats plankton as a continuum, as if it were a chemical, whose concentration represents a biomass. Eulerian models have the advantage of being simple and computationally economical compared to their Lagrangian counterpart.

For this reason early models of marine ecosystems were implemented using the Eulerian approach. They were initially simple due to the infancy of the discipline and the technological constraints of available computing facilities. They started with “NPZD” models in which nutrients, phytoplankton, zooplankton and detritus constitute the main model structure (e.g. Fasham *et al.*, 1990) and gradually got more complex to represent more complex food webs and processes (e.g. European Regional Seas Ecosystem Model – ERSEM – Baretta-Bekker *et al.*, 1997).

Eulerian modelling has the merit of opening the way to modelling ecology and does a good job in predicting the bulk properties of a system such as chlorophyll and primary production (Fasham, 1993, Anderson and Pondaven, 2003). However when tackling more complex investigations, such as the transfer of biomass up the trophic chain, an over-simplistic description of biology and its interaction with the environment can lead to wrong conclusions (Flynn, 2005).

Classical models available to fisheries management use parameterisations of complex processes such as mortality, density-dependent survival, etc. (Cushing, 1996). In population-based models the demographic properties of a population are used directly as state variables. These use equations, based on observations of the bulk properties of the population, rather than on the physiology of its individuals.

This has a number of disadvantages. The information about individual organisms is not available. All individuals of a population are assumed to be in the same state. Population dynamics are represented by differential equations that describe the changes in population size or biomass as a relatively simple function of one or a few state variables (e.g. age, size, etc.). So, even if the parameterisation is successful in matching observations, the intrinsic causes that led the system to that state remain

unknown. This approach incorporates a “principle of induction”: starting from observations it assumes that the future will be like the past. However this does not realistically account for inter-annual variation in the weather, which is one of the principal factors driving the ecosystem. Also, it should be noted that observations are in the vast majority of cases geographically sparse and qualitatively inadequate. This constrains the reliability and therefore the usefulness of predictions.

This type of parametrisation risks oversimplifying certain processes, which may be crucial (e.g. mortality, food availability to animals, etc.).

Anderson (2005) pointed out that two different models (Hood *et al.*, 2004 and Lenos *et al.*, 2005) studying the distribution of nitrogen fixers in the subtropical Atlantic and Caribbean both generated results which broadly matched observations using different parameterisations. This raises two issues. The first is the robustness of Eulerian models. This can be assessed by integrating the model over a variety of different scenarios and comparing the output with observations. But in reality, this is not often achievable as there are not enough reliable observations to compare with. The second is whether Eulerian models get the right answer by asking the wrong questions. It is possible that two wrongs make a right but this is also difficult to verify as the biology is abstracted in the form of differential equations for the population as a whole (Flynn, 2005).

The difficulties of PBM lie in the short life-scale and high responsiveness of the population to environmental variables (e.g. temperature, salinity, etc.). These are routinely monitored and may exert a direct effect on the organisms. However these are only proxies for other variables such as ocean currents that advect larvae and juveniles, or food supply at appropriate times (Agnew *et al.*, 2000; Boyle and Rodhouse, 2005).

2.2.3 Individual-based modeling (IBM)

A promising alternative is individual-based modelling in which an individual is the biological unit of the population, and the population demography “emerges” from

the balance between births and deaths of the individuals of a population interacting with the environment.

The use of IBMs has been growing rapidly during the last twenty years for two reasons:

- the fast increase in computing power that made it possible to simulate a much larger number of particles, and
- the possibility to understand ecosystem complexity and its emergence from the variability and physiology of individual organisms. (Grimm and Railsback, 2005).

The advantages of individual-based modelling are that:

- the biology (physiology and behaviour) is mechanically explicit and not hidden away in differential equations;
- it explores how individuals within a population adapt and interact with the environment. (in IBMs this interaction is clearly detailed);
- it allows for intra-population variability, resulting from the different life-histories of the organisms.

This opens up new horizons for investigating the dynamics of an ecosystem. After all, it is the physiological and behavioural properties of individuals that determine the state of the ecosystem. During their lives, organisms are exposed to different environmental conditions (e.g. temperature, food, light, etc.), as they sink, migrate or are advected by turbulence. This causes intrapopulation variability in the internal state of the individuals composing the population. Most importantly, different internal and external conditions generate differences in the way organisms adapt to their ambient environment, which often determines their chances of survival. IBMs have a great potential for making realistic predictions if the biology and the key processes affecting it are represented correctly (Doney, 1999). As the effort of marine biologists is concentrated on producing equations to describe the behaviour and physiology of thousands of species of plankton in the oceans, it is increasingly possible to describe plankton ecosystems using individual-based modelling.

2.2.4 Lagrangian Ensemble metamodel (LEM)

The main problem with IBMs is the high computational cost associated with running them. To give the model results statistical significance, a large number of individuals have to be modelled. The more individuals, and/or the more complex biology of an individual, the more acute the computational costs.

In the Lagrangian Ensemble metamodel (LEM - Woods, 2005), this problem is solved by introducing the concept of subpopulations. These group together individual plankters, which, following the same trajectories and being exposed to the same ambient environment, share the same life history. The introduction of subpopulations greatly reduces the integration time. Increasing the number of agents may improve the statistical significance of results, but at the cost of computation time. The model designer should choose the compromise, depending on available computing resources and required statistical error control.

Virtual Plankton Ecology (VPE) is a new branch of biological oceanography (Woods and Onken, 1982; Woods, 2005). It provides an alternative to the traditional approach to marine ecology founded on population-based modelling and a way of making IBMs computationally feasible. VPE is based on the Lagrangian Ensemble (LE) metamodel, which integrates the BPEs separately along the trajectory of individual plankters as they are advected by turbulence. This results in the exposure to different environmental conditions and the development of different life histories for each of them and reveals explicitly intra-population variability.

LEM was used successfully to prove the inherent stability of the plankton ecosystem (Woods *et al.*, 2005). If an ecosystem is stable, it would respond in the same way to the same external forcing. After a transient period, in which initialisation errors had enough time to decay, the ecosystem adjusts to an attractor, in which the inter-annual variability is a small percentage of the multi-year stability. The inter-annual variability is caused by the random displacement of plankton above the turbocline. Stability determines the limits to predictability and is the base condition for what-if predictions, in which changing the external forcing causes the ecosystem to adjust to the new environment (Woods *et al.*, 2005). The demography of a population is a

function of the integrated life histories of all plankters within it. This is an emergent property of the model, unlike the populations in PBM, which are prescribed by the model equations. Furthermore, the LE method considers how the environment, both physical and chemical, is in turn affected by the demographic state of the population, in terms of biofeedback (fig.2.6). A good example is self-shading, caused by the large biomass of phytoplankton in the surface water during spring blooms (Woods and Barkmann, 1993). This increases the turbidity of the water, effectively reducing the vertical propagation of light through the water column (bio-optical feedback).

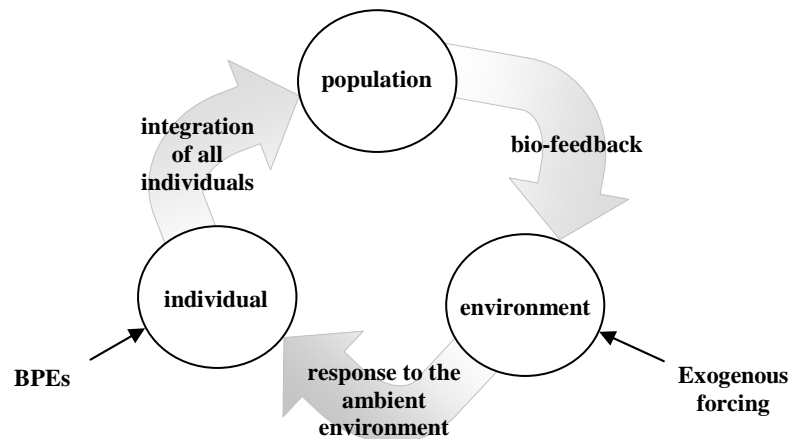


Fig. 2.6 – Lagrangian Ensemble Method

All the links between the three components of a plankton ecosystem are integrated together using LEM.

The final product of the LE integration process is a Virtual Plankton Ecosystem. It consists of a large data set documenting the life history of each individual plankter within a subpopulation, the demography of every population, and the chemical and physical environment for each layer of the water column. During the integration process this is computed every time step (typically half an hour). The richness of the data set produced by the integration limits the spatial and temporal complexity of a simulation or the number of species included in it.

2.2.5 Virtual Ecology Workbench, VEW

LE models are complicated to write. One must consider not only the interactions between individuals and their ambient environment, but also the demography (number of individuals represented) of agents. For this purpose, the Virtual Ecology Workbench (VEW) has been created (Hinsley, 2005). It allows a biologist without particular programming skills, to create a biological model of the plankton ecosystem, using a suite of custom-built tools. The model is then compiled into Java classes which can be executed on any Java-compliant platform.

The VEW allows creation of functional groups, which represent a set of plankton of shared behaviour. It also supports a mechanism for modelling staged growth. Behaviour is defined by rules, which are written from the perspective of an individual plankter of a functional group. Rules consist mostly of standard mathematical statements. However, when an interaction between a plankter and its environment is required, a special function is provided, and the simulation kernel handles that function. This is necessary in agent-based models, since one agent's actions will affect the others in its locality. There are seven such functions, which handle uptake and remineralisation, reproduction, cell division and changes in growth stage.

Having written a model, various other specification options are set:

- Species of each functional group are set up.
- Ingestion relationships (by species and stage) are defined
- The simulation takes place in a mesocosm which can be anchored or can drift with OCCAM currents. Climate data for each timestep is provided.
- Agent-management rules can set limits on how many, or how few agents of each stage and species should be permitted.
- Chemical and physical profiles for the beginning of the simulation are set.
- The biological profiles are set – distributions of plankton of a given species and stage, and their initial properties.
- An exogenous trophic closure is set, in which the concentration, size and depth of the top predators can be prescribed.

- Exogenous events can be set to force changes in the environment at a given time, to facilitate “What-If experiments”.
- The variables required for logging are selected; aggregate totals, field variables, and the properties of individuals can all be selected for logging.

CHAPTER 3 - The Lagrangian Ensemble Recruitment Model with Parameterised Squid (LERM-PS)

LERM-PS uses the Lagrangian Ensemble metamodel to represent a classical NPZD trophic chain with three nutrients, one explicit phytoplankton species, one explicit zooplankton species, two parametrised top predator species to provide trophic closure (fig.3.1). The model comprises phenotypic equations derived from reproducible laboratory experiments. The emergent demography and bio-feedback to the environment are calculated from the individuals. This ecosystem adjusts to changes in external forcing.

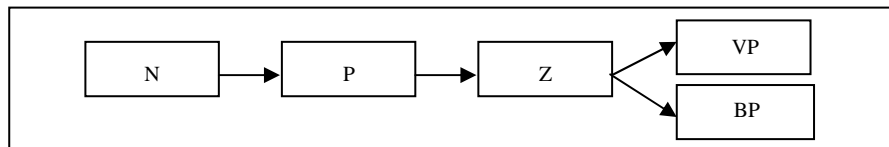


Fig.3.1 – LERM-PS. N: nutrients, P: phytoplankton, Z: zooplankton, VP: visual predators, BP: basal predators

3.1 Phytoplankton

The phytoplankton species group is typical of midsize diatom (cross-section diameter 20 μ m). Each individual is characterised by its depth and four state variables (carbon pool, nitrogen pool, silicon pool, chlorophyll-a pool), which determine its physiological state. The Lagrangian Ensemble subpopulation is described by a demographic variable: the number of individuals. Fig. 3.2 provides a roadmap of the diatom model. It shows the biological state variables (green box), the biological processes (inputs in red and outputs in blue) and ambient environment (in yellow) which affect them.

3.1.1 Stoichiometry

Each diatom has an internal pool for each of the dissolved chemicals (nitrogen and silicon), one for carbon and one for chlorophyll. At any time, it exists in one of two states: dead or alive. Table 3.1 shows the stoichiometric composition of an individual diatom, the maximum observed range in the internal ratio of the chemical elements and the physiological processes in which they are involved.

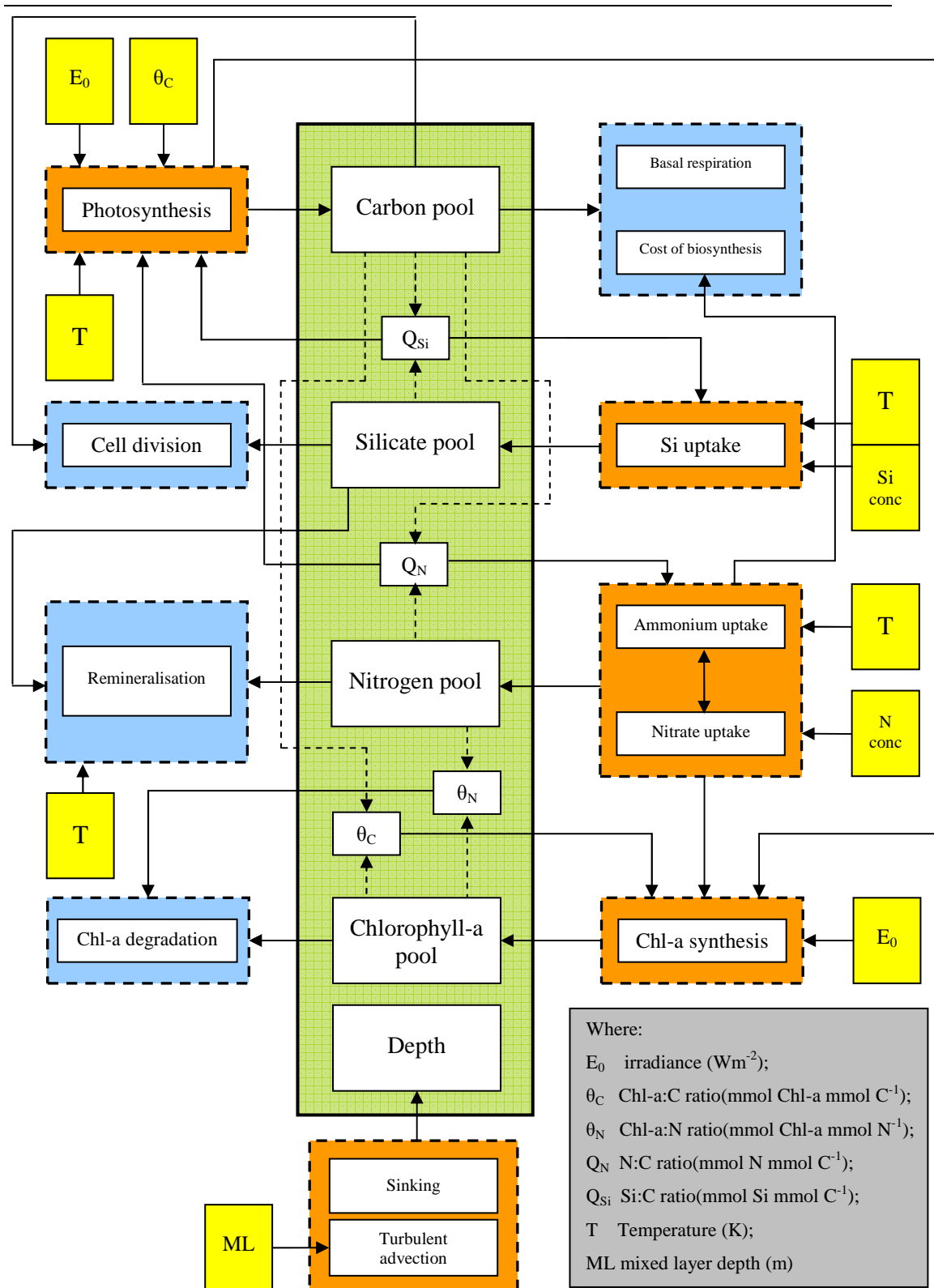


Fig. 3.2 – Roadmap of the diatom model. Biological state variables (in the green box), processes (inputs in orange and outputs in blue) and factors affecting processes (in yellow).

a)	Units	Min	Max	Functions	Reference
C	mmol C	8.5×10^{-9}	2.6×10^{-8}	State variable	Strathmann, 1967 Gilpin <i>et al.</i> , 2004
N	mmol N	7.8×10^{-10}	1.44×10^{-9}	State variable	Geider <i>et al.</i> 1998
Si	mmol Si	1.0×10^{-9}	2.1×10^{-9}	State variable	Brzezinski, 1985
Chl-a ¹	mmol Chl-a	0	3.7×10^{-12}	State variable	Geider <i>et al.</i> , 1998

b)					
N:C	mmol N : mmol C	0.03	0.17	Max photosynthesis Max N uptake	Geider <i>et al.</i> , 1998
Si:C	mmol Si : mmol C	0.04	0.15	Max photosynthesis Max Si uptake	Brzezinski, 1985
Chl:C	mmol Chl-a: mmol C	0	4.3×10^{-4}	Photosynthesis Chl-a synthesis	Geider <i>et al.</i> , 1998
Chl:N	mmol Chl-a: mmol N	0	4.7×10^{-3}	Chl-a synthesis Chl-a degradation	Geider <i>et al.</i> , 1998

Tab. 3.1 – a) Stoichiometry and b) cellular ratios of chemicals

3.1.2 Processes

Table 3.2 shows the list of processes that are modelled explicitly.

<u>Processes</u>	<u>Characteristics</u>	<u>References</u>
Photoadaptation	Dynamic adaptation	Geider <i>et al.</i> , 1998
Photosynthesis	Geider photoadaptive model	Geider <i>et al.</i> , 1998
Nutrient uptake	Droop dynamics Internal quotas to regulate uptake	Paasche, 1973 Geider <i>et al.</i> , 1998 Tett and Droop, 1998
Chlorophyll synthesis	Geider photoadaptive model	Geider <i>et al.</i> , 1998
Respiration	Basal metabolism cost Cost of biosynthesis	Geider <i>et al.</i> , 1998
Cell division	Carbon threshold for cell division Silicon threshold for cell division	Woods and Barkmann, 1994 Brzezinski, 1985
Motion	Constant sinking speed	Woods and Barkmann, 1994
Mortality	Calculated for a nutrient starvation period of 18 days	Berges and Falkowski, 1998 Veldhuis <i>et al.</i> , 2001

Tab. 3.2 – Diatom processes

¹ LERM measures Chlorophyll-a in mg Chl-a, as VEW requires it in this form for the calculation of bio-optical feedback. The molar mass of Chlorophyll-a ($C_{55}H_{72}MgN_4O_5$) is $893.509 \text{ g mol}^{-1}$.

3.1.2.1 Photoadaptation

Photoadaptation allows optimisation of growth rate under inclement conditions; in particular it maximises growth rate at low irradiance and minimises the risk of photo-oxidative damage at high irradiance². Photoadaptation is modelled using phenotypic equations, derived by cell culture experiments³. Growth rate and chlorophyll content of a cell vary with irradiance, temperature and nutrient concentration at the depth of the particle (called “ambient”) nutrient concentrations. Diatom growth is a function of environmental variables and cellular stoichiometric composition. This is modeled explicitly by describing the internal state of the organism, using independently varying chemical internal quotas. In particular, the individual internal ratio of chlorophyll-a : carbon (θ_c) is a function of its light history and nitrogen : carbon (Q_N) is a function of nutrients limitation and variability⁴.

3.1.2.2 Photosynthesis

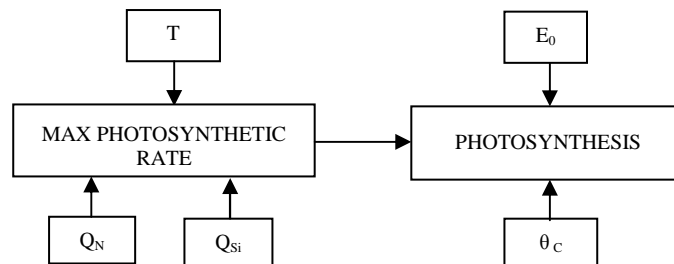


Fig. 3.3 – Photosynthesis components, internal and external controlling factors

The maximum photosynthetic rate ($\text{mmolC mmolC}^{-1} \text{ h}^{-1}$) is a function of temperature, T ($^{\circ}\text{K}$), nitrogen : carbon internal quota, Q_N ($\text{mmol N mmol C}^{-1}$), and silica : carbon internal quota, Q_{Si} ($\text{mmol Si mmol C}^{-1}$) (fig.3.3, Eq.I.9). If dissolved silicate becomes limiting, diatoms in the reproductive phase stop fixing carbon if the internal ratio of Si:C drops below the minimum Si:C ratio⁵. The rate of carbon specific photosynthesis ($\text{mmolC mmolC}^{-1} \text{ h}^{-1}$) is a function of the maximum photosynthetic rate, the ratio of chlorophyll a : carbon, θ_c ($\text{mg Chl-a mmol C}^{-1}$) and the incident irradiance in the PAR (photo-active radiation) part of the spectrum, E_0

² Raven, 1980

³ Geider *et al.*, 1998

⁴ Geider *et al.*, 1998

⁵ $0.04 \text{ mmol Si mmol C}^{-1}$, according to Brzezinski, 1985

[W m⁻²] (fig. 3.3, Eq.I.7). In particular, photosynthetic rate is sensitive to nitrogen : carbon internal quota when light is saturated, to chlorophyll-a : carbon internal quota when light is limited and to silica : carbon internal quota when ambient silica is depleted. At low irradiance photosynthetic rate is higher when chlorophyll-a : carbon internal quota is high (black lines). At high irradiance it is controlled by the maximum rate of photosynthesis, and therefore by the nitrogen : carbon internal quota (red triangle and black cross). The irradiance at which the initial slope of light-limited intercepts the light saturated rate, represents the light saturation parameter, E_K .

3.1.2.3 Nutrients uptake

Specific rates of nutrient uptake are modelled using pools⁶. The maximum uptake rate of a nutrient depends on temperature and the internal quota of the nutrient : carbon⁷ (Eq.I.13 and I.15). This modulates the potential uptake to its stoichiometric composition. The uptake rate of the nutrient to the nutrient pool is a function of the maximum uptake rate and the ambient concentration of such nutrient (i.e. the nutrient concentration at its current depth, fig.3.4, Eq.I.14 and I.16).

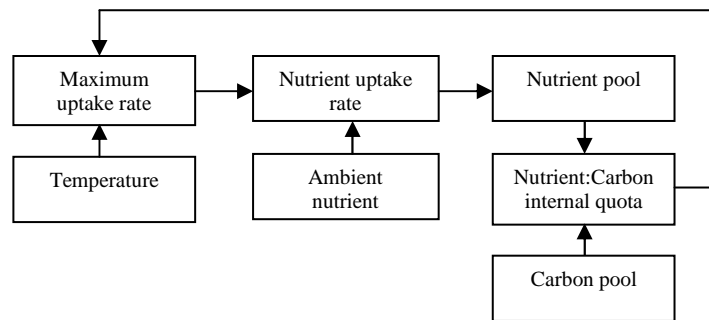


Fig. 3.4 – Nutrients uptake mechanism

3.1.2.3.1 Ammonia and nitrate uptake

Carbon specific nitrate and ammonia uptake rate are modeled using the traditional saturation kinetics model (Michaelis-Menten equation⁸). Ammonia is uptaken

⁶ Droop, 1973

⁷ Geider et al. 1998

⁸
$$v = \frac{v_m \times S}{K_s + S}$$

Where: v is the uptake rate, S the ambient concentration of nutrient, v_m the maximum uptake rate at nutrient saturation and K_s the half-saturation parameter.

preferentially over nitrate⁹ and low level of ammonia inhibits significantly nitrate uptake¹⁰.

3.1.2.3.2 Silicate uptake

Diatoms start uptaking silicate, when they approach their reproductive phase (i.e. when carbon pool reaches 90% of the carbon threshold for cell division)¹¹. Silicate uptake rate is modelled in the same way as ammonia; the only difference is that the Michaelis-Menten equation is silicon specific rather than carbon specific.

3.1.2.4 Chlorophyll synthesis

The amount of chlorophyll produced per timestep within the organism is a function of the level of ambient irradiance (Eq.I.12). Photoadaptation is modelled as a dynamic allocation of cell material between light-harvesting components (L), energy storage compounds (R), such as polysaccharides and lipids, and biosynthetic apparatus (E), consisting of enzymes involved in carbon fixation and new cell elaboration¹² (fig. 3.5).

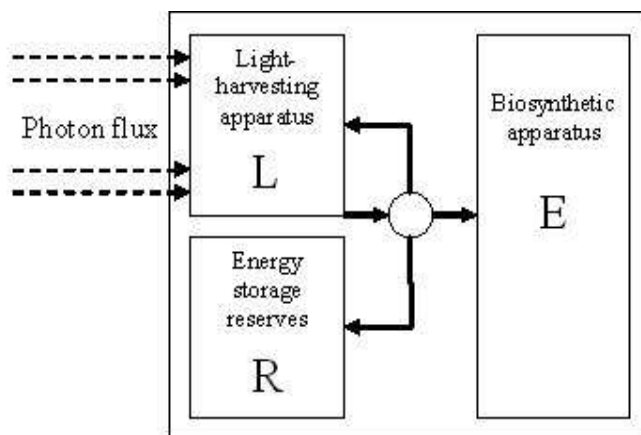


Fig. 3.5 – Photoadaptation (adapted from Geider *et al.*, 1996)

⁹ Experimental results have shown that ammonia is used preferentially over nitrate for the full range of nitrogen concentrations, nanomolar to micromolar (Harrison *et al.*, 1996, Flynn *et al.*, 1997)

¹⁰ Low level of ammonia is capable of significant inhibition of nitrate uptake (Wheeler and Kokkinakis, 1990; Harrison *et al.*, 1996). This was introduced to provide the basis for future research on new and regenerated production and the transition from a diatom dominated ecosystem to a flagellate dominated one.

¹¹ Diatoms acquire most of the silicate needed just before cell division (Brzezinski, 1985),

¹² Geider *et al.*, 1996

Carbon fixation is a function of L and E. Light-limited photosynthesis is controlled by L, while light-saturated photosynthesis is controlled by E (fig. 3.6). The rate of chlorophyll synthesis is therefore a function of ambient irradiance, the value of the light saturation parameter and nitrogen assimilation.

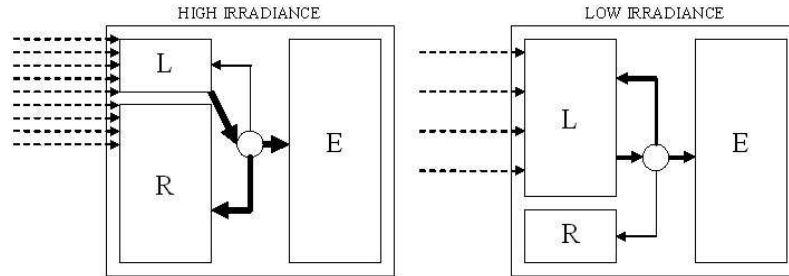


Fig. 3.6 – (Adapted from Geider *et al.*, 1996)

3.1.2.5 Respiration

Respiration rate is defined as the carbon loss due to metabolic activities (Eq.I.20-21).

The total respiration rate is temperature dependent and it has two parts:

- cost of basal metabolism, assumed to be constant
- cost of biosynthesis, which is a function of nitrogen uptake¹³.

3.1.2.6 Cell division

When the carbon pool has reached 90% of the threshold for cell division, diatom starts to uptake silicate to build its valve (Eq.I.22-23). The cell divides when both carbon pool and silicon pool have reached the threshold value for division. After cell division the daughters and parents have the same amounts of carbon, nitrogen, silicon and chlorophyll-*a*, which are half the value in the parent cell before division.

3.1.2.7 Motion

In the mixing layer diatoms are randomly advected by turbulence (eq.I.6). Below the thermocline, a diatom sinks at a constant speed of 1 m day^{-1} ¹⁴. The turbocline marks the boundary between mixing layer and thermocline.

¹³ Geider *et al.*, 1998

¹⁴ Woods and Barkmann, 1994.

3.1.2.8 Mortality

The diatom dies when its carbon reserve pool is fully exhausted (Eq.I.24). The carbon threshold for death was estimated for a diatom with carbon pool at the threshold for cell division, nutrient starved for a period of 18 days¹⁵. During this period they burn carbon to cover basal metabolism. The carbon left at the end of this period is the threshold for cell death.

3.2 Zooplankton

The zooplankton species is based on *Calanus finmarchicus*. LERM assumes that all copepods are female. The phenotypic equations for behaviour and physiology were derived mainly from Carlotti and Wolf (1998). Each copepod features a pool for each of the chemicals present in diatoms (tab.3.3), except for silica and chlorophyll as they play no part in copepod physiology. Copepods reach the mature stage, after a fixed number of successive development stages (staged growth). Molting from one stage to the next is triggered by size (i.e. protein pool).

The copepod physiological state is determined by ten biological state variables: carbon pool – including proteins (nitrogenous carbon, C_N), lipids (non-nitrogenous carbon, C_{NN}) and carapace (made of chitin, C_{shell}) –, nitrogen pool, gut content, gut fullness, gut volume, stage and age.

3.2.1 Stoichiometry

Assimilated carbon is dynamically allocated to lipids, proteins and carapace in different ratios depending on the life stage. The amount of ingested carbon allocated to lipid reserve per timestep depends on the development state they are in. The ratio of N:C for proteins is assumed to be constant¹⁶. The total amount N is regulated by a minimum and maximum ratio of nitrogen:carbon, Q_N ¹⁷.

¹⁵ Berges and Falkowski, 1998; Veldhuis *et al.*, 2001

¹⁶ 0.27 mmolN:mmolC, according to Anderson *et al.*, 2005

¹⁷ 0.12-0.23 mmolN:mmolC according to Huntley and Nordhausen, 1995

a)	Units	Min	Max	Functions	Reference
C	mmol C	10^{-5}	Not fixed	State variable	Carlotti and Wolf, 1998
Protein	mmol C	4.75×10^{-6}	8.33×10^{-3}	State variable	Carlotti and Wolf, 1998
Lipid	mmol C	4.75×10^{-6}	Not fixed	State variable	Carlotti and Wolf, 1998
Shell	mmol C	5×10^{-7}	4.2×10^{-4}	State variable	Carlotti and Wolf, 1998
N	mmol N	1.2×10^{-6}	23% of C	State variable	Huntley and Nordhausen, 1995
b)					
N:C	mmol N : mmol C	0.12	0.23	Excretion	Huntley and Nordhausen, 1995

Tab. 3.3 – Stage independent a) stoichiometry and b) cellular ratios of chemicals

3.2.2 Processes

3.2.2.1 Molting

LERM-PS uses the Carlotti and Wolf (1998) model for copepod staged growth. An individual copepod can only be in one particular development stage at any time. As it grows and its protein pool reaches a threshold value, it molts and passes into the next stage (tab.3.4 and fig.3.7).

3.2.2.2 Ingestion

Ingestion rate (prey s^{-1}) is based on midgut capacity and depends on copepod filtration rate ($\text{cm}^3 \text{s}^{-1}$), prey concentration (prey cm^{-3}), feeding activity (wd) and maximum ingestion rate (prey s^{-1} , Eq.II.22-24)¹⁸. Filtration rate increases with size defined by prosome length. Feeding activity is determined by gut capacity (cm^3) and the fraction of time spent in feeding activity, which is a function of prey concentration. Maximum ingestion rate is limited by the handling time for prey.

¹⁸ Caparroy and Carlotti, 1996

Development stage	Stage description	LERM ID #	Protein threshold for molting (mmol C)	Prosome length (mm)	Frontal Surface Area cm ²	Body vol mm ³	Max swimming speed at 10C m/h
N3	Nauplius III	0	1.00×10 ⁻⁵	0.27	1.46×10 ⁻⁴	1.00×10 ⁻³	5.09
N4	Nauplius IV	1	1.70×10 ⁻⁵	0.32	1.70×10 ⁻⁴	1.64×10 ⁻³	5.93
N5	Nauplius V	2	2.50×10 ⁻⁵	0.36	1.94×10 ⁻⁴	2.50×10 ⁻³	6.77
N6	Nauplius VI	3	3.75×10 ⁻⁵	0.41	2.22×10 ⁻⁴	3.79×10 ⁻³	7.74
C1	Copepodite I	4	6.25×10 ⁻⁵	0.48	2.62×10 ⁻⁴	6.42×10 ⁻³	9.14
C2	Copepodite II	5	9.20×10 ⁻⁵	0.55	2.97×10 ⁻⁴	9.53×10 ⁻³	10.36
C3	Copepodite III	6	2.10×10 ⁻⁴	0.72	3.88×10 ⁻⁴	2.22×10 ⁻²	13.53
POW4	Pre-overwintering CIV	7	5.83×10 ⁻⁴	1.00	5.42×10 ⁻⁴	6.42×10 ⁻²	18.91
POW5	Pre-overwintering CV	8	1.25×10 ⁻³	1.29	6.95×10 ⁻⁴	0.14	24.24
OWD4	Overwintering descent CIV	9	5.83×10 ⁻⁴	1.00	5.42×10 ⁻⁴	6.42×10 ⁻²	18.91
OWD5	Overwintering descent CV	10	1.25×10 ⁻³	1.29	6.95×10 ⁻⁴	0.14	24.24
OW4	Overwintering CIV	11	5.83×10 ⁻⁴	1.00	5.42×10 ⁻⁴	6.42×10 ⁻²	18.91
OW5	Overwintering CV	12	1.25×10 ⁻³	1.29	6.95×10 ⁻⁴	0.14	24.24
OWA4	Overwintering ascent CIV	13	5.83×10 ⁻⁴	1.00	5.42×10 ⁻⁴	6.42×10 ⁻²	18.91
OWA5	Overwintering ascent CV	14	1.25×10 ⁻³	1.29	6.95×10 ⁻⁴	0.14	24.24
C4	Copepodite IV	15	5.83×10 ⁻⁴	1.00	5.42×10 ⁻⁴	6.42×10 ⁻²	18.91
C4OW	Copepodite IV after OW	16	5.83×10 ⁻⁴	1.00	5.42×10 ⁻⁴	6.42×10 ⁻²	18.91
C5	Copepodite V	17	1.25×10 ⁻³	1.29	6.95×10 ⁻⁴	0.14	24.24
C6	Copepodite VI	18	3.33×10 ⁻³	1.77	9.56×10 ⁻⁴	0.39	33.35
Ad	Adult	19	7.50×10 ⁻³	2.31	1.25×10 ⁻³	0.89	43.60
Ma	Mature	21	8.33×10 ⁻³	2.39	1.29×10 ⁻³	1.00	45.00
Se	Senescent	22		2.39	1.29×10 ⁻³	1.00	45.00
Nauplius	Nauplius	20					
P	Pellet	23					
D	Dead	24					

Tab. 3.4 – Copepod stages

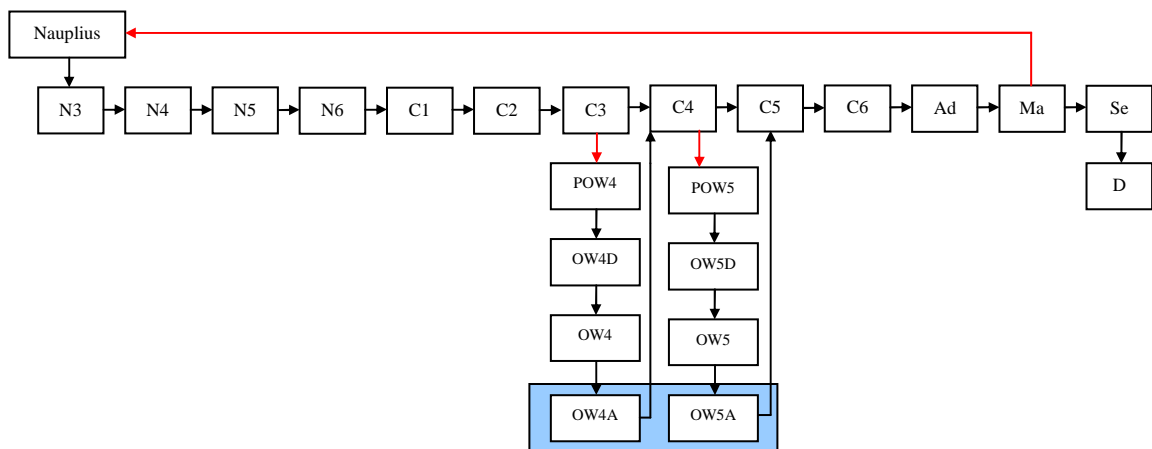


Fig. 3.7 – Stages implemented in a copepod. Red arrows indicate the creation of a new agent. OW4A and OW5A migrates to the surface waters after spending the whole winter as overwintering.

3.2.2.3 Gut processes

In the midgut of a copepod two main processes occur simultaneously on the ingested prey: gut transit and assimilation (fig. 3.8).

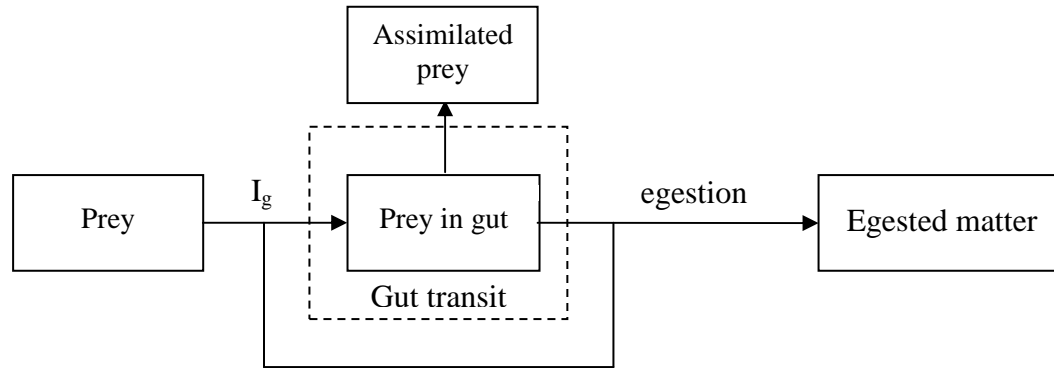


Fig. 3.8 – Copepod digestion. (Adapted from Caparroy and Carlotti, 1996)

The time that food is kept in the gut for digestion is inversely related to how full the gut is (Eq.II.33)¹⁹. It may vary from half hour, when the gut is full, to one hour, when it contains little food²⁰. The fuller the stomach, the quicker the clearance rate (eq.II.34). Gut passage time has a great impact on the assimilation of food. The residence time of food in the gut determines the amount of breakdown and assimilation of the larger insoluble macromolecules in cell walls and membranes. Assimilation efficiency is therefore a function of gut passage time (Eq.II.35-36)²¹. The ingested food that is not assimilated is egested as a faecal pellet.

3.2.2.4 Faecal pellets production

Unassimilated food is expelled as a faecal pellet (Eq.II.38)²². It is accumulated in the gut and expelled when its volume reaches a volume threshold (Eq.II.25)²³. The volume of a faecal pellet produced increases proportionally with copepod size (i.e. prosome length)²⁴. Pellet sinking rate is a function of its volume (Eq.II.26)²⁵.

¹⁹ Kjørboe and Tiselius, 1987

²⁰ Caparroy and Carlotti, 1996

²¹ Van den Bosch and Gabriel, 1994; Caparroy and Carlotti, 1996

²² Woods and Barkmann, 1994

²³ Caparroy and Carlotti, 1996

²⁴ Uye and Kaname, 1994

²⁵ Paffenhöfer and Knowles, 1979

3.2.2.5 Allocation of assimilated carbon

Assimilated carbon can be allocated either to storage, growth or carapace (fig. 3.9). A fixed proportion (5%) is allocated to production of carapace²⁶. The rest is allocated to lipids and proteins depending on the copepod development stage (App.II.2.3). Young copepods (Nauplius to C3) allocate it equally to lipids and proteins (the fraction allocated to lipids, $\gamma = 0.5$). Older copepods (C4 to Senescent) allocate it more to lipids ($\gamma = 0.7$)²⁷.

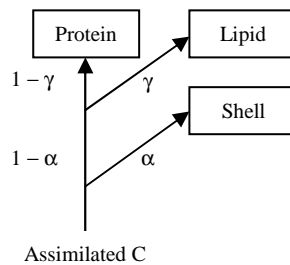


Fig. 3.9 - Dynamic allocation of assimilated C. α is the fraction of assimilated C allocated to carapace building and γ is the fraction allocated to lipid reserve.

Copepods preparing to overwinter (POW4, POW5, OWD4 and OWD5) allocate assimilate carbon exclusively to lipids²⁸.

3.2.2.6 Respiration

Copepods use lipids preferentially to cover metabolic costs. Lipids are more energy-rich than proteins and therefore more efficient in covering the metabolic costs²⁹. The physiological state of the copepod (i.e. lipids in their pool) determines the impact of respiration expressed in term of carbon. Starved individuals using proteins for respiration will consume more carbon compared to those with a lipid reserve. The metabolic rate of an animal is defined with respect to the following activities: basal metabolism, specific dynamic action (SDA), and activity metabolism (Eq.II.12). Basal metabolism is the carbon consumption rate for maintaining bodily functions only and is a function of the size (i.e. proteins in their pools) of the animal

²⁶ Vidal, 1980

²⁷ Fiksen and Carlotti, 1998

²⁸ Carlotti and Wolf, 1998

²⁹ Båmstedt, 1986

and its ambient temperature (Eq.II.15)³⁰. Specific Dynamic Action (SDA) is the katabolic cost associated with digestive processes (assimilation and gut clearance) and biomass formation. This is modelled as proportional to the ingestion rate (Eq.II.16)³¹. Activity metabolism is the carbon consumption rate³² due to swimming. It is calculated as the power expenditure of a copepod swimming at speed U , as a function of: seawater density, cephalothorax length of the copepod, the projected area of swimming copepod and the velocity of swimming (Eq.II.17-21)³³.

3.2.2.7 Excretion

Proteins and carapace have a fixed ratio of N:C, lipids are assumed nitrogen free³⁴. Nitrogen is excreted in the form of ammonia, whenever proteins are used to cover metabolic costs or when the maximum ratio of N:C is exceeded (Eq.II.39).

3.2.2.8 Maximum swimming speed

An adult copepod can swim vertically up to a speed of 45 m h^{-1} at a temperature of 10°C ³⁵. Maximum vertical swimming speed, m h^{-1} , is a function of the stage of development and temperature, $^\circ\text{C}$ (Table.3.4).

3.2.2.9 Diel migration

Copepods migrate dielily pursuing a target isolume³⁵. At daytime, a copepod swims towards a depth, at which irradiance is relatively low so that the risk of being eaten by visual predators is reduced (Eq.II.43-44). However, if starved, they target a less dim isolume, offsetting the higher risk of being predated against the benefits of grazing on the higher concentration of food available in shallower water. The degree of starvation is represented by its gut fullness. Gut fullness ranges from zero (starved) to one (satiated).

³⁰ Carlotti and Wolf, 1998

³¹ Kjørboe *et al.*, 1985; Fiksen and Carlotti, 1998; Carlotti and Wolf, 1998

³² The equation calculates the power expenditure of swimming at speed U (J s^{-1}). This is converted to oxygen consumption using the oxycaloric coefficient ($20.3 \text{ kJ l O}_2^{-1}$ according to Ikeda *et al.*, 2000) and to carbon consumption as a function of the respiratory quotient of lipids or proteins (Parsons *et al.*, 1984)

³³ Caparroy and Carlotti, 1996

³⁴ Carlotti and Wolf, 1998

³⁵ Woods and Barkmann, 1994

3.2.2.10 Foraging

During the night copepods migrate to the surface to feed (Eq.II.45). As they swim upwards, they pass through a number of layers with varying concentration of prey. Their ingestion rate in each layer is a function of the time spent in that layer and the concentration of prey encountered³⁶. If, as they swim, the concentration of encountered prey decreases, copepods reverse the direction of swimming in order to optimise feeding.

3.2.2.11 Over-wintering

At the moment of molting to C4 or to C5 (i.e. at the timestep when their protein pool reaches the threshold for molting to the next stage), a fraction of individuals enter a pre-overwintering stage (POW4 or POW5), the rest molt to the next development stage (C4 or C5). The probability that an individual enters the pre-overwintering stage is 30% before the 1st August and 50% after (fig.3.10). During pre-overwintering all the assimilated food is allocated to lipid storage³⁷.

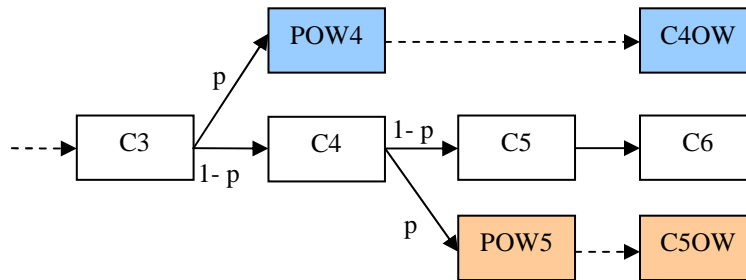


Fig. 3.10 – Copepod pre-overwintering. P represents the probability of an individual entering pre-overwintering. Before the 1st Aug $p = 0.3$, after $p = 0.5$. Each colour represents an agent.

When the lipid reserve is full, copepods swim down to a depth below 375 m and over-winter there until mid-March. During overwintering, the animal does not swim or feed. Basal metabolism is reduced to 20% and fueled preferentially by lipids or, if depleted, from the structural proteins. At the end of the overwintering period copepods migrate back to the surface to feed.

³⁶ Wood and Barkmann, 1994

³⁷ Carlotti and Wolf, 1998

3.2.2.12 Reproduction

Once a copepod has reached the adult stage, it enters a period of egg production (20 days³⁸). The number of eggs produced depends on how well it fed during that period. After 20 days, the copepod is ready to lay eggs. If the lipid pool is larger than the ingested matter during this period, then egg production is limited by proteins, otherwise it is limited by lipids³⁹.

The egg stage is not modeled explicitly, but an instantaneous mortality of 90% is assumed³⁸. The survivors are initialized in stage N3, each with a prescribed amount of carbon and nitrogen.

3.2.2.13 Mortality

Other than by being ingested by a top predator, a copepod may die of natural causes: starvation or senescence. A copepod is assumed to die of starvation when its carbon pool gets below half of its maximum achieved carbon pool (Eq.II.47). During twenty days following reproduction, the spawning population is assumed to die of senescence at a randomly chosen date (Eq.II.48)³⁸. Dead copepod sinking rate is a function of its surface area .

3.3 Top predators

Trophic closure to LERM-PS is provided by two top predators that feed on copepods: one, based on squid, feeds visually, the other feeds as a function of prey abundance.

Top predators are declared in the model as a special type of functional group⁴⁰. They differ from all other functional groups in the fact that their demography is set in the scenario using a series of exogenous equations, rather than by emerging from the Virtual Ecosystem. The only interaction between predator and prey is through ingestion which is unilateral: top predators feed on prey species, but are not affected by any biological feedback from the virtual ecosystem (fig.3.11).

³⁸ Woods and Barkmann, 1994

³⁹ Carlotti and Wolf, 1998

⁴⁰ Woods, 2005

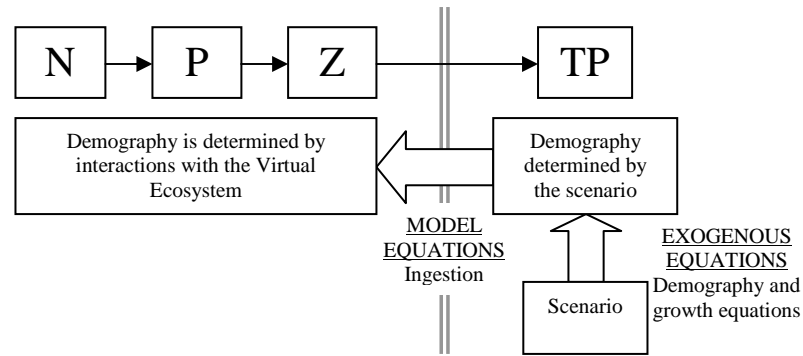


Fig. 3.11 – Top predators demography and interaction with prey. N:Nutrients, P:Phytoplankton, Z:Zooplankton, and TP:Top Predators.

3.3.1 Visual top predators

For the Azores scenario, LERM-PS visual top predators represent a population of squid *Loligo forbesii*. It is an abundant species at the Azores and it is known to graze on copepods during the early phase of its life.

3.3.1.1 Exogenous equations (Top predator demography)

Exogenous equations defined in the scenario describe the demographic state of the predator population, in particular, its growth rate, its annual distribution and its vertical distribution.

Predator growth

Laboratory experiments on *Loligo forbesii* estimated daily growth rates of 7% of its mantle length (ML) in its first months of life, when it feeds on copepods. The maximum ML at which predator feeds on copepods is assumed to be 40 mm⁴¹. It takes about 100 days for a young squid, growing at a daily rate of 7% of its mantle length, to switch diet (Eq.IV.1).

⁴¹ During the first month since hatching squid feed on planktonic organisms, mainly copepods. When squid reach a size of 4 cm, it switches to a diet made of euphausiids and arrow worms (Vovk and Khvichiya, 1980; Vovk, 1985).

Predator annual distribution

Squid eggs all hatch simultaneously on the 1st April, they feed on copepods until mid-July, before switching diet. The mortality rate of predator population is assumed to follow a negative exponential function of the time of the year (Eq.IV.2). Every year the concentration of predators is set back to its initial value.

Vertical distribution of predators

The concentration of visual top predators is assumed to be homogeneous in the top 100m.

3.3.1.1 Endogenous equations

Ingestion

The maximum rate of ingestion is modeled as the maximum daily percentage of body weight that can be consumed (Eq.IV.5)⁴². Maximum ingestion rate is therefore a function of the weight of the predator and the weight of the prey. Ingestion rate depends on the concentration and visibility of prey and ambient temperature (Eq.IV.6). The visibility of the prey is determined by the ambient irradiance and the surface area of the prey (fig.3.12). Ingestion rate can never exceed maximum ingestion rate.

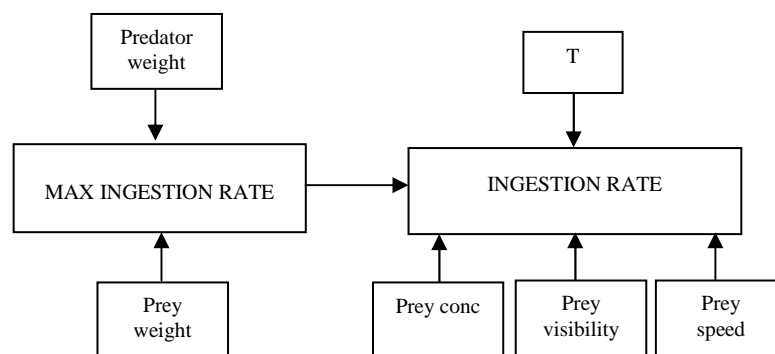


Fig. 3.12 – Predator ingestion rate, internal and external controlling factors

⁴² Koueta and Boucaud-Camou, 2001

Faecal pellets

A pellet, containing all the nitrogen and carbon ingested, is released every timestep. As it sinks at a constant speed of 10 m h^{-1} , it is remineralised by an implicit bacteria population. Pellets remineralization is modelled as temperature dependent⁴³.

3.3.2 Basal top predators

3.3.2.1 Exogenous equations (Top predator demography)

Background top predators are assumed to maintain a constant size (40 mm). They are present all year at a constant concentration (3000 m^{-2}), and they are homogeneously distributed in the top 100m.

3.3.2.2 Endogenous equations

The maximum rate of ingestion for background predators is based on the equation used for visual predators. It is calculated as the maximum daily percentage of body weight that can be consumed. As the weight of the predator is kept constant, maximum ingestion rate depends on the weight of the prey (Eq.IV.7). The bigger the prey the less can be ingested by the predator, and vice versa. Ingestion rate is a function of the ambient concentration of prey and temperature (fig.3.13, Eq.IV.9). Ingestion rate can never exceed maximum ingestion rate.

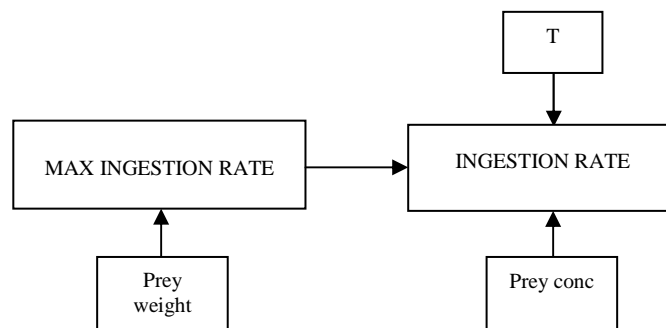


Fig. 3.13 – Predator ingestion rate, internal and external controlling factors

Faecal pellets are produced, sink and get remineralised in exactly the same way as for visual top predators.

⁴³ Heath et al, 1997

3.4 Particle management

As described in Chapter 2 on the Lagrangian Ensemble metamodel, each particle represents a collection of identical individuals sharing the same life-history. Each particle has a variable depth and a demographic variable describing the number of individuals carried in the agent's sub-population.

3.4.1 Phytoplankton

Diatom particles are initialised in the living stage with a sub-population size of 50,000 individuals. There are twenty particles per metre between 0-200 m, for a total of 4,000 particles. The number of particles per layer is kept between twenty and forty. If the number of particles in the living stage falls below twenty diatoms the largest particles are split, while if the number of particles exceeds forty then the smallest particles get merged. Dead diatom particles are merged so that there can only be one particle per metre. When a diatom cell divides, the number of individuals within the sub-population doubles, but no new particle is created.

3.4.2 Zooplankton

Copepod particles are initialised in overwintering stages (OW4 and OW5) each with twenty copepods in its subpopulation. There are 10 particles per metre between 375-405 m, for a total of 300 particles for each stage. Contrary to what happens with diatoms, copepod particles are never split. They are merged once a year when they enter overwintering for reasons that will become clear below. Dead copepods and pellet particles are merged so that there can only be one particle of each per metre. New particles are created in the case of faecal pellets egestion, reproduction and pre-overwintering. A faecal pellet is released as a new agent, but it is immediately merged with the other pellets in the same layer.

In the case of reproduction, the mother particle spawns a new particle containing the offspring. The overall number of particles is doubled for a period of 20 days, during which the mothers die of senescence (fig.3.14).

At the moment of molting to C4 or C5 (i.e. at the timestep when their protein pool reaches the threshold for molting to the next stage), a fraction of individuals are

transferred to a new agent in the pre-overwintering stage (POW4 or POW5), the rest molts to the next development stage (C4 or C5) and eventually die (fig.3.14). The creation of new particles for POW4 and POW5 causes an annual doubling of copepod particles in the water column (fig.3.14, years 2 and 3). In order to avoid the explosion of copepod agents, LERM-PS merges copepod particles as they enter overwintering (OW4 and OW5). This is a time where individuals are very similar biochemically (i.e. they have the same pool of lipids and proteins) and the least active (i.e. they only respire).

In LERM-PS the threshold for merging of OW4 and OW5 is 300 agents. This ensures that at the start of each year the virtual ecosystem contains no more than 600 agents: 300 in OW4 and 300 in OW5.

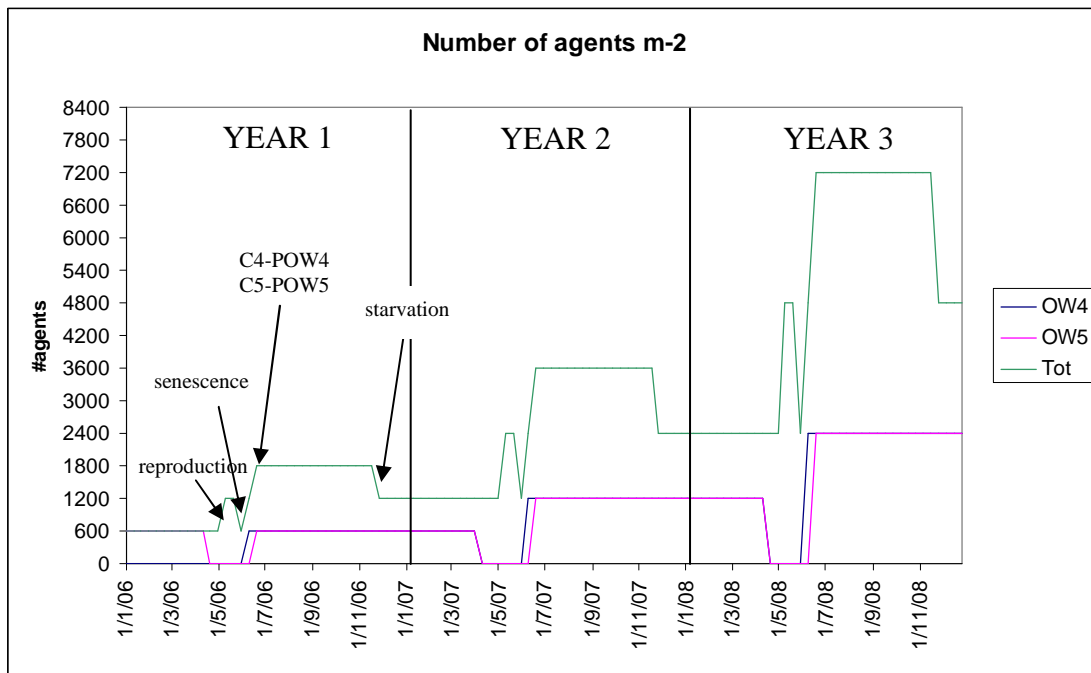


Fig. 3.14 – Copepod particles doubling problem.

3.4.3 Top predators

Both top predators are initialised in the existence stage, with a subpopulation of 30 individuals per particle. There is one particle per metre between 0-100 m, for a total of 100 particles. Particles in the existence stage are never split or merged. Faecal pellets, released as a new agent, are immediately merged with the other pellets in the same layer.

CHAPTER 4 - The Lagrangian Ensemble Recruitment Model with Explicit Squid (LERM-ES)

LERM-ES extends LERM-PS (Chapter 3) by including an explicit population of squid (fig. 4.1). Two top predators are included in the model to provide trophic closure: (1) a background top predator, as before, feeding on zooplankton, and (2) a visual top predator feeding on squid. All species but squid and visual top predators are unchanged from LERM-PS.

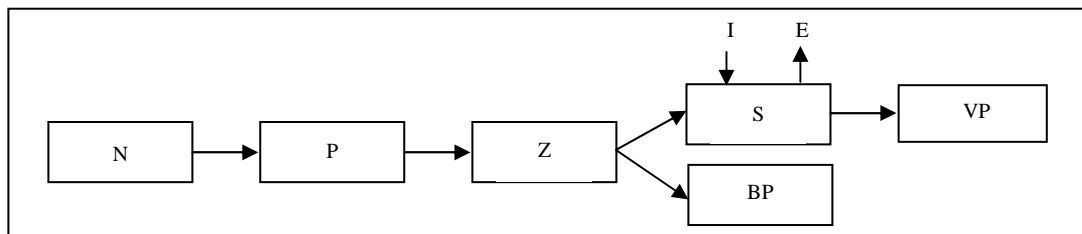


Fig.4.1 – LERM-ES: N: Nutrients , P: Phytoplankton, Z: Zooplankton, S: Squid paralarvae, VP: visual predators, BP: background predators, I: immigrant squids; E: emigrant squids

Unlike the copepods, which exist in the virtual mesocosm generation after generation, squid are a transient population in the virtual mesocosm. Immigration (spawning) is handled as an exogenous event in which eggs are injected in the water (cfr.4.1.2.1). Emigration (recruitment) represents the metamorphosis to a stage that is no longer tracked in the virtual ecosystem (cfr.4.1.2.4.7). In this version of LERM-ES, there is no link between the demography of emigrants and immigrants.

4.1 Squid

The species of choice is squid. Its fishery is growing in importance and landings as the abundance of fish stocks has been reducing through over-fishing (Caddy and Rodhouse, 1998). Due to their short life-cycle (one year) and their semelparity (death after a single reproduction), the exploited stock is composed almost entirely of recently recruited animals of a similar age (Agnew *et al.*, 2002). So, knowledge of recruitment variability is highly desirable for managing purposes.

As squid populations are not characterized by the presence of several year classes living contemporaneously, squid provides a perfect candidate for testing fisheries

recruitment hypotheses (Rodhouse, 2001). The availability of an extensive dataset of the biology and fisheries of this species allows for comparison between the emergent properties of the model and observations.

The explicit squid is based on *Loligo opalescens* (California market squid) physiology and behaviour, which have been studied extensively. This is a small squid (mantle length ML up to 160mm) of the family of Loliginidae. It is found in the Eastern Pacific Ocean from Baja Mexico to Alaska at latitudes similar to that of the Azores site (fig. 4.2). It lives less than one year. Its fishery is of great economic importance: since 1993 it has become the first fishery in California with landings of 118,000 tons and \$41 million in 2000.

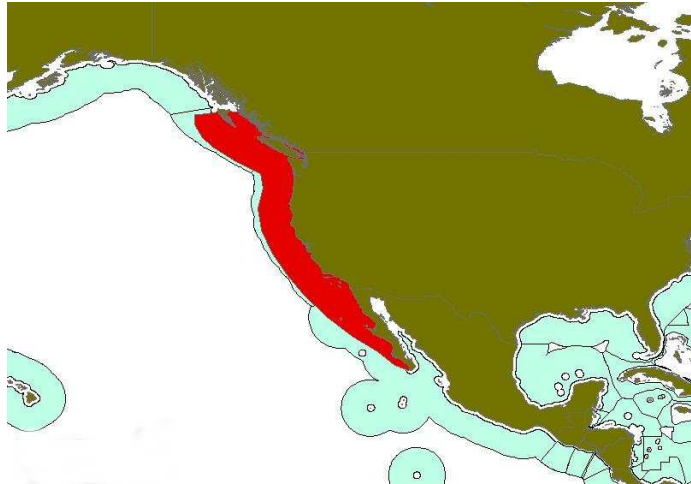


Fig. 4.2 – *Loligo opalescens* geographical distribution (Source: FAO, 1984)

4.1.1 Stoichiometry

Each squid has a pool for each of the chemicals present in copepods. Carbon ingested is allocated to proteins and lipids. In LERM-ES squids have a 15% DW maximum lipids content¹. Body nitrogen is coupled to proteins through a fixed ratio (0.15 mmolN mmolC⁻¹).

¹ Squid has an uncommon stoichiometry. Its wet weight, WW, is made up by 18% protein, 79% water with just 3% left for all other biochemical compounds needed for life. In contrast to fishes, cephalopods contain 20% more protein, 80% less ash, 50-100% less lipid and 50-100% less carbohydrate (Bouchaud and Galois, 1990; Lee, 1994). Lee (1994) reported lipid contents of cephalopods ranging between 0.34-3.4% WW. Bouchaud and Galois (1990) in laboratory experiments on *Sepia officinalis* found that hatchlings' lipid content was close to 15% Dry Weight, DW, (14.5-15.9%DW) independently of temperature and duration of development. Assuming a body water percentage of 75-80%, the total lipids content is 3-4 % WW.

a)	Units	Min	Max	Functions
C	mmol C	0.05	0.70	State variable
Protein, C_{NN}	mmol C	0.05	0.70	State variable
Lipid, C_N	mmol C	0	0.09	State variable
N	mmol N	7.5×10^{-3}	0.10	State variable

b)				
N:C	mmol N mmol C ⁻¹	0.13	0.15	Excretion

Tab. 4.1 – a) Stoichiometry and b) cellular ratios of chemicals

4.1.2 Stages

Unlike copepods, whose growth is staged for molting of the carapace, squid body growth is continuous and unstaged. However, in order to allow for size specific predation by the visual top predator (tab.4.2), squid paralarvae have been allocated to size classes S1 to S7, based on their mantle length (ML). A small paralarvae is less visible to visual top predators than a large one, but is slower in its escape (cfr. 4.2.2.1). S1 represents the squid at hatching, S7 represents the recruited squid, which leave the virtual mesocosm. A squid can only be in one particular development stage at any time. As it grows and its ML increases by one millimeter it moves into the next stage (fig.4.2).

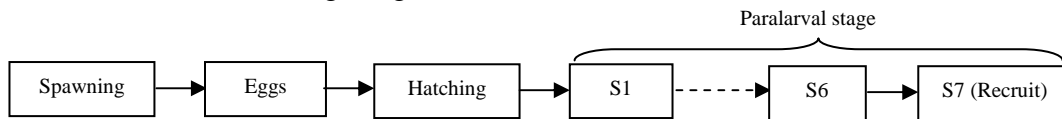


Fig.4.2 – Squid stages

STAGE	Max ML mm	MW mm	DW mgC	DW mmol C	S m ²	Ave DW mmol C	Ave S m ²	Max speed m h ⁻¹
S1	~ 2.80	1.84	0.69	0.06	2.7×10^{-6}	0.06	2.8×10^{-6}	11.3
	2.99	1.92	0.81	0.07	2.9×10^{-6}			
S2	3.00	1.92	0.81	0.07	2.9×10^{-6}	0.10	3.5×10^{-6}	14.3
	3.99	2.30	1.60	0.13	4.1×10^{-6}			
S3	4.00	2.30	1.61	0.13	4.1×10^{-6}	0.18	4.9×10^{-6}	19.8
	4.99	2.68	2.72	0.23	5.6×10^{-6}			
S4	5.00	2.68	2.73	0.23	5.6×10^{-6}	0.29	6.5×10^{-6}	26.3
	5.99	3.06	4.19	0.35	7.3×10^{-6}			
S5	6.00	3.06	4.21	0.35	7.4×10^{-6}	0.43	8.3×10^{-6}	33.7
	6.99	3.44	6.05	0.50	9.3×10^{-6}			
S6	7.00	3.44	6.07	0.51	9.3×10^{-6}	0.60	1.0×10^{-5}	42.0
	7.99	3.82	8.30	0.69	1.1×10^{-5}			
S7	≥ 8.00	-	-	-	-	-	-	-

Tab. 4.2 – Squid stages. ML: mantle length, MW: mantle width, DW: dry weight, S: frontal surface area, AVE DW: stage specific dry weight, AVE S: stage specific surface area

4.1.2.1 Spawning

An exogenous population of mature squid lays a batch of 300 eggs m⁻² at 50 m every year at a prescribed date set in the experiment (10th April in preliminary tests)². Spawners exit the mesocosm immediately after laying the eggs.



Fig. 4.3 – *L. opalescens* egg mass (www.elasmodiver.com)

4.1.2.2 Egg stage

4.1.2.2.1 Embryogenesis

In nature the duration of cephalopod embryogenesis depends mainly on egg size and ambient temperature³. LERM-ES assumes that all eggs have the same size, so that temperature is the only factor affecting the duration of embryogenesis ((Eq.III.10). Embryonic development is estimated using daily accumulated temperature, DAT, as it is common practice for loliginid species⁴. DAT is accumulated from the time eggs are laid. Eggs hatch when DAT exceeds 600°C days⁵. Hatching within an egg mass occurs within a period of 4-6 days⁶. The intra-population variability in hatching date is modelled as a variation of the initial DAT and justified as a consequence of the variation in egg size, which in the current version of the model is not modeled explicitly.

² In Monterey Bay (latitude ~37°N) *L. opalescens* spawn from April to November (Zeidberg and Hamner, 2002).

³ Laptikhovsky, 1991.

⁴ Baron, 2000.

⁵ For *L. opalescens* embryonic development requires ~ 30-40 days at 15°C (Yang *et al.*, 1986).

⁶ In *L. opalescens* and *L. forbesi*, the period from the first paralarva hatching to the emergence of the last took 4-6 and 7 days, respectively (Yang *et al.*, 1986; Segawa *et al.*, 1988 From Arkhipkin and Middleton, 2003 pp 132).

4.1.2.3 Hatching

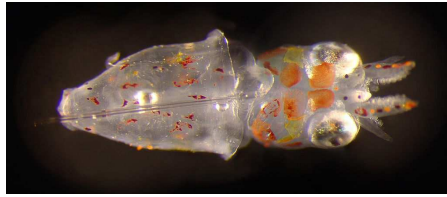


Fig. 4.4 - *Loligo opalescens* paralarva (www.flickr.com/photos/toddography/38447140)

Squid paralarvae hatch at night⁷, when visual predators are not feeding. Mean incubation temperature during embryogenesis controls the weight and volume of yolk reserves in the hatchlings of *L. opalescens*⁸. Regression equations are used to link incubation temperature to: size of hatchling (mantle length and width, frontal surface area, protein, lipid and nitrogen pools, Eg.III.11-19, yolk content and stoichiometric composition of hatchling (lipids and proteins). Independently of temperature, yolk weight is proportional to body weight (Eq.III.20)⁹. Egg yolk lipid represents 15% wet weight of the paralarva at hatching¹⁰. Body nitrogen is coupled to protein through a fixed proportion (15%).

4.1.2.4 Paralarva stages

4.1.2.4.1 Yolk absorption rate

During the very early post-embryonic life, embryonic and post-embryonic nutrition overlap¹¹. Until depleted, the yolk provides the energy to fuel metabolism (Eq.III.25-26). The caloric value of yolk in *L. opalescens* is 1.71 Kcal/WW¹².

4.1.2.4.2 Motion

Paralarvae are inefficient swimmers which cannot usefully change their local environment by swimming horizontally. However they are capable of changing it by swimming vertically¹³.

⁷ Fields, 1965.

⁸ Squid eggs incubated at lower mean temperatures hatched larvae, which were larger, heavier and have more yolk than those incubated at higher mean temperature (Vidal *et al.*, 2002).

⁹ Vidal *et al.*, 2002.

¹⁰ Bouchaud and Galois, 1990; Vidal *et al.*, 2002

¹¹ Vidal *et al.*, 2002

¹² Giese, 1969.

¹³ Zeidberg and Hamner, 2002

Swimming speed

Squid swimming speed is proportional to its mantle length (Eq.III.21)¹⁴. They migrate in the virtual mesocosm at a routine migration speed (tab. 4.2), which is about 40 % less than the maximum jet speed used to escape attacks¹⁵.

Diel migration

Diel migration is modelled using target isolumines, as for copepods (chapter 3). During the day a squid keeps to a depth at which irradiance is low enough to reduce the risk of being eaten (Eq.III.23)¹⁶. This depth is a function of squid visibility. Squid visibility is determined by its size and ambient irradiance. During night-time squid ascend the water column swimming at its routine speed.

Foraging

Prey attack is elicited by visual stimuli¹⁷. The impossibility of implementing lunar phase in the current version of VEW meant that during night-time squid are unable to detect the prey and feed. Predator-prey encounter occurs during the day (from dawn until dusk) as they both migrate in the virtual mesocosm in search of their target isolume (Eq.III.23).

4.1.2.4.3 Ingestion

Ingestion is based on gut capacity as for copepods (chapter 3).

Size specific ingestion

Post-hatching squids feed on all stages of copepods, except for pellets, dead and over-wintering copepods¹⁸.

¹⁴ Zeidberg, 2004

¹⁵ Zeidberg, 2004

¹⁶ In situ observations in Monterey Bay on the distribution of *L. opalescens* paralarvae revealed that diel migration starts immediately after hatching (Zeidberg and Hamner, 2002). Paralarvae are vertically distributed above 80m, with the maximum concentration occurring at 15 m during the night and 30 m during the day (Okutani and McGowan, 1969; Zeidberg and Hamner, 2002).

¹⁷ Boletzky, 1974.

¹⁸ The diet during the post-embryonic phase is restricted to specific prey. The prey size changes as the individual grows. Very young planktonic cephalopods attack prey of approximately their own size (Boletzky, 1974b) and are only successful in capturing relatively slow prey such as crustacean

Maximum ingestion rate

Max ingestion rate is a function of the volume of gut not yet filled with prey (i.e. gut volume minus the volume of food in gut and not yet ingested (Eq.III.28)¹⁹.

Efficiency of prey capture

Mastery of copepod capture is a skill that is acquired in an experience-dependent manner early in post-hatching life and is a function of ML²⁰. The velocity of the prey is another factor affecting the efficiency of capture, in relation to the swiftness of the predator. Hunting efficiency is modeled as a function of the ratio of squid ML and the stage-specific copepod maximum swimming speed (Eq.III.27).

Ingestion rate

Ingestion rate is a function of prey visibility (size and ambient irradiance), predator hunting efficiency, prey stage specific speed of escape, prey concentration²¹, squid gut volume and fullness (Eq.III.29-33).

4.1.2.4.4 Gut processes

Gut volume

Gut volume increases proportionally to mantle length and so does its feeding potential (Eq.III.46).

Gut content

Gut content represents the volume of prey in the gut. It increases by feeding and decreases by digestion and egestion (Eq.III.47-48). Copepod carapace is discarded²².

larvae and copepods (Boletzky, 1974a). *Loligo opalescens* reared in laboratory during the first 60 days after hatching selected copepods less than 4mm in length (Yang *et al.*, 1983). As maximum prosome length is 2.4 mm, squid are capable of feeding on all stages of copepod.

¹⁹ A regulation of the quantity of food eaten is present in all cephalopods. They all reject any excess food. It is impossible, by offering food, to overfeed experimentally a cephalopod (Koueta and Boucaud-Camou, 2001).

²⁰ Mastery of copepod capture develops progressively, culminating for *L. opalescens* by approximately 40 days post-hatching in adult-like prey capture behaviour (Chen *et al.*, 1996). Absolute attack speed increases in proportion to ML (Chen *et al.*, 1996)

²¹ There is no clear evidence of a relationship between prey density and survival of *L. opalescens*. One experiment compared the survival rate of *L. opalescens* raised with twice as much food per squid than another experiment, and survival rate was not significantly different (Yang *et al.*, 1986).

However, another study reported that increasing prey density increases the incidence of encounter between predator and prey (Vidal *et al.*, 2002). In the latter experiments prey density never fell below 50 prey l⁻¹ (50 × 10⁶ prey m⁻³).

Digestion

Digestion duration is highly influenced by temperature²³. Digestion rate doubles with an increase of 10°C over a reference temperature²⁴. Rate of digestion is assumed to decrease exponentially with time²⁵. The rate of digestion (volume of food, protein, lipid digested per hour) is a function of temperature, time since last fed and size of meal (fig. 4.5, Eq.III.35-36).

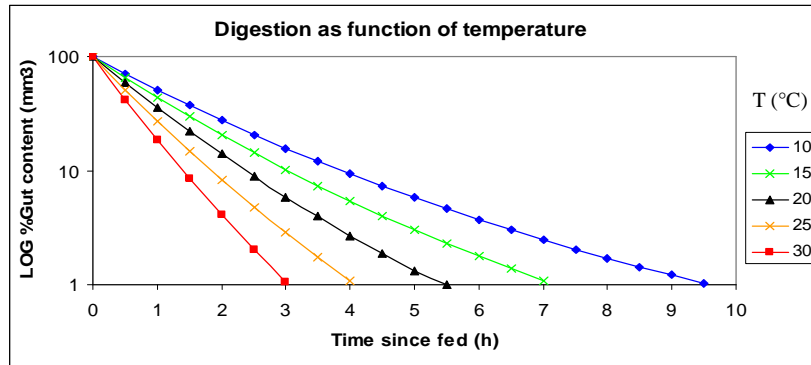


Fig.4.5 – Digestion rate as a function of temperature and time since feeding²⁶

Assimilation

Assimilation rate for lipid and proteins is a fixed ratio of the digested rate of each (Eq.III.37-39). Assimilation efficiency for lipids (50%) is much lower than for protein (80-95%)²⁷. Unassimilated lipids and proteins are egested as faecal pellets (Eq.III.41-43).

²² Young squid are capable of removing exoskeletons crustaceans prior to ingestion (Vecchione, 1999; Kasugai, 2001).

²³ The total time necessary to digest a meal varies from one species of cephalopods to the other, and within the same species it is strongly influenced by temperature (Boucaud Camou and Boucher Rodoni, 1983).

²⁴ The only study on the effect of temperature on digestion duration was carried out for the octopus *Eledone cirrhosa* (Boucher-Rodoni, 1973). The digestion lasted 15 hours at 20°C, 20 hours at 15°C and 30 hours at 10°C (Boucher-Rodoni, 1973).

²⁵ The rate of digestion is very high at the beginning and then slows down gradually (Wallace *et al.*, 1981). The rate of food digested represents a fairly constant percentage of the quantity ingested and decreases with time after feeding (Boucher-Rodoni, 1975).

²⁶ Comparable results of digestion time with Karpov and Cailliet, 1978, in which *L. opalescens* completes digestion of a meal digestion at 18°C in about six hours.

²⁷ O'Dor *et al.*, 1984; Lee 1994.

4.1.2.4.5 Respiration

Respiration is a heterogeneous process, whose separate components vary independently²⁸. Respiration rate (Eq.III.50), expressed in calories per hour, is the sum of the costs associated with maintenance (basal metabolism), new tissues production (Specific Dynamic Action, SDA) and movement. Basal respiration is a function of the size of the squid and temperature (Eq.III.51)²⁹. SDA is proportional to the energy of lipid and protein assimilated (Eq.III.52)³⁰. Swimming cost is a function of the animal size, swimming speed and water density (Eq.III.53-57)³¹.

4.1.2.4.6 Energetics

During the first few days after hatching metabolic costs are covered by the energy provided by the yolk (Eq.III.25-26)³². When the yolk sac is completely exhausted, lipids are used preferentially to cover metabolic costs over proteins (Eq.III.58-603)³³.

4.1.2.4.7 Recruitment

Recruitment occurs when a paralarva reaches a ML of 8 mm³⁴. It is then assumed to switch diet and exit the virtual mesocosm.

4.1.2.4.8 Starvation

A squid is assumed to die of starvation if its daily feeding rate was below 10% body weight for 3 days³⁵ or if its carbon pool falls below three quarters of the maximum obtained carbon pool (App.III.5.10).

²⁸ Wells and Clarke, 1996

²⁹ O'Dor *et al.*, 1986

³⁰ Perry, 1983

³¹ O'Dor *et al.*, 1986

³² Bouchaud and Galois, 1990; Vidal *et al.*, 2002.

³³ Wells and Clarke, 1996.

³⁴ For *L. opalescens*, the mastery of copepod capture develops progressively, culminating by approximately 40 days post-hatching in adult-like prey capture behaviour.(Chen *et al.*, 1996). Different studies reported different ML for *L. opalescens* reared in tanks forty days after hatching: 6mm at 17-18°C (Chen *et al.*, 1996), 8 mm at 15-17°C (Hurley, 1976) and 10 mm at 15°C (Yang *et al.*, 1986).

³⁵ LaRoe, 1971.

4.1.2.4.9 Excretion

Nitrogen is excreted in the form of ammonia, whenever proteins are used to cover metabolic costs or when the ratio of nitrogen to protein is exceeded (Eq.III.44-45).

4.1.2.4.10 Egestion

Unassimilated food is expelled as a faecal pellet (Eq.III.41-43). In absence of information, the pellets are assumed to sink at a constant rate of ten metres per hour.

4.2 Visual top predator

LERM-ES visual top predators represent a population of larger *Loligo forbesii*.

4.2.1 Exogenous equations

Loligo forbesii juveniles (15 mm ML) grow at a rate of 2% of its mantle length (ML) and feed on the explicit squid population until they reach 40 mm ML (Eq.IV.1).

They are present from the 1st April until they reach 40 mm ML (~1st August). The mortality rate of the predator population is assumed to follow a negative exponential function of the time of the year (Eq.IV.2). Every year the concentration of predators is set back to its initial value. The concentration of these visual top predators is assumed to be homogeneous in the top 100m.

4.2.2 Endogenous equations

Ingestion

The maximum rate of ingestion is modelled as the maximum daily percentage of body weight that can be consumed (Eq.IV.5). Maximum ingestion rate is therefore a function of the weight of the predator and the weight of the prey. Ingestion rate depends on the concentration and visibility of prey and ambient temperature (Eq.IV.6) The visibility of the prey is determined by the ambient irradiance and the surface area of the prey (fig.4.6). Ingestion rate can never exceed maximum ingestion rate.

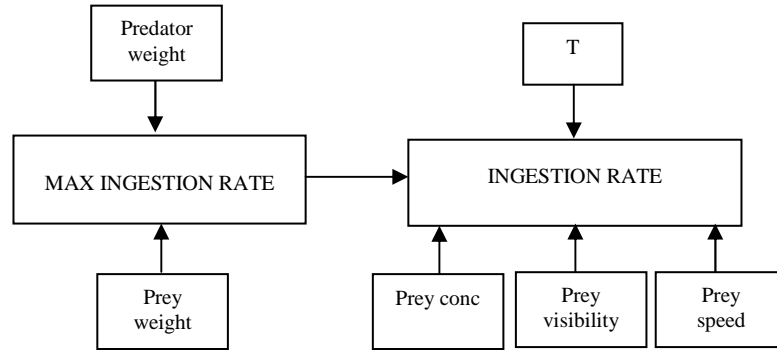


Fig. 4.6 – Predator ingestion rate, internal and external controlling factors

Faecal pellets

A pellet, containing all the nitrogen and carbon ingested, is released every timestep. As it sinks at a constant speed of 10 mh^{-1} , it is remineralised by an implicit bacteria population, following the rule for copepods in LERM-PS (chapter 3). The rate of pellets remineralisation is temperature dependent³⁶.

4.3 Particle management

4.3.1 Squid

Squid particles are initialised as spawning, whose immigration is being controlled exogenously as an event. Each particle represents a single spawner. As an initial scenario there are 300 particles in total at a depth of fifty metres. Particles representing paralarvae are never split or merged. Dead squid and pellet particles are merged so that there can only be one particle of each per metre. Particles that reach the S7 recruit stage leave the mesocosm.

4.3.2 Visual top predator

Visual top predators are initialised in the existence stage, with a subpopulation of 30 individuals per particle. There is one particle per metre between 0-100 m, for a total of 100 particles. Particles in the existence stage are never split or merged. Faecal pellets, released as a new agent, are immediately merged with the other pellets in the same layer.

³⁶ Heath et al, 1997

CHAPTER 5 – NUMERICAL EXPERIMENTS

The first group of the numerical experiments provides the pre-requisites for the project: to prove that LERM-ES achieves multi-year stability and that the Lagrangian Ensemble method can be used successfully to test Cushing’s match-mismatch hypothesis (fig.5.1). This is done in the following stages:

1. first, showing that after 15 years VEs converge to an attractor independently of initial conditions;
2. then, testing the ergodicity of the VE.

The successive series of experiments explore the sensitivity of recruitment to different exogenous scenarios, in particular changes to:

1. nutrients load,
2. abundance in competitors for food (basal predator),
3. predation,
4. spawning magnitude,
5. spawning time.

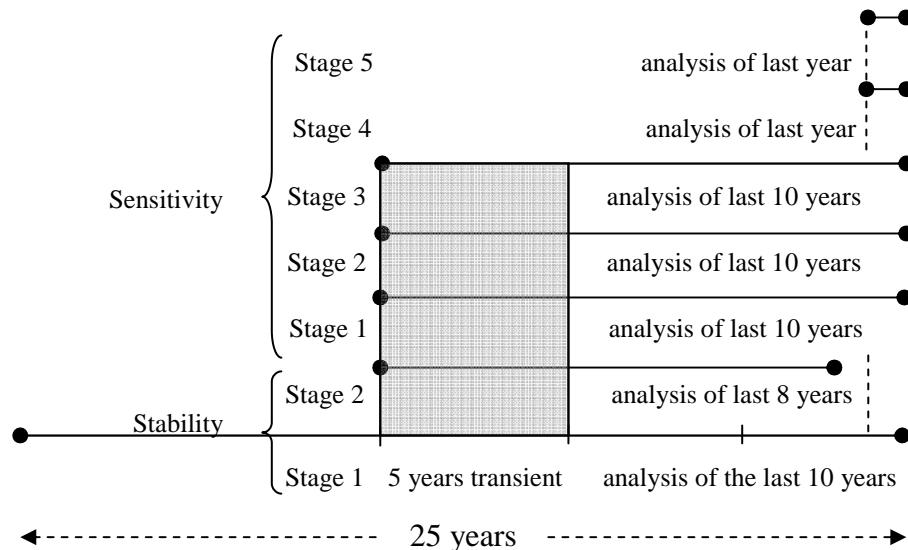


Fig.5.1 – Numerical experiments

Community

All numerical experiments in this thesis were performed using the LERM-ES community (fig.5.2).

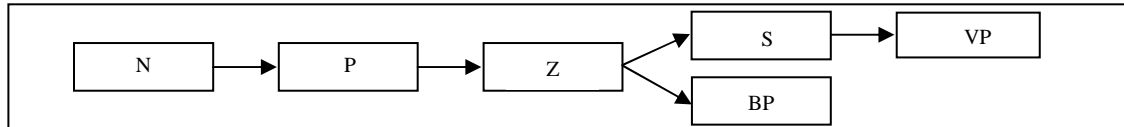


fig.5.2 – LERM-ES: N: Nutrients , P: Phytoplankton, Z: Zooplankton, S: Squid paralarvae, BP: background predators and VP: visual predators

5.1 Stability experiments

5.1.1 Stage 1 – Does LERM-ES at the Azores have a VE that is on attractor after 15 years?

This was tested by running LERM-ES for 25 years with five different initial concentrations of P and Z to see if the VEs adjust to a stable attractor that is independent of initial conditions¹.

Initialisation

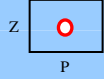
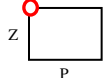
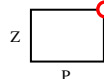
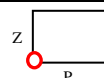
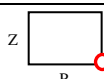
The initial chemical concentration for chemicals was derived from the NOAA Ocean Atlas (2002). Plankton populations were initialised using the Azores WB ecosystem attractor, tab.5.1 (Woods *et al.*, 2005). Squid initial population was composed of 300 adults, represented by 300 agents.

	In. state	Agents per layer	Ind. agent ⁻¹	Top depth	Bottom depth	Date
Diatom	Living	20	50000	0	200	1 Jan 2005 6am
Copepod	OW4	10	20	375	405	1 Jan 2005 6am
Squid	Spawning	2	1	200	350	Every 1 Jan 6am
VP	Existence	1	30	0	100	1 Jan 2005 6am
BP	Existence	1	30	0	100	1 Jan 2005 6am

Tab. 5.1 – Plankton initialization in the base run

¹ Previous work has proven that virtual ecosystems created under the aegis of the LE metamodel can be intrinsically stable (Woods *et al.*, 2005). A community is defined stable, or on attractor, if the inter-annual variation of species biomass or demography is lower than the demographic noise. This condition being reached after an initial transient period, and the population gets in balance with its ambient environment independently of initial conditions.

The test of stability is that the annual cycles of the plankton populations should be insensitive to initial conditions. This was tested by repeating the base run, with four different initial P and Z concentrations (tab.5.2).

Experiment	Initial P and Z vertically integrated concentration		
	P (ind m ⁻²)	Z (ind m ⁻²)	Symbol
BASE RUN	2×10^8	6,000	
P05Z2	1×10^8	12,000	
P2Z2	4×10^8	12,000	
P05Z05	1×10^8	3,000	
P2Z05	4×10^8	3,000	

Tab.5.2 – Numerical experiments to test for stability

Location

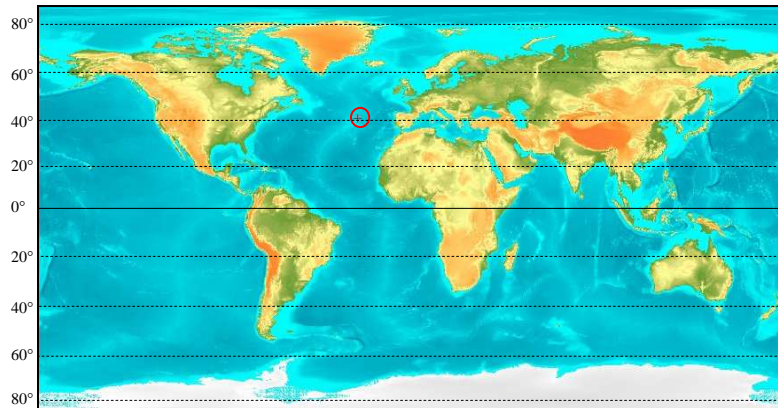


Fig. 5.3 – Experiments site

The virtual mesocosm is anchored at a fixed location north of the Azores, 41°N, 27°W (fig.5.3). This is a familiar location (Woods *et al.*, 2005), which was chosen as it lies close to the trans-Atlantic line, where the annual surface heat budget is zero (solar heating equals cooling to the atmosphere).

External forcing

The virtual ecosystem, VE, is driven by a stationary annual cycle of external forcing, derived from Bunker climatology (Isemer and Hasse, 1987).

Physics

The physical model comprised solar radiation in 25 wavebands, Morel optics and Woods-Barkmann mixed layer model (Woods and Barkmann, 1986).

Experiment

The experiment is initialised on the 1st of January and run for 25 years. On the 10th April of each year a batch of squid eggs are released in the virtual mesocosm by an exogenous population of spawning adults.

Logging

Analysis of the last 10 years of the simulation is performed on the ecosystem on attractor.

The variables logged are divided into 8 categories and listed in tab. 5.3:

1. Demography
 - a. Vertically integrated concentration of individuals
 - b. Mortality causes (predation or starvation)
2. Biomass
 - a. Vertically integrated biomass
 - b. Carbon transfer through the trophic chain (fig.5.4)
3. Number of agents
4. Physical environment
5. Chemical environment
6. VE variability on the 1st Jan
7. Timing of maximum D and C biomass and squid eggs hatching
8. Audit trails (life history of individuals)

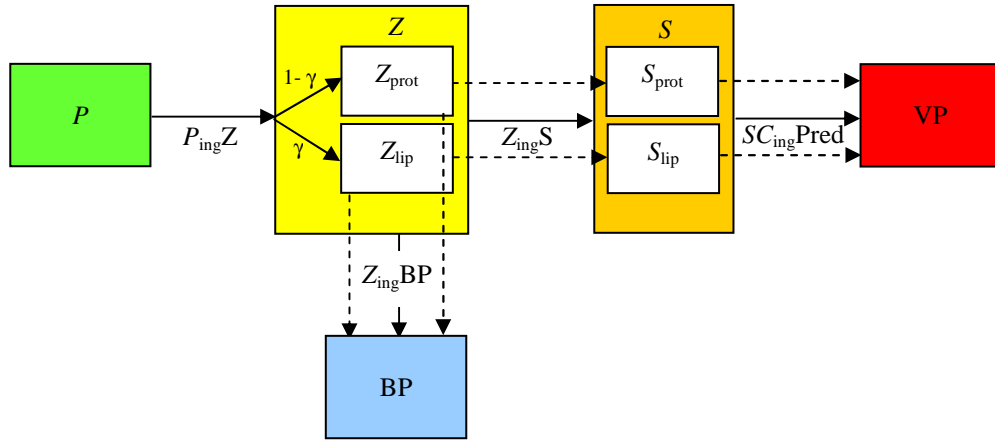


Fig. 5.4 – Carbon transfer along the trophic chain. P : diatom carbon biomass (mmol C m^{-2}), $P_{\text{ing}Z}$: transfer of diatom carbon to copepods; γ : copepod stage-specific allocation of ingested carbon to lipid; Z : copepod carbon biomass (mmolC m^{-2}); Z_{prot} : copepod protein biomass (mmolC m^{-2}); Z_{lip} : copepod lipid biomass (mmolC m^{-2}); $Z_{\text{ing}S}$ and $Z_{\text{ing}BP}$: transfer of copepod carbon to squid and BP respectively; S : squid carbon biomass (mmolC m^{-2}); S_{prot} : squid protein biomass (mmolC m^{-2}); S_{lip} : squid lipid biomass (mmolC m^{-2}); $S_{\text{ing}Pred}$: transfer of squid carbon to VP. BP: background top predator; VP: visual top predator. Dotted lines represent the relative amount of lipid and protein transfer.

	Variables	units	Analysis	
			1 y	10 y
1a	P, Z, S, R	ind m^{-2}	*	*
1b	$P_{\text{ing}}, P_{\text{starve}}, Z_{\text{ing}S}, Z_{\text{ing}BP}, Z_{\text{starve}}, S_{\text{ing}Pred}, S_{\text{starve}}$	$\text{ind m}^{-2} \text{ts}^{-1}$	*	*
2a	$P, Z, Z_{\text{prot}}, Z_{\text{lip}}, S, S_{\text{prot}}, S_{\text{lip}}$	mmol C m^{-2}	*	*
2b	$P_{\text{ing}Z}, Z_{\text{ing}S}, Z_{\text{prot-ing}S}, Z_{\text{lip-ing}S}, Z_{\text{ing}BP}, Z_{\text{prot-ing}BP}, Z_{\text{lip-ing}BP}, S_{\text{ing}VP}, S_{\text{prot-ing}Pred}, S_{\text{lip-ing}Pred}$	$\text{mmol C m}^{-2} \text{ts}^{-1}$	*	*
3	$P_{\text{ag}}, Z_{\text{ag}}, S_{\text{ag}}$	# agents	*	*
4	N, Si $N[0], Si[0]$	mmol N,Si m^{-2} mmol N,Si m^{-3}	*	*
5	$T[0], Irr[0], MLD$	$^{\circ}\text{C}, \text{Wm}^{-2}, \text{m}$	*	*
6	$P, Z, P, Z, Z_{\text{prot}}, Z_{\text{lip}}, P_{\text{ag}}, Z_{\text{ag}}, MLD, N[0], Si[0], T[0]$			*
7	$\text{Max}P, \text{Date Max}P, \text{Max}Z, \text{Date Max}Z, \text{Max}Z_{\text{prot}}, \text{Max}Z_{\text{lip}}, \text{Date } S_{\text{hatch}}, R$			*
8	Squid Audit trails		*	

Tab. 5.3 – Variables logged. Where P , diatom; Z , copepod; S , squid; R : squid in stage 7 (recruited) BP, background predator; VP, visual predator; X_{ing} , X individuals ingested; $X_{\text{ing}Y}$, X individuals ingested by Y ; X_{starve} : X individuals dead by starvation; X : X biomass, X_{prot} : X protein biomass; X_{lip} : X lipid biomass X_{ag} : number of X agents; [0] surface value; N and Si , total nitrogen and silicon in mesocosm (dissolved + particulate); $T[0]$, sea surface temperature; Irr , irradiance; MLD depth of mixed layer.

Requirements

Total integration time (at a rate of 3 hours per simulated year) is about 75 hours on one Intel Pentium 4 (2.8 GHz) processor producing about 6 GB of data.

5.1.2 Stage 2 – Testing the ergodicity of the virtual ecosystem

Location and external forcing

Same as in stage 1.

Experiment

Stage 2 is concerned with assessing if the system is ergodic or not (i.e. it is ergodic if there is no significant difference between the inter-annual and inter-instance noise). This is done by repeating the final eight years of stage 1 eight times, each with a different random seed (an ensemble of eight runs).

Logging

Demography, biomass and agents for the last 8 years.

Requirements

Total number of runs required: 8 (13 years).

Total integration time (at a rate of 3hours per simulated year) is about 40 hours per run on one Intel Pentium 4 (2.8 GHz) processor producing about 2 GB of data.

5.2 Sensitivity experiments

5.2.1 Stage 1 – Sensitivity of recruitment to a change in mesocosm dissolved silicate and nitrogen load

Location and external forcing

Same as in stage 1, but with a event that doubles the dissolved chemical concentration in the mixed layer on the 1st Jan of the first year.

Experiment

This experiment aims to assess the sensitivity of squid recruitment to variation of the nutrients load of the ecosystem, which limits primary production.

The experiments involve re-running the last 15 years of stage 1, doubling the dissolved silicate concentration above the turbocline ($\sim 0.6 \text{ mmol Si m}^{-3}$) on the 1st January of year 10 (2015). The maintenance of a stable 1st January dissolved silicate

concentration above in the mixed layer for the successive years is provided by the chemical conservation rule described in Appendix V. The same procedure was repeated doubling the dissolved nitrogen concentration ($\sim 4 \text{ mmol N m}^{-3}$).

Logging

Analysis of the last 10 years with the VE on attractor, including all variables logged in stage 1.

Requirements

Total number of runs required: 2 (15 years). Total integration time (at a rate of 3 hours per simulated year) is about 90 hours on one Intel Pentium 4 (2.8 GHz) processor producing about 12 GB of data.

5.2.2 STAGE 2 - Sensitivity of recruitment to abundance of basal predator

Location and external forcing

As in stage 1.

Experiment

This experiment investigates the sensitivity of recruitment to variation of inter-population competition for food. The simulation restarts from year 10 (1st Jan 2015) of the base run with double the initial concentration of basal predators feeding on copepods from 3000 to 6000 ind m^{-2} .

Logging

Analysis of the last 10 years after the VE has converged to the new attractor, including all variables logged in stage 1.

Requirements

Total number of runs required: 1 (15 years).

Total integration time (at a rate of 3hours per simulated year) is about 45 hours on one Intel Pentium 4 (2.8 GHz) processor producing about 6 GB of data.

5.2.3 STAGE 3 - Sensitivity of recruitment to predation

Location and external forcing

As in stage 1.

Experiment

The first experiment investigates the sensitivity of squid recruitment to variation of predator pressure directly on the squid population. This is done by repeating the last 15 years of stage 1, doubling the visual predator initial concentration from 3000 to 6000 ind m⁻².

Logging

Analysis of the last 10 years after the VE has converged to the new attractor, including all variables logged in stage 1.

Requirements

Total number of runs required: 1 (15 years).

Total integration time (at a rate of 3hours per simulated year) is about 45 hours on one Intel Pentium 4 (2.8 GHz) processor producing about 6 GB of data.

5.2.4 STAGE 4 - Sensitivity of recruitment to spawning magnitude

This set of numerical experiments focuses on investigating the effect of spawning magnitude on recruitment success, to investigate the causes of the possible density-dependent effect discussed by Agnew *et al.* (2000).

Location and external forcing

As in stage 1.

Experiments

This is done by repeating the last year of stage 1 increasing the number of eggs being laid annually, from 100 to 700 m⁻².

Logging

Analysis of one year restarted from the last year of the base run, with the VE on attractor. Logging includes all variables logged in stage 1, except audit trails.

Requirements

Total number of runs required: 7 (1 year).

Total integration time (at a rate of 3 hours per simulated year) is about 21 hours on one Intel Pentium 4 (2.8 GHz) processor producing about 4 GB of data.

5.2.5 STAGE 5 - Sensitivity of recruitment to spawning date

This stage focuses on the numerical experiments to test Cushing's match-mismatch hypothesis in the context of the Lagrangian Ensemble metamodel.

The day of maximum prey biomass is an emergent property of the simulation. Also the day of squid hatching, D_H , is emergent and function of day of spawning, D_S , and the temperature at which eggs are incubated.

Location and external forcing

As in stage 1.

Experiments

This set of numerical experiments is designed to test the hypothesis that there is a correlation between recruitment and the difference in time between squid spawning date, D_S , and the date of maximum prey biomass, D_P (fig.5.5).

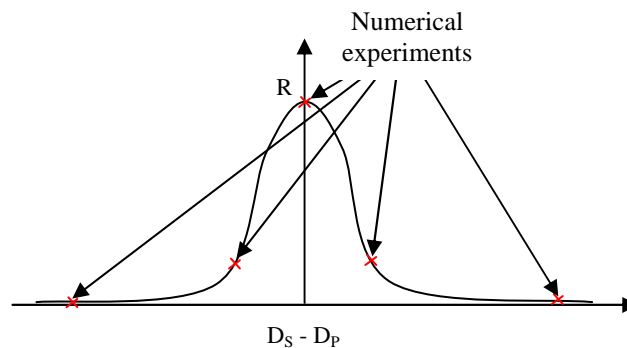


Fig.5.5 – Hypothetical match-mismatch curve

In all previous experiments, squid eggs were laid by an exogenous spawning stock as an event on day 100 (10th April) every year. In this experiments, fifteen repetitions of the last year of the base run will be made with eggs being laid at four days interval from day 88 (29th March) to day 144(24th May).

Logging

Analysis of 1 year, including all variables logged in stage 1, and audit trails, describing the life histories of one recruiting and one non-recruiting squid.

Requirements

Total number of runs required: 15 (1 year).

Total integration time (at a rate of 3hours per simulated year) is about 45 hours on one Intel Pentium 4 (2.8 GHz) processor producing about 9 GB of data.

6.1.1.1 Poincaré plots of vertically integrated biomasses

Experiment	Duration	Biomass	Ave	s.d.	% Var
BASE	25 YRS	P	390.4	27.8	7.1
		Z	83.7	8.0	9.6
		S	1.8	0.4	21.4
	LAST 10 YRS	P	395.1	9.4	2.4
		Z	80.7	4.9	6.1
		S	1.9	0.2	9.2
P05Z2	25 YRS	P	396.1	32.7	8.3
		Z	99.8	25.0	25.1
		S	1.8	0.6	36.8
	LAST 10 YRS	P	404.3	14.9	3.7
		Z	90.4	6.0	6.6
		S	1.7	0.2	11.3
P2Z2	25 YRS	P	379.3	38.5	10.2
		Z	92.0	17.5	19.0
		S	2.0	1.2	59.5
	LAST 10 YRS	P	390.8	8.9	2.3
		Z	91.6	4.0	4.4
		S	1.7	0.2	8.9
P05Z05	25 YRS	P	393.0	11.0	2.8
		Z	81.4	5.6	6.9
		S	1.6	0.3	19.9
	LAST 10 YRS	P	395.7	11.2	2.8
		Z	83.9	7.2	8.6
		S	1.5	0.2	11.0
P2Z05	25 YRS	P	394.4	0.3	0.1
		Z	87.3	6.2	7.1
		S	1.6	0.1	9.0
	LAST 10 YRS	P	390.7	3.8	1.0
		Z	87.8	4.5	5.2
		S	1.6	0.1	5.3

Tab.6.2 –Diatom (P); Copepod (Z); Squid (S) on 28th May at 6am (mmolC m⁻²)

Base run

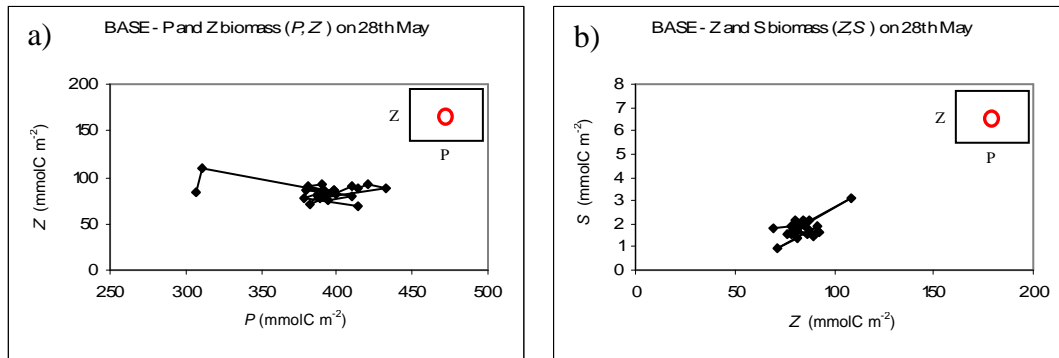


Fig.6.1 - P, Z and S vertically integrated biomass on the 28th May at 6am for all 25 years.

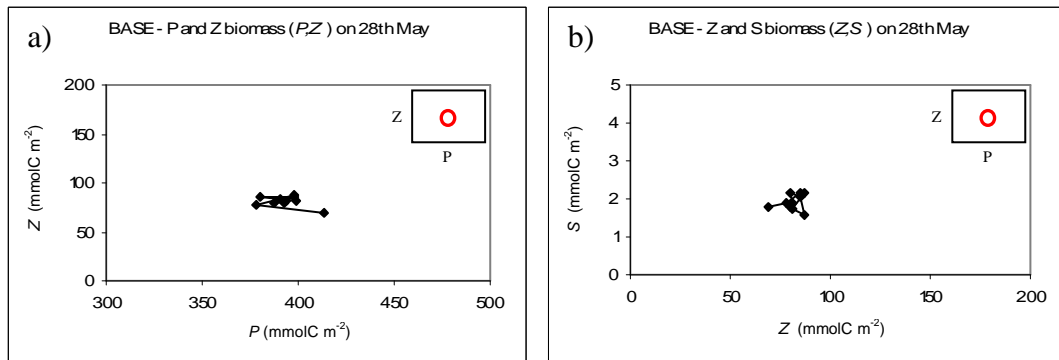


Fig.6.2 - P,Z and S vertically integrated biomass on the 28th May at 6am for the last 10 years.

Runs initialized with half and double the P and Z concentrations on the 1st Jan

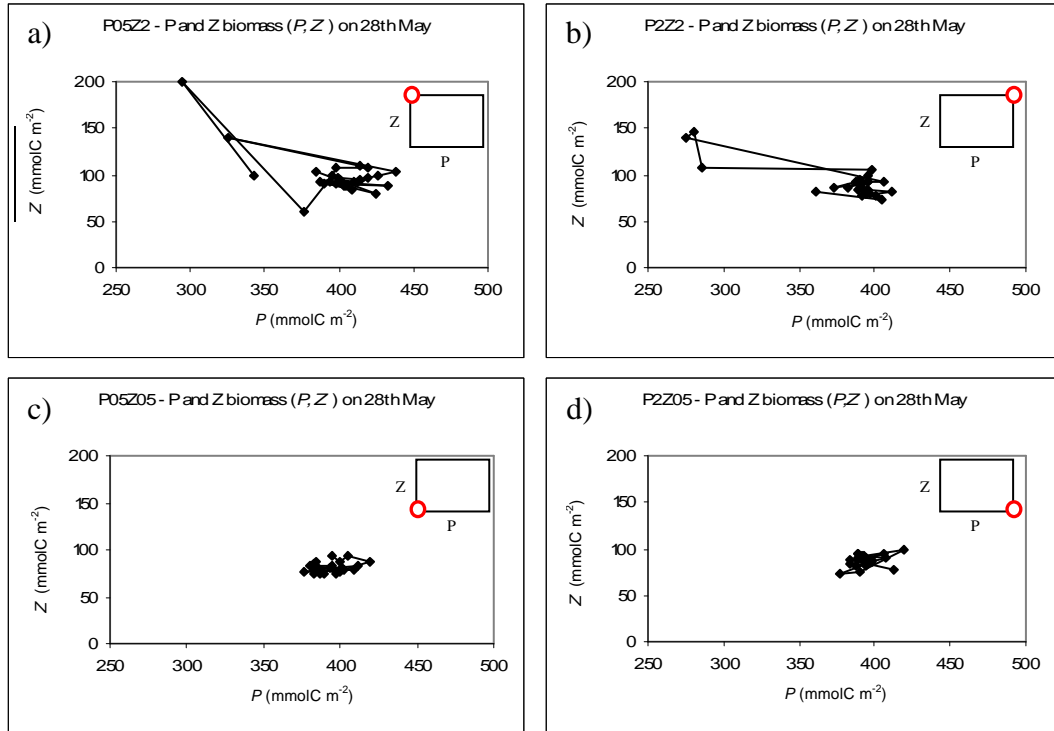


Fig.6.3 – P and Z vertically integrated biomass on the 28th May at 6am for **all 25 years**.

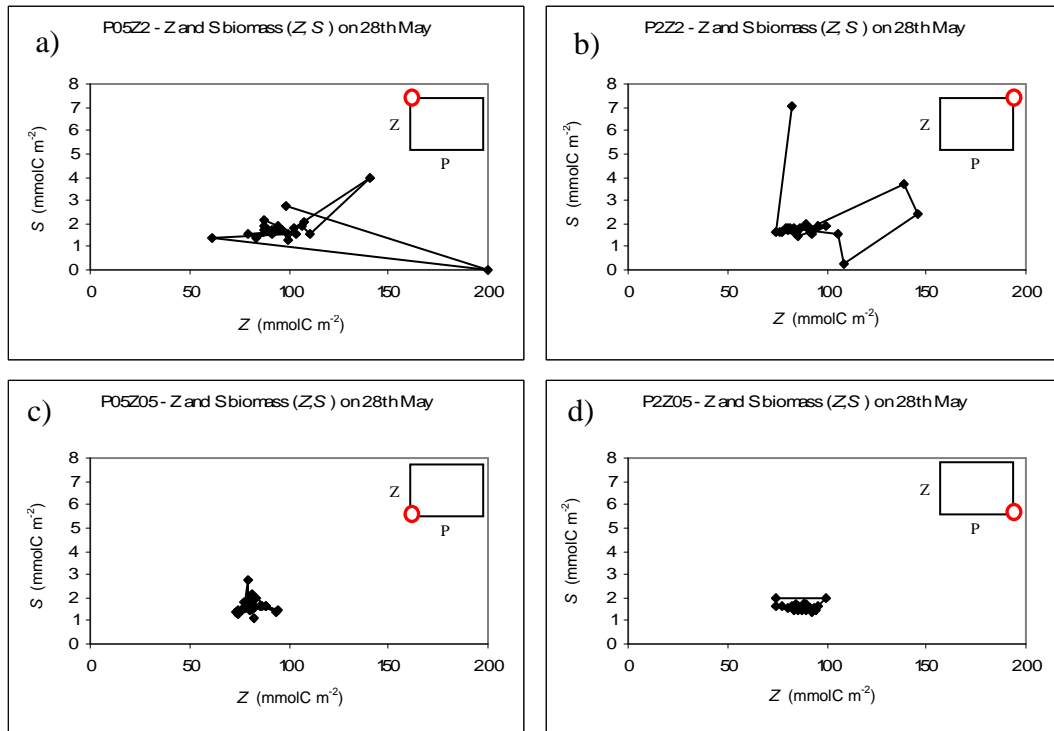


Fig. 6.4 - Z and S vertically integrated biomass on the 28th May at 6am for **all 25 years**.

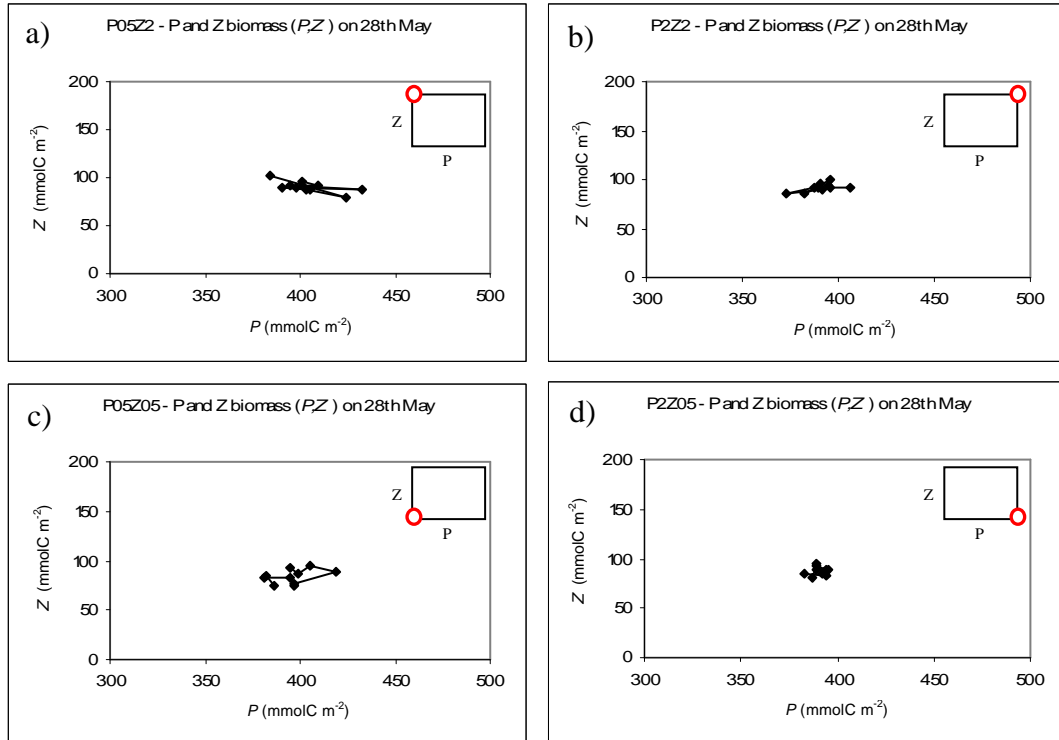


Fig. 6.5 - P and Z vertically integrated biomass on the 28th May at 6am for the last 10 years.

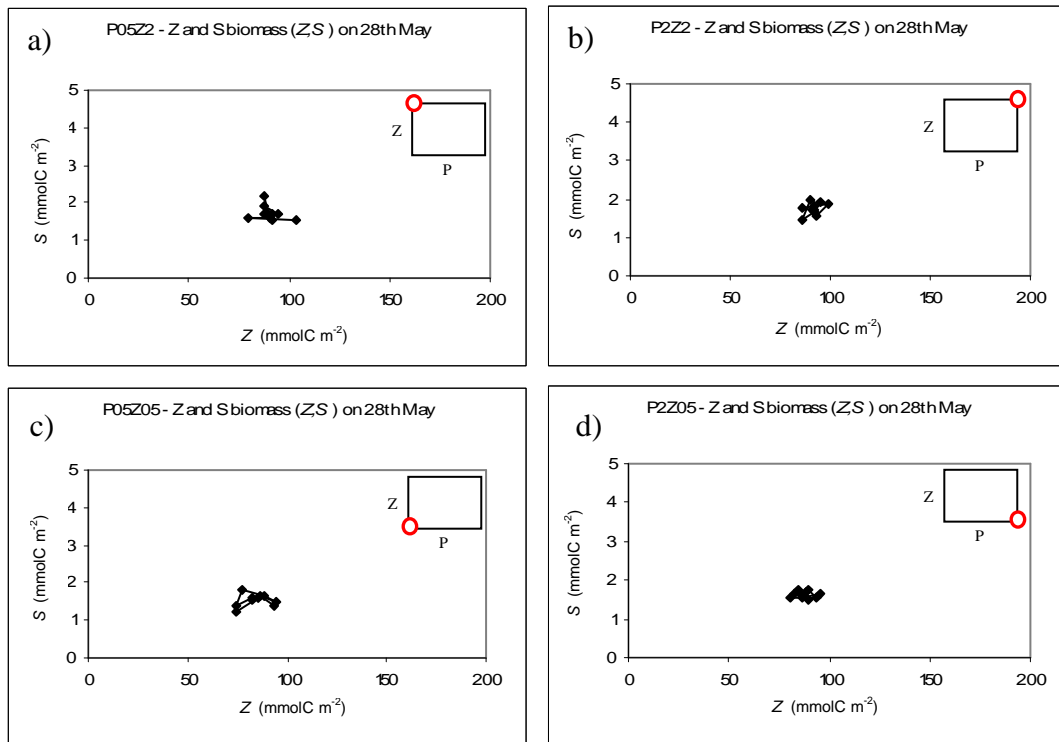


Fig.6.6 - Z and S vertically integrated biomass on the 28th May at 6am for the last 10 years

6.1.1.2 Poincaré plots of vertically integrated concentrations

Experiment	Duration	Abundance	Ave	s.d.	% Var
BASE	25 YRS	P	2.0×10^{10}	1.3×10^9	6.3
		Z	25546.7	3806.4	14.9
		S	11.6	1.9	16.1
	LAST 10 YRS	P	2.0×10^{10}	6.0×10^8	2.9
		Z	24823.8	2655.6	10.7
		S	11.6	1.5	13.0
P05Z2	25 YRS	P	2.2×10^{10}	1.5×10^9	6.9
		Z	29682.5	4657.0	15.7
		S	12.00	3.1	26.1
	LAST 10 YRS	P	2.1×10^{10}	8.2×10^8	3.8
		Z	29028.6	3772.8	13.0
		S	11.9	1.5	12.8
P2Z2	25 YRS	P	2.0×10^{10}	2.0×10^9	9.7
		Z	27503.7	6124.9	22.3
		S	12.5	3.5	27.8
	LAST 10 YRS	P	2.1×10^{10}	8.1×10^8	3.9
		Z	27224.8	2147.3	7.9
		S	11.8	1.5	12.9
P05Z05	25 YRS	P	2.0×10^{10}	7.5×10^8	3.7
		Z	24868.6	2677.8	10.8
		S	11.2	1.8	16.1
	LAST 10 YRS	P	2.0×10^{10}	9.0×10^8	4.4
		Z	25664.5	3206.9	12.5
		S	10.8	1.6	14.9
P2Z05	25 YRS	P	2.1×10^{10}	1.1×10^9	5.0
		Z	27189.2	3093.6	11.4
		S	11.5	1.2	10.2
	LAST 10 YRS	P	2.1×10^{10}	6.1×10^8	3.0
		Z	27387.6	1801.0	6.6
		S	11.5	1.3	11.4

Tab.6.3 – Diatom (P); Copepod (Z); Squid (S) on 28th May at 6am (ind m⁻²):

Base run

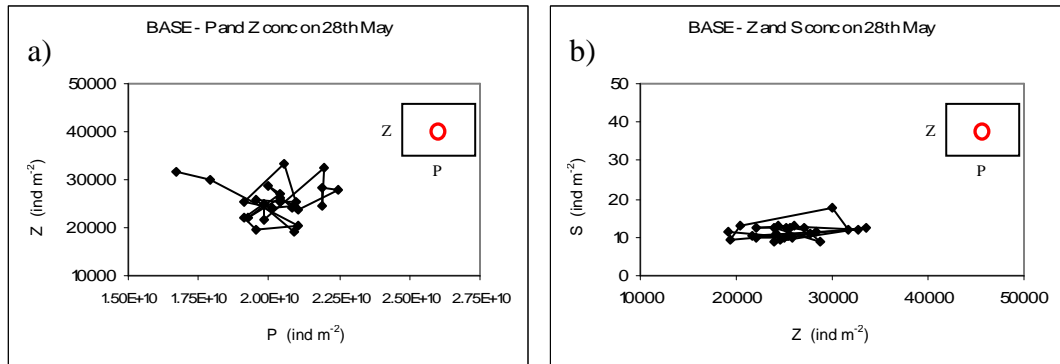


Fig. 6.7 – P,Z and S vertically integrated concentration on the 28th May at 6am for all 25 years.

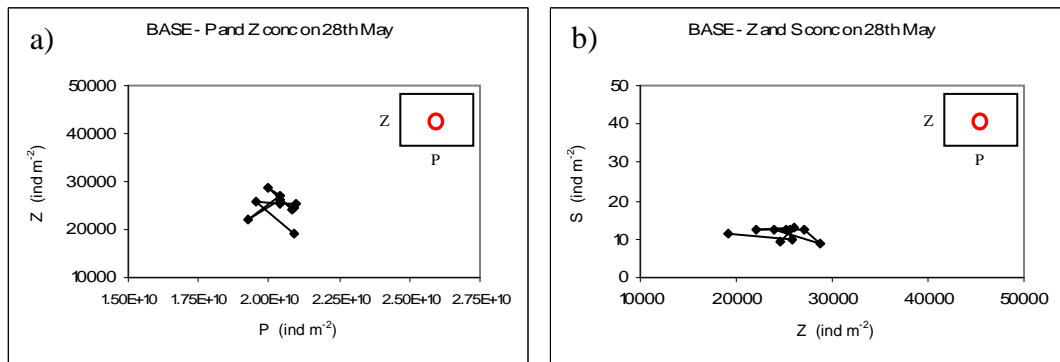


Fig. 6.8 – P,Z and S vertically integrated concentration on the 28th May at 6am for the last 10 years.

Runs initialized with half and double the P and Z concentrations on the 1st Jan

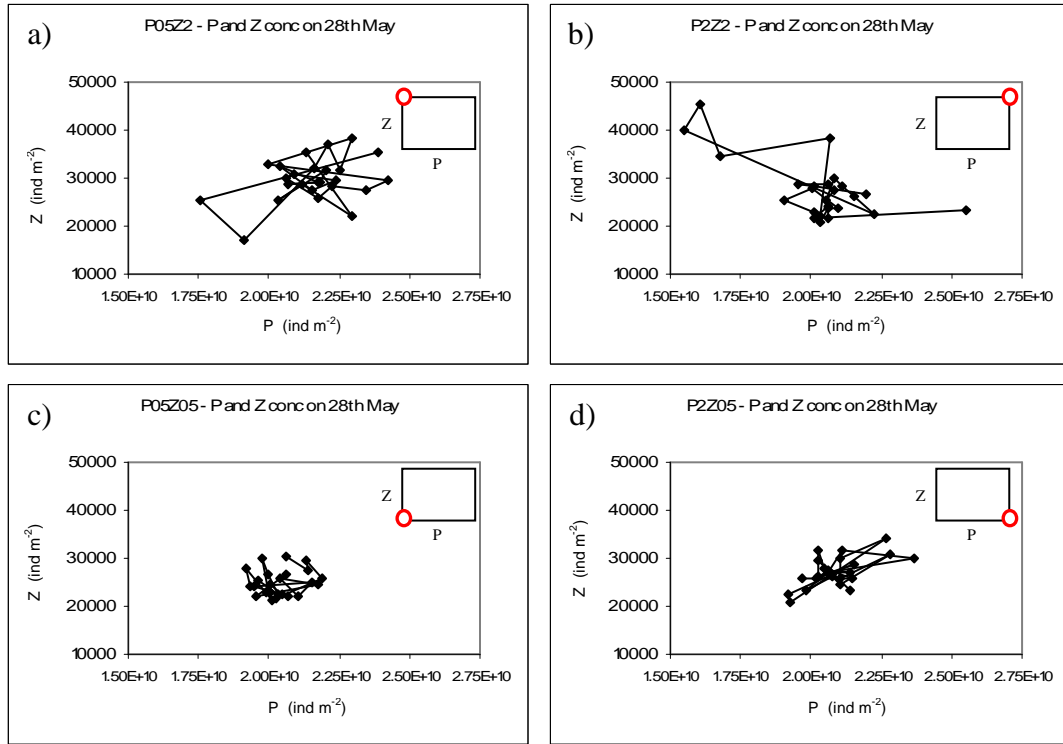


Fig. 6.9 – P and Z vertically integrated concentration on the 28th May at 6am for **all 25 years**.

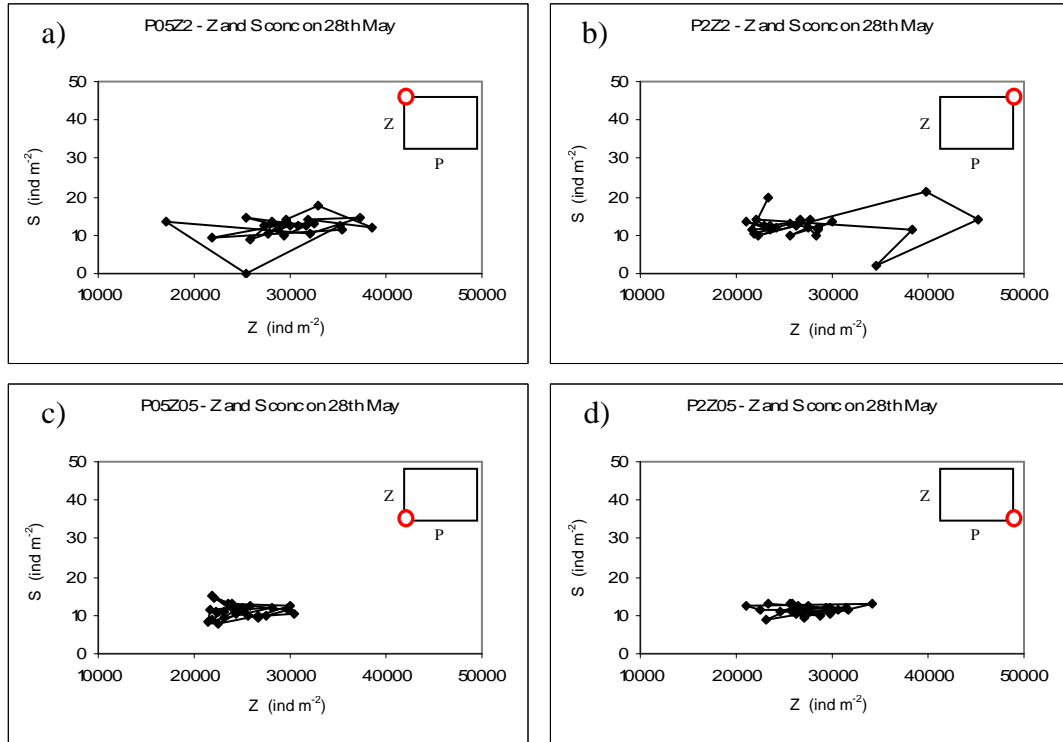


Fig. 6.10 - Z and S vertically integrated concentration on the 28th May at 6am for **all 25 years**.

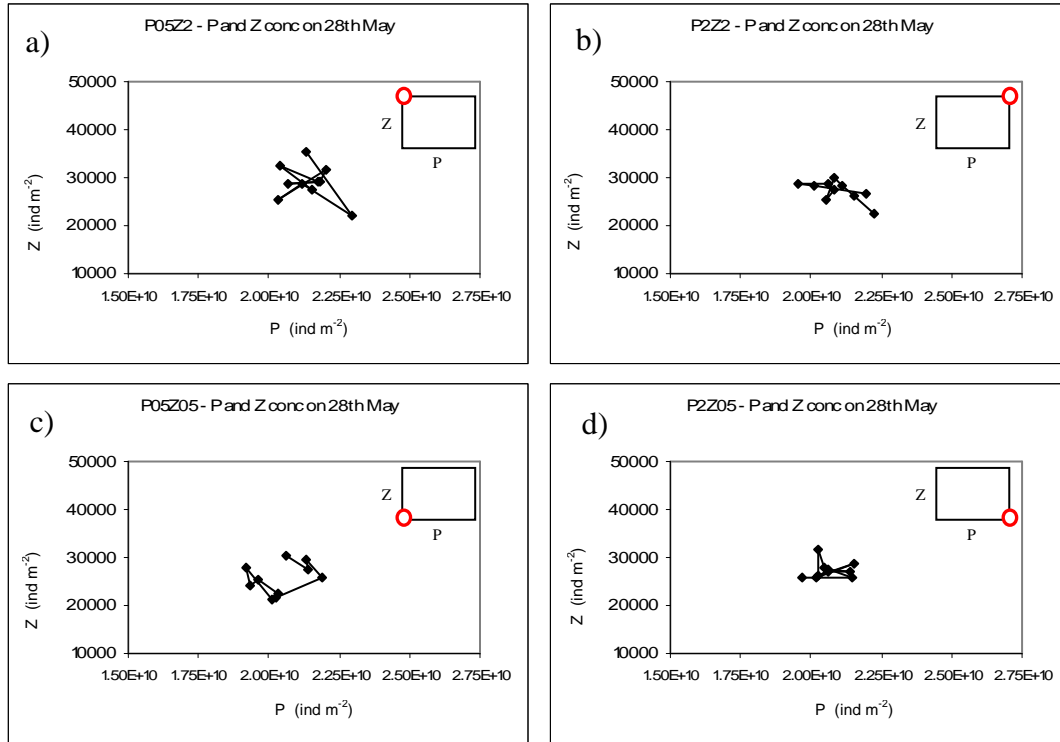


Fig. 6.11 - P and Z vertically integrated concentration on the 28th May at 6am for the last 10 years.

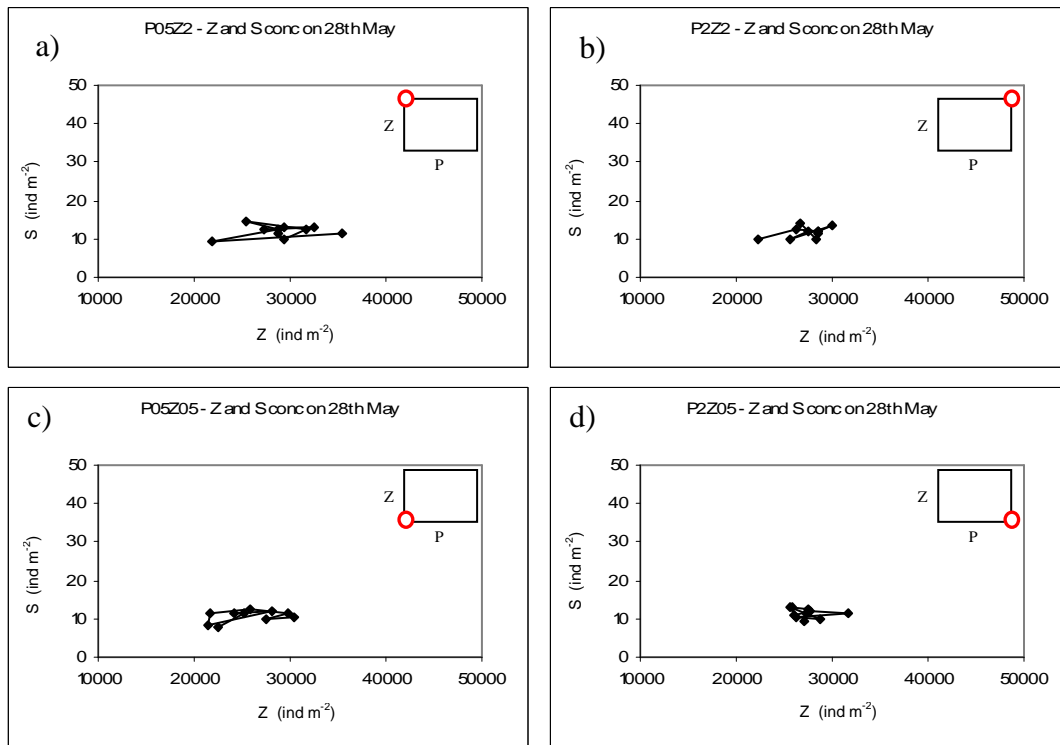


Fig. 6.12 - Z and S vertically integrated concentration on the 28th May at 6am for the last 10 years.

6.1.1.3 Error distribution around the mean

Sample data for P, Z, S and P, Z, S on the 28th May of the last 10 years of the five VEs on attractor ($n=50$) were standardised by subtracting the sample mean and dividing by the sample standard deviation and distributed in 18 bins (tab.6.4). These were plotted against a normal distribution (fig.6.13-6.14). A chi-squared test was performed to assess whether the errors were normally distributed, and the results showed that, for all the variables considered, the errors from the mean approximate a Gaussian distribution (tab.6.4).

# s.d. from mean	Gaussian	P	Z	S	P	Z	S
(< -4.0)	0.0	0	0	0	0	0	0
(-4.0, -3.5)	0.0	0	0	0	0	0	0
(-3.5, -3.0)	0.1	0	0	0	0	0	0
(-3.0, -2.5)	0.5	0	2	0	0	2	2
(-2.5, -2.0)	1.6	0	0	2	0	0	2
(-2.0, -1.5)	4.3	4	6	4	6	8	6
(-1.5, -1.0)	9.1	10	8	8	8	4	14
(-1.0, -0.5)	15.1	14	10	22	14	10	8
(-0.5, 0.0)	19.3	28	20	22	26	24	8
(0.0, 0.5)	19.3	24	22	18	12	20	22
(0.5, 1.0)	15.1	8	18	12	16	20	24
(1.0, 1.5)	9.1	4	10	2	10	4	8
(1.5, 2.0)	4.3	2	2	2	6	6	6
(2.0, 2.5)	1.6	2	2	8	0	0	0
(2.5, 3.0)	0.5	2	0	0	2	2	0
(3.0, 3.5)	0.1	2	0	0	0	0	0
(3.5, 4.0)	0.0	0	0	0	0	0	0
(>4.0)	0.0	0	0	0	0	0	0
%	100	100	100	100	100	100	100
χ^2		27.85	6.22	19.22	7.94	13.98	13.66
Significance		0.05	0.99	0.32	0.97	0.67	0.69

Tab.6.4 – Error frequency distribution (%) of P, Z, S, P, Z, S . Each bin represents a half s.d. range. Gaussian represents the expected normal distribution. χ^2 and significance report how well the observed values approximate a normal distribution, where 1 indicates normal distribution.

Errors for Z and P were almost perfectly normally distributed (significance of chi-test for normal distribution 0.99 and 0.97 respectively), while P, S, Z and S showed slightly larger tails than a normal distribution (fig.6.13-6.14). The fatter tails, however, are not the product of a single VE, but all VEs contribute.

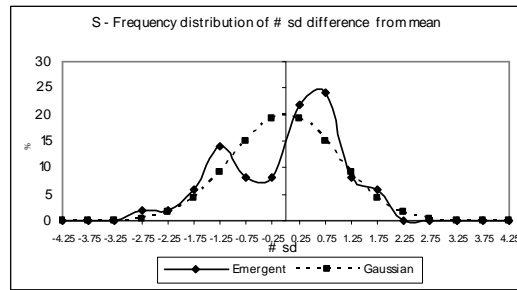
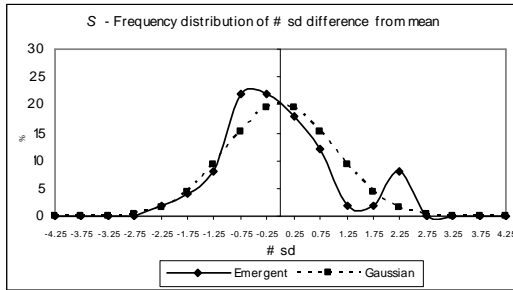
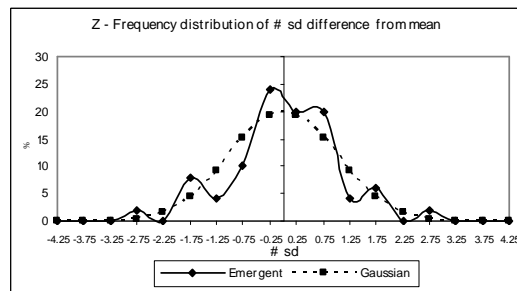
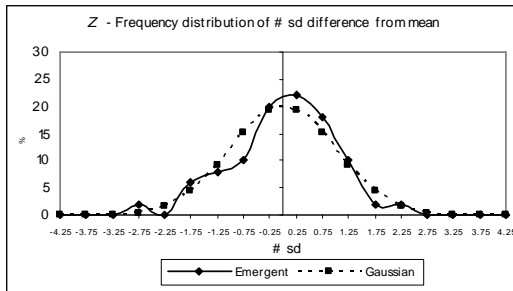
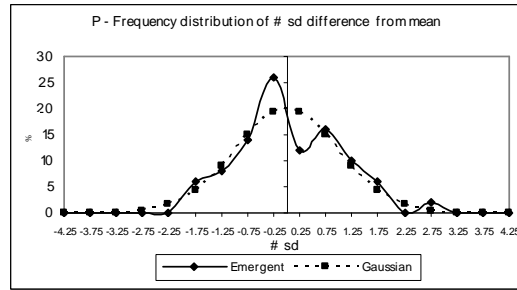
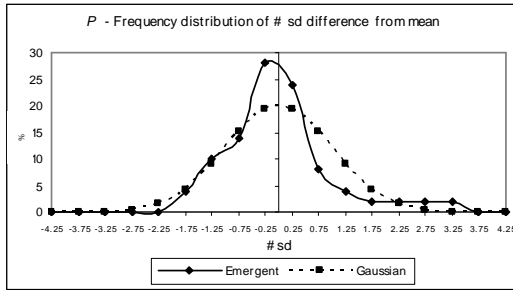


Fig. 6.13 - Error frequency distribution (%) of P,Z,S on the 28th May.

Fig. 6.14 - Error frequency distribution (%) of P,Z,S on the 28th May.

6.1.2 On attractor (last 10 years)

Fig.6.15-6.56 illustrate the VE from the period 2020-2030 (a) and in 2029-2030 (b), after settling to its attractor.

6.1.2.1 Demography

	Units	Year 16-25		
		Ave	s.d.	% var
P	ind m ⁻²	9.1×10 ¹⁰	1.5×10 ⁹	1.7
Z	ind m ⁻²	156087.6	10313.1	6.6
C _{OW}	ind m ⁻²	7935.8	344.4	4.3
S	ind m ⁻²	140.7	4.7	3.3
SHD	h	3256.0	0.9	0
R	ind m ⁻² yr ⁻¹	3.96	0.48	12.2

Tab. 6.5 - Average value, s.d. and percentage variation from the mean. Where:

P: Max vertically integrated P concentration; Z: Max vertically integrated Z concentration;
 C_{OW}: Max vertically integrated concentration of over-wintering copepods; S: Max vertically integrated S concentration; SHD: Hours since 1st Jan when squid hatching occurs.
 R: vertically integrated total number of squid that reached stage 7.

6.1.2.1.1 Vertically integrated concentration of plankton

Fig.6.15-6.19 show the vertically integrated concentrations of the plankton populations on attractor. Diatom had an average annual maximum concentration of 9.1×10^{10} ind m⁻² (s.d. 1.5×10^9 ind m⁻²; percentage variation from the mean was 1.7; tab.6.5). Fig.6.15b shows the annual demography of the diatom population. It can be seen that the population reached its peak by mid-April. After that, it started to decline. It showed smaller peaks in the period June-July and September-October.

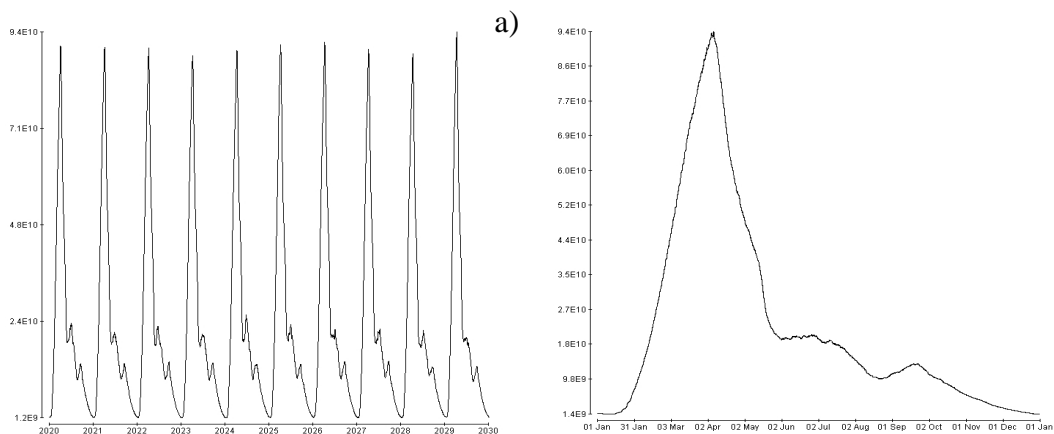


Fig. 6.15 - Vertically integrated P concentration (ind m⁻²).

Copepod population in spring was composed exclusively by copepods that entered over-wintering in the previous summer (fig. 6.16a). Their average concentration as over-wintering was $7,936 \text{ ind m}^{-2}$ (s.d. 344 ind m^{-2} ; percentage variation from the average = 4.3%; tab. 6.5). The average annual peak in copepod concentration was about $156,000 \text{ ind m}^{-2}$ (s.d. $10,300 \text{ ind m}^{-2}$; percentage variation from the average = 6.6%; tab. 6.5). Every year over-wintering copepods emerged from diapause on the 15th March and reproduced between the 13th and 14th of May. All over-wintering copepods had already left the surface water by mid July. The population of non over-wintering copepods survived until the beginning of September.

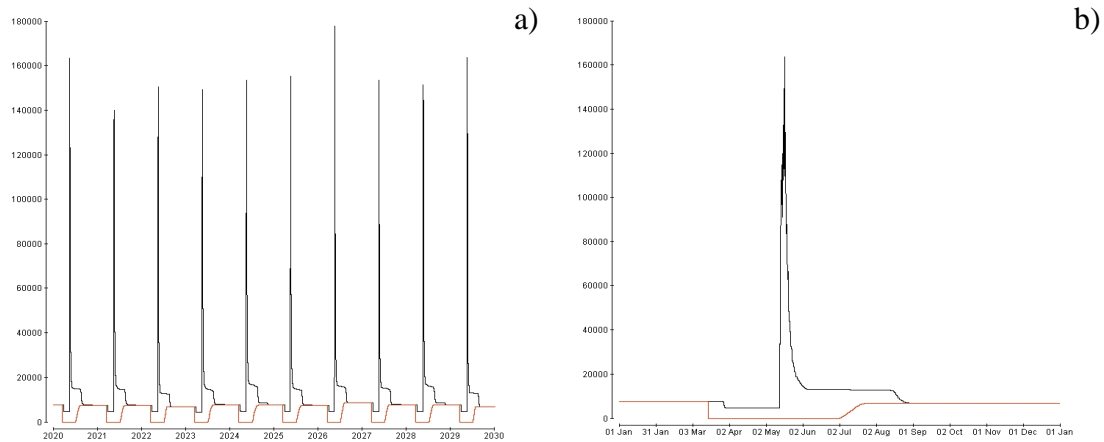


Fig. 6.16 - Vertically integrated Z concentration (black:all stages; red: over-wintering) (ind m^{-2})

The annual maximum concentration in squid (fig. 6.17) was 161 ind m^{-2} (s.d. 3.7 ind m^{-2} ; percentage variation from the average = 3.3%; tab. 6.5). Every year eggs were injected in the water column on the 10th April and hatching started on the 15th May every year (fig.6.17 and tab.6.5). The average annual recruitment between 2020-2030 was $4.0 \text{ ind m}^{-2} \text{ yr}^{-1}$ (s.d. $0.5 \text{ ind m}^{-2} \text{ yr}^{-1}$; percentage variation from the mean of 12.2%; fig.6.19a and tab.6.5). Recruitment occurred within the first week of June (fig. 6.18b). The vertically integrated concentration of top predators is exogenous (fig.6.19). The vertically integrated concentration of visual predators feeding on squid decreases with time, while that of basal predator feeding on copepods does not vary in time.

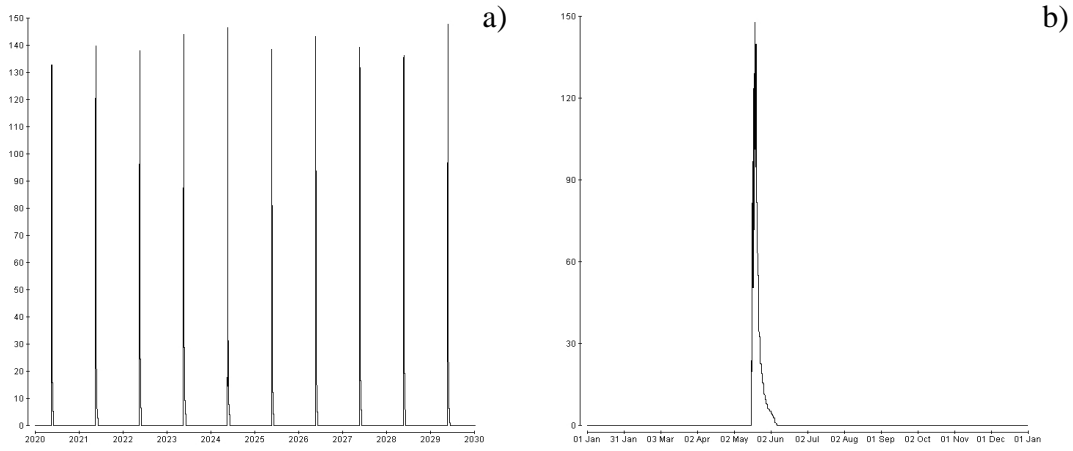


Fig. 6.17 - Vertically integrated concentration of squid (S1-S6) (ind m^{-2})

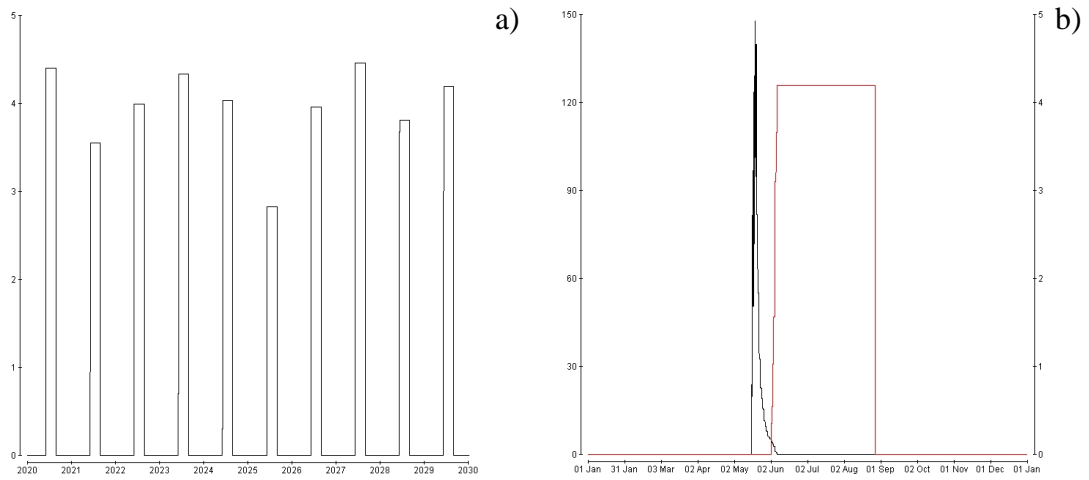


Fig. 6.18 – Annual squid recruitment ($\text{ind m}^{-2} \text{ yr}^{-1}$)

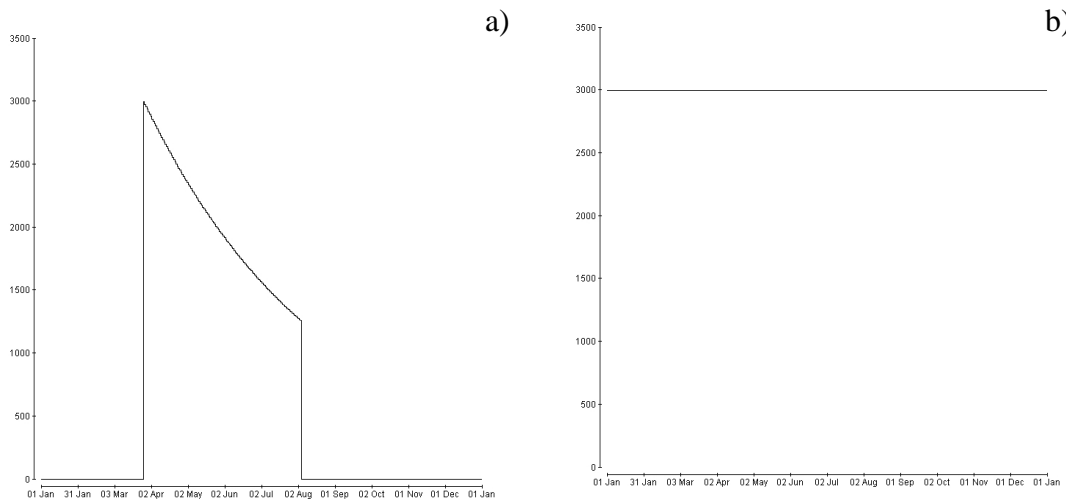


Fig. 6.19 – Parametrised top predators vertically integrated concentration (ind m^{-2})
 a) Visual predator feeding on squid; b) basal predator feeding on copepods

Fig.6.20-6.21 illustrate the stability of the ecosystem. Every year the vertically integrated concentration of diatom and copepod on a particular day was very similar in all ten years analysed (fig.6.20). The vertically integrated concentration of copepod in relationship with vertically integrated concentration of squid shows some variation in the copepod concentration on the day squid eggs hatched (fig.6.21).

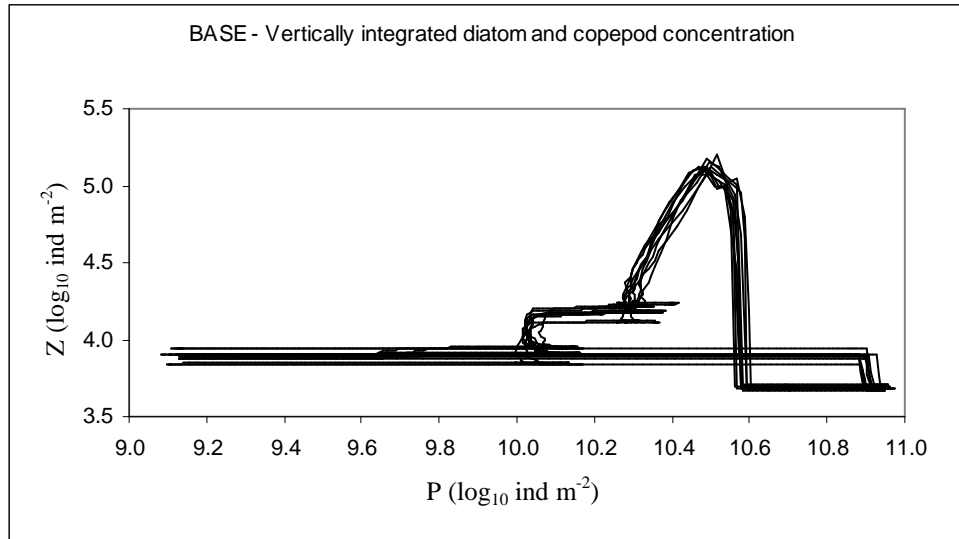


Fig. 6.20 – Poincaré map showing vertically integrated concentration of diatom and copepod every day at 6am from 1st Jan 2020 to 31st Dec 2029.

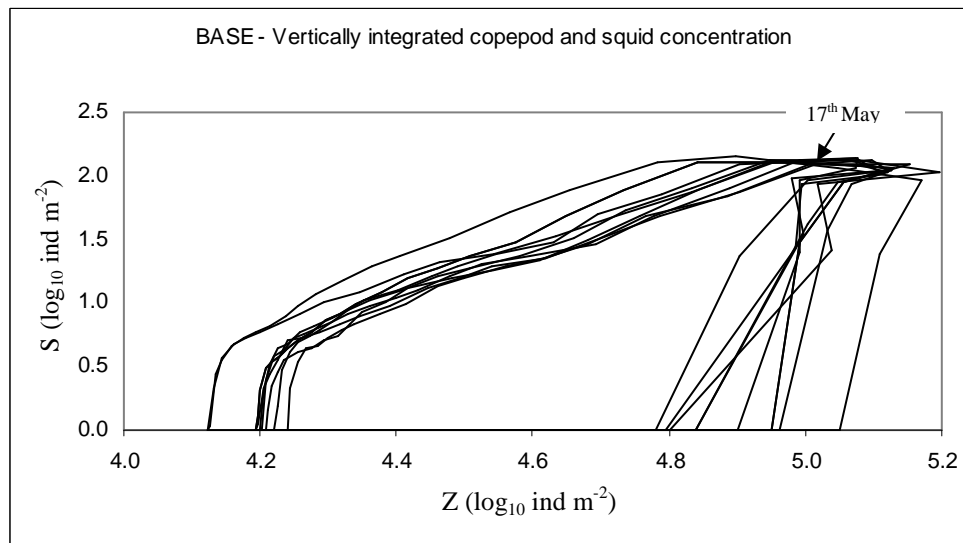


Fig. 6.21 – Poincaré map showing vertically integrated concentration of copepod and squid every day at 6am from 15th May to 1st July of years 2020 to 2029 (anti-clockwise).

6.1.2.1.2 Causes of mortality

Year	PingZ ind m ⁻² yr ⁻¹	ZingS ind m ⁻² yr ⁻¹	ZingBP ind m ⁻² yr ⁻¹	SingPred ind m ⁻² yr ⁻¹	Pstarve ind m ⁻² yr ⁻¹	Zstarve ind m ⁻² yr ⁻¹	Sstarve ind m ⁻² yr ⁻¹
2020	1.1×10 ¹¹	190846.1	197983.6	295.6	2.0×10 ¹¹	7092.4	0.0
2021	1.1×10 ¹¹	153530.5	221294.2	296.4	1.9×10 ¹¹	7125.2	0.0
2022	1.0×10 ¹¹	168305.7	209281.7	296.0	2.0×10 ¹¹	5763.7	0.0
2023	1.0×10 ¹¹	160264.4	200598.4	295.7	1.9×10 ¹¹	6271.0	0.0
2024	1.2×10 ¹¹	168141.4	225335.6	296.0	2.0×10 ¹¹	8063.0	0.0
2025	1.0×10 ¹¹	145379.0	233250.0	297.2	2.0×10 ¹¹	6880.8	0.0
2026	1.1×10 ¹¹	156258.2	217359.9	296.0	2.0×10 ¹¹	6691.3	0.0
2027	1.1×10 ¹¹	163381.7	229086.0	295.5	1.9×10 ¹¹	6748.4	0.0
2028	1.1×10 ¹¹	160108.8	224364.8	296.2	1.9×10 ¹¹	7655.4	0.0
2029	9.7×10 ¹⁰	124739.8	251190.4	295.8	1.9×10 ¹¹	5952.3	0.0
Ave	1.1×10 ¹¹	159095.6	220974.5	296.0	2.0×10 ¹¹	6824.3	0.0
s.d.	6.3×10 ⁹	17006.5	15824.2	0.5	2.9×10 ⁹	715.4	0.0
% var	5.9	10.7	7.2	0.2	1.5	10.5	0.0

Tab. 6.6 – Causes of mortality. Where: PingZ = Diatoms ingested by copepods; ZingS = Copepods ingested by squid; ZingBP = Copepods ingested by basal predator; SingPred= Squid ingested by visual predator; Pstarve = Diatoms died of energy starvation; Zstarve = Copepods died of starvation; Sstarve = Squid died of starvation.

Table 6.6 summarises the causes of mortality of each population annually. It shows the total number of individuals lost to predation and starvation each year, between 2020-2030 (year 16-25), with the average, standard deviation and percentage variation from the mean during this period. On average, 1.1×10^{11} diatoms m⁻² get ingested by copepods every year (s.d.= 6.3×10^9 diatoms m⁻² yr⁻¹; percentage variation from the mean = 5.9%), and 2.0×10^{11} diatoms m⁻² yr⁻¹ are lost through energy starvation each year (s.d. = 2.9×10^9 diatoms m⁻² yr⁻¹; percentage variation from the mean = 1.5%). The average number of copepods annually ingested by squid is about 160,000 m⁻² yr⁻¹ (s.d. = 17,000 copepods m⁻² yr⁻¹; percentage variation from the mean = 10.7%), while those ingested by basal predator is about 221,000 m⁻² yr⁻¹ (s.d. = 15,800 copepods m⁻² yr⁻¹; percentage variation from mean = 7.2%). Every year about 6,800 copepods m⁻² die of starvation (s.d. = 715 copepods m⁻² yr⁻¹; percentage variation from the mean = 10.5%). Mortality of squid is caused exclusively by predation by visual predators. On average 296 squid m⁻² are eaten annually (s.d. = 0.5 squid m⁻² yr⁻¹; percentage variation from mean = 0.2%).

Predation

Fig. 6.22-6.25 show the instantaneous mortality rate due to predation. Every year diatoms are grazed between the end of March and the beginning of September, with a peak in diatoms consumption in mid-May (fig.6.22).

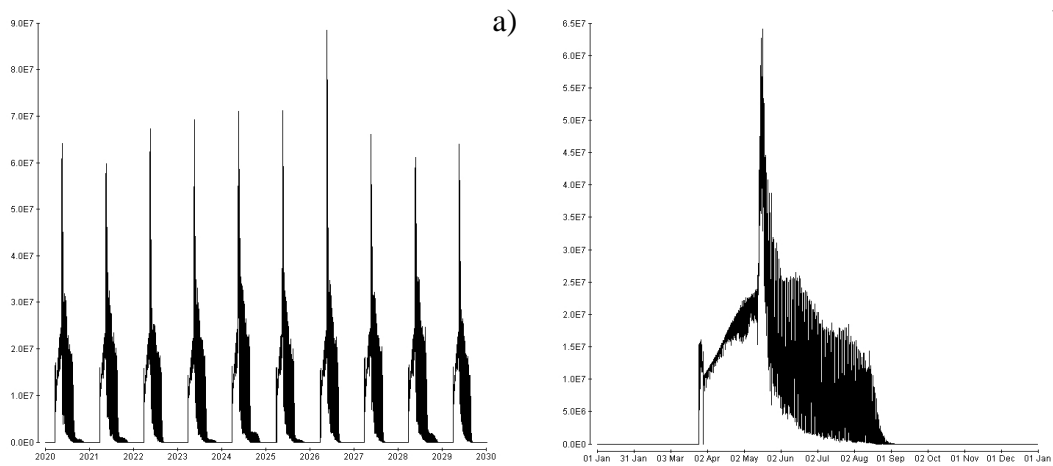


Fig. 6.22 – Diatoms ingested by copepods ($\text{ind m}^{-2} \text{ts}^{-1}$)

Predation on copepods is concentrated in the period between mid-May and the first week of June (fig.6.23-6.24). The maximum instantaneous rate of copepod predated was about 25,000 copepods m^{-2} per half-hour timestep by squid (fig.6.23) and about 7,000 copepods m^{-2} per timestep by basal predator (fig.6.24).

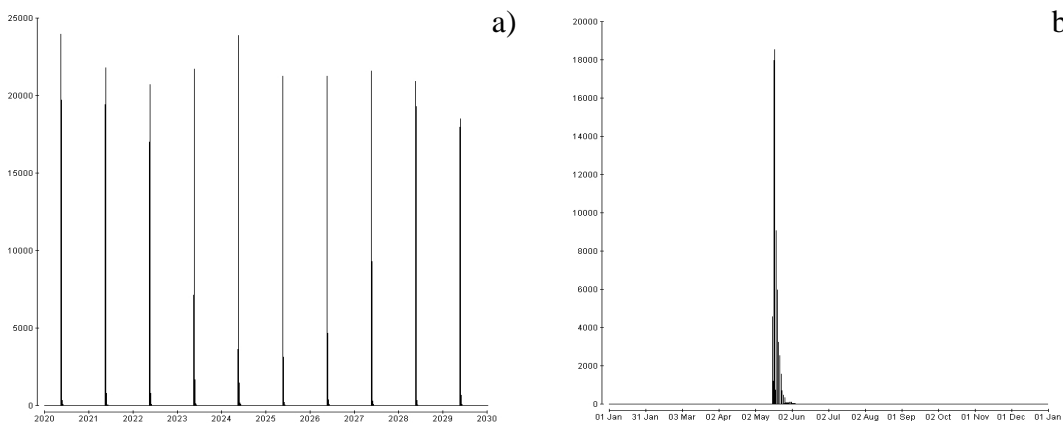


Fig. 6.23 – Copepods ingested by squid ($\text{ind m}^{-2} \text{ts}^{-1}$)

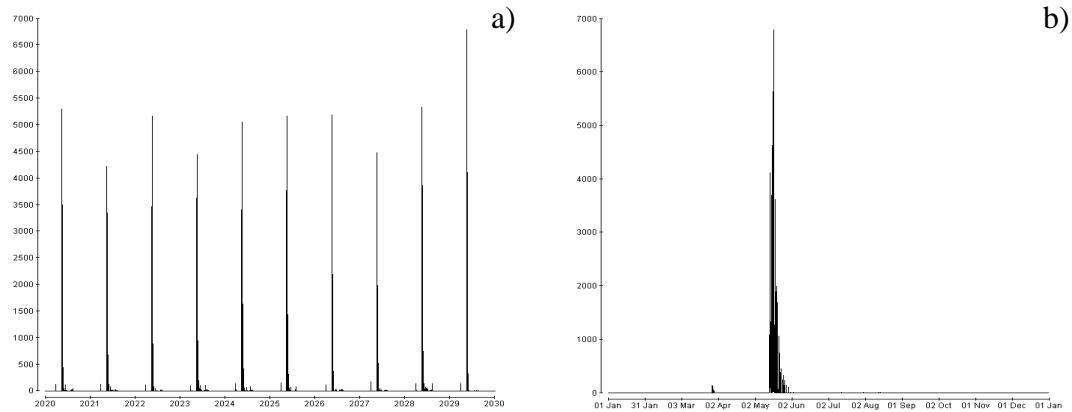


Fig. 6.24 – Copepods ingested by basal predator (ind m⁻² ts⁻¹)

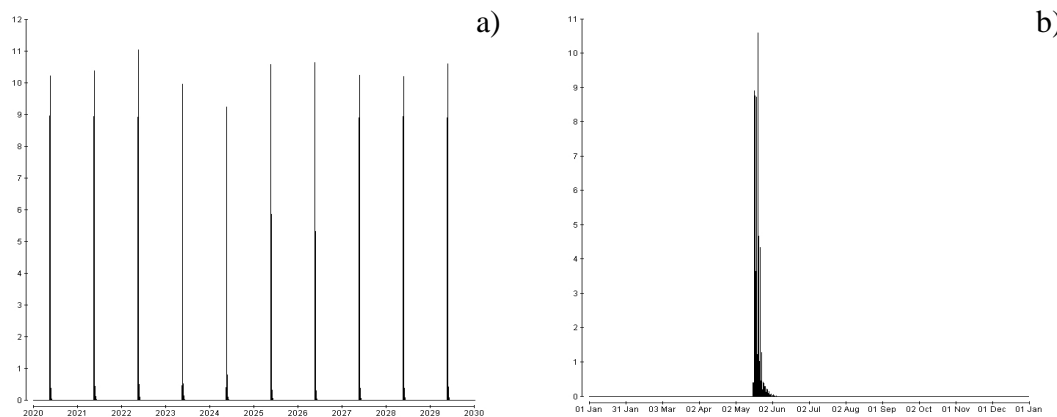


Fig. 6.25 – Squid ingested by visual predator (ind m⁻² ts⁻¹)

Year	S1	S2	S3	S4	S5	S6
2020	203.3	83.7	6.5	1.3	0.5	0.4
2021	202.8	85.5	6.5	1.2	0.3	0.2
2022	203.4	82.0	6.2	2.4	1.2	0.8
2023	204.1	82.3	5.8	2.1	0.8	0.7
2024	205.8	83.2	5.0	1.3	0.3	0.4
2025	205.6	82.4	5.6	2.2	0.9	0.4
2026	187.8	98.0	6.5	2.1	1.0	0.7
2027	199.9	86.1	6.6	1.6	0.7	0.6
2028	204.1	83.5	5.2	1.9	1.0	0.5
2029	193.1	93.0	6.6	1.5	1.0	0.6
Ave	201.0	86.0	6.0	1.8	0.8	0.5
s.d.	5.9	5.3	0.6	0.4	0.3	0.2
% var	2.9	6.2	10.1	24.8	39.6	33.8

Tab. 6.7 – Stage specific mortality due to predation

Squid mortality due to predation occurs throughout the period of squid permanence in the mesocosm (mid-May to the 1st week of June), with a peak soon after hatching (fig.6.25). Looking at the squid stage-specific annual mortality due to predation, it can be seen that it is highest on the newly hatched S1 squid, and it progressively decreases in successive stages (tab.6.7). Squid recruitment is perfectly correlated to the number of squid eaten annually by the predator.

Starvation

Fig. 6.26-6.27 show the instantaneous mortality rate due to starvation. Diatoms died of energy starvation throughout the whole year (fig. 6.26), however their mortality peaked between mid-March to mid-May, July to August and October-November. Copepod died of starvation mostly between mid-August to mid-September, with some deaths due to starvation occurring also during November (fig.6.27). As already said, no squid die of starvation (tab.6.7).

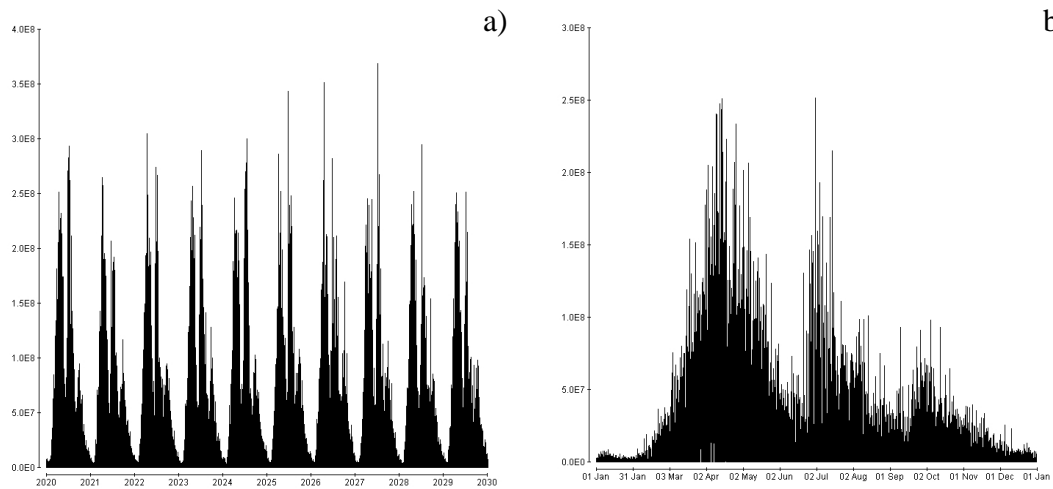


Fig. 6.26 – Diatom death by energy starvation (ind m⁻² ts⁻¹)

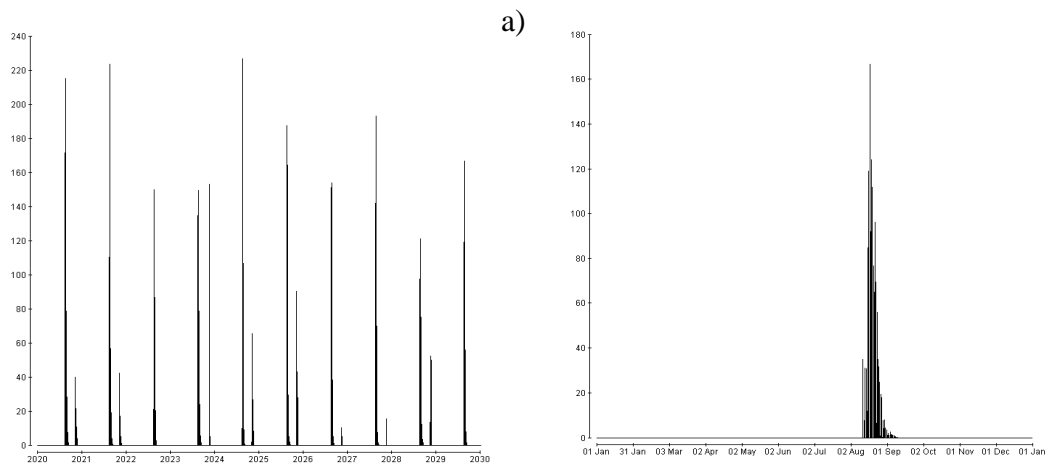


Fig. 6.27 – Copepod death by energy starvation (ind m⁻² ts⁻¹)

6.1.2.2 Plankton biomass

	Units	Ave	s.d.	% var
<i>P</i>	mmol C m ⁻²	1696.5	29.2	1.7
<i>PD</i>	h	2503.3	17.7	0.7
<i>Z</i>	mmol C m ⁻²	229.4	9.7	2.3
<i>Zprot</i>	mmol C m ⁻²	68.5	1.6	2.4
<i>Zlip</i>	mmol C m ⁻²	160.9	3.7	2.3
<i>Z_1st Jan</i>	mmol C m ⁻²	42.6	2.5	5.8
<i>Zprot 1st Jan</i>	mmol C m ⁻²	6.5	0.4	6.2
<i>ZD</i>	h	3212.7	9.9	0.3
<i>S</i>	mmol C m ⁻²	9.9	0.4	3.8
<i>Sprot</i>	mmol C m ⁻²	8.1	0.3	3.6
<i>Slip</i>	mmol C m ⁻²	1.8	0.1	5.3
<i>SprotD</i>	h	3357.6	7.6	0.2
<i>SHD</i>	h	3256.0	0.9	0

Tab. 6.8 - Average value, s.d. and percentage variation from the mean. Where:

P: Annual maximum vertically integrated P biomass; *PD*: Hours since 1st Jan when max vertically integrated P biomass occurs; *Z*: Max vertically integrated Z biomass [lipid + protein]; *Zprot*: Max vertically integrated Z protein biomass; *Zlip*: Max vertically integrated Z lipid biomass; *Z_1st Jan*: Vertically integrated Z biomass [lipid + protein] on the 1st Jan; *Zprot_1st Jan*: Vertically integrated Z protein biomass on the 1st Jan; *ZD*: Hours since 1st Jan when max vertically integrated Z biomass occurs; *S*: Max vertically integrated S biomass [lipid + protein]; *Sprot*: Max vertically integrated S protein biomass; *Slip*: Max vertically integrated S lipid biomass; *SprotD*: Hours since 1st Jan when maximum S protein occurs; *SHD*: Hours since 1st Jan when squid hatching occurs.

6.1.2.2.1 Vertically integrated biomass of plankton

Fig.6.28-6.34 show the vertically integrated biomass of each population on attractor. Diatom had an average annual maximum biomass of 1696.5 mmol C m⁻² (s.d. 29.2 mmol C m⁻²; percentage variation from the mean = 1.7%; tab.6.8). Fig.6.30b shows the annual biomass of the diatom population. It can be seen that the maximum carbon biomass was reached on the 14th April each year (s.d. 17.7 hours; variation from the mean = 0.7%). From that date diatom biomass started to decline. Compared to its vertically integrated concentration (fig.6.15b), the summer (June-July) and autumn blooms (September-October) were less pronounced.

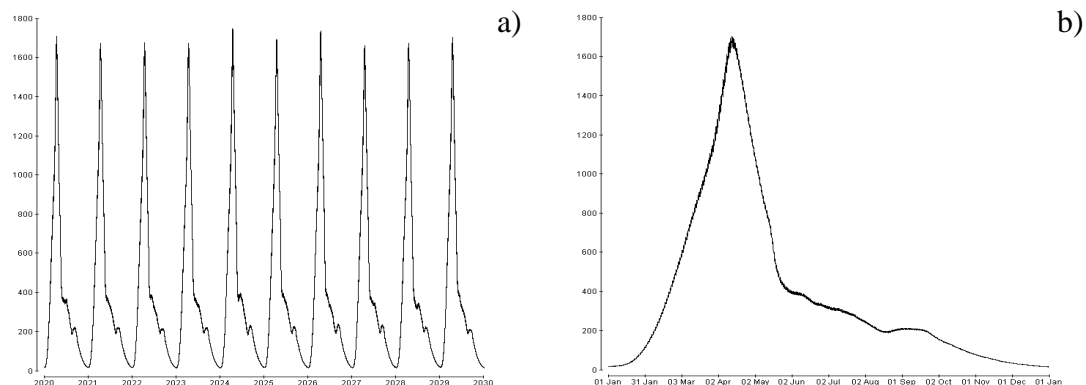


Fig 6.28 – Diatom total biomass (mmol C m⁻²)

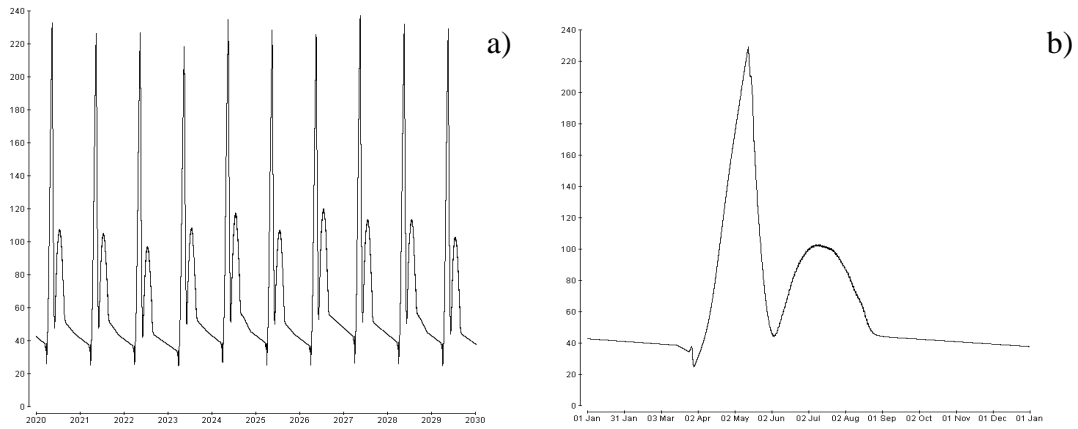


Fig 6.29 - Copepod total biomass – all stages (mmol C m^{-2})

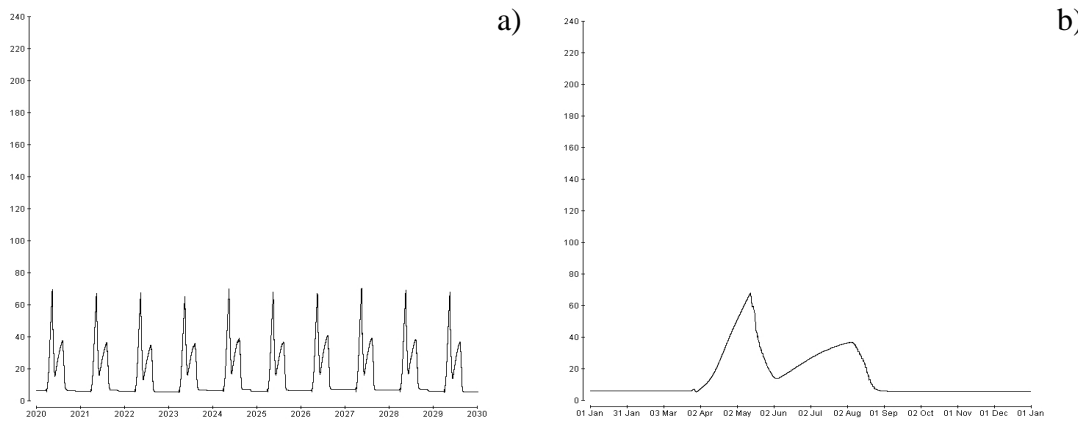


Fig 6.30 - Copepod protein biomass – all stages (mmol C m^{-2})

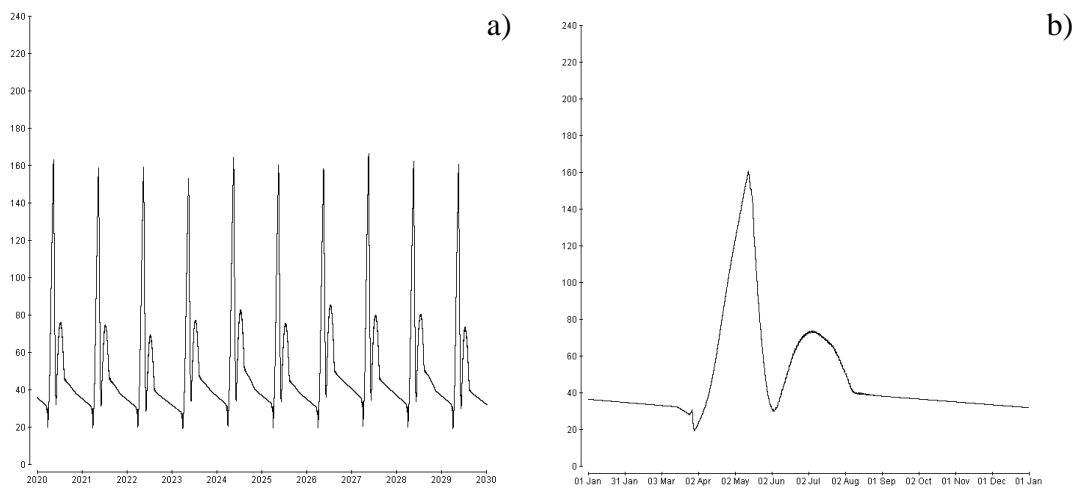


Fig 6.31 - Copepod lipid biomass – all stages (mmol C m^{-2})

Copepod biomass reached an average maximum annual value of $229.4 \text{ mmol C m}^{-2}$ (s.d. $9.7 \text{ mmol C m}^{-2}$; percentage variation from the mean = 2.3%; tab.6.8 and fig. 6.29) every year on the 13th May (s.d. 10 hours; percentage variation from the mean 0.3%). This date also coincides with the beginning of copepod reproduction. Then, newborn copepods are fiercely predated. The second peak in biomass consists of surviving copepods that are putting on weight, in terms of lipids, for pre-overwintering and a mixture of proteins and lipids for non-overwintering copepods trying to achieve reproduction. Protein biomass constituted about one third of the total copepod biomass (fig. 6.29-6.31 and tab.6.8).

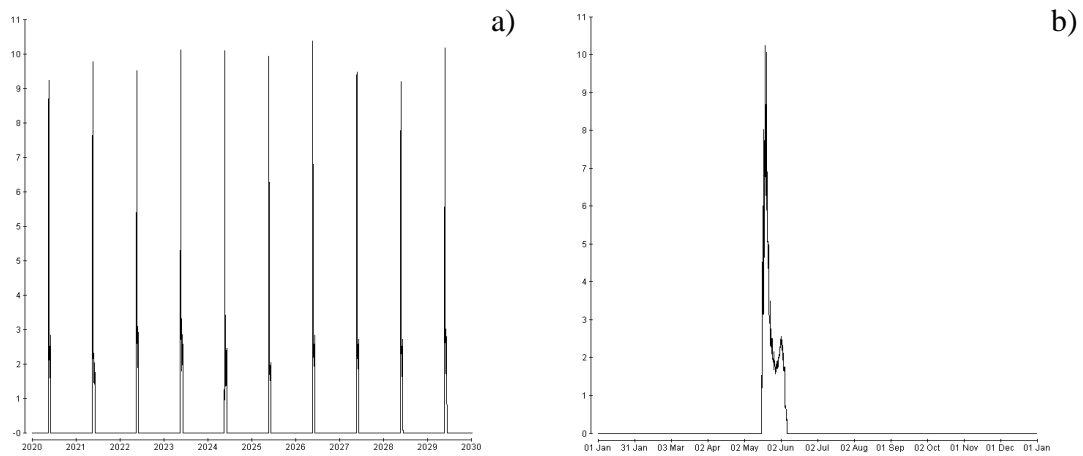


Fig 6.32 - Squid biomass – all stages (mmol C m^{-2})

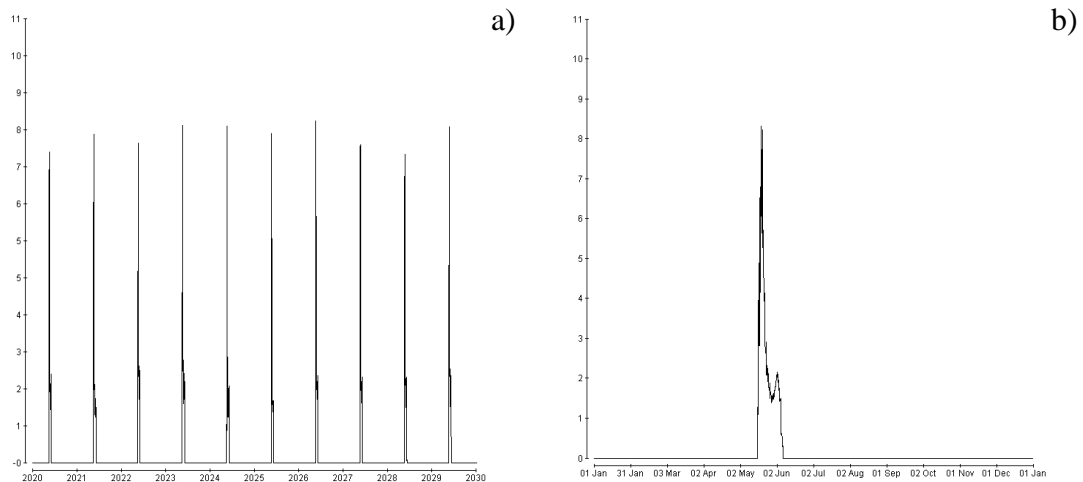


Fig 6.33 - Squid protein biomass – all stages (mmol C m^{-2})

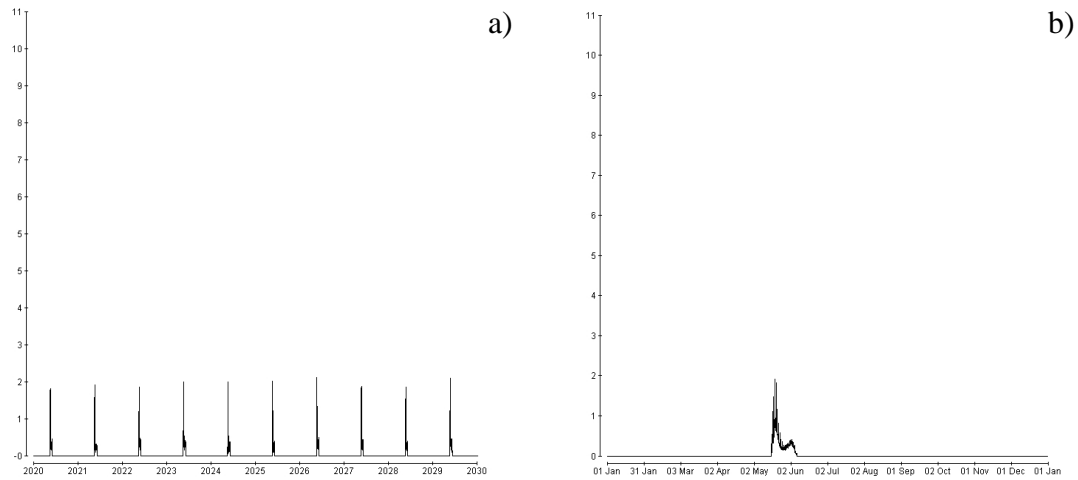


Fig 6.34 - Squid lipid biomass – all stages (mmol C m^{-2})

Squid hatched every year on the 15th May (s.d. 1 hour). The population biomass increased rapidly to a maximum of about 10 mmol C m^{-2} (s.d. 0.4; percentage variation from the mean = 2.3; tab.6.8), which was reached every year on the 20th May (s.d. 7.6 hours). Protein constituted over 80% of the total biomass (Fig. 6.32-6.34 and tab.6.8).

Fig. 6.35-6.36 provide further proof of the stability of the ecosystem. Every year the vertically integrated diatom and copepod biomass on a particular day was very similar in all ten years analyzed (fig.6.35). This is true also for the vertically integrated copepod and squid biomass on a particular day (fig.6.36).

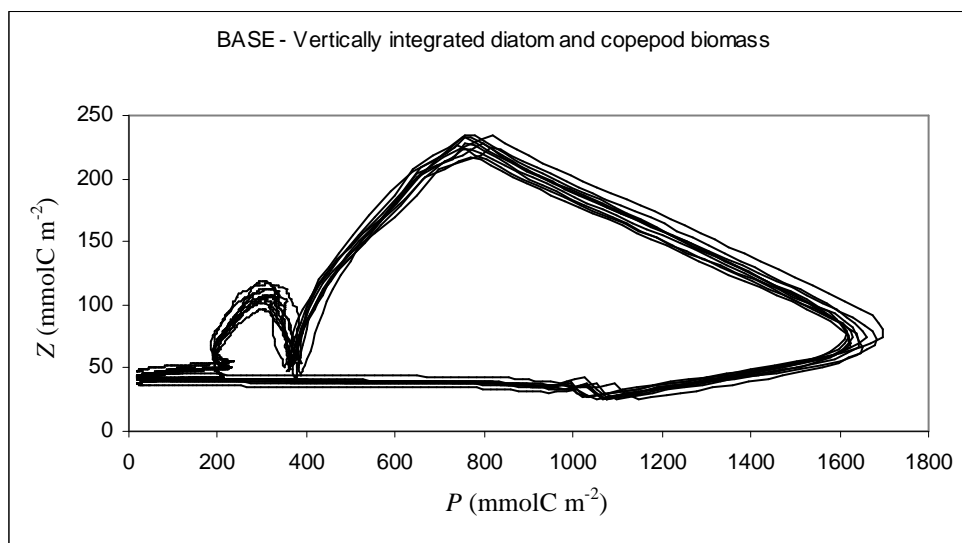


Fig. 6.35 – Poincaré map showing vertically integrated diatom and copepod biomass every day at 6am from 1st Jan 2020 to 31st Dec 2029.

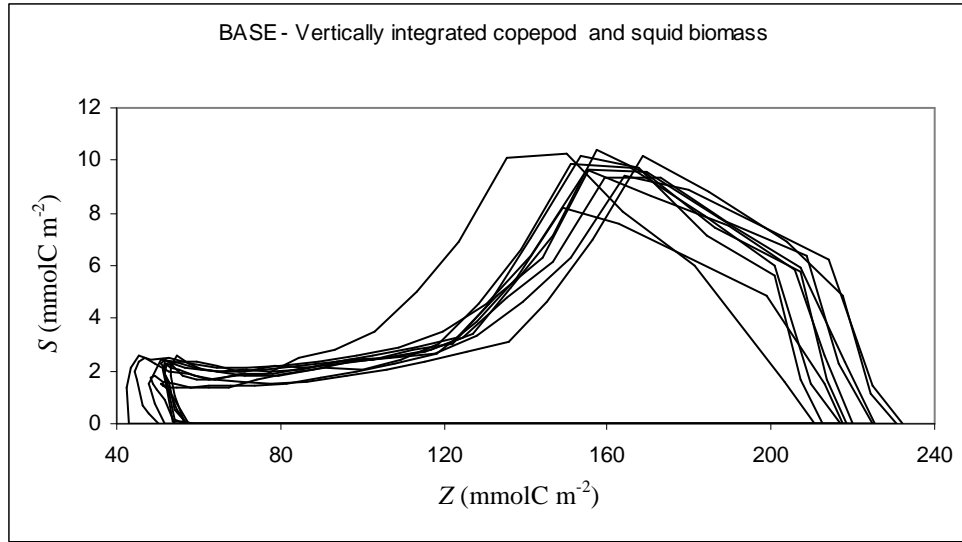


Fig. 6.36 – Poincaré map showing vertically integrated copepod and squid biomass every day at 6am from 15th May to 1st July of years 2020 to 2029 (anti-clokwise).

6.1.2.2.2 Carbon transfer through the trophic chain

Fig. 6.37-6.42 show the instantaneous carbon ingestion rate for all populations. Every year copepod ingested carbon from diatoms between the end of March and the beginning of September, with a peak in mid-May (fig.6.37). Squid carbon ingestion occurred throughout the period of their permanence in the mesocosm, between mid-May and the first week of June (fig.6.38). The carbon ingested by squid was composed in about equal parts of proteins and lipids (Fig.6.39-6.40).

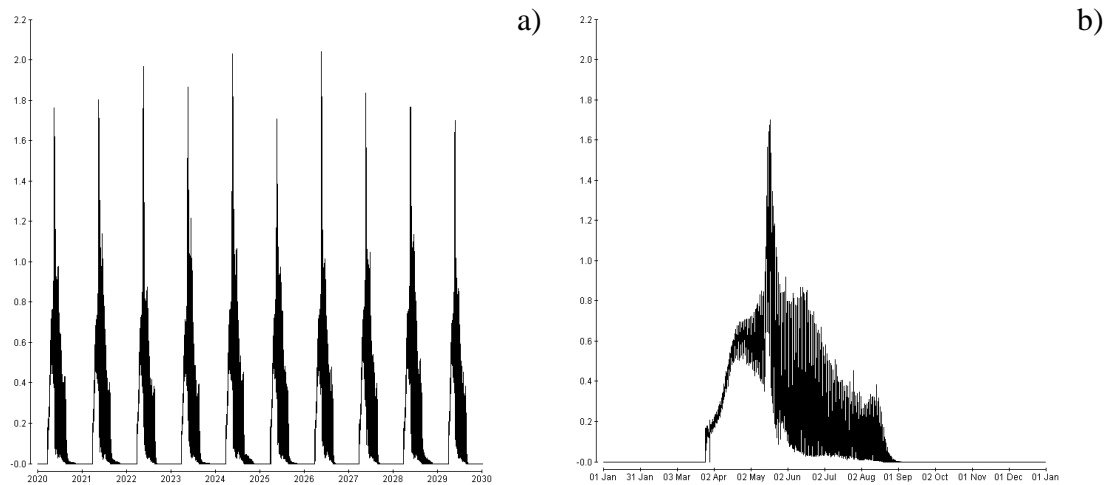


Fig 6.37 – Carbon ingested by copepods ($\text{mmol C m}^{-2} \text{ts}^{-1}$)

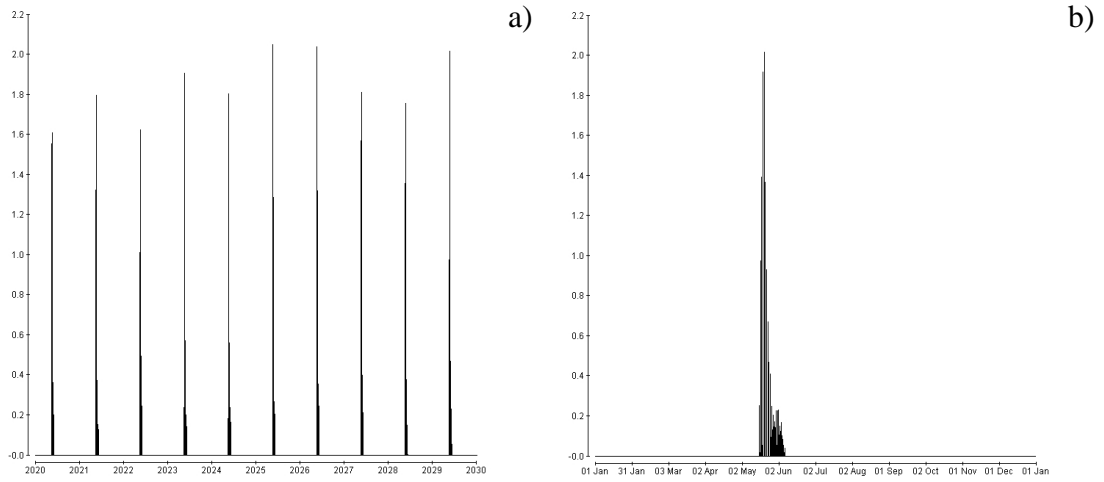


Fig 6.38 – Carbon ingested by squid (mmol C m⁻² ts⁻¹)

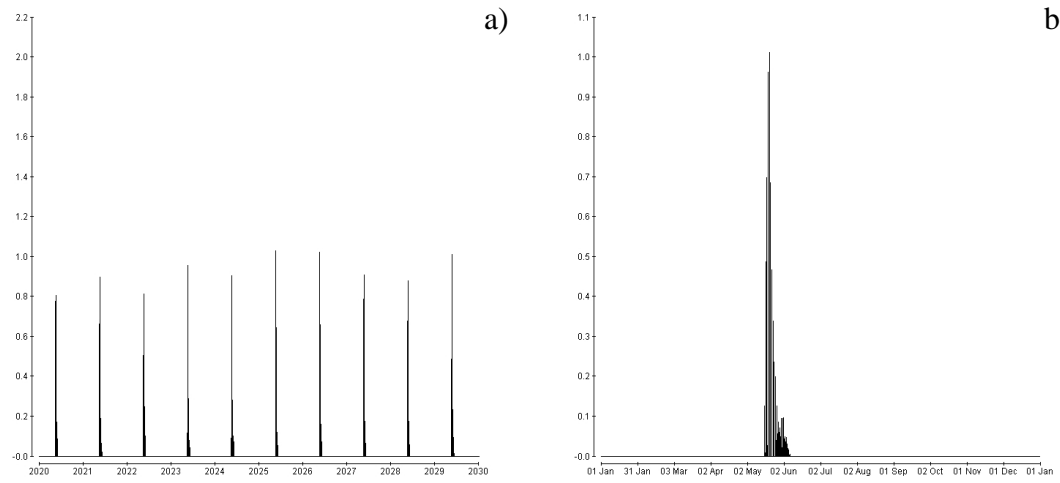


Fig 6.39 – Protein ingested by squid (mmol C m⁻² ts⁻¹)

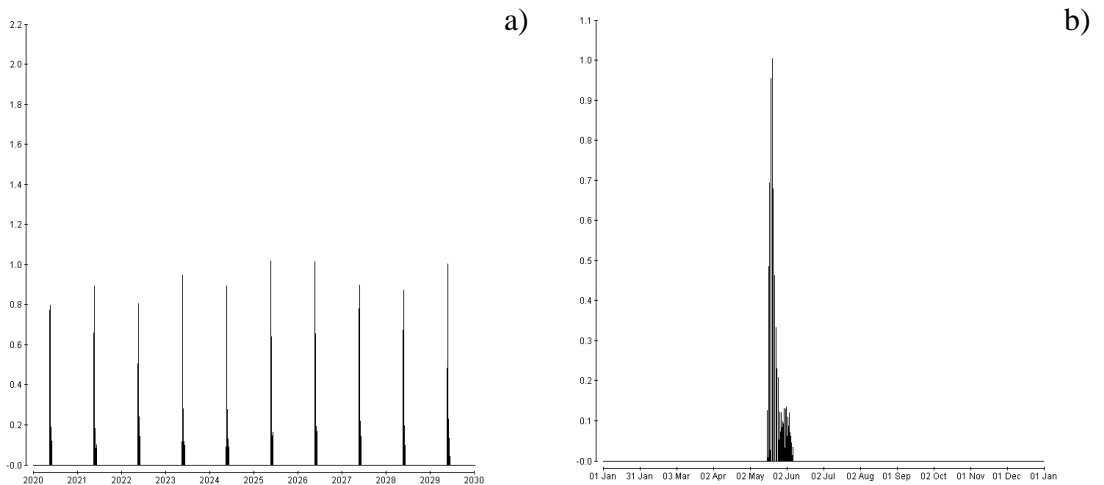


Fig 6.40 – Lipid ingested by squid (mmol C m⁻² ts⁻¹)

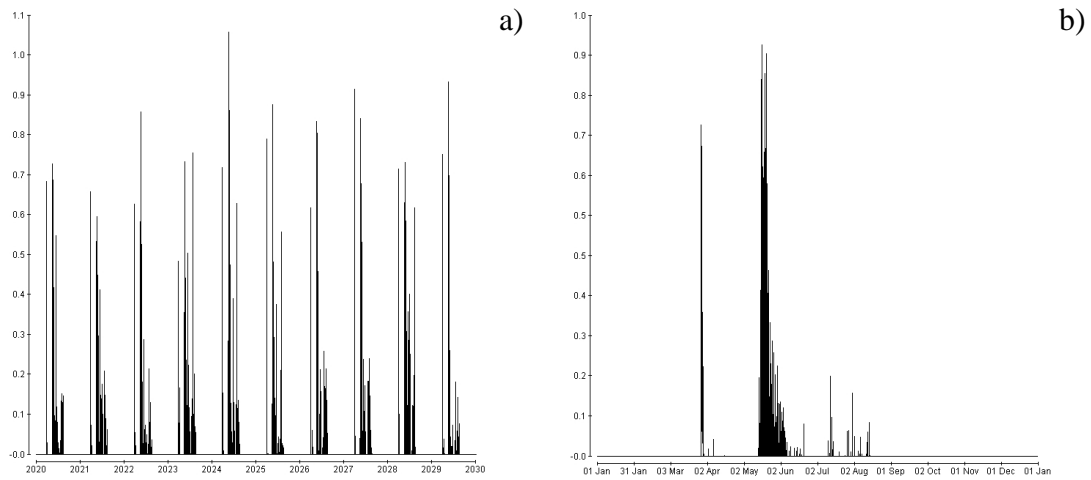


Fig 6.41 – Carbon ingested by basal predator feeding on copepods ($\text{mmol C m}^{-2} \text{ts}^{-1}$)

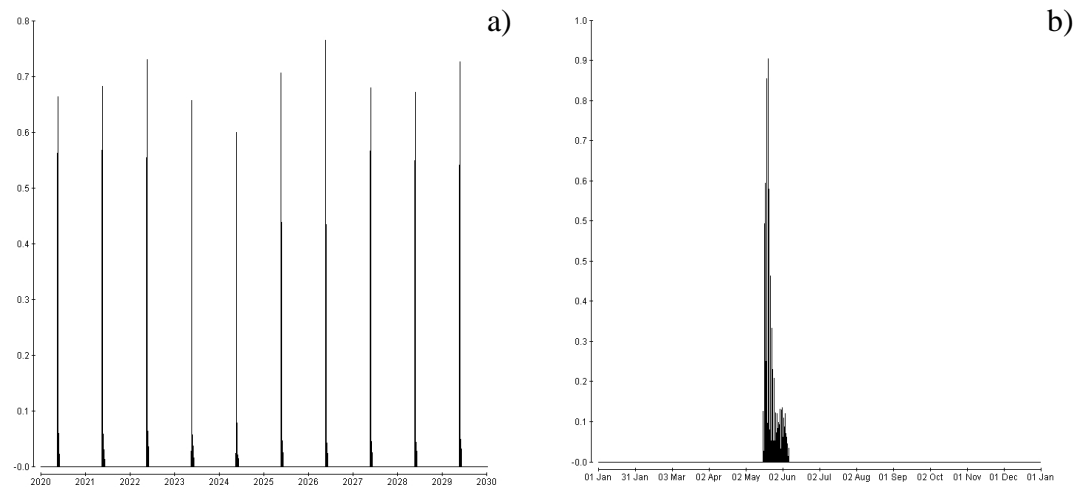


Fig 6.42 – Carbon ingested by predator feeding on squid ($\text{mmol C m}^{-2} \text{ts}^{-1}$)

Carbon ingestion rate by basal predator is concentrated between mid-May and July (fig.6.41). By comparing basal predator carbon ingestion rate (fig.6.41) and copepod ingestion rate (fig.6.23), it can be seen how ingestion before May and in July-August brought in more carbon per prey than in the period May-June. Visual predator carbon ingestion rate was obviously limited to the period of permanence of squid in the mesocosm and shows a major peak soon after squid hatching, and a second peak starting from the end of May (Fig.6.42).

Year	PingZ mmolC m ⁻² yr ⁻¹	ZingS mmolC m ⁻² yr ⁻¹	Zprot_ingS mmolC m ⁻² yr ⁻¹	Zlip_ingS mmolC m ⁻² yr ⁻¹	ZingBP mmolC m ⁻² yr ⁻¹	SingPred mmolC m ⁻² yr ⁻¹
2020	2592.5	21.6	9.8	11.8	57.5	22.2
2021	2559.8	20.1	9.1	11.0	63.1	22.0
2022	2440.6	22.6	10.2	12.4	56.1	23.0
2023	2549.2	23.0	10.2	12.8	65.6	22.6
2024	2780.4	20.8	9.4	11.4	74.1	22.1
2025	2562.1	20.9	9.2	11.7	65.4	22.6
2026	2666.3	23.8	10.6	13.2	66.8	23.4
2027	2645.4	23.4	10.3	13.1	64.4	22.7
2028	2684.9	21.7	9.9	11.8	66.4	22.7
2029	2437.0	23.2	10.3	12.9	53.9	22.8
Ave	2591.8	22.1	9.9	12.2	63.3	22.6
s.d.	107.1	1.2	0.5	0.8	6.0	0.4
% var	4.1	5.6	5.2	6.2	9.5	1.9

Tab. 6.9 – Carbon transfer through the trophic chain. Where:

PingZ = Carbon ingested annually by copepods; ZingS = Carbon ingested annually by squid; Zprot_ingS = Protein ingested annually by squid; Zlip_ingS = Lipid ingested annually by squid; ZingBP = Carbon ingested annually by basal predator; SingPred = Carbon ingested annually by visual predator.

The amount of carbon transferred from diatoms to copepods was on average 2,592 mmolC m⁻² yr⁻¹ (s.d. 107 mmolC m⁻² yr⁻¹; percentage variation from the mean = 4.1 %; tab.6.9). The average carbon transferred annually from copepod to predators was 85.4 mmol C m⁻² yr⁻¹. Squid ingested 22 mmolC m⁻² yr⁻¹ (s.d. 1.2 mmolC m⁻² yr⁻¹; percentage variation from the mean = 5.6 %; tab.6.9), of which about 10 mmolC m⁻² yr⁻¹ was made up protein. The remaining 63.3 mmol C m⁻² yr⁻¹ (s.d. 6 mmolC m⁻² yr⁻¹; percentage variation from the mean = 9.5 %; tab.6.9) was ingested by the basal predator. Visual predator ingested on average 22.6 mmolC m⁻² yr⁻¹ from the squid biomass (s.d. 0.4 mmolC m⁻² yr⁻¹; percentage variation from the mean = 1.9 %; tab.6.9).

6.1.2.3 Number of agents

The number of diatom agents varied between about 2,100-4,500. On the 1st January the population of diatom was represented by 3,600. It dropped to about 3,000 in the beginning of February and then increased gradually to annual average maximum of about 4,700 in the beginning of April. It then dropped sharply to the annual average minimum of about 2,100 agents in the beginning of May and gradually increased to about 3,600 agents until the 1st January of the following year (fig.6.43).

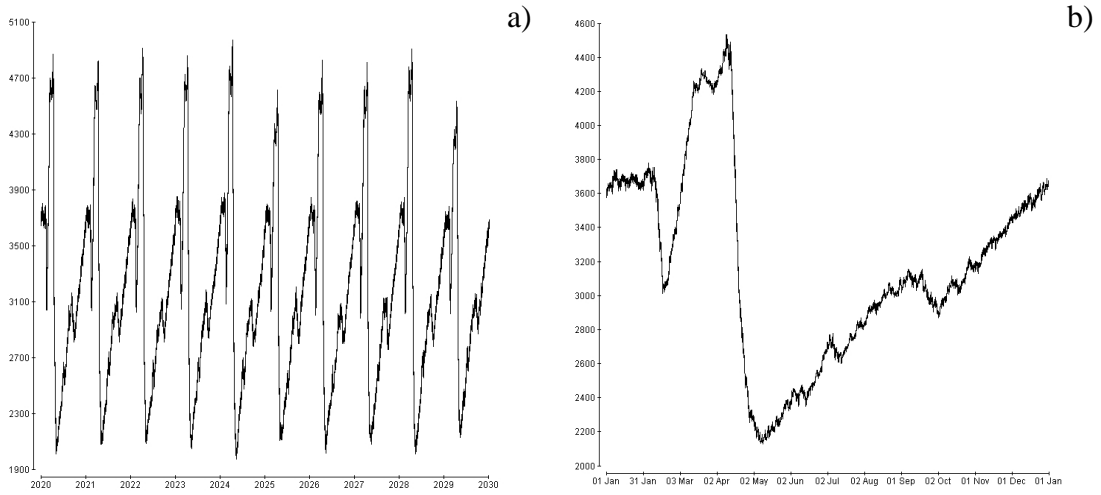


Fig 6.43 - Number of diatom agents

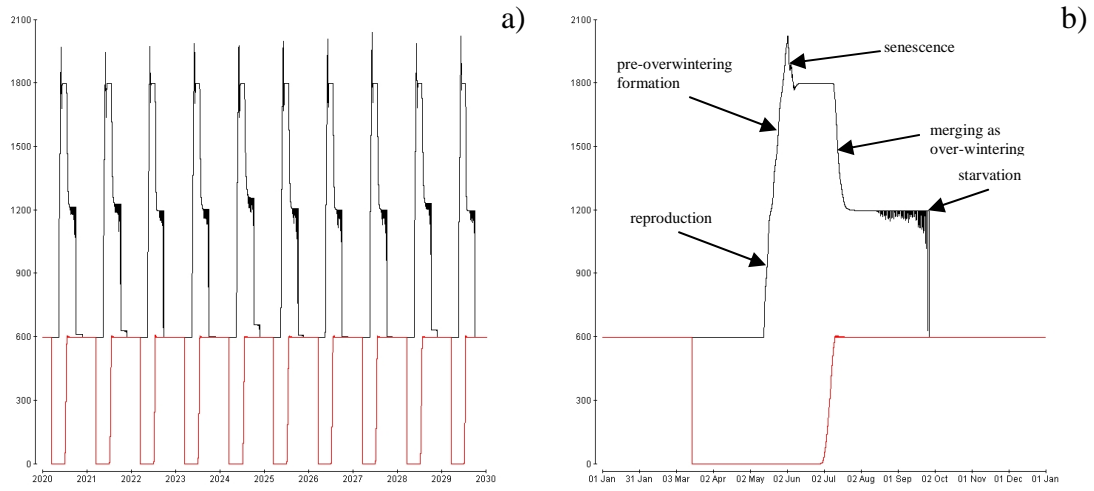


Fig 6.44 - Number of copepod agents. Red: over-wintering. Black: all other stages.

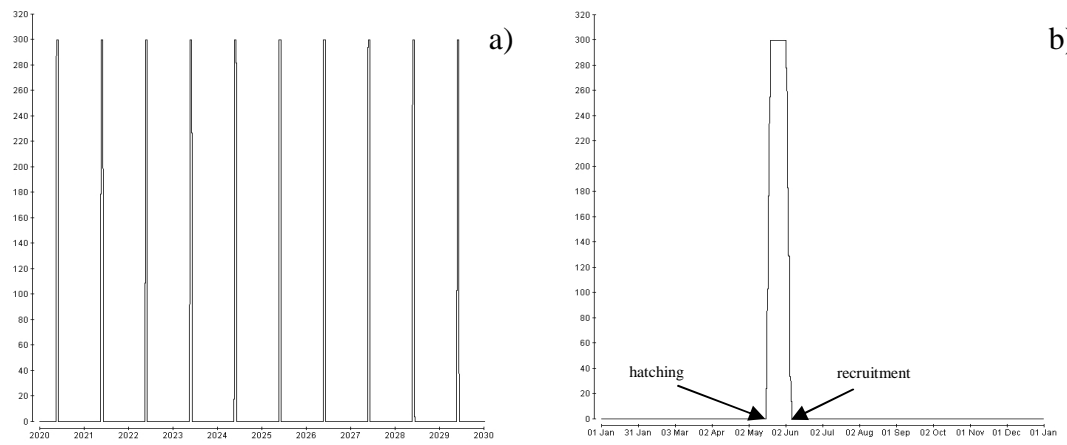


Fig 6.45 - Number of squid agents S1-S6

The number of copepod agents increased in May from 600 to about 2,000. In the beginning of June it dropped to 1,800. In the beginning of July it dropped to 1,200, and eventually to 600 agents in the end of September. From October to March the entire copepod population was represented by 600 agents (fig.6.44). The number of squid agents in stage S1-S6 increased to 300 in mid-May and dropped to zero during the first week of June (fig.6.45).

6.1.2.4 Physical environment

	Units	Year 16-25		
		Ave	s.d.	% var
MLD_{max}	m	155.9	4.4	2.8
$T_{min}[0]$	°C	14.5	0.01	0.1
$T_{max}[0]$	°C	29.3	0.1	0.3
$Si[0]$	mmol Si m ⁻³	1.7	0.1	4.5

Tab. 6.10 – Surface minimum and maximum average temperature and annual average maximum mixed layer depth, standard deviation and percentage variation from the average. Where:

MLD_{max} : Annual maximum mixed layer depth;

$T_{min}[0]$ and $T_{max}[0]$: Annual minimum and maximum average surface temperature.

Mixed layer depth varied seasonally (fig.6.46) reaching its average annual maximum depth of about 156 m (s.d. 4.4 m; percentage variation from the mean = 2.8 %; tab.6.10) every year in mid-March. The average sea surface temperature varied from an annual minimum of 14.5°C (s.d. 0.01°C; percentage variation from the mean = 0.1 %; tab.6.10) in March to an annual maximum of 29.3 °C (s.d. 0.1°C; percentage variation from the mean = 0.3 %; tab.6.10) in August (fig.6.47).

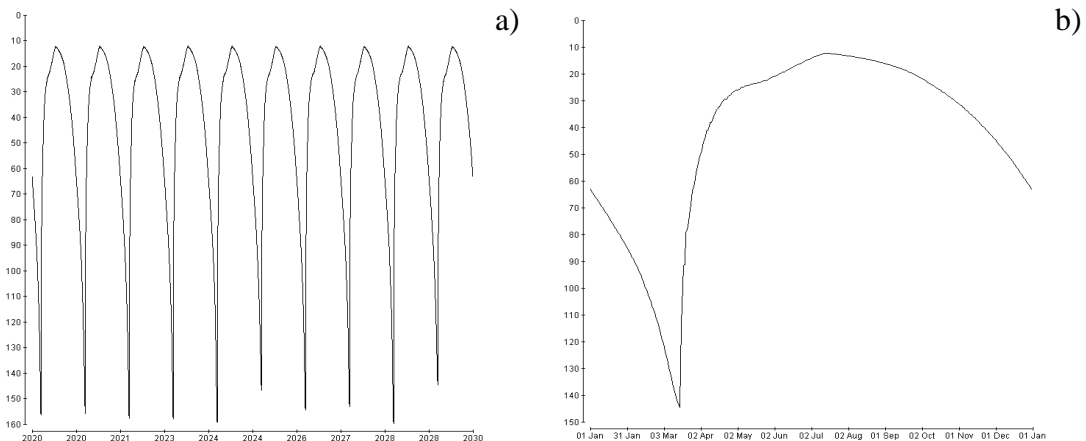


Fig 6.46 – Mixed layer depth at 6am (m)

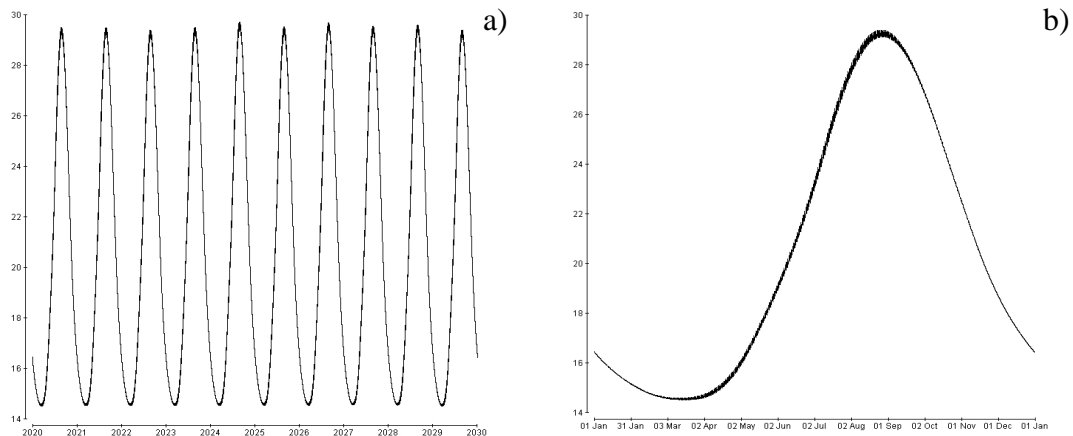


Fig 6.47 – Surface temperature (°C)

6.1.2.5 Chemical environment

	Units	Year 16-25		
		Ave	s.d.	% var
N [0]	mmol N m ⁻³	6.0	0.1	2.3
Si [0]	mmol Si m ⁻³	1.7	0.1	4.5

Tab. 6.11 – Surface nutrients average concentration, standard deviation and percentage variation from the average. Where: N[0]: Maximum dissolved N concentration at surface; Si[0]: Maximum dissolved Si concentration at surface.

The total mesocosm nitrogen, comprising particulate and dissolved nitrogen, showed a positive drift (fig.6.48), increasing by about 0.35 mmol N m⁻² annually. Conversely, the total mesocosm silicate decreased by about 0.1 mmol Si m⁻² annually (fig.6.49).

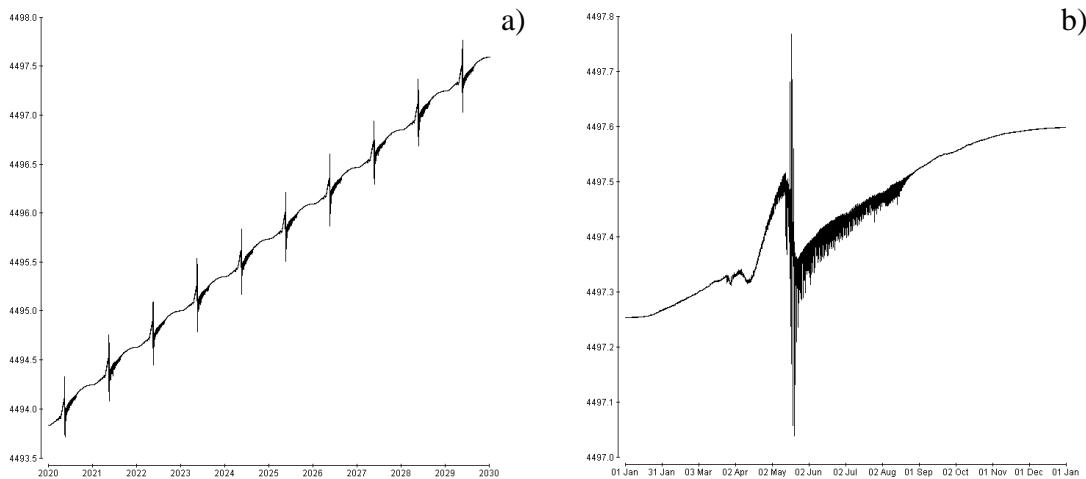


Fig 6.48 –Total mesocosm nitrogen (dissolved + particulate) (mmol N m⁻²)

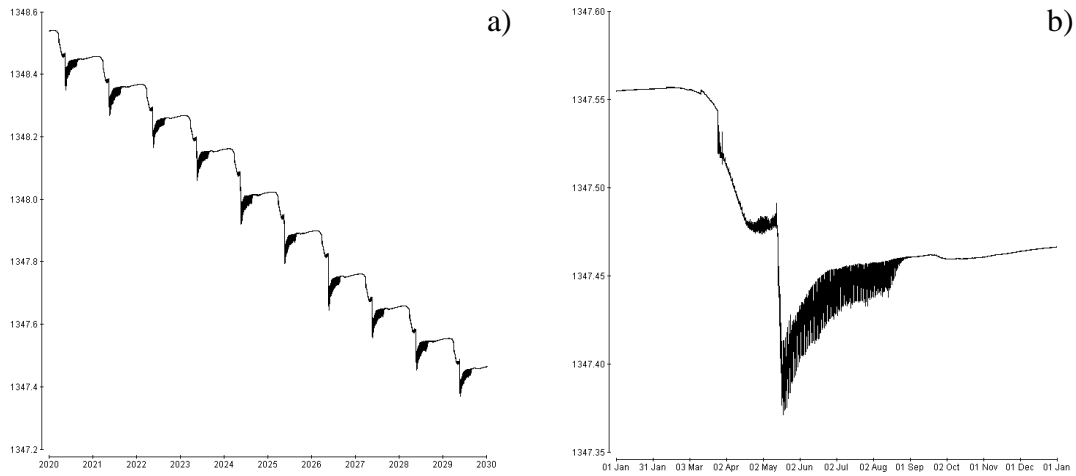


Fig 6.49 – Total mesocosm silicon (dissolved + particulate) (mmol Si m^{-2})

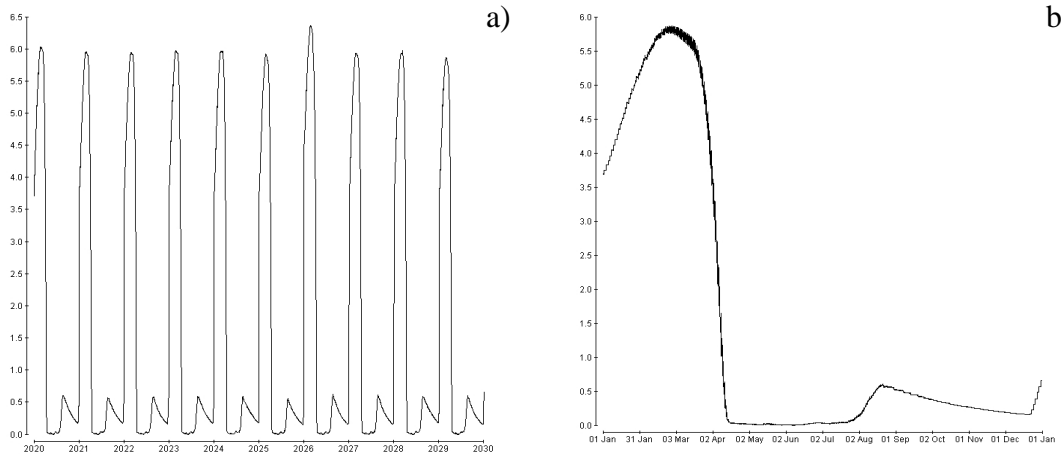


Fig 6.50 – Surface dissolved nitrogen (mmol N m^{-3})

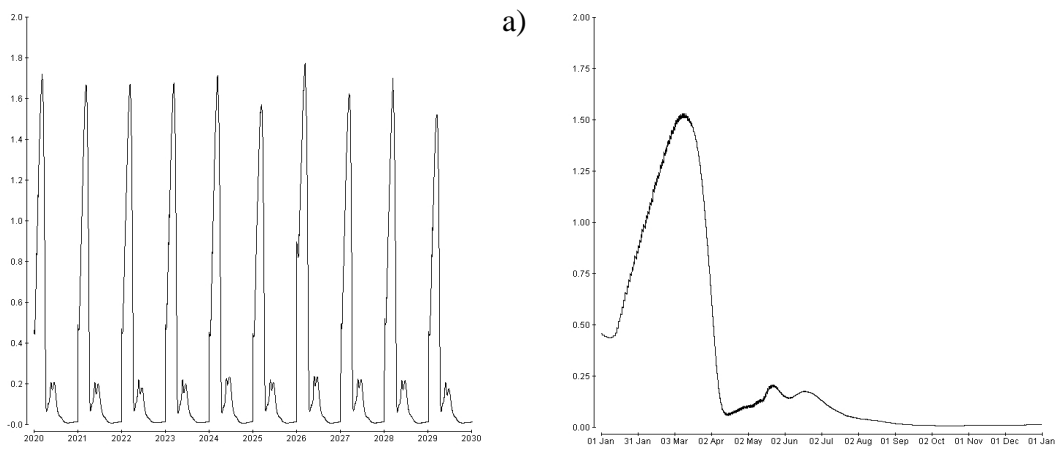


Fig 6.51 – Surface dissolved silicon (mmol Si m^{-3})

Sea surface dissolved nitrogen and silicate concentrations increased until the beginning of March as the depth of the mixed layer reached the annual maximum bringing extra nutrients (Fig. 6.46, 6.50-6.51). Dissolved nitrogen and silicate reached an average maximum surface concentration of $6.0 \text{ mmol N m}^{-3}$ and $1.7 \text{ mmol Si m}^{-3}$ respectively (Tab.6.11). Their inter-annual variation was small (for nitrogen, s.d. $0.1 \text{ mmol N m}^{-3}$; percentage variation from the average = 2.3%; for silicate, s.d. $0.1 \text{ mmol Si m}^{-3}$; percentage variation from the average = 4.5%; tab.6.11). The dissolved concentration of nutrients in the mixed layer increases from May to July for silicate and from July to August for nitrogen. On the 1st January nutrients lost from the annual maximum mixed layer are re-injected in the surface (chemical conservation rule, § Appendix V). Fig.6.52 and 6.53, show that the silicate nutricline is subducted from the mixed layer at a depth of about 50m as it gets exhausted from the surface water in the beginning of April. The nitrogen nutricline is subducted at a depth of about 35m, as it gets exhausted a few days after silicate. Fig.6.54 shows the formation and sinking of the deep chlorophyll maximum. Its depth ranges from about 40-80 m between May and June, sinking at a rate of almost 10 m per month, reaching a depth 50-100 m between August and September.

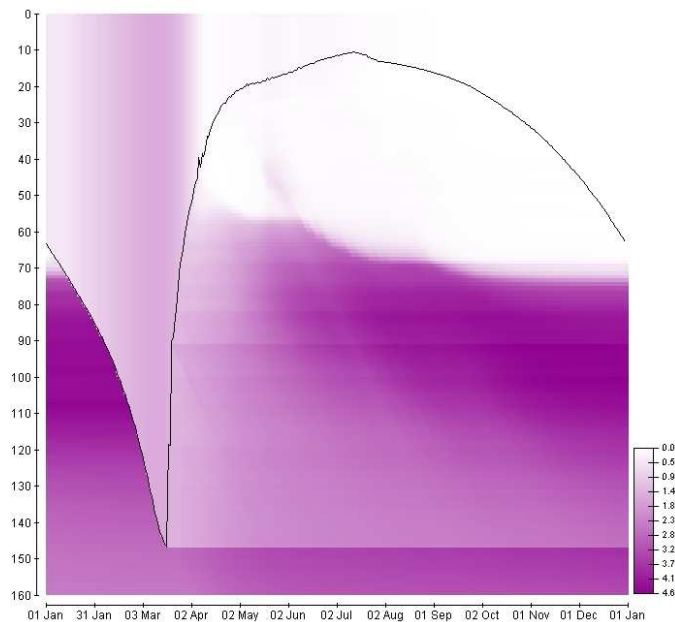


Fig 6.52 –Silicate in the top 160 m (mmol Si m^{-3}) and the mixed layer depth at 7am (black line)

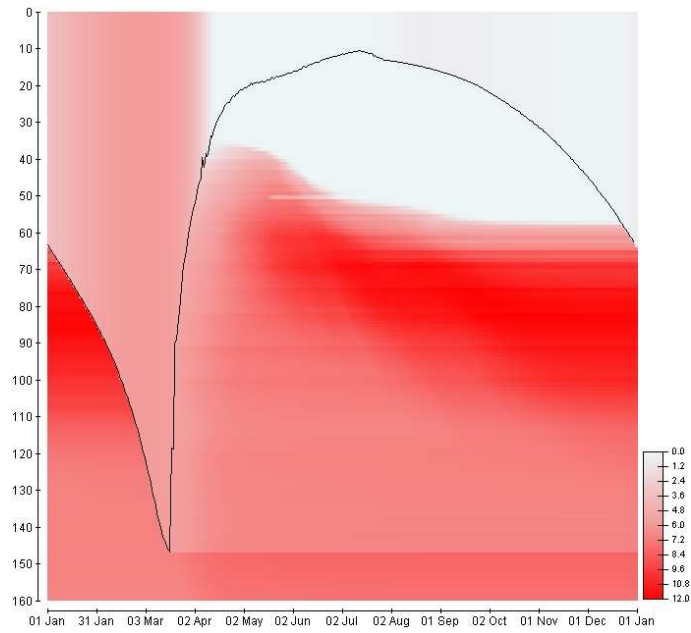


Fig 6.53 – Nitrogen in the top 160 m (mmol Si m^{-3}) and the mixed layer depth at 7am (black line)

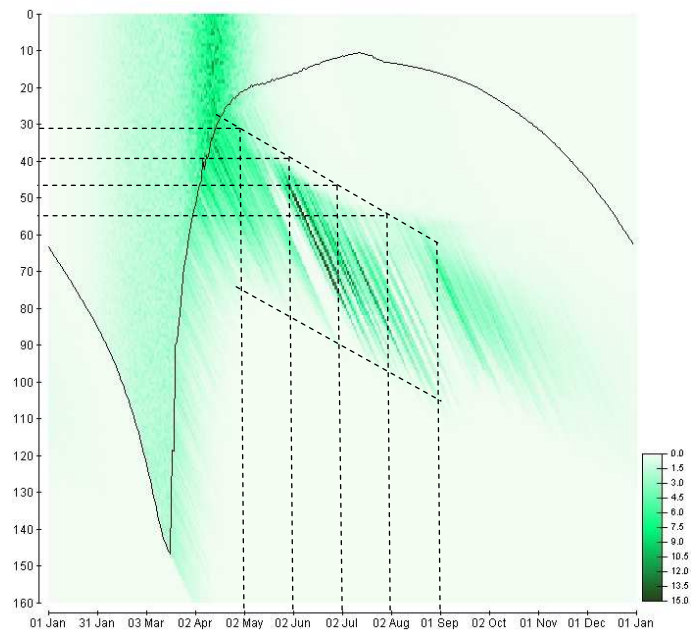


Fig 6.54 – Chlorophyll in the top 160 m (mmol Si m^{-3}) and the mixed layer depth at 7am (black line)

6.2 Ergodicity

a)	Seed numbers										
Year	16628	19856	30640	33485	43833	54498	61663	72824	Ave	s.d.	% Var
2020	4.29	3.71	3.98	4.05	4.35	5.02	3.77	5.05	4.28	0.52	12.10
2021	3.75	5.38	3.12	4.74	3.36	3.35	3.68	4.17	3.95	0.78	19.70
2022	5.14	3.82	4.37	3.71	3.52	4.39	3.06	4.29	4.04	0.64	15.94
2023	5.21	3.67	3.80	4.70	4.48	4.16	3.33	4.66	4.25	0.63	14.76
2024	5.15	4.31	3.61	4.83	4.40	4.92	4.36	4.34	4.49	0.48	10.63
2025	4.35	5.28	3.63	4.03	3.83	4.40	4.30	4.65	4.31	0.51	11.87
2026	3.90	4.37	3.34	5.02	3.07	4.74	3.98	6.04	4.31	0.96	22.23
2027	4.95	4.82	3.72	4.84	3.63	4.69	3.94	4.51	4.39	0.54	12.28
Ave	4.59	4.42	3.70	4.49	3.83	4.46	3.80	4.71	4.25	0.63	14.94
SD	0.59	0.68	0.38	0.48	0.53	0.53	0.45	0.60			
% Var	12.89	15.46	10.31	10.80	13.72	11.94	11.78	12.78			
t-test	0.55	0.91	0.03	0.71	0.05	0.83	0.06	0.30			

Tab. 6.12 – Ergodicity experiment results: inter-annual (2020-2027) and inter-instance variation in recruitment

The biomass of diatoms, copepods and squid were taken from an ensemble of 8 runs with different seeds, started from a simulation that had settled on an attractor after 15 years. The successive 8 years were considered. Results from a students t-test show that recruitment inter-annual (years 2020-2027) and inter-instance (year 2027) variation are not significantly different at least at the 3% significance level (tab.6.12). The daily (1st Jan - 31st Dec) diatom, copepod and squid biomass averaged over the period 2021-2030 (excluding leap years:2024 and 2028) for one instance of the VE (seed 43833) and averaged over the eight different instances of the VE for the period 1st Jan 2027 to 31st Dec 2027 overlap almost perfectly (fig.6.55a-6.57a). The inter-annual variation (2021-2030, excluding 2024 and 2028) from the average for the single instance (seed 43833), and the inter-instance variation for a single year (year 2027) for diatom biomass (fig.6.55b), copepod biomass (fig.6.56b) deviate from the average at some time during the year by not more than 3%. The maximum squid biomass deviation from the average is about 25%, and occurs during the periods of squid immigration and emigration from the mesocosm (fig.6.57b). Results from paired students t-test comparing the inter-instance (8 instances, year 2027, tab.6.13a) and the inter-annual (1 instance: seed 43833, years 2021-2030, excl.2024 and 2028, tab.6.13b) diatom, copepod and squid biomass on the 28th May reveal that they are not significantly different at the 3%, 97% and 20% respectively (tab.6.13c). The same analysis as in section 6.1.1.2 was performed, but the sample data were standardised by subtracting the last 10 years mean in the base run and dividing by the inter-instance standard deviation and distributed in 18 bins (tab.6.14). Results from a chi-squared test for normal

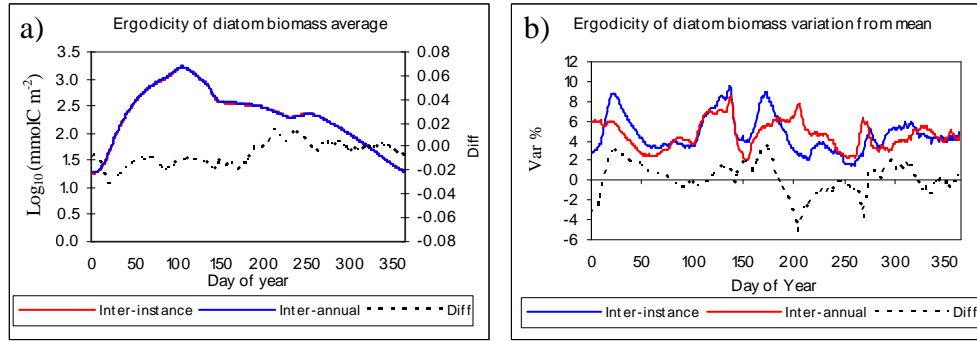


Fig 6.55 – Ergodicity of P biomass every day at 6 am: a) Inter-annual average 2021-2030 (seed 43833) and inter-instance average in 2027 (8 instances); b) Inter-annual variation 2021-2030 (seed 43833) and inter-instance in 2027 (8 instances)

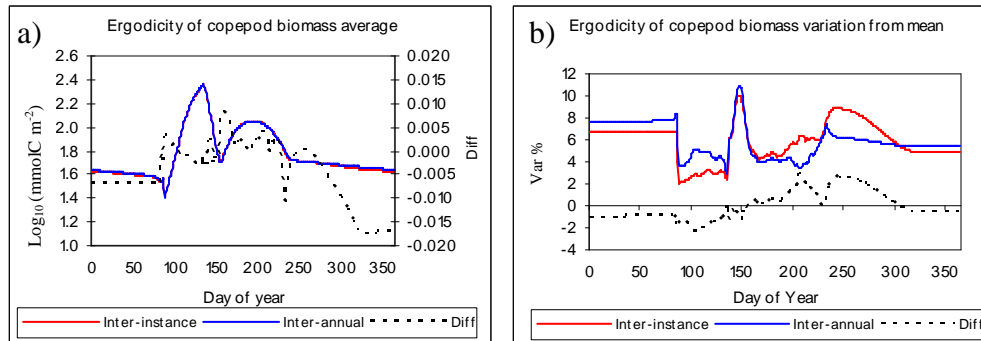


Fig 6.56 – Ergodicity of Z biomass every day at 6 am: a) Inter-annual average 2021-2030 (seed 43833) and inter-instance average in 2027 (8 instances); b) Inter-annual variation 2021-2030 (seed 43833) and inter-instance in 2027 (8 instances)

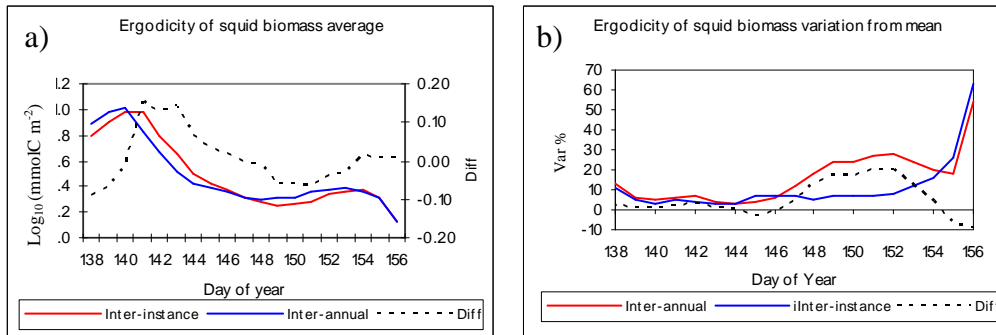


Fig 6.57 – Ergodicity of S biomass every day at 6 am: a) Inter-annual average 2021-2030 (seed 43833) and inter-instance average in 2027 (8 instances); b) Inter-annual variation 2021-2030 (seed 43833) and inter-instance in 2027 (8 instances)

a)	Seed #	(28-May-2027)								Ave	s.d.	Var
	16628	19856	30640	33485	43833	54498	61663	72824				
P	376.9	396.4	379.3	387.1	407.9	402.7	361.2	403.8	389.4	16.2	4.2	
Z	75.4	91.4	95.2	80.3	96.4	78.2	95.5	81.5	86.7	8.7	10.1	
S	2.3	2.0	1.7	1.4	2.1	1.7	2.4	1.7	1.9	0.3	17.6	
b)	28-May	(Seed: 43833)								Ave	s.d.	Var
	2021	2022	2023	2025	2026	2027	2029	2030				
P	412.8	392.1	400.3	417.7	405.3	407.9	381.1	409.2	403.3	11.8	2.9	
Z	86.9	83.3	87.8	68.8	100.0	96.4	82.5	89.4	86.9	9.5	10.9	
S	2.1	2.3	2.0	1.9	2.3	2.1	1.9	2.0	2.1	0.1	6.7	
c)	T-test significance level											
P	0.04											
Z	0.97											
S	0.20											

Tab.6.13 – a) Inter-instance biomass variation for P,Z and S on 28 May 2027 at 6am; b) Inter-annual biomass variation for P,Z and S on 28 May 2021-2030, (2024-2028 excluded; seed 43833); c) T-test results comparing the similarity of inter-annual and inter-instance P,Z,S biomass on 28th May

distribution revealed that the error distribution of all variables, apart from *S* (sign=0.0003), approximates a normal distribution at least at the 0.01 significance level (tab.6.14). In the case of *P,Z* and *P,Z* errors are not normally distributed around the inter-annual mean of the base run, showing an higher kurtosis, which is indicative of low variation from the inter-annual mean in the base run.

# s.d. from mean	Gaussian	<i>P</i>	<i>Z</i>	<i>S</i>	<i>P</i>	<i>Z</i>	<i>S</i>
(-4.0,-3.5)	0.0	0	0	0	0	0	0
(-3.5,-3.0)	0.1	0	0	0	0	0	0
(-3.0,-2.5)	0.5	0	0	0	0	0	0
(-2.5,-2.0)	1.6	0	0	0	0	0	2
(-2.0,-1.5)	4.3	0	0	2	0	0	4
(-1.5,-1.0)	9.1	2	0	4	0	0	6
(-1.0,-0.5)	15.1	14	2	26	12	2	14
(-0.5,0.0)	19.3	28	4	36	24	8	4
(0.0,0.5)	19.3	38	14	16	30	10	10
(0.5,1.0)	15.1	8	16	6	22	34	22
(1.0,1.5)	9.1	4	30	10	10	34	24
(1.5,2.0)	4.3	4	22	0	2	8	8
(2.0,2.5)	1.6	2	8	0	0	2	4
(2.5,3.0)	0.5	0	2	0	0	2	2
(3.0,3.5)	0.1	0	2	0	0	0	0
(3.5,4.0)	0.0	0	0	0	0	0	0
n	100						
χ^2		20.46	31.9	41.51	14.96	28.44	15.7
Significance		0.25	0.02	0.0003	0.60	0.04	0.5

Tab.6.14 – Error frequency distribution (%) of *P,Z,S,P,Z,S*. Each bin represents a half s.d. range.

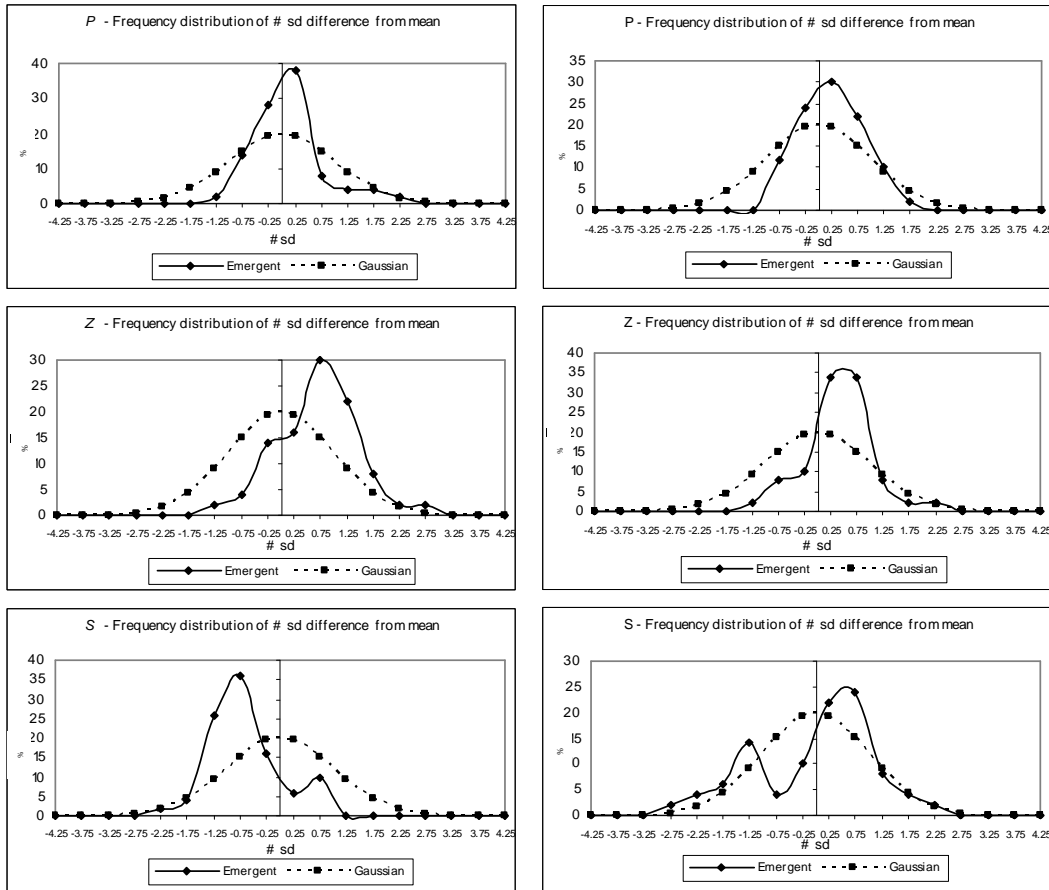


Fig.6.58 – Error frequency distribution (%) of *P,Z,S* on the 28th May.

Fig.6.59 – Error frequency distribution (%) of *P,Z,S* on the 28th May.

6.3 Sensitivity of stability

Run	Av. Recr.	s.d.	% var	
BASE	4.0	0.5	12.2	
CHEMICALS				
DOUBLE Si	Y: 2020-2030	5.2	3.4	65.0
	Y: 2021-2031	4.4	0.7	16.7
DoubleN (results not shown. Comments in discussion)		4.8	0.8	24.3
COMPETITION				
DOUBLE BP		3.1	0.5	17.0
PREDATION				
DOUBLE PRED		1.7	0.5	30.4

Tab. 6.15 – Sensitivity of stability experiment results

6.3.1 Doubling the 1st Jan dissolved silicate concentration

Restarted from a VE snapshot on the 1st Jan 2015 of the base run. On the 1st January 2015 the initial silicate profile of the ecosystem on attractor was doubled from 0.6 mmol Si m⁻³ to 1.2 mmol Si m⁻³. The simulation was allowed to adjust to its new attractor for 5 years before analysing the final 10 years of the VE.

6.3.1.1 Vertically integrated concentration of plankton

	Units	Year 16-25		
		Ave	s.d.	% var
P	ind m ⁻²	9.6×10 ¹⁰	2.0×10 ⁹	2.1
Z	ind m ⁻²	155618.7	8870.6	5.7
Z _{ow}	ind m ⁻²	8309.2	440.1	5.3
S	ind m ⁻²	147.0	5.3	3.6
SHD	h	3258.3	3.0	0.05
R1	ind m ⁻² yr ⁻¹	5.2	3.4	65.1
R2	ind m ⁻² yr ⁻¹	4.4	0.7	16.7

Tab. 6.16 - Average value, s.d. and percentage variation from the mean for years 2021-2031. Where:

P: Max P concentration; Z: Max Z concentration; Z_{ow}: Max concentration of over-wintering copepods; S: Max S concentration; SHD: Hours since 1st Jan when squid hatching occurs; R1: total number of squid that reached stage 7 between 2020-2030; R2: total number of squid that reached stage 7, between 2021-2031.

Fig. 6.60-6.62 show the vertically integrated concentration of the explicitly modeled populations. Year 2020 exhibited an extremely high squid recruitment compared with all successive years. In 2020, the annual recruitment was almost 15 ind m⁻², while the average between 2021-2031 was 4.4 ind m⁻² yr⁻¹ (s.d. 0.7 ind m⁻² yr⁻¹; percentage variation from the mean of 16.7%; fig.6.62 and tab.6.16). This high recruitment had good reasons to occur, as explained in section 6.3.1.7, but for the stability analysis it will be discarded. The ten year analysis will be performed using years 2021-2031. In that period, diatom had an average annual maximum concentration of 9.6×10¹⁰ ind m⁻² (s.d. 2.0×10⁹ ind m⁻²; percentage variation from

the mean was 2.1; tab.6.16 and fig.6.60), which is slightly higher than its annual maximum in the base run (tab.6.5).

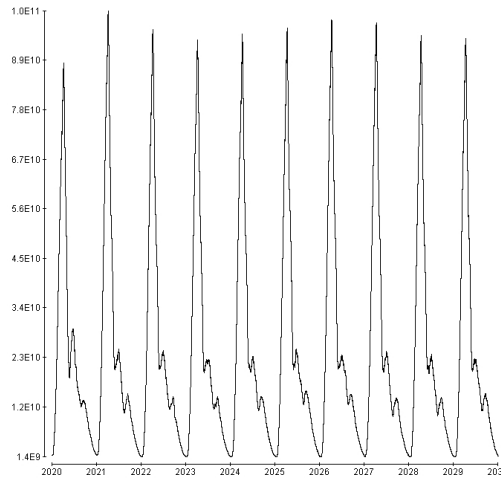


Fig. 6.60 - Vertically integrated P concentration (ind m⁻²)

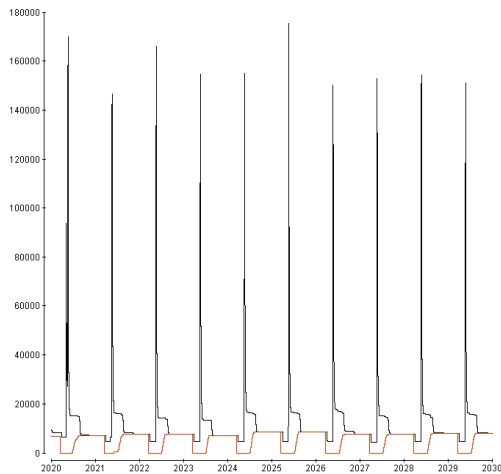


Fig. 6.61 - Vertically integrated copepod concentration (black:all stages; red:over-wintering - ind m⁻²)

Contrary to all years in the base run and all the successive years, in 2020 the copepod population in January is not exclusively made up of over-wintering copepods (fig. 6.61). On the 1st January, 9,600 copepods were present in the mesocosm. Of these, only 7,140 were over-wintering, the rest were made up by copepods that failed to enter overwintering in the previous year, and managed to survive through the winter feeding on the reduced diatom winter population. The average annual peak in copepod concentration was slightly below 155,600 ind m⁻² (s.d. 8,870 ind m⁻²; percentage variation from the average = 5.7%; tab.6.16).

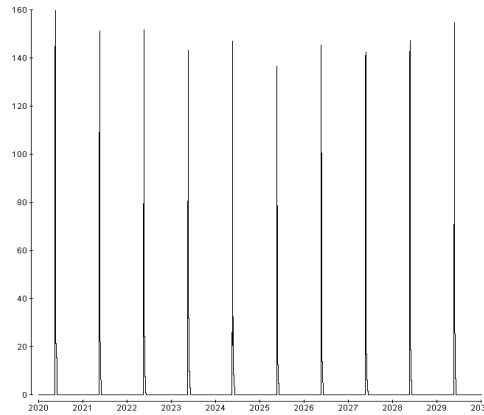


Fig. 6.62 - Vertically integrated concentration of squid (S1-S6 - ind m⁻²)

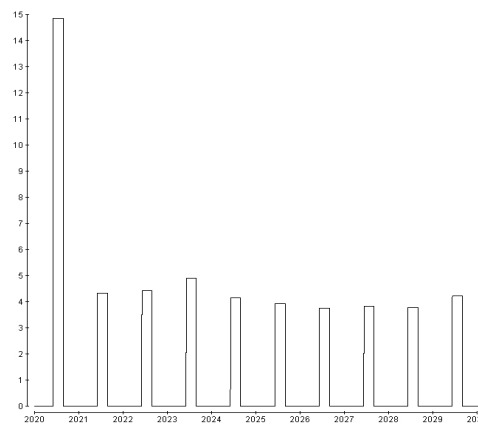


Fig. 6.63 - Annual squid recruitment (ind m⁻² yr⁻¹)

The annual maximum concentration in squid (fig. 6.62) was 147 ind m⁻² (s.d. 5.3 ind m⁻²; percentage variation from the average = 3.6%; tab. 6.17). Every year eggs were injected in the water column on the 10th April and hatching started on the 15th May every year (fig.6.62 and tab.6.16). The average annual recruitment between 2021-2031 was 4.4 ind m⁻² yr⁻¹ (s.d. 0.7 ind m⁻² yr⁻¹; percentage variation from the mean of 16.7%; fig.6.63 and tab.6.16).

6.3.1.2 Causes of mortality

Table 6.18 summarizes the causes of mortality of each population annually. It shows the total number of individuals lost to predation and starvation each year, between 2020-2030, with the average, standard deviation and percentage variation from the mean during this period. On average, 1.1×10^{11} diatoms m⁻² get ingested by copepods every year (s.d.= 4.7×10^9 diatoms m⁻² yr⁻¹; percentage variation from the mean = 4.1%), and 2.1×10^{11} diatoms m⁻² yr⁻¹ are lost through energy starvation (s.d.

Year	PingZ ind m ⁻² yr ⁻¹	ZingS ind m ⁻² yr ⁻¹	ZingBP ind m ⁻² yr ⁻¹	SingPred ind m ⁻² yr ⁻¹	Pstarve ind m ⁻² yr ⁻¹	Zstarve ind m ⁻² yr ⁻¹	Sstarve ind m ⁻² yr ⁻¹
2020	1.5×10 ¹¹	190113.5	313426.3	285.1	1.9×10 ¹¹	8626.2	0
2021	1.1×10 ¹¹	177090.0	200713.7	295.7	2.1×10 ¹¹	7795.8	0
2022	1.1×10 ¹¹	176313.3	217848.9	295.6	2.1×10 ¹¹	6046.9	0
2023	1.1×10 ¹¹	180141.0	198439.0	295.1	2.1×10 ¹¹	6048.4	0
2024	1.2×10 ¹¹	188930.9	183332.7	295.8	2.1×10 ¹¹	7130.5	0
2025	1.2×10 ¹¹	177178.6	217750.5	296.1	2.1×10 ¹¹	7261.6	0
2026	1.2×10 ¹¹	189733.1	204489.3	296.2	2.1×10 ¹¹	8414.0	0
2027	1.1×10 ¹¹	192078.3	178317.8	296.2	2.1×10 ¹¹	6427.4	0
2028	1.1×10 ¹¹	175244.0	205017.6	296.2	2.0×10 ¹¹	6597.7	0
2029	1.2×10 ¹¹	187033.6	198361.3	295.8	2.1×10 ¹¹	7234.5	0
2030	1.2×10 ¹¹	173589.5	221800.4	293.8	2.1×10 ¹¹	6717.9	0
Ave	1.1×10 ¹¹	181733.2	202607.1	295.6	2.1×10 ¹¹	6967.5	0
s.d.	4.7×10 ⁹	6940.7	14297.8	0.7	3.6×10 ⁹	756.2	-
% var	4.1	3.8	7.1	0.2	1.7	10.9	-

Tab. 6.17 – Causes of mortality. Where: PingZ = P ingested by Z; ZingS = Z ingested by S; ZingBP = Z ingested by BP; SingPred= S ingested by VP; Pstarve = P died of energy starvation; Zstarve = Z died of starvation; Sstarve = S died of starvation.

= 3.6×10⁹ diatoms m⁻² yr⁻¹; percentage variation from the mean = 1.7%). The average number of copepods annually ingested by squid was about 181,700 m⁻² yr⁻¹ (s.d. = 6,940 copepods m⁻² yr⁻¹; percentage variation from the mean = 3.8%), while those ingested by basal predator is about 202,000 m⁻² yr⁻¹ (s.d. = 14,300 copepods m⁻² yr⁻¹; percentage variation from the mean = 7.1%). Every year about 6,970 copepods m⁻² die of starvation (s.d. = 756 copepods m⁻² yr⁻¹; percentage variation from the mean = 10.9%). Also in this VE mortality of squid is caused exclusively by predation by visual predators (tab.6.17). On average 295.6 squid m⁻² are eaten every year (s.d. = 0.6 squid m⁻² yr⁻¹; percentage variation from the mean = 0.2%), and therefore recruitment was perfectly correlated with the number of squid being annually predated. As already seen in the base run (tab.6.7), newly hatched S1 squid were the most predated, which progressively decreased in successive stages (tab.6.18).

Year	S1	S2	S3	S4	S5	S6
2020	269.6	7.8	3.4	2.1	1.2	0.9
2021	201.1	86.8	4.7	1.7	1.0	0.5
2022	193.1	93.1	5.6	1.9	1.0	0.7
2023	209.5	76.1	5.7	2.0	1.2	0.7
2024	203.0	84.3	5.6	2.1	0.6	0.3
2025	198.7	88.7	5.9	1.7	0.7	0.4
2026	208.2	78.1	6.8	1.9	0.8	0.4
2027	209.5	79.2	4.4	1.7	0.8	0.6
2028	217.6	70.6	5.1	1.5	0.9	0.6
2029	196.8	91.1	5.2	1.4	0.8	0.5
2030	206.1	78.4	5.3	2.2	1.2	0.7
Ave	204.3	82.6	5.4	1.8	0.9	0.5
s.d.	7.3	7.3	0.7	0.3	0.2	0.1
% var	3.6	8.8	12.4	14.4	22.2	24.2

Tab. 6.18 – Stage specific squid mortality due to starvation predation

6.3.1.3 Vertically integrated biomass of plankton

	Units	Ave	s.d.	% var
<i>P</i>	mmol C m ⁻²	1794.5	29.4	1.6
<i>PD</i>	h	2534.5	10.6	0.42
<i>Z</i>	mmol C m ⁻²	230.7	4.9	2.1
<i>Z</i> _{prot}	mmol C m ⁻²	68.8	1.5	2.2
<i>Z</i> _{lip}	mmol C m ⁻²	161.9	3.5	2.2
<i>ZD</i>	h	3236.9	5.3	0.16
<i>S</i>	mmol C m ⁻²	10.1	0.3	3.0
<i>S</i> _{prot}	mmol C m ⁻²	8.3	0.2	2.9
<i>S</i> _{lip}	mmol C m ⁻²	1.8	0.1	4.0
<i>SHD</i>	h	3258.3	1.6	0.05

Tab.6.19 - Average value, s.d. and percentage variation from the mean. Where: *P*: Annual maximum vertically integrated P biomass; *PD*: Hours since 1st Jan when max vertically integrated P biomass occurs; *Z*: Max vertically integrated Z biomass [lipid + protein]; *Z*_{prot}: Max vertically integrated Z protein biomass; *Z*_{lip}: Max vertically integrated Z lipid biomass; *ZD*: Hours since 1st Jan when max vertically integrated Z biomass occurs; *S*: Max vertically integrated S biomass [lipid + protein]; *S*_{prot}: Max vertically integrated S protein biomass; *S*_{lip}: Max vertically integrated S lipid biomass; *SHD*: Hours since 1st Jan when squid hatching occurs.

Fig. 6.64-6.70 show the vertically integrated biomass of each population on attractor. Diatom had an average annual maximum biomass of 1794.5 mmol C m⁻² (s.d. 29.4 mmol C m⁻²; percentage variation from the mean = 1.6%; tab.6.19 and fig.6.64 on the 15th April (s.d. 10.6 hours; percentage variation from the mean = 0.4 %; tab.6.19). Compared to the base run, annual maximum biomass was on average almost 100 mmol C m⁻² higher and occurred one day later (tab.6.8-6.19).

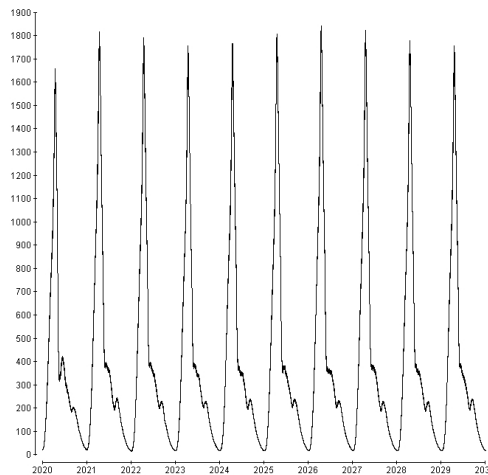


Fig 6.64 Diatom total biomass (mmol C m⁻²)

Copepod biomass reached an average maximum annual value of 230.7 mmol C m⁻² (s.d. 4.9 mmol C m⁻²; percentage variation from the mean = 2.1%; tab.6.19 and fig. 6.65) every year on the 14th May (s.d. 5 hours; percentage variation from the mean

0.2%). Total copepod biomass was made up by about one third protein and two thirds lipid (fig. 6.66-6.67 and tab.6.19). Squid hatched every year on the 15th May (s.d. 1 hour). The population biomass increased rapidly to a maximum of about 10 mmol C m⁻² (s.d. 0.3 mmol C m⁻²; percentage variation from the mean = 3.0%; tab.6.19). Protein constituted over 80% of the total biomass (Fig. 6.68-6.70 and tab.6.19). Compared to the base run, the annual maximum copepod biomass in this VE was not significantly higher, only 1.3 mmol C m⁻², which is lower than the standard deviation in both VEs (tab.6.8-6.19). As for the annual maximum diatom biomass date of occurrence, the annual maximum copepod biomass occurred on average one day later than in the base run.

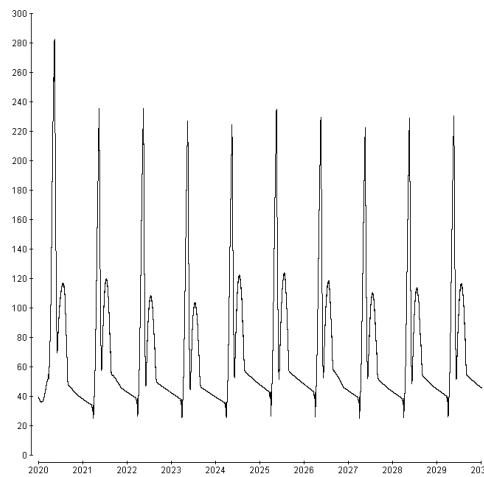


Fig 6.65 - Copepod total biomass – all stages (mmol C m⁻²)

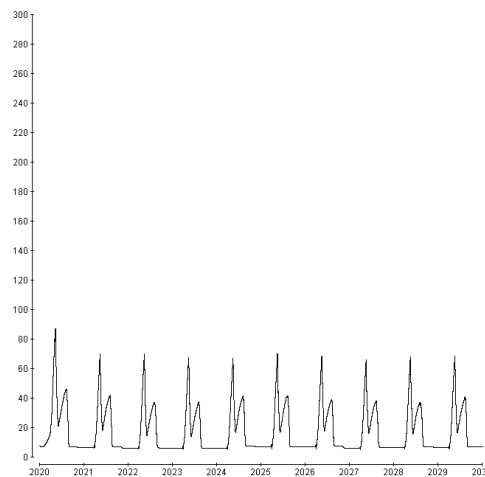


Fig 6.66 - Copepod protein biomass – all stages (mmol C m⁻²)

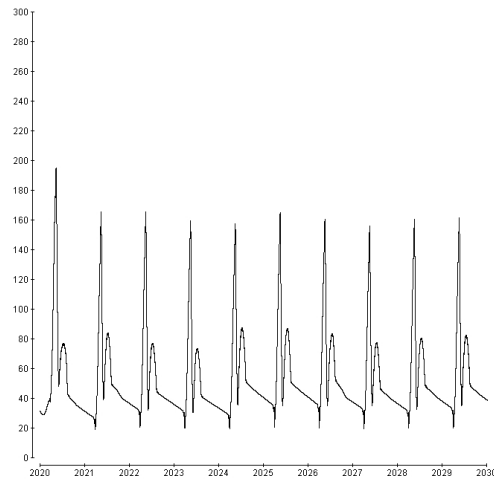


Fig 6.67 - Copepod lipid biomass – all stages (mmol C m^{-2})

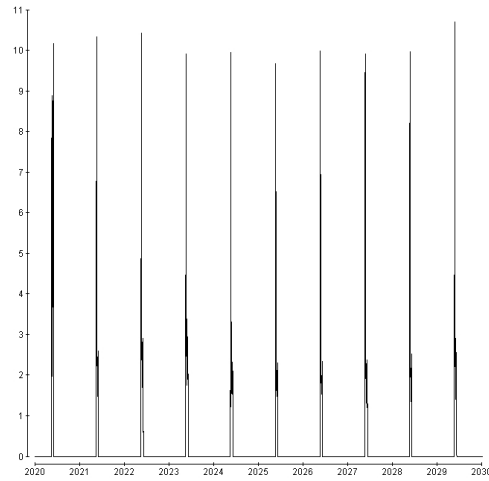


Fig 6.68 - Squid biomass – all stages (mmol C m^{-2})

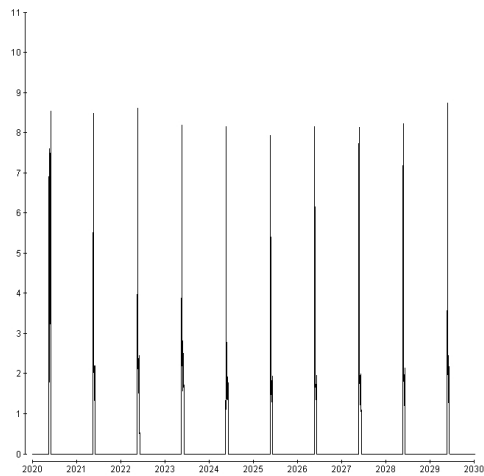
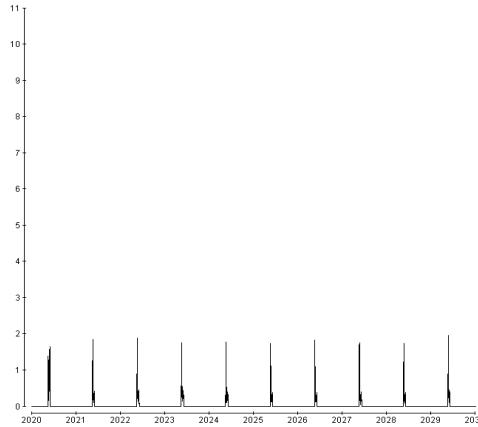


Fig 6.69 - Squid protein biomass – all stages (mmol C m^{-2})

Fig 6.70 - Squid lipid biomass – all stages (mmol C m⁻²)

Carbon transfer

Year	PingZ mmolC m ⁻² yr ⁻¹	ZingS mmolC m ⁻² yr ⁻¹	Zprot_ingS mmolC m ⁻² yr ⁻¹	Zlip_ingS mmolC m ⁻² yr ⁻¹	ZingBP mmolC m ⁻² yr ⁻¹	SingPred mmolC m ⁻² yr ⁻¹
2020	3221.3	40.6	13.7	26.9	72.4	18.7
2021	2645.0	21.3	10.0	11.4	51.8	22.5
2022	2592.7	23.4	10.4	13.1	60.9	22.8
2023	2508.4	23.5	10.5	12.9	57.2	22.6
2024	2667.4	21.7	9.7	11.9	63.5	22.2
2025	2747.1	21.6	9.7	11.9	74.4	22.5
2026	2727.8	20.5	9.4	11.1	74.5	22.3
2027	2571.3	21.3	9.4	12.0	63.4	22.2
2028	2633.1	20.2	9.2	11.1	67.2	22.0
2029	2667.3	21.8	9.9	11.9	63.8	22.5
2030	2674.8	25.1	11.3	13.8	66.1	22.5
Ave	2643.5	22.1	9.9	12.1	64.3	22.4
s.d.	71.6	1.5	0.6	0.9	7.0	0.2
% var	2.7	6.8	6.3	7.4	10.9	1.1

Tab. 6.20 – Carbon transfer through the trophic chain. Where: PingZ = Carbon ingested annually by copepods; ZingS = Carbon ingested annually by squid; Zprot_ingS = Protein ingested annually by squid; Zlip_ingS = Lipid ingested annually by squid; ZingBP = Carbon ingested annually by basal predator; SingPred = Carbon ingested annually by visual predator.

The amount of carbon transferred from diatoms to copepods was on average higher compared to the base run: 2,643.5 mmolC m⁻² yr⁻¹ (s.d. 71.6 mmolC m⁻² yr⁻¹; percentage variation from the mean = 2.7 %; tab.6.20), against the 2,592 mmolC m⁻² yr⁻¹ transfer in the base run. The carbon transferred annually from copepod to predators was only slightly higher than that in base run, with an average value 86.4 mmol C m⁻² yr⁻¹ compared to 85.4 mmol C m⁻² yr⁻¹. This extra 1 mmol C m⁻² yr⁻¹ was transferred to the basal predator population. Squid ingested 22.1 mmolC m⁻² yr⁻¹ (s.d. 1.5 mmolC m⁻² yr⁻¹; percentage variation from the mean = 6.8%; tab.6.20), of which about 10 mmol C m⁻² yr⁻¹ was made up protein, showing no variation with the base run. Basal predator ingested on average 64.3 mmol C m⁻² yr⁻¹ (s.d. 7.0 mmolC m⁻² yr⁻¹; percentage variation from the mean = 10.9 %; tab.6.20). Visual

predator average annual carbon ingested (tab.6.20) showed little variation with the base run: $22.6 \text{ mmolC m}^{-2} \text{ yr}^{-1}$ from the squid biomass (s.d. $0.4 \text{ mmolC m}^{-2} \text{ yr}^{-1}$; percentage variation from the mean = 1.9 %; tab.6.9).

6.3.1.4 Number of agents

The number of diatom agents varies between about 2,000-4,700 (fig.6.71), with the same trend observed in the base run (fig.6.43). The number of copepod agents varies from a minimum of 600 (all over-wintering during the winter) to about 2,000. It kept the same trend in the base run (fig.6.44), except for year 2020, in which the initial number of copepods is about 500, only 100 of which overwintering (fig.6.72).

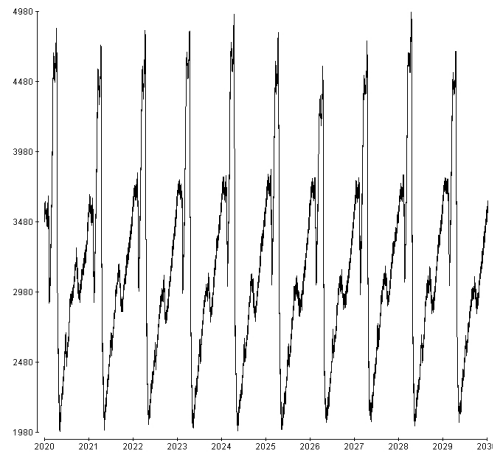


Fig 6.71 - Number of diatom agents

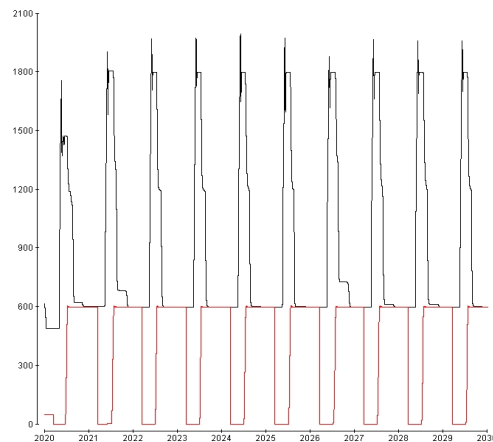


Fig 6.72 - Number of copepod agents

Squid agents in stages S1-S6 are always maintained to a number of 300 in the period between hatching and recruitment (fig.6.73).

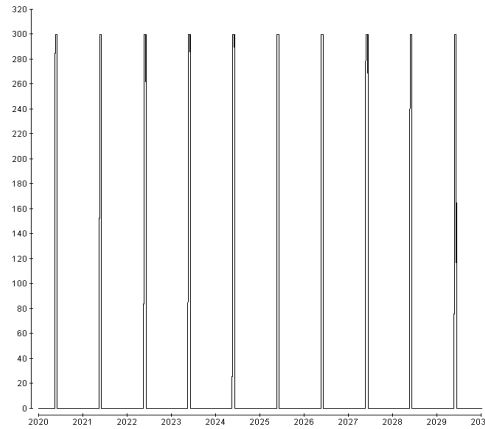


Fig 6.73 - Number of squid agents S1-S6

6.3.1.5 Physical environment

	Units	Year 16-25		
		Ave	s.d.	% var
MLD _{max}	m	156.0	4.0	2.6
T _{min} [0]	°C	14.4	0.01	0.1
T _{max} [0]	°C	29.2	0.1	0.3

Tab. 6.21 – Surface minimum and maximum average temperature and annual average maximum mixed layer depth, standard deviation and percentage variation from the average. Where:

MLD_{max}: Annual maximum mixed layer depth;

T_{min}[0] and T_{max}[0]: Annual minimum and maximum average surface temperature.

The physical environment was largely unchanged by the increase in surface dissolved silicate. The average annual maximum mixed layer depth (fig.6.74) was 156.0 m (s.d. 4.0 m; percentage variation from the mean = 2.6 %; tab.6.21), which is not significantly different from the average annual maximum reached in the base run (tab.6.10) every year in mid-March.

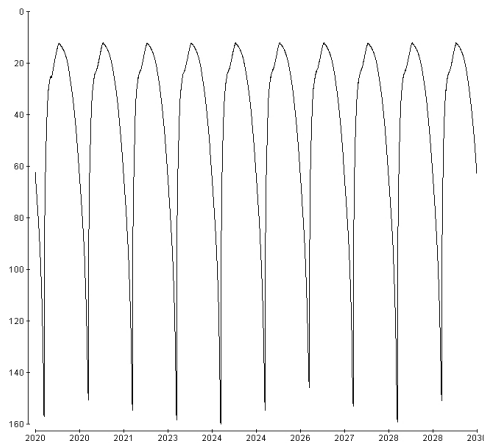


Fig 6.74 – Turbocline depth at 6 am.

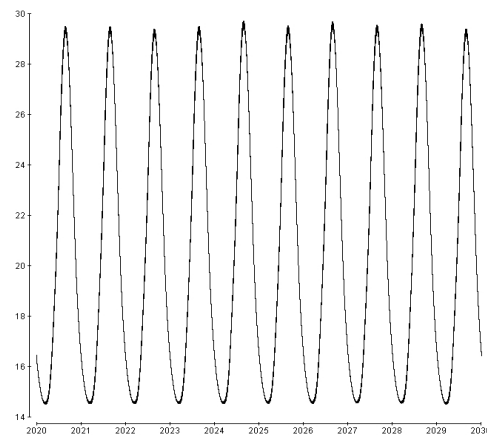


Fig 6.75 – Sea surface temperature

The average sea surface temperature varied from an annual minimum of 14.4°C (s.d. 0.01°C; percentage variation from the mean = 0.1 %; tab.6.21) in March to an annual maximum of 29.2 °C (s.d. 0.1°C; percentage variation from the mean = 0.3 %; tab.6.21) in August (fig.6.75). It did not differ significantly from the base run the average sea surface temperature in the base run (tab.6.10).

6.3.1.6 Chemical environment

	Units	Year 16-25		
		Ave	s.d.	% var
N [0]	mmol N m ⁻³	5.9	0.2	3.1
Si [0]	mmol Si m ⁻³	1.8	0.1	4.5

Tab. 6.22 – Surface nutrients average concentration, standard deviation and percentage variation from the average. Where: N[0]: Maximum dissolved N concentration at surface; Si[0]: Maximum dissolved Si concentration at surface.

The total (dissolved + particulate) mesocosm nitrogen and silicate (fig.6.76-6.77) had a small drift as observed in the base run (fig.6.48-6.49). Total mesocosm nitrogen was mostly unchanged, drifting from 4,493.8 to 4,497.5 mmol N m⁻² in 10 years in both experiments (fig.6.48 and fig.6.76). The maximum total mesocosm silicate was obviously higher in this run, but it showed the same rate in annual silicate loss: in 10 years it decrease from 1,384.5 to 1,383.4 mmol Si m⁻² compared with the the base run variation from 1,348.5 to 1,347.4 mmol Si m⁻² (fig.6.49 and fig.6.77).

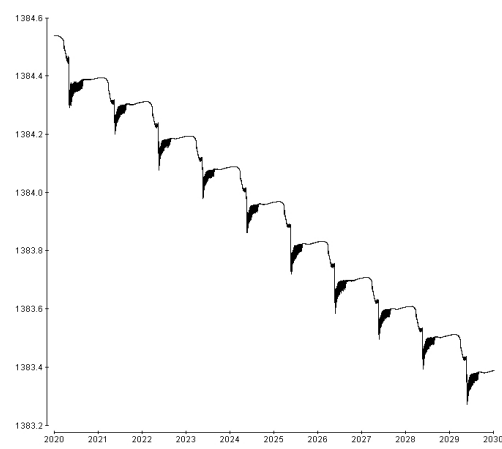
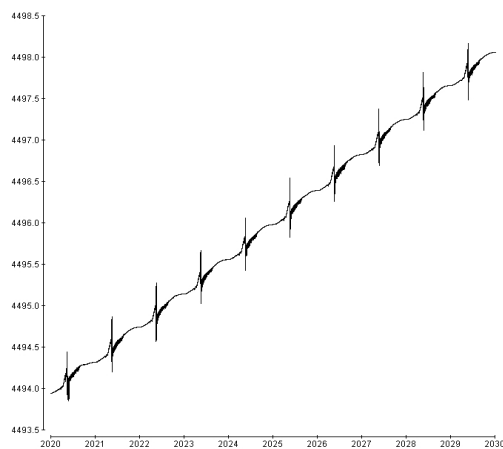


Fig 6.76 – Total mesocosm nitrogen (mmol N m⁻²) Fig 6.77 –Total mesocosm silicon (mmol Si m⁻²)

Dissolved nitrogen and silicate (fig.6.78-6.79) reached an average maximum surface concentration respectively of $5.9 \text{ mmol N m}^{-3}$ (s.d. $0.1 \text{ mmol N m}^{-3}$; percentage variation from the average = 2.3%; tab.6.22) and $1.8 \text{ mmol Si m}^{-3}$ (s.d. $0.1 \text{ mmol Si m}^{-3}$; percentage variation from the average = 4.5%; tab.6.22). These average annual maximum surface concentrations were not significantly different from those in the base run (tab.6.11).

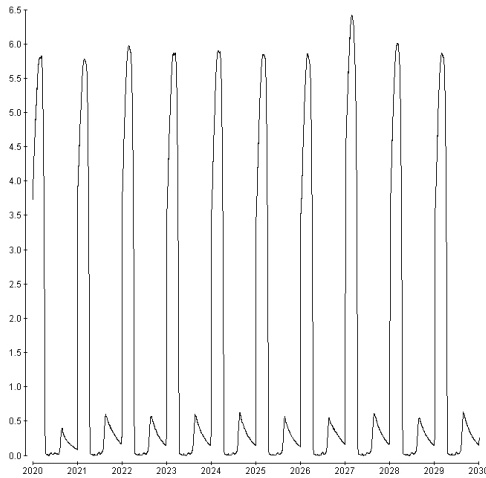


Fig 6.78 – Surf. dissolved nitrogen (mmolN m^{-3})

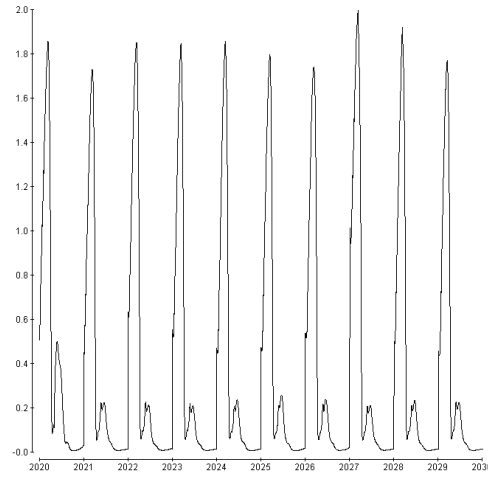


Fig 6.79 – Surf. dissolved silicon (mmolSi m^{-3})

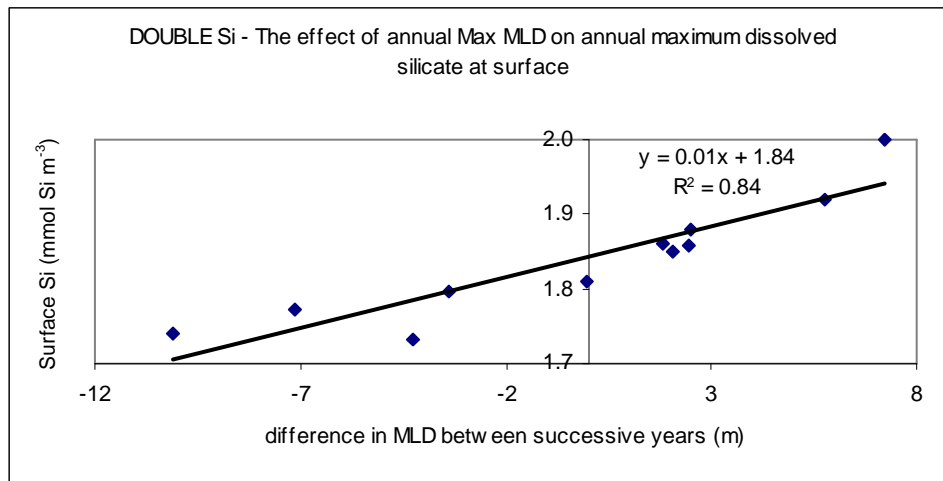


Fig. 6.80 – The effect of variation in annual maximum mixed layer depth on annual maximum dissolved silicate at surface

The variation in annual maximum dissolved silicate concentration was correlated to the variation in annual maximum mixed layer depth in successive years (fig.6.80).

6.3.1.7 Causes of high recruitment event in year 16 (2020)

The first noticeable difference with the base run, and all other years in this experiment is that year 16 is the only year in which the copepod stage composition on the 1st Jan is not entirely composed by over-wintering copepods.

In the previous year, some copepod survived through the winter (fig.6.61 and 6.81-6.82). The survivors were those copepods that entered pre-overwintering in the previous year, but did not manage to store enough lipids to enter overwintering. Nevertheless, they stored enough lipids to sustain them through the winter on the limited diatom winter population.

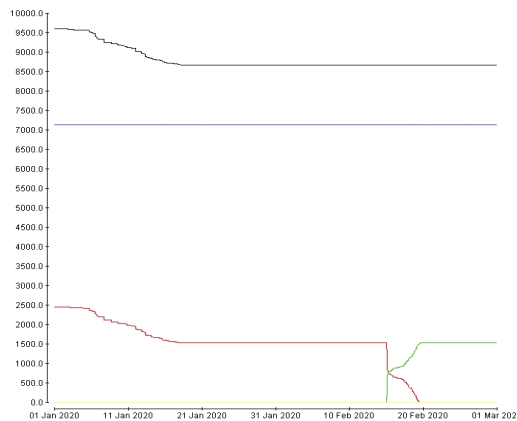


Fig.6.81 – Black: copepod concentration (all stages); Blue: overwintering copepod concentration; Red: concentration of copepod that failed to overwinter and survived through the winter as C4(ow); Green: C5 copepod concentration (ind. m⁻²).

As, this cohort of survivors grew, it constituted an extra portion of copepod biomass available as food for the squid population. As a consequence of this, year 16 was the year with the biggest copepod biomass (fig.6.65-6.67).

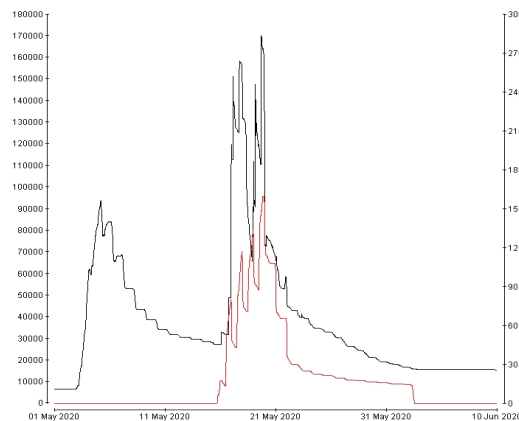


Fig.6.82 – Copepod (Black, left: ind m⁻²) and squid (Red: right: ind m⁻²) abundance in year 16

Year	<i>P</i>	<i>PD</i>	<i>Z</i>	<i>ZD</i>	<i>SHD</i>	<i>SHD-ZD</i>	<i>R</i>
2018	1641.6	2506.5	235.6	3240.0	3259.0	19.0	3.1
2019	1813.6	2529.5	283.9	3256.5	3258.0	1.5	6.8
2020	1660.4	2554.5	282.8	3218.0	3258.0	40.0	14.9
2021	1818.0	2556.0	235.8	3238.0	3258.5	20.5	4.3
2022	1694.4	2529.5	235.6	3236.5	3256.0	19.5	4.4
2023	1658.2	2529.5	226.0	3242.5	3256.0	14.5	4.9
2024	1668.2	2553.0	224.9	3235.0	3256.5	21.5	4.2
2025	1808.2	2529.5	235.1	3242.5	3256.5	14.0	3.9
2026	1844.8	2529.0	229.6	3239.0	3258.5	19.5	3.8
2027	1825.4	2529.0	222.5	3242.0	3258.5	16.5	3.8
2028	1680.9	2530.0	229.0	3235.5	3259.0	23.5	3.8
2029	1658.1	2529.5	230.6	3226.5	3261.0	33.5	4.2
2030	1689.0	2530.0	236.2	3229.0	3260.5	31.5	6.2
Ave	1694.5	2534.5	230.6	3236.9	3258.3	21.5	4.4
s.d.	29.4	10.6	4.9	5.3	1.6	6.6	0.6
% var	1.6	0.4	2.1	0.2	0.0	30.6	16.6

Tab.6.23 – Where: *P*: Max vertically integrated P biomass (mmolC m^{-2}); *PD*: Time (hurs since 1st Jan) of max vertically integrated P biomass; *Z*: Max vertically integrated Z biomass [lipid and protein] (mmolC m^{-2}); *ZD*: Time (Hours since 1st Jan) of max vertically integrated Z biomass; *SHD*: Squid hatching time (Hours since 1st Jan); *SHD-ZD*: time difference (hours) between *SHD* and *ZD* *R*: vertically integrated total number of squid that reached stage 6 (recruited m^{-2})

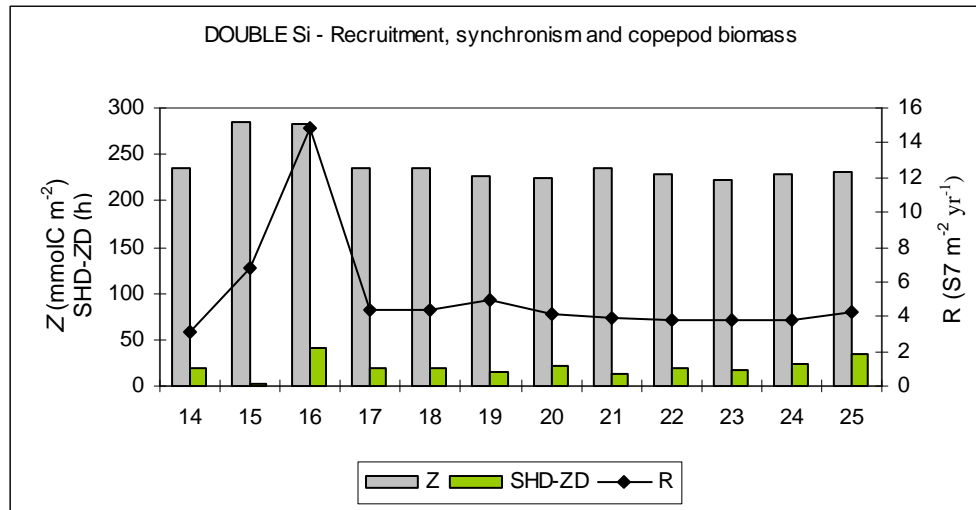


Fig.6.83 – The effect of hatching-copepod biomass synchronism and max copepod biomass on recruitment.

Comparing recruitment with the magnitude of copepod biomass and timing between its occurrence and squid hatching (fig.6.83), it can be seen that:

- The synchronism (time difference between copepod maximum vertically integrated biomass and hatching) was better (i.e. smaller difference) in year 15 than year 16, 1.5 hours and 40 hours respectively (fig.6.84).
- Year 15 and 16 had similar maximum copepod biomass (fig.6.85).
- However, recruitment in year 16 is higher than in year 15.

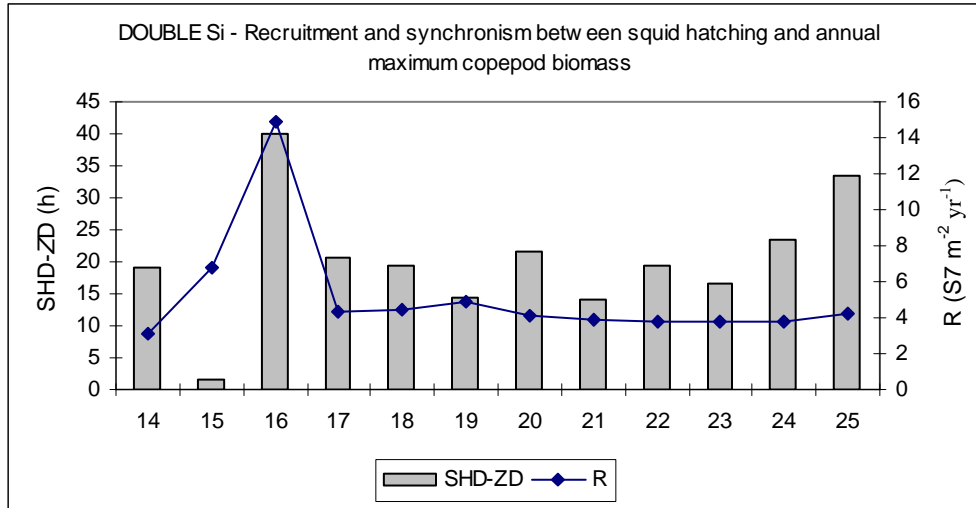


Fig.6.84 – The effect of hatching-copepod biomass synchronism on recruitment.

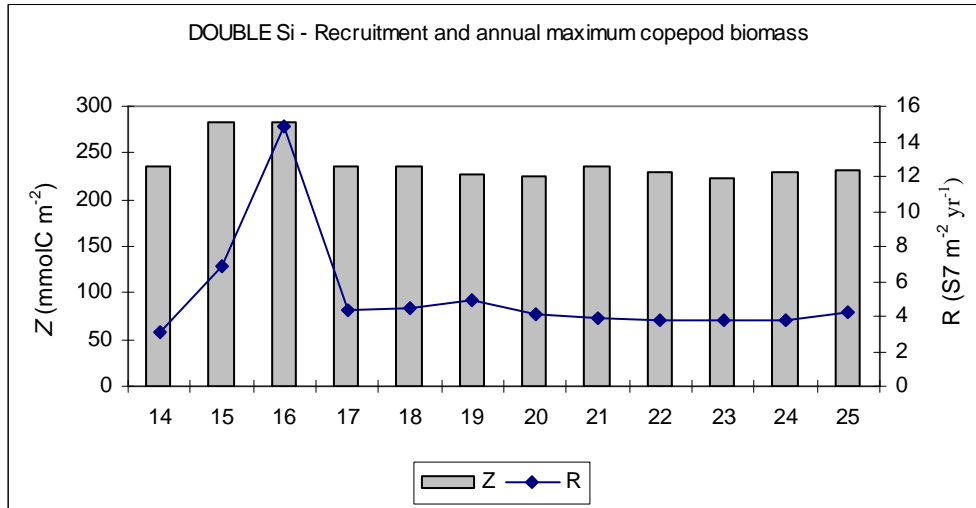


Fig.6.85 – The effect of max copepod biomass on recruitment.

Possible causes to explain the high recruitment in year 16 would be:

- Less competition for food
- Less predation
- More food ingested

Competition

In year 16 the annual ingestion of copepod biomass by the basal predator population is not smaller to that of other years with lower squid recruitment (fig.6.86).

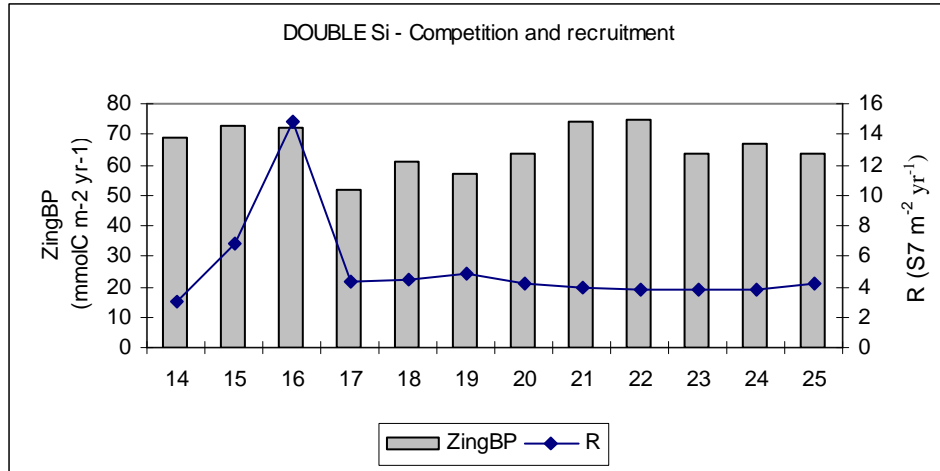


Fig.6.86 – Annual carbon ingested by basal predator and recruitment

The number of copepods that get ingested annually by basal predator reaches a minimum in year 15 and a maximum in year 16 (fig.6.87).

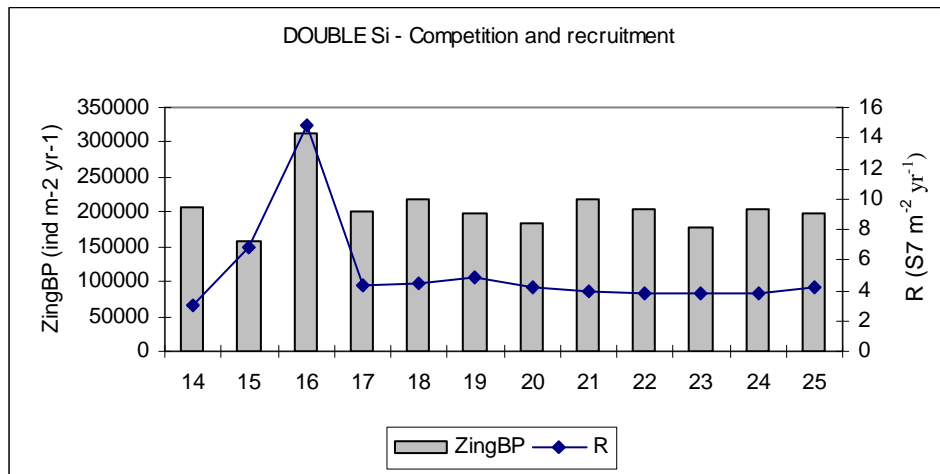


Fig.6.87 – Annual number of copepods ingested by basal predator and recruitment

However, when considering the period in which squid is present in the mesocosm, the picture is different. The amount of copepod biomass consumed by the basal predator in 2016 is considerably lower than all other years (fig.6.88). The amount of copepod biomass ingested by the basal predator competing for food is negatively correlated to recruitment (fig.6.89). On the other hand, the number of ingested copepods is the highest (fig.6.90).

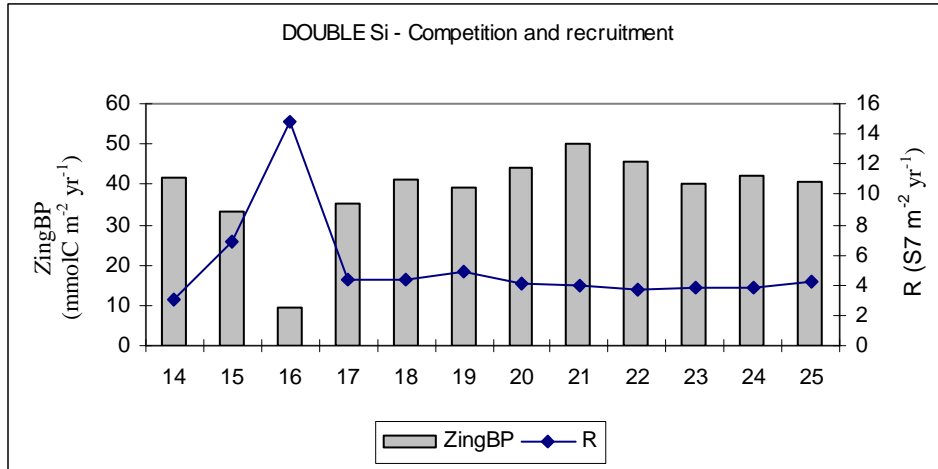


Fig.6.88 – Carbon ingestion by basal predator during the period in which squid is present and recruitment

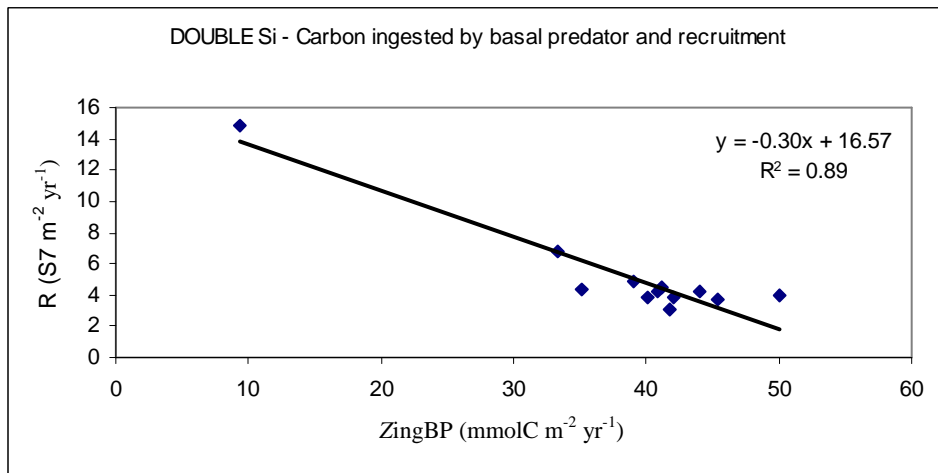


Fig.6.89 – Correlation between carbon ingested by basal predator and recruitment

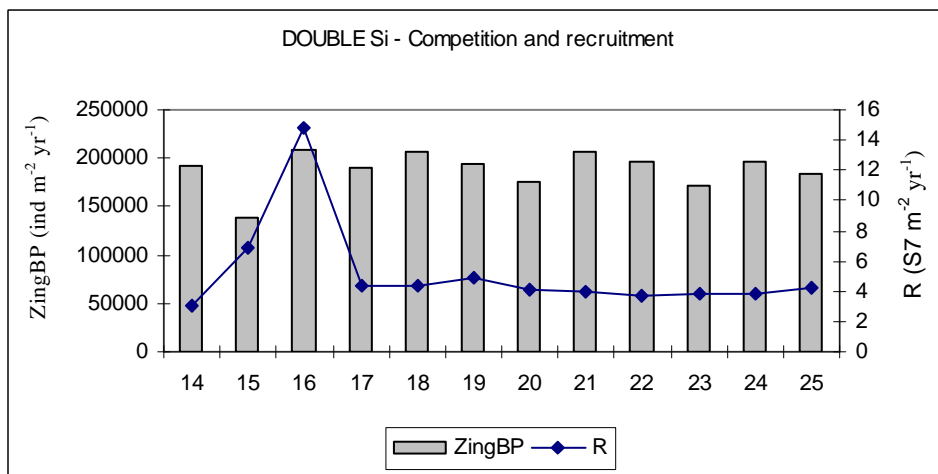


Fig.6.90 – Copepods ingested by basal predator during the period in which squid is present and recruitment

Predation

Year 16 was the year with the lowest amount of squid biomass consumed by the parametrised population of visual predators (fig.6.91). The amount of squid biomass consumed by the top predator shows a negative correlation with recruitment (fig.6.92). When analyzing the number of squid ingested by top predators (fig.6.93), it can be seen that annual predation on squid was higher in year 15 than in year 16 and that it correlates perfectly with recruitment.

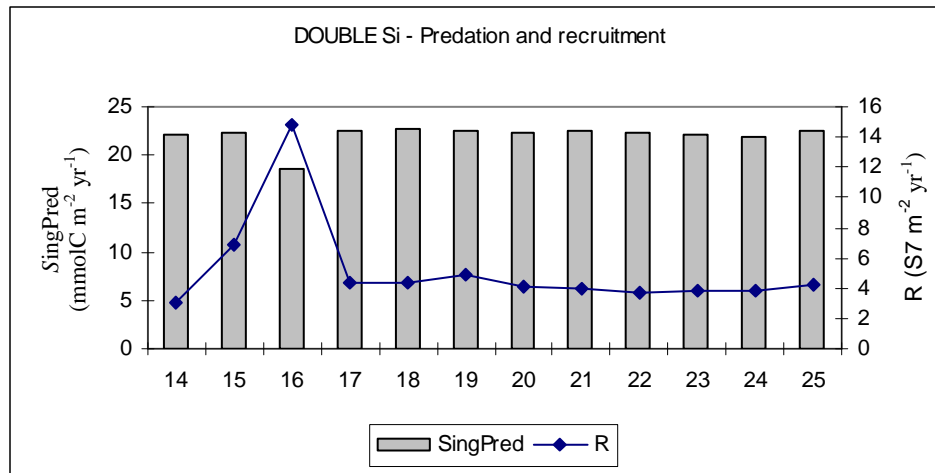


Fig.6.91 – Annual carbon ingestion by visual predator and recruitment

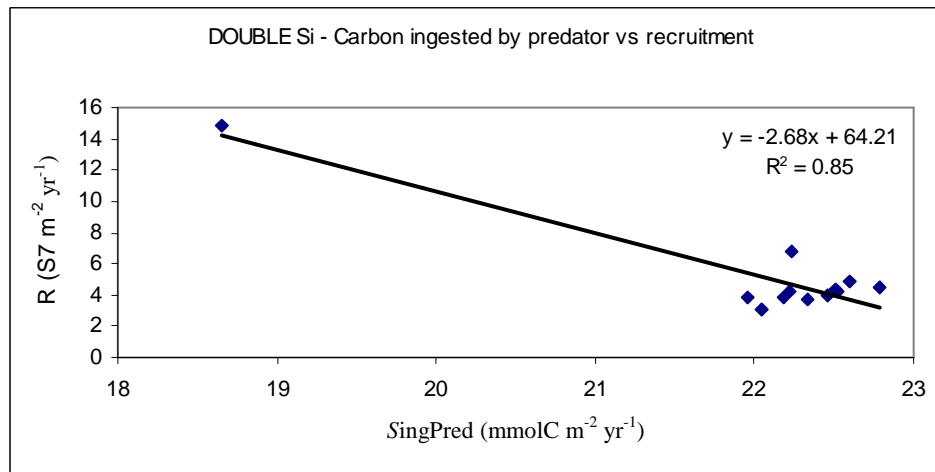


Fig.6.92 – Correlation between carbon ingested by visual predator and recruitment

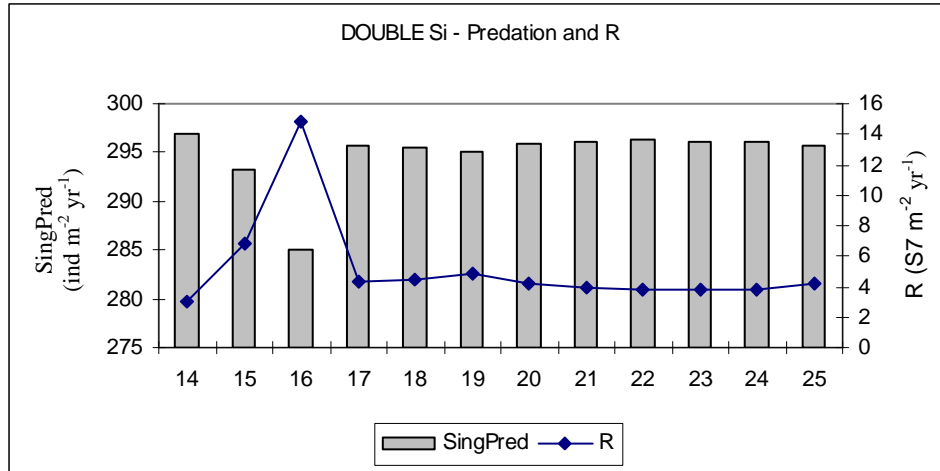


Fig.6.93 – Annual squid ingested by visual predator and recruitment

However when comparing predation on different squid stages in year 15 and 16 (tab.6.24), it can be seen that in both years smaller squid are more vulnerable to predation. During year 16, about 270 squid in stage S1 were victim of predation against 217 in year 15 (fig.6.94).

Squid stage	Y15	Y16
S1	217.1	269.6
S2	64.3	7.8
S3	7.2	3.4
S4	2.6	2.1
S5	1.2	1.2
S6	0.8	0.9
Total	293.2	285.1

Tab.6.24 – Predation of different squid stages (ind m⁻² yr⁻¹) in years 15 and 16.

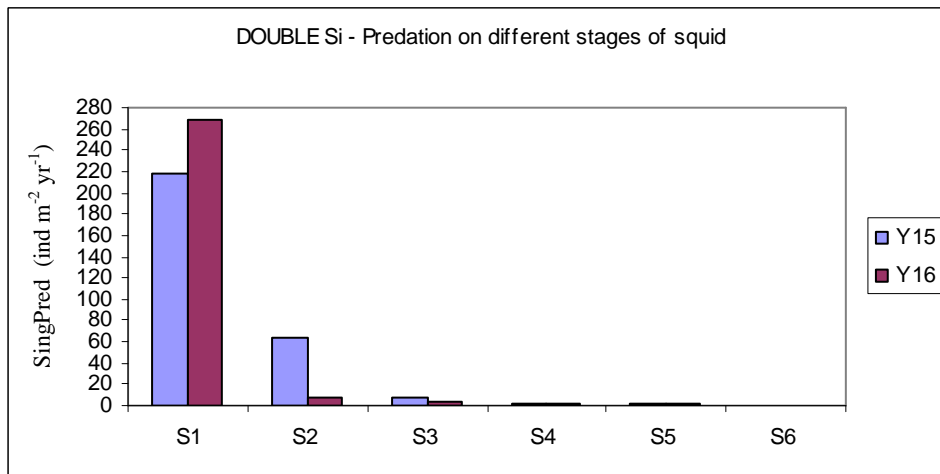


Fig. 6.94 – Annual predation on different squid stages, Sing, in year 15 and 16

The population of visual predators is parametrised (§ 4.2), so that its abundance and vertical distribution are exogenous and designed to be the same in different years. At the time of squid hatching the predator feeding potential in year 15 and 16 is therefore identical. To explain the causes of the difference in predation between the two years, we need to compare the feeding of each squid stage.

Feeding

Comparing the magnitude of recruitment to the number of copepod ingested annually (fig.6.95), it is not sufficient to explain the high recruitment exhibited by year 16. The number of annually ingested copepods in year 16 is not significantly higher than that of the other years. An interesting observation arises from the fact that year 15 is the year in which squid ate the most copepods, but still had less recruitment than year 16.

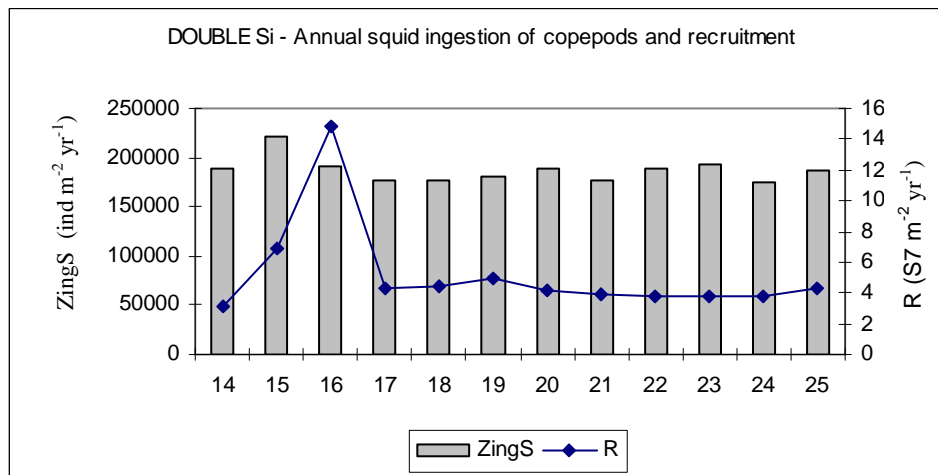


Fig. 6.95 – Annual squid ingestion on copepods

When comparing the annual amount of carbon ingested by squid and recruitment in the different years (fig.6.96), it can be seen that squid in year 16 had ingested the highest amount of copepod biomass of all other years. Squid recruitment is positively related with the amount of carbon ingested in a particular year (fig.6.97).

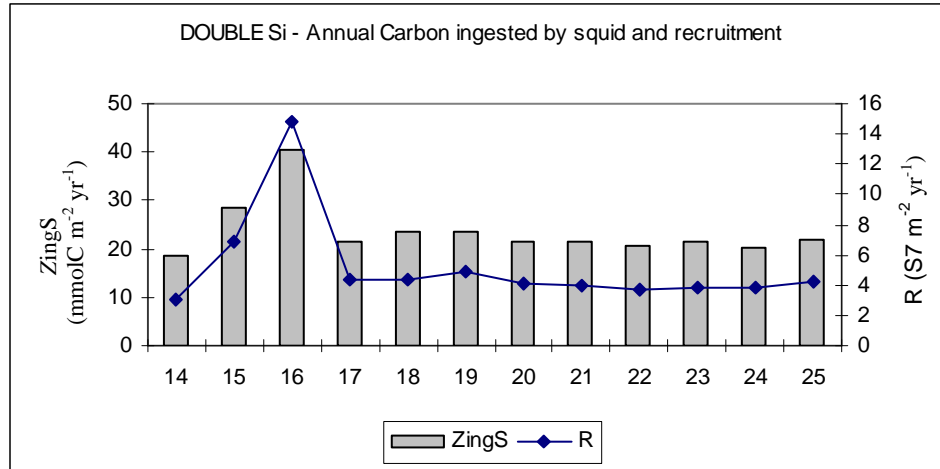


Fig. 6.96 – Annual carbon ingested by squid and recruitment

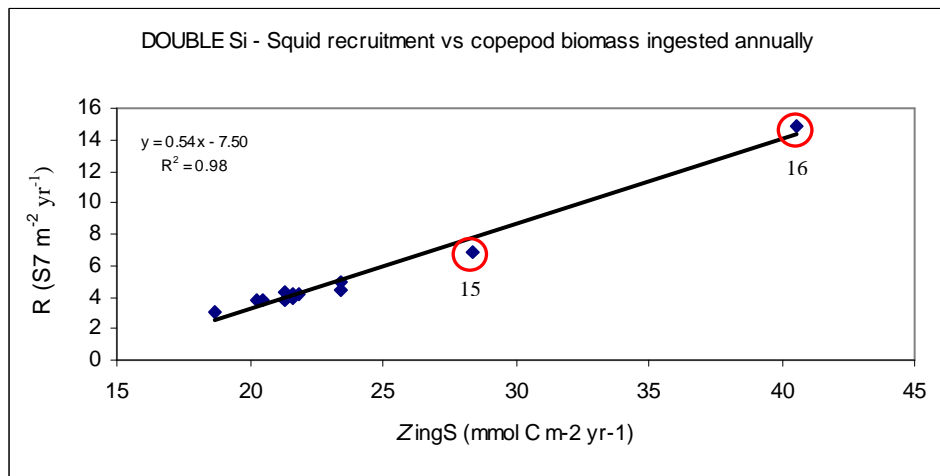


Fig.6.97 – Linear correlation between squid recruitment and copepod biomass ingested annually

As already said, during year 15 squid have eaten more copepods than during year 16 (fig.6.95). However in year 15, the annual amount of copepod biomass consumed by squid was smaller than in year 16 (fig.6.96). This is an interesting observation. In year 15 squid ingested more copepods than in year 16 but got less carbon out of it. When comparing squid ingestion relative to their stage of development, it can be noticed that, in year 15, squid in early stages (S1, S2 and S3), especially in S2, ingested more copepods than their counterparts in year 16 (tab.6.25). Later stages of squid (S4, S5 and S6) experienced a larger consumption of copepods in year 16 than in year 15. This shift in trend is more evident when considering the amount of protein ingested by different squid stages in year 15 and 16 (fig. 6.97).

Stages	Y15		Y16	
	Zing (ind m ⁻² yr ⁻¹)	Zprot_ingS (mmol C m ⁻² yr ⁻¹)	Zing (ind m ⁻² yr ⁻¹)	Zprot_ingS (mmol C m ⁻² yr ⁻¹)
S1	173698.7	3.8	166540.2	2.0
S2	36002.5	2.5	7657.0	1.8
S3	4907.1	1.4	4619.0	2.1
S4	2777.8	1.3	5060.3	2.3
S5	2727.0	1.3	3663.1	2.6
S6	2361.2	1.4	2573.9	2.9
Sum	222474.3	11.7	190113.5	13.7

Tab. 6.25 – Copepod (Zing) and protein ingested (Zprot_ingS) by different squid stages

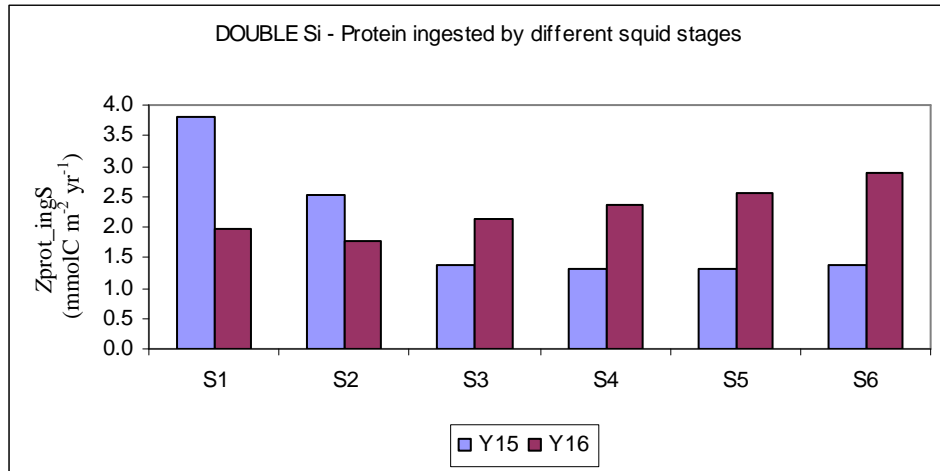


Fig. 6.98 - Protein ingested annually by different squid stages, Zprot_ingS, in year 15 and 16

Squid in stage S1 ingested almost double the amount of protein in year 15 compared to year 16. Also in stage S2 squid the amount of protein ingested was higher than in year 16. However, the amount of protein ingested by squid from stage S3 onwards presents an inverted trend. While the amount of protein ingested by larger squid stages (S3-S6) in year 15 was about constant, in year 16 they ingested progressively more proteins as they grew, and therefore transit to the successive stage (fig.6.98).

Growth rate

The amount of protein ingested is reflected in the time required for squid to move to the successive stage. Fig.6.99-6.100 show the stage composition of the squid population in years 15 and 16. It is interesting to notice that in year 15, stage S1 squid ingested more protein than in year 16 (tab.6.25; fig.6.98), and this is reflected in the time needed for squid S1 to move to stage S2 (tab.6.26; fig.6.101). In year 15 squid in S1 grew faster than in year 16, with the first transition to S2 taking 1.6 days

and 6.4 days respectively. As a consequence of this faster growth in year 15, the number of S1 squid lost to predation was less than in year 16 (tab.6.24). Conversely, S2 squid in year 15 grew slower than in year 16, so they got predated more (tab.6.24). The same trend is true in all other years.

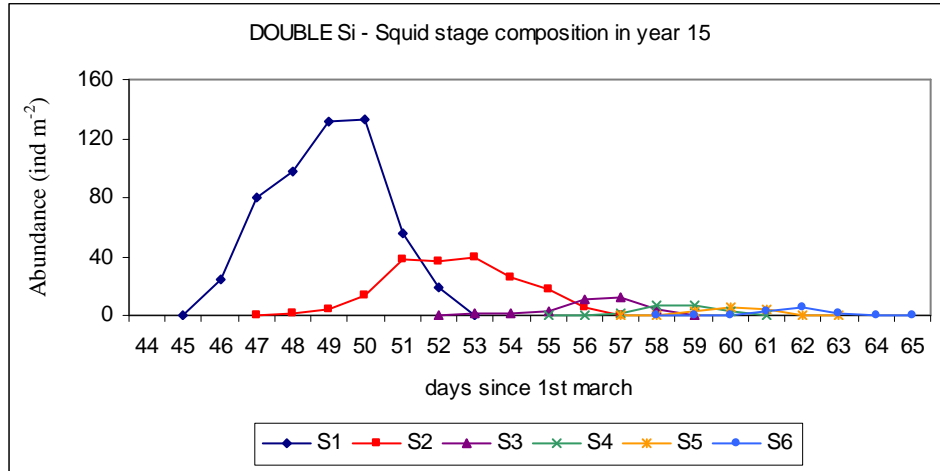


Fig.6.99- Squid stage composition in year 15

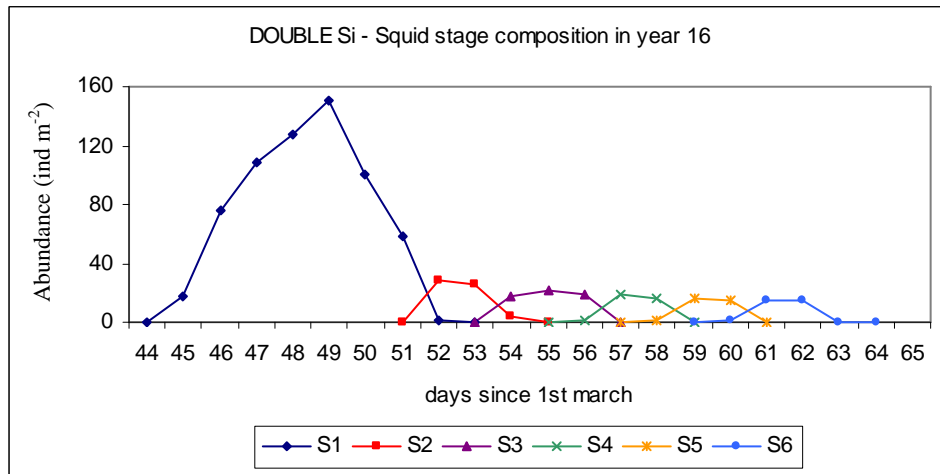


Fig.6.100 - Squid stage composition in year 16

Stage	Y15 (days)	Y16 (days)
S1	1.6	6.4
S2	4.9	2.1
S3	3.0	2.2
S4	2.1	2.0
S5	1.3	1.9
S6	1.9	2.1

Tab.6.26 – Time needed for the first squid to pass to the successive stage in years 15 and 16

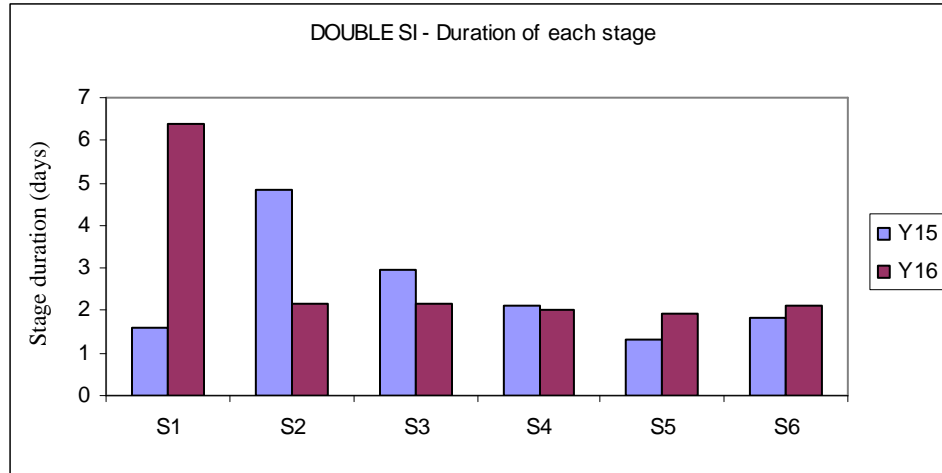


Fig.6.101 – Time needed for the first squid to pass to the successive stage in years 15 and 16

6.3.2 Increasing the inter-population competition for food (basal predator)

Restarted from a VE snapshot on the 1st Jan 2015 of the base run. The vertically integrated concentration of basal predators feeding on copepods is doubled from 3,000 ind m⁻² to 6,000 ind m⁻², in order to investigate the effect of competition for food on annual squid recruitment.

6.3.2.1 Vertically integrated concentration of plankton

Units	Year 16-25		
	Ave	s.d.	% var
P ind m ⁻²	9.1×10 ¹⁰	1.6×10 ⁹	1.8
Z ind m ⁻²	120855.7	8603.4	7.1
Z _{ow} ind m ⁻²	6840.5	412.5	6.0
S ind m ⁻²	140.7	3.2	2.3
SHD h	3255.9	0.7	0.02
R ind m ⁻² yr ⁻¹	3.1	0.5	17.0

Tab. 6.27 - Average value, s.d. and percentage variation from the mean for years 2020-2030. Where:
 P: Max vertically integrated P concentration; Z: Max vertically integrated Z concentration;
 Z_{ow} : Max vertically integrated concentration of over-wintering copepods; S: Max vertically integrated S concentration; SHD: Hours since 1st Jan when squid hatching occurs;
 R: vertically integrated total number of squid that reached stage 7 between 2020-2030;

Fig. 6.102-6.107 show the vertically integrated concentration of the populations between years 2020-2030. During that period, diatom had an average annual maximum concentration of 9.1×10¹⁰ ind m⁻² (s.d. 1.6×10⁹ ind m⁻²; percentage variation from the mean was 1.8; tab.6.27 and fig.6.102), which is not significantly different from the maximum observed in the base run (tab.6.5).

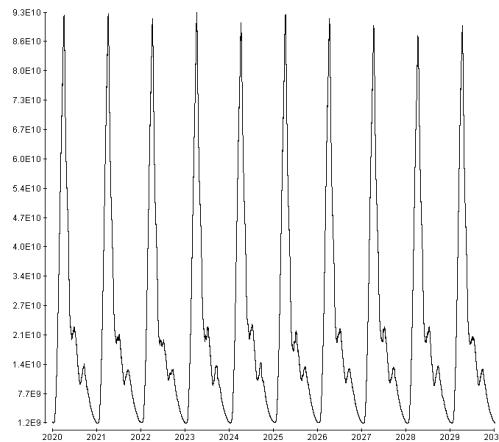


Fig. 6.102 - Vertically integrated P concentration (ind m⁻²)

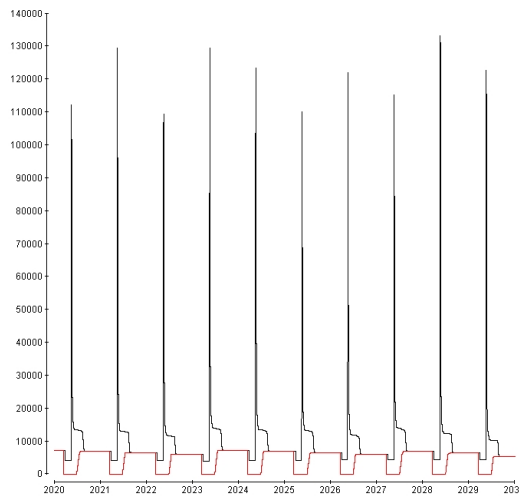


Fig. 6.103 - Vertically integrated Z concentration (black:all stages; red: over-wintering) (ind m⁻²)

Copepod population in spring was composed exclusively of copepods that entered over-wintering in the previous summer (fig.6.103). The annual average concentration of copepod that entered over-wintering was about 14% lower than in the base run (tab.6.5): 6,840 ind m⁻² (s.d. 413 ind m⁻²; percentage variation from the average = 6.0%; tab.6.27). Also the average annual peak in copepod concentration was smaller than in the base run (tab.6.5): about 121,000 ind m⁻² (s.d. 8,600 ind m⁻²; percentage variation from the average = 7.1%; tab.6.27). The population of non over-wintering copepods survived until the beginning of September (fig.6.103).

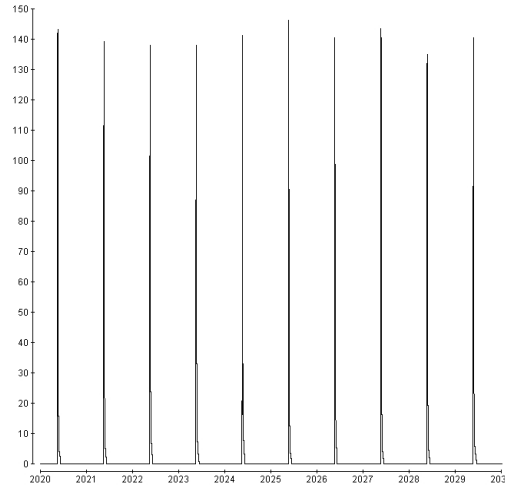


Fig. 6.104 - Vertically integrated concentration of squid (S1-S6) (ind m⁻²)

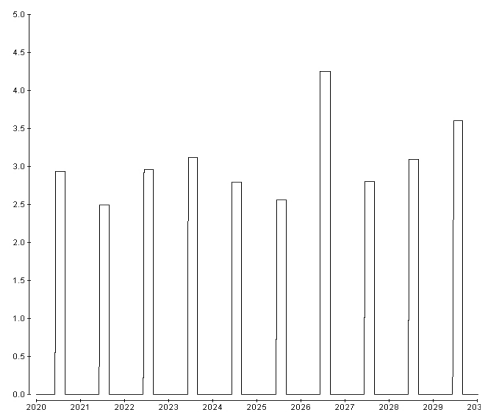


Fig. 6.105 - Annual squid recruitment (ind m⁻² yr⁻¹)

The annual maximum concentration in squid (fig. 6.104) was 141 ind m⁻² (s.d. 3.2 ind m⁻²; percentage variation from the average = 2.3%; tab.6.27). Every year eggs were injected in the water column on the 10th April and hatching started on the 15th May (tab.6.27). The average annual recruitment was 3.1 ind m⁻² yr⁻¹ (sd 0.5 ind m⁻² yr⁻¹; percentage variation from the mean of 17.0%; fig.6.105 and tab.6.27), which is almost one quarter less than recruitment in the base run (tab.6.5).

6.3.2.2 Causes of mortality

Table 6.29 summarizes the annual losses to mortality due to predation and starvation between 2020-2030, with average, standard deviation and percentage variation from the mean during this period.

Year	PingZ ind m ⁻² yr ⁻¹	ZingS ind m ⁻² yr ⁻¹	ZingBP ind m ⁻² yr ⁻¹	SingPred ind m ⁻² yr ⁻¹	Pstarve ind m ⁻² yr ⁻¹	Zstarve ind m ⁻² yr ⁻¹	Sstarve ind m ⁻² yr ⁻¹
2020	9.7×10 ¹⁰	163074.1	175831.8	297.1	2.0×10 ¹¹	5819.5	0.0
2021	9.4×10 ¹⁰	121175.0	214912.1	297.4	1.9×10 ¹¹	5952.2	0.1
2022	8.8×10 ¹⁰	135461.1	204665.7	297.0	2.0×10 ¹¹	5194.6	0.0
2023	9.8×10 ¹⁰	128592.4	192595.2	295.4	2.0×10 ¹¹	5882.8	1.5
2024	1.0×10 ¹¹	138212.4	201560.7	297.2	2.0×10 ¹¹	5801.7	0.0
2025	9.5×10 ¹⁰	135697.1	200566.8	297.3	2.0×10 ¹¹	5718.2	0.1
2026	9.5×10 ¹⁰	118788.8	240700.5	295.7	2.0×10 ¹¹	5150.7	0.0
2027	9.5×10 ¹⁰	122659.0	228880.2	297.2	1.9×10 ¹¹	5871.1	0.0
2028	9.6×10 ¹⁰	156847.8	203856.3	296.9	1.9×10 ¹¹	5738.3	0.0
2029	9.0×10 ¹⁰	123084.3	232103.2	296.1	1.9×10 ¹¹	4907.0	0.3
Ave	9.5×10 ¹⁰	134359.2	209567.3	296.7	2.0×10 ¹¹	5603.6	0.2
s.d.	3.9×10 ⁹	15135.2	19738.8	0.7	2.2×10 ⁹	372.1	0.5
% var	4.1	11.3	9.4	0.2	1.1	6.6	231.3

Tab. 6.28 – Causes of mortality. Where: PingZ = Diatoms ingested by copepods; ZingS = Copepods ingested by squid; ZingBP = Copepods ingested by basal predator; SingPred= Squid ingested by visual predator; Pstarve = Diatoms died of energy starvation; Zstarve = Copepods died of starvation; Sstarve = Squid died of starvation.

The average number of diatoms consumed by copepods annually (tab.6.28) was $9.5 \times 10^{10} \text{ m}^{-2} \text{ yr}^{-1}$ (s.d.= 3.9×10^9 diatoms $\text{m}^{-2} \text{ yr}^{-1}$; percentage variation from the mean = 4.1%) which is about 15% lower than in base run (tab.6.6). On the other hand the number of diatoms lost due to energy starvation is not significantly different from the base run (tab.6.6): 2.0×10^{11} diatoms $\text{m}^{-2} \text{ yr}^{-1}$ (s.d. = 2.2×10^9 diatoms $\text{m}^{-2} \text{ yr}^{-1}$; percentage variation from the mean = 1.1%, tab.6.28). The average number of copepods annually ingested by squid was slightly less than $135,000 \text{ ind m}^{-2} \text{ yr}^{-1}$ (s.d. = $15,135$ copepods $\text{m}^{-2} \text{ yr}^{-1}$; percentage variation from the mean = 11.3%, tab.6.28), which is about 15% less than what they ingested in the base run (tab.6.6). The average number of annually ingested copepods by basal predator was about $210,000 \text{ ind m}^{-2} \text{ yr}^{-1}$ (s.d. = $19,800$ copepods $\text{m}^{-2} \text{ yr}^{-1}$; percentage variation from the mean = 9.4%, tab.6.28), which is slightly lower compared to the based run (tab.6.6). The average number of copepods annually lost due to starvation was $5,600 \text{ ind m}^{-2} \text{ yr}^{-1}$ (s.d. = 370 copepods $\text{m}^{-2} \text{ yr}^{-1}$; percentage variation from the mean = 6.6%, tab.6.28), which is about almost 20% less than the average annual value in base run (tab.6.6). Squid mortality was largely due to predation by top predators: 296.7 squid $\text{m}^{-2} \text{ yr}^{-1}$ (s.d. = 0.7 squid $\text{m}^{-2} \text{ yr}^{-1}$; percentage variation from the mean = 0.2%, tab.6.28). Contrary to the base run, a small number of squid died of starvation: 0.2 squid $\text{m}^{-2} \text{ yr}^{-1}$ (s.d. = 0.5 squid $\text{m}^{-2} \text{ yr}^{-1}$; percentage variation from the mean = 231%, tab.6.28). As already seen in the base run (tab.6.7), newly hatched S1 squid were subject to the highest predation, which progressively decreased in successive stages (tab.6.29).

Year	S1	S2	S3	S4	S5	S6
2020	208.67	82.95	4.63	0.40	0.23	0.17
2021	210.88	82.82	1.92	1.06	0.41	0.25
2022	224.63	67.45	3.22	1.18	0.37	0.19
2023	208.63	85.85	0.64	0.11	0.09	0.10
2024	204.66	86.69	4.39	0.86	0.33	0.27
2025	225.32	67.19	3.78	0.66	0.23	0.16
2026	217.37	71.47	3.87	1.51	1.03	0.50
2027	229.50	63.73	2.47	0.79	0.51	0.20
2028	222.16	70.09	3.40	0.87	0.22	0.17
2029	209.73	84.43	1.84	0.07	0.03	0.04
Ave	216.15	76.27	3.01	0.75	0.35	0.21
s.d.	8.73	9.03	1.27	0.46	0.28	0.12
% var	4.04	11.84	42.18	61.23	81.37	60.07

Tab. 6.29 – Stage specific squid mortality due to predation

6.3.2.3 Vertically integrated biomass of plankton

	Units	Ave	s.d.	% var
<i>P</i>	mmol C m ⁻²	1717.3	37.8	2.2
<i>PD</i>	h	2510.2	21.5	0.9
<i>Z</i>	mmol C m ⁻²	207.8	6.9	3.3
<i>Z</i> _{prot}	mmol C m ⁻²	62.3	2.1	3.4
<i>Z</i> _{lip}	mmol C m ⁻²	145.6	4.8	3.3
<i>Z</i> _{1st Jan}	mmol C m ⁻²	36.8	2.2	6.0
<i>Z</i> _{prot_1st Jan}	mmol C m ⁻²	5.9	0.4	6.2
<i>ZD</i>	h	3215.7	11.0	0.3
<i>S</i>	mmol C m ⁻²	9.6	0.3	3.4
<i>S</i> _{prot}	mmol C m ⁻²	7.9	0.2	2.8
<i>S</i> _{lip}	mmol C m ⁻²	1.7	0.1	6.0
<i>SHD</i>	h	3255.9	0.7	0.02

Tab. 6.30 - Average value, s.d. and percentage variation from the mean. Where:

P: Annual maximum vertically integrated *P* biomass; *PD*: Hours since 1st Jan when max vertically integrated *P* biomass occurs; *Z*: Max vertically integrated *Z* biomass [lipid + protein];
*Z*_{prot}: Max vertically integrated *Z* protein biomass; *Z*_{lip}: Max vertically integrated *Z* lipid biomass;
*Z*_{1st Jan}: Vertically integrated *Z* biomass [lipid + protein] on the 1st Jan; *Z*_{prot_1st Jan}: Vertically integrated *Z* protein biomass on the 1st Jan; *ZD*: Hours since 1st Jan when max vertically integrated *Z* biomass occurs; *S*: Max vertically integrated *S* biomass [lipid + protein];
*S*_{prot}: Max vertically integrated *S* protein biomass; *S*_{lip}: Max vertically integrated *S* lipid biomass;
SHD: Hours since 1st Jan when squid hatching occurs.

Fig.6.106-6.112 show the vertically integrated biomass of each population on attractor. Diatom had an average annual maximum biomass of 1717.3 mmol C m⁻² (s.d. 37.8 mmol C m⁻²; percentage variation from the mean = 2.2%; tab.6.30 and fig.6.106), which is not significantly different to the value in the base run (tab.6.8). It occurred on the 14th April (s.d. 21.5 hours; percentage variation from the mean = 0.9 %; tab.6.30), as in the base run (tab.6.8). The average annual maximum copepod biomass was about 208 mmol C m⁻² (s.d. 6.9 mmol C m⁻²; percentage variation from the mean = 3.3%; tab.6.30 and fig.6.107). This is about 10% lower

than the value in the base run (tab.6.8), but it occurred within 3 hours difference from the date in which it occurred in the base run (tab.6.30 and 6.8).

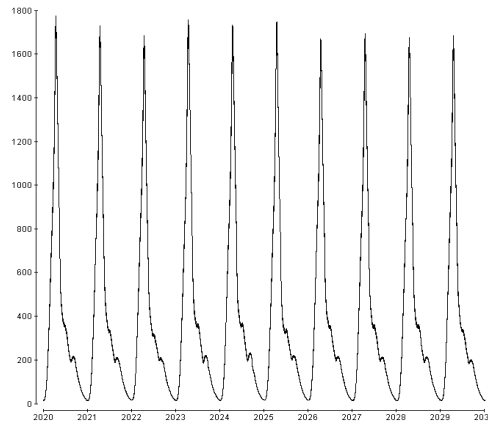


Fig 6.106 – Diatom total biomass (mmol C m^{-2})

As in the base run, total copepod biomass was made up of about one third protein and two thirds lipid (fig. 6.107-6.109 and tab.6.30). The biomass of over-wintering copepods on the 1st Jan was about 15% lower than in the base run: $36.8 \text{ mmol C m}^{-2}$ (s.d. $2.2 \text{ mmol C m}^{-2}$; percentage variation from the mean = 6.0%; tab.6.30). Squid hatching date did not vary from the date in the base run (tab.6.8), occurring on the 15th May each year (s.d. 0.7 hour, tab.6.30). Squid population biomass reached an average annual maximum of $9.6 \text{ mmol C m}^{-2}$ (s.d. $0.3 \text{ mmol C m}^{-2}$; percentage variation from the mean = 3.4%; tab.6.30). Protein constituted over 80% of the total biomass (Fig. 6.110-6.112 and tab.6.30). Compared to the base run, the annual maximum squid biomass in this VE was only $0.3 \text{ mmol C m}^{-2}$ lower.

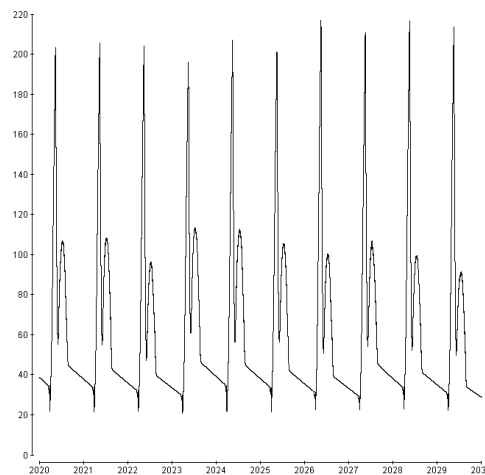


Fig 6.107 - Copepod total biomass – all stages (mmol C m^{-2})

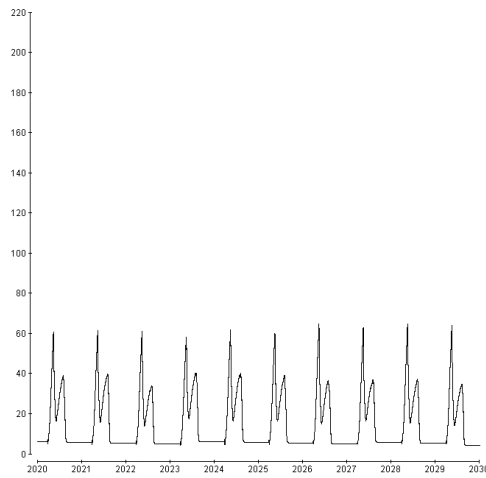


Fig 6.108 - Copepod protein biomass – all stages (mmol C m⁻²)

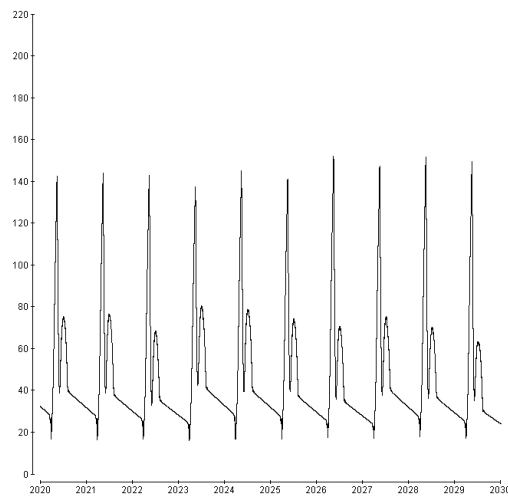


Fig 6.109 - Copepod lipid biomass – all stages (mmol C m⁻²)

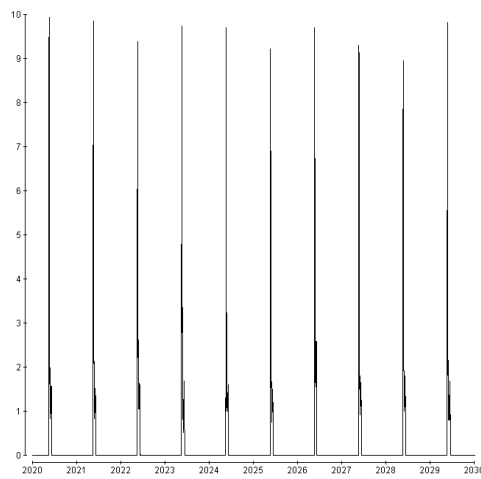


Fig 6.110 - Squid biomass – all stages (mmol C m⁻²)

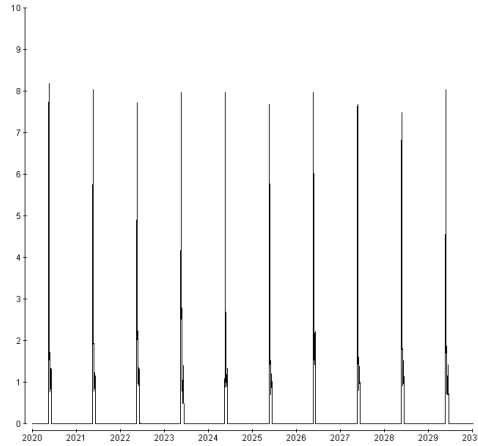


Fig 6.111 - Squid protein biomass – all stages (mmol C m⁻²)

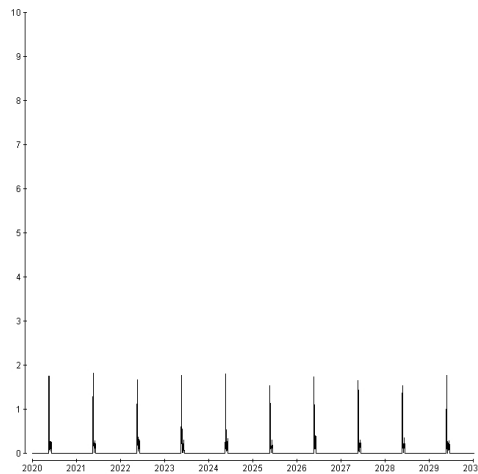


Fig 6.112 - Squid lipid biomass – all stages (mmol C m⁻²)

Carbon transfer

Year	<i>PingZ</i> mmolC m ⁻² yr ⁻¹	<i>ZingS</i> mmolC m ⁻² yr ⁻¹	<i>Zprot_ingS</i> mmolC m ⁻² yr ⁻¹	<i>Zlip_ingS</i> mmolC m ⁻² yr ⁻¹	<i>ZingBP</i> mmolC m ⁻² yr ⁻¹	<i>SingPred</i> mmolC m ⁻² yr ⁻¹
2020	2385.7	19.4	8.3	11.1	56.2	21.6
2021	2350.2	19.2	8.0	11.2	48.4	21.6
2022	2222.3	18.8	7.9	10.9	45.6	21.2
2023	2397.5	19.1	7.9	11.2	55.7	20.9
2024	2453.3	19.8	8.4	11.4	59.8	21.9
2025	2333.9	18.9	7.7	11.2	50.7	21.2
2026	2367.5	22.8	9.3	13.5	45.7	21.7
2027	2372.1	18.4	7.5	10.9	47.4	20.8
2028	2378.8	19.1	8.0	11.1	47.9	21.1
2029	2272.9	20.4	7.8	12.6	43.3	20.6
Ave	2353.4	19.6	8.1	11.5	50.1	21.3
s.d.	65.2	1.3	0.5	0.9	5.4	0.4
% var	2.8	6.5	6.2	7.5	10.8	2.0

Tab. 6.31 – Carbon transfer through the trophic chain. Where:

PingZ = Carbon ingested annually by copepods; *ZingS* = Carbon ingested annually by squid; *Zprot_ingS* = Protein ingested annually by squid; *Zlip_ingS* = Lipid ingested annually by squid; *ZingBP* = Carbon ingested annually by basal predator; *SingPred* = Carbon ingested annually by visual predator.

The amount of carbon transferred from diatoms to copepods was on average 10% lower than that of the base run (tab.6.9): $2,353.4 \text{ mmolC m}^{-2} \text{ yr}^{-1}$ (s.d. $65.2 \text{ mmolC m}^{-2} \text{ yr}^{-1}$; percentage variation from the mean = 2.8 %; tab.6.31). The carbon transferred annually from copepod to predators (squid and basal predators) was about 20% less than in the base run (tab.6.9): $69.7 \text{ mmol C m}^{-2} \text{ yr}^{-1}$, of which $19.6 \text{ mmol C m}^{-2} \text{ yr}^{-1}$ (s.d. $1.3 \text{ mmolC m}^{-2} \text{ yr}^{-1}$; percentage variation from the mean = 6.5 %; tab.6.31) was transferred to the squid population and the remaining $50.1 \text{ mmol C m}^{-2} \text{ yr}^{-1}$ (s.d. $5.4 \text{ mmolC m}^{-2} \text{ yr}^{-1}$; percentage variation from the mean = 10.8 %; tab.6.31) went to the basal predator population. Compared to the amount of carbon transferred from the copepod population to the higher trophic levels in the base run (tab.6.9), the amount of carbon transferred to the squid population was about 12% less. When considering the protein ingested by squid, the reduction from the base run was almost 20%. The average annual carbon transferred from squid to visual predator was about 6% lower than that in the base run (tab.6.9): $21.3 \text{ mmol C m}^{-2} \text{ yr}^{-1}$ (s.d. $0.4 \text{ mmol C m}^{-2} \text{ yr}^{-1}$; percentage variation from the mean = 2.0 %; tab.6.31).

6.3.2.4 Number of agents

The number of diatom agents varied between about 2,100-4,850 (fig.6.113), with the same trend observed in the base run (fig.6.43). The number of copepod agents varied from a minimum of 600 (all over-wintering during the winter) to about 2,200 (fig.6.114). It kept the same trend as in the base run (fig.6.44).

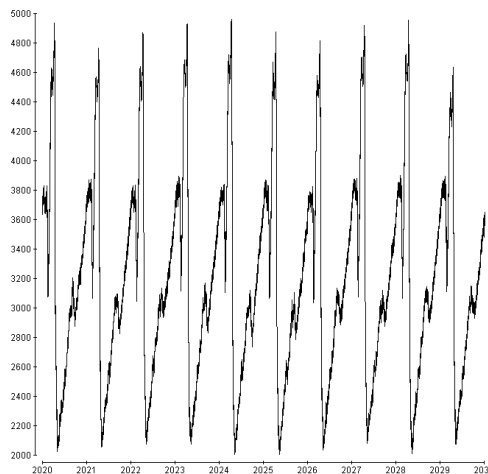


Fig 6.113 - Number of diatom agents

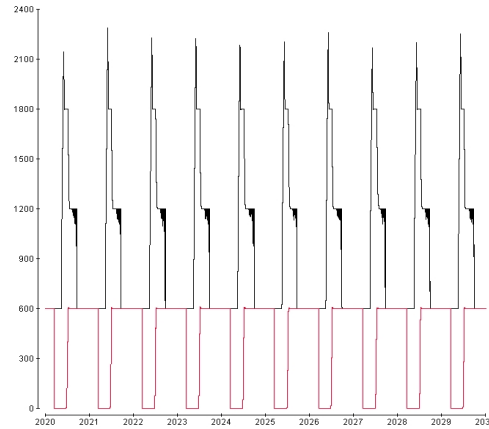


Fig 6.114 - Number of copepod agents

Squid agents in stages S1-S6 are always maintained to a number of 300 in the period between hatching and recruitment (fig.6.115).

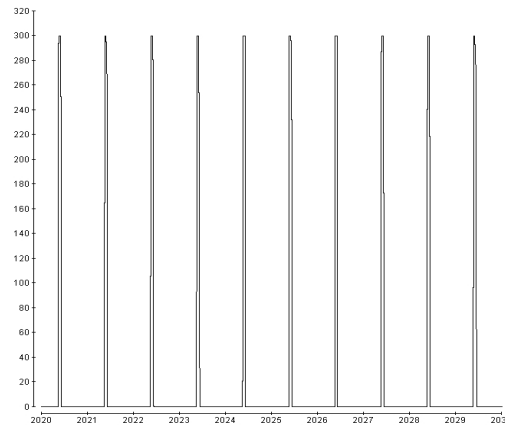


Fig 6.115 - Number of squid agents S1-S6

6.3.2.5 Physical environment

	Units	Year 16-25		
		Ave	s.d.	% var
MLD _{max}	m	156.4	2.7	1.8
T _{min} [0]	°C	14.5	0.01	0.1
T _{max} [0]	°C	29.3	0.09	0.3

Tab. 6.32 – Surface minimum and maximum average temperature and annual average maximum mixed layer depth, standard deviation and percentage variation from the average. Where:

MLD_{max}: Annual maximum mixed layer depth;

T_{min}[0] and T_{max}[0]: Annual minimum and maximum average surface temperature.

The physical environment was largely unchanged by the increase in basal predator abundance. The average annual maximum mixed layer depth (fig.6.116) was 156.4 m (s.d. 2.7 m; percentage variation from the mean = 1.8 %; tab.6.32), which is not

significantly different from the average annual maximum reached in the base run (tab.6.10) every year in mid-March. The average sea surface temperature varied

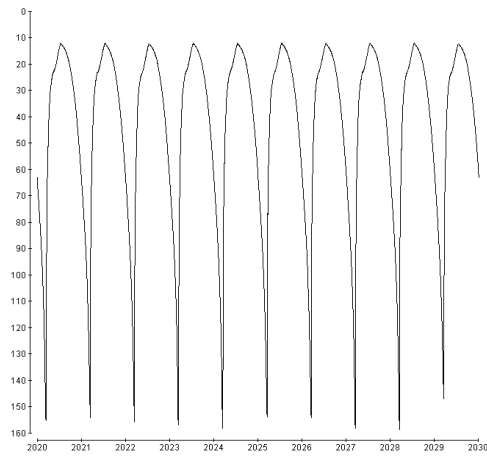


Fig 6.116 – Turbocline depth at 6 am (m)

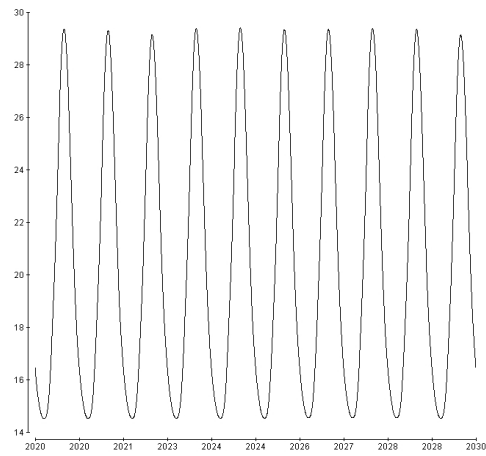


Fig 6.117 – Sea surface temperature (°C)

from an annual minimum of 14.5°C (s.d. 0.01°C; percentage variation from the mean = 0.1 %; tab.6.32) in March to an annual maximum of 29.3 °C (s.d. 0.1°C; percentage variation from the mean = 0.3 %; tab.6.32) in August (fig.6.117). It did not differ significantly from the average sea surface temperature in the base run (tab.6.10).

6.3.2.6 Chemical environment

	Units	Year 16-25		
		Ave	s.d.	% var
N [0]	mmol N m ⁻³	6.0	0.1	0.8
Si [0]	mmol Si m ⁻³	1.7	0.1	3.0

Tab. 6.33 – Surface nutrients average concentration, standard deviation and percentage variation from the average. Where: N[0]: Maximum dissolved N concentration at surface; Si[0]: Maximum dissolved Si concentration at surface.

The total (dissolved + particulate) mesocosm nitrogen and silicate (fig.6.118-6.119) had a small drift as observed in the base run (fig.6.48-6.49). Both total mesocosm nitrogen and silicon concentrations were mostly unchanged from the base run. They drifted from 4,493.8 to 4,497.7 mmol N m⁻² and from 1348.5 to 1347.5 mmol Si m⁻², respectively (fig.6.48-6.49 and fig.6.118-6.119).

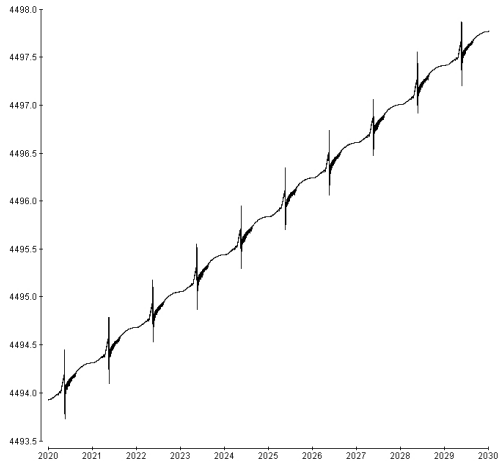


Fig 6.118 – Total mesocosm nitrogen (mmol N m^{-2})

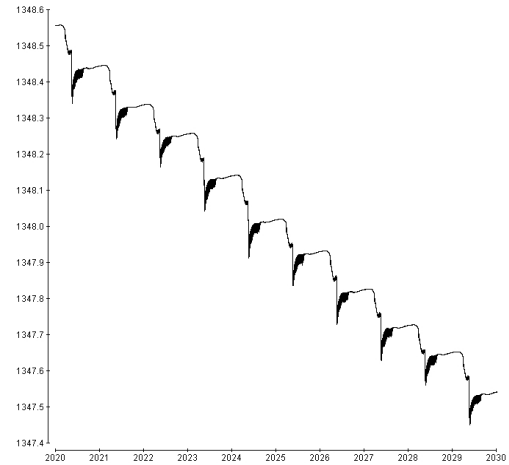


Fig 6.119 – Total mesocosm silicon (mmol Si m^{-2})

Dissolved nitrogen and silicate (fig.6.120-6.121) reached an average maximum surface concentration respectively of $6.0 \text{ mmol N m}^{-3}$ (s.d. $0.1 \text{ mmol N m}^{-3}$; percentage variation from the average = 0.8%; tab.6.33) and $1.7 \text{ mmol Si m}^{-3}$ (s.d. $0.1 \text{ mmol Si m}^{-3}$; percentage variation from the average = 3.0%; tab.6.33). These average annual maximum surface concentrations were not significantly different from those in the base run (tab.6.11).

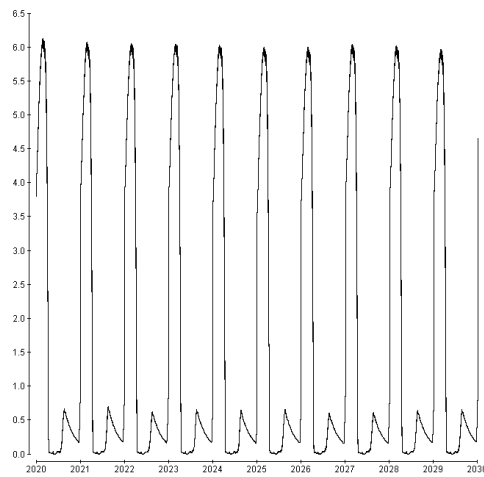


Fig 6.120 – Surf. dissolved nitrogen (mmolN m^{-3})

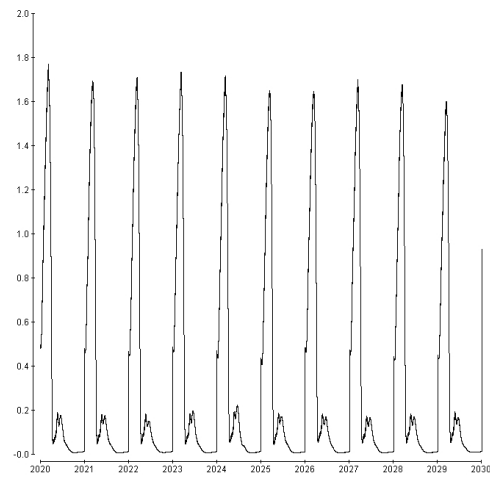


Fig 6.121 – Surf. dissolved silicon (mmolSi m^{-3})

6.3.3 Increasing predation pressure (visual predator)

Restarted from a VE snapshot on the 1st Jan 2015 of the base run. The vertically integrated concentration of visual predators feeding on the squid population is doubled from 3,000 ind m⁻² to 6,000 ind m⁻², in order to investigate the effect of predation pressure on annual squid recruitment.

6.3.3.1 Vertically integrated concentration of plankton

	Units	Year 16-25		
		Ave	s.d.	% var
P	ind m ⁻²	8.9×10 ¹⁰	5.9×10 ⁹	6.6
Z	ind m ⁻²	158034.3	16441.7	10.4
Z _{OW}	ind m ⁻²	6132.9	523.0	8.5
S	ind m ⁻²	95.3	3.3	3.5
SHD	h	3255.6	1.0	0.03
R	ind m ⁻² yr ⁻¹	1.7	0.5	30.1

Tab. 6.34 - Average value, s.d. and percentage variation from the mean for years 2020-2030. Where:

P: Max vertically integrated P concentration; Z: Max vertically integrated Z concentration;

Z_{OW}: Max vertically integrated concentration of over-wintering copepods; S: Max vertically integrated S concentration; SHD: Hours since 1st Jan when squid hatching occurs;

R: vertically integrated total number of squid that reached stage 7 between 2020-2030;

Fig.6.122-125 show the vertically integrated concentration of the populations between years 2020-2030. During that period, diatom had an average annual maximum concentration of 8.9×10¹⁰ ind m⁻² (s.d. 5.9×10⁹ ind m⁻²; percentage variation from the mean was 6.6; tab.6.34 and fig.6.122), which is not significantly different from the maximum observed in the base run (tab.6.5).

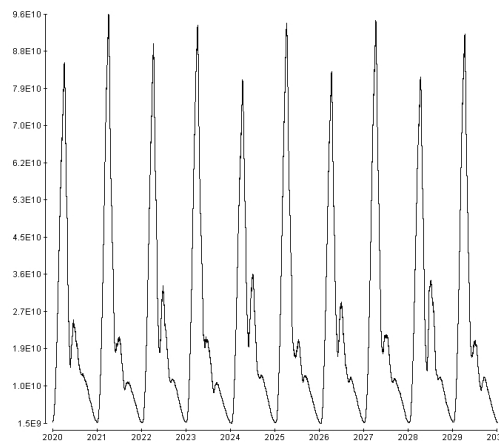


Fig. 6.122 - Vertically integrated P concentration (ind m⁻²)

However, the maximum diatom concentration fluctuated inter-annually and exhibited a higher standard deviation than in base run (tab.6.34 and 6.5).

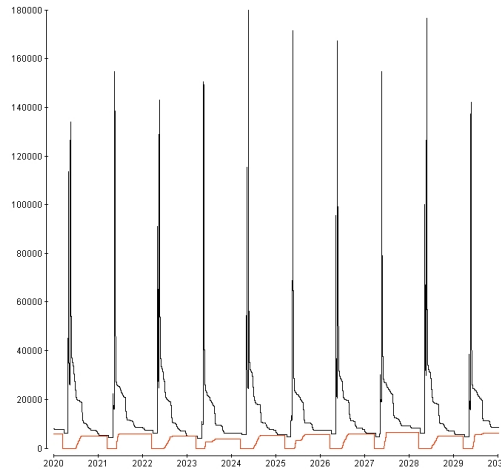


Fig. 6.123 - Vertically integrated Z concentration (black:all stages; red: over-wintering) (ind m⁻²)

Contrary to what happened in the base run, every winter some copepods survived the winter without overwintering (fig. 6.123). The annual average concentration of copepod that entered over-wintering was lower than in the base run (tab.6.5): 6,133 ind m⁻² (s.d. 523 ind m⁻²; percentage variation from the average = 8.5%; tab.6.34). The average annual peak in copepod concentration was not significantly different from that in the base run (tab.6.5): about 158,000 ind m⁻² (s.d. 16,400 ind m⁻²; percentage variation from the average = 10.4%; tab.6.34).

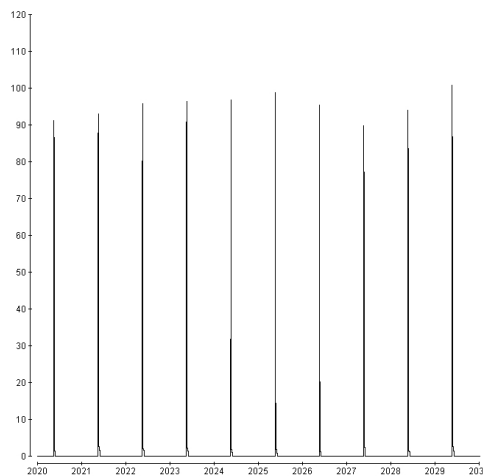


Fig. 6.124 - Vertically integrated concentration of squid (S1-S6) (ind m⁻²)

The annual maximum concentration in squid (fig. 6.124) was much smaller than in the base run (tab.6.5): 95.3 ind m⁻² (s.d. 3.3 ind m⁻²; percentage variation from the average = 3.5%; tab.6.34). Every year eggs started to hatch on the 15th (tab.6.34). The average annual recruitment was 1.7 ind m⁻² yr⁻¹ (s.d. 0.5 ind m⁻² yr⁻¹; percentage variation from the mean of 30.1%; fig.6.125 and tab.6.34), which is less than half the recruitment in the base run (tab.6.5).

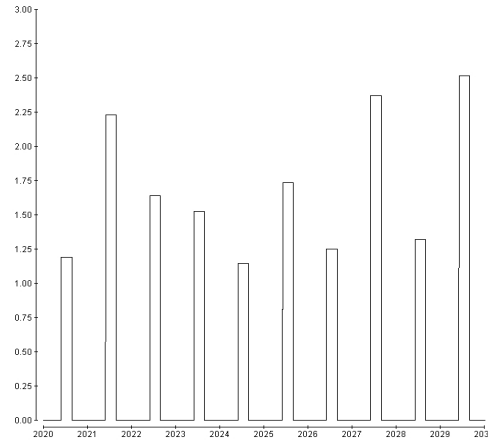


Fig. 6.125 - Annual squid recruitment (ind m⁻² yr⁻¹)

6.3.3.2 Causes of mortality

Table 6.36 summarizes the annual losses to mortality due to predation and starvation between 2020-2030, with average, standard deviation and percentage variation from the mean during this period.

The average number of diatoms consumed by copepods annually (tab.6.35) was 1.5×10^{11} m⁻² yr⁻¹ (s.d. = 1.7×10^{10} diatoms m⁻² yr⁻¹; percentage variation from the mean = 11.7%) which is almost one third higher than in base run (tab.6.6). On the other hand the number of diatoms lost due to energy starvation is about one tenth lower than in base run (tab.6.6): 1.8×10^{11} diatoms m⁻² yr⁻¹ (s.d. = 6.9×10^9 diatoms m⁻² yr⁻¹; percentage variation from the mean = 3.8%, tab.6.35). The average number of copepods annually ingested by squid was about one third less than in the base run (tab.6.6): 107,000 ind m⁻² yr⁻¹ (s.d. = 23,740 copepods m⁻² yr⁻¹; percentage variation from the mean = 22.2%, tab.6.35). The percentage variation from the mean was however double than in the base run. The average number of annually ingested copepods by basal predator was about one third more than what they ingested in the

base run (tab.6.6): 312,000 ind m⁻² yr⁻¹ (s.d. = 67,350 copepods m⁻² yr⁻¹; percentage variation from the mean = 21.6%, tab.6.35). The percentage variation from the mean was three times higher than in the base run (tab.6.6 and 6.35). The average number of copepods annually lost due to starvation was 12,185 ind m⁻² yr⁻¹ (s.d. = 911 copepods m⁻² yr⁻¹; percentage variation from the mean = 7.5%, tab.6.35), which is almost double the average annual value in base run (tab.6.6). Squid mortality was caused exclusively by top predator predation: 298.3 squid m⁻² yr⁻¹ (s.d. = 0.5 squid m⁻² yr⁻¹; percentage variation from the mean = 0.2%, tab.6.35). As already seen in the base run (tab.6.9), newly hatched S1 squid were subject to the highest predation, which progressively decreased in successive stages (tab.6.36). However, predation on different squid stages oscillated yearly (tab.6.36).

Year	PingZ ind m ⁻² yr ⁻¹	ZingS ind m ⁻² yr ⁻¹	ZingBP ind m ⁻² yr ⁻¹	SingPred ind m ⁻² yr ⁻¹	Pstarve ind m ⁻² yr ⁻¹	Zstarve ind m ⁻² yr ⁻¹	Sstarve ind m ⁻² yr ⁻¹
2020	1.7×10 ¹¹	140310.5	340659.9	298.8	1.7×10 ¹¹	12429.6	0
2021	1.4×10 ¹¹	109107.4	250766.4	297.8	1.9×10 ¹¹	12334.2	0
2022	1.6×10 ¹¹	124441.2	361031.9	298.4	1.8×10 ¹¹	14137.1	0
2023	1.2×10 ¹¹	107907.9	231313.5	298.5	1.9×10 ¹¹	10872.2	0
2024	1.6×10 ¹¹	58653.4	391415.4	298.9	1.8×10 ¹¹	11007.4	0
2025	1.3×10 ¹¹	115180.9	270905.5	298.3	1.9×10 ¹¹	12241.1	0
2026	1.6×10 ¹¹	83879.1	381605.0	298.7	1.8×10 ¹¹	12106.1	0
2027	1.4×10 ¹¹	111602.3	259892.7	297.6	1.9×10 ¹¹	12671.7	0
2028	1.6×10 ¹¹	89333.7	392721.2	298.7	1.8×10 ¹¹	11737.9	0
2029	1.4×10 ¹¹	126518.9	239414.0	297.5	1.8×10 ¹¹	12327.1	0
Ave	1.5×10 ¹¹	106693.5	311972.5	298.3	1.8×10 ¹¹	12186.4	0
s.d.	1.7×10 ¹⁰	23737.6	67351.2	0.5	6.9×10 ⁹	911.0	-
% var	11.7	22.2	21.6	0.2	3.8	7.5	-

Tab. 6.35 – Causes of mortality. Where:

PingZ = Diatoms ingested by copepods; ZingS = Copepods ingested by squid; ZingBP = Copepods ingested by basal predator; SingPred = Squid ingested by visual predator; Pstarve = Diatoms died of energy starvation; Zstarve = Copepods died of starvation; Sstarve = Squid died of starvation.

Year	S1	S2	S3	S4	S5	S6
2020	287.02	11.29	0.28	0.12	0.05	0.04
2021	283.34	14.10	0.24	0.03	0.01	0.03
2022	292.36	5.75	0.15	0.06	0.03	0.02
2023	277.10	21.11	0.14	0.07	0.03	0.02
2024	295.18	3.51	0.09	0.04	0.02	0.02
2025	277.09	20.82	0.18	0.10	0.02	0.03
2026	289.75	8.41	0.32	0.19	0.06	0.02
2027	276.36	21.06	0.12	0.01	0.05	0.03
2028	296.74	1.85	0.04	0.01	0.03	0.01
2029	283.82	13.48	0.13	0.02	0.02	0.01
Ave	285.88	12.14	0.17	0.07	0.03	0.02
s.d.	7.59	7.28	0.09	0.06	0.02	0.01
% var	2.65	59.97	52.16	86.87	52.37	47.85

Tab. 6.36 – Stage specific squid mortality due to predation

6.3.3.3 Vertically integrated biomass of plankton

	Units	Ave	s.d.	% var
<i>P</i>	mmol C m ⁻²	1648.5	80.9	4.9
<i>PD</i>	h	2515.7	30.5	1.2
<i>Z</i>	mmol C m ⁻²	267.0	15.6	5.9
<i>Z</i> _{prot}	mmol C m ⁻²	79.4	5.0	6.3
<i>Z</i> _{lip}	mmol C m ⁻²	188.1	11.3	6.0
<i>ZD</i>	h	3203.0	32.7	1.0
<i>S</i>	mmol C m ⁻²	5.3	0.2	4.2
<i>S</i> _{prot}	mmol C m ⁻²	4.5	0.2	3.6
<i>S</i> _{lip}	mmol C m ⁻²	1.0	0.2	15.3
<i>SHD</i>	h	3255.6	1.0	0.03

Tab. 6.37 - Average value, s.d. and percentage variation from the mean. Where:

P : Annual maximum P biomass; *PD*: Hours since 1st Jan when max P biomass occurs; *Z*: Max Z biomass [lipid + protein]; *Z*_{prot}: Max Z protein biomass; *Z*_{lip}: Max Z lipid biomass; *ZD*: Hours since 1st Jan when max Z biomass occurs; *S*: Max S biomass [lipid + protein]; *S*_{prot}: Max S protein biomass; *S*_{lip}: Max S lipid biomass; *SHD*: Hours since 1st Jan when squid hatching occurs.

Fig. 6.126-6.132 show the vertically integrated biomass of each population on attractor. Diatom had an average annual maximum biomass of 1648.5 mmol C m⁻² (s.d. 80.9 mmol C m⁻²; percentage variation from the mean = 4.9%; tab.6.37 and fig.6.126), which is slightly lower than the value in the base run (tab.6.8). It occurred on the 14th April (s.d. 30.5 hours; percentage variation from the mean = 1.2%; tab.6.37), as in the base run (tab.6.8). The average annual maximum copepod biomass was 267 mmol C m⁻² (s.d. 15.6 mmol C m⁻²; percentage variation from the mean = 5.93%; tab.6.37 and fig.6.127). This is about 15% higher than the value in the base run (tab.6.8) and occurred within 10 hours from the date in which it occurred in the base run (tab.6.37 and 6.8).

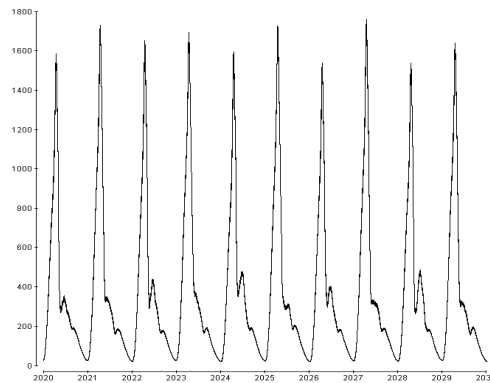


Fig 6.126 – Diatom total biomass (mmol C m⁻²)

The total copepod biomass was made up of about one third protein and two thirds lipid (fig. 6.127-6.129 and tab.6.37). Squid hatching date did not vary from the date in the base run (tab.6.8) occurring on the 15th May each year (s.d. 0.7 hour, tab.6.37). Squid biomass reached an average annual maximum of 5.3 mmol C m⁻²

(s.d. $0.2 \text{ mmol C m}^{-2}$; percentage variation from the mean = 4.2%; tab.6.37), which is almost half the maximum biomass obtained in the base run. Protein constituted over 80% of the total biomass (Fig. 6.130-6.132 and tab.6.37).

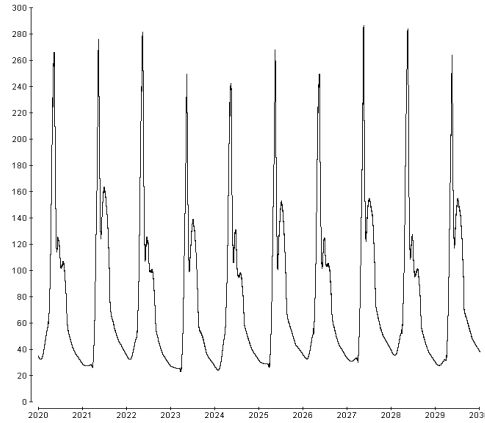


Fig 6.127 - Copepod total biomass – all stages (mmol C m^{-2})

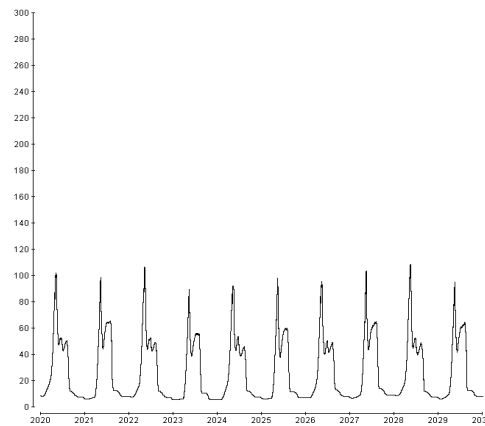


Fig 6.128 - Copepod protein biomass – all stages (mmol C m^{-2})

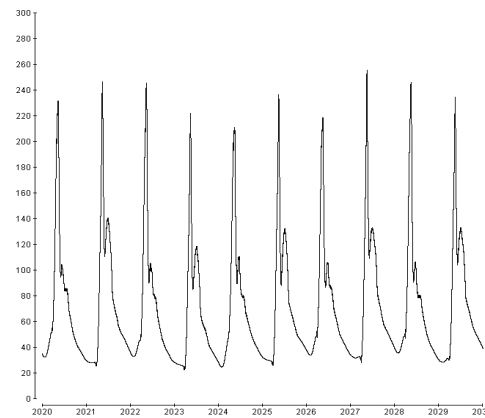


Fig 6.129 - Copepod lipid biomass – all stages (mmol C m^{-2})

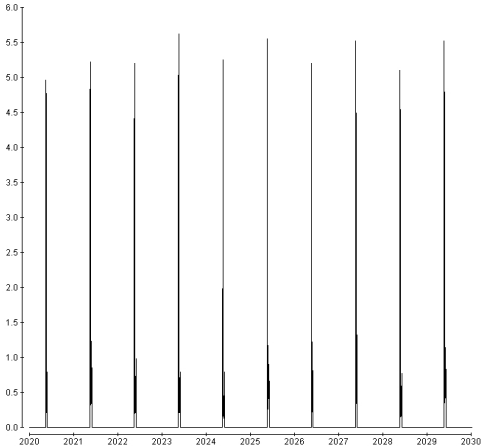


Fig 6.130 - Squid biomass – all stages (mmol C m^{-2})

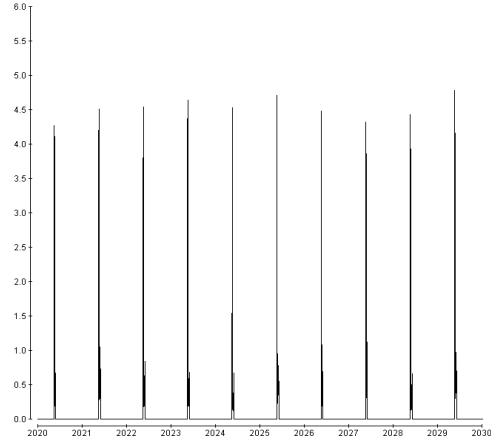


Fig 6.131 - Squid protein biomass – all stages (mmol C m^{-2})

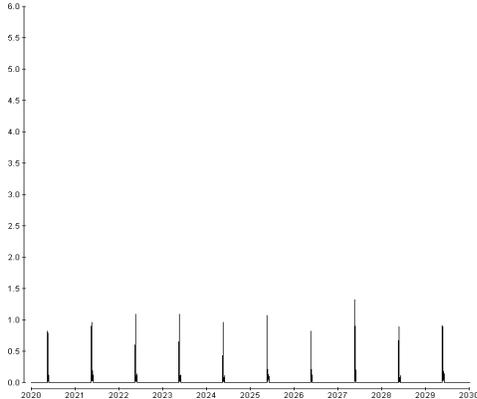


Fig 6.132 - Squid lipid biomass – all stages (mmol C m^{-2})

6.3.3.4 Comparison between 1st Jan vertically integrated biomass of diatom and copepod with base run

	Units	Base run			Double Pred		
		Ave	s.d.	% var	Ave	s.d.	% var
<i>P</i>	mmol C m ⁻²	18.7	0.8	4.5	25.3	2.6	10.3
<i>Z</i>	mmol C m ⁻²	42.6	2.5	5.8	32.5	3.9	12.1

Tab.6.38 – 1st Jan diatom and copepod biomass multi-year average, standard deviation and percentage variation

Compared to the base run, the percentage variation from the mean of diatom and copepod biomass on the 1st January increased by more than double (tab.6.38, fig. 6.133-134).

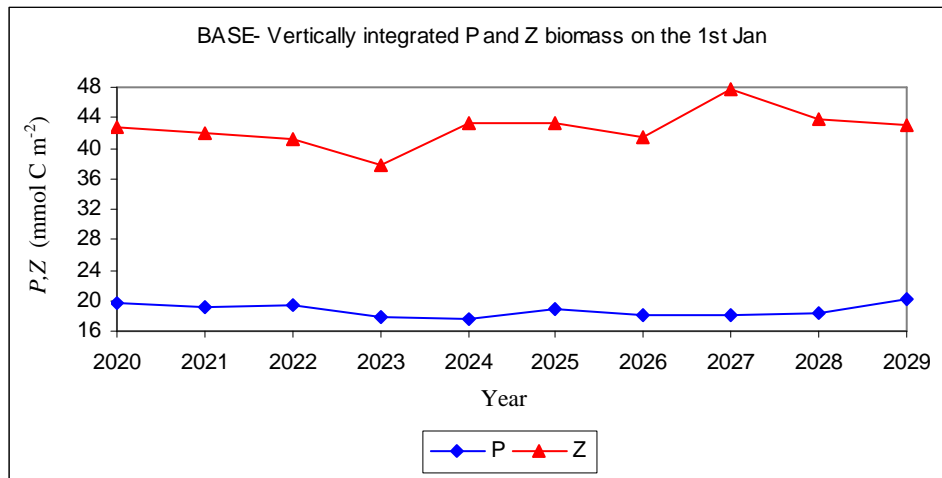


Fig 6.133 – Vertically integrated diatom (*P*, mmol C m⁻²) and copepod (*Z*, mmol C m⁻²) biomass on the 1st Jan each year of the base run

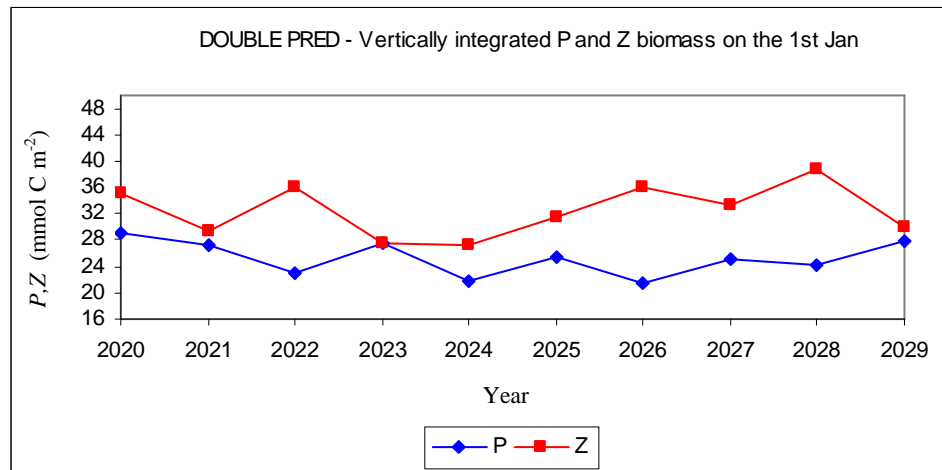


Fig 6.134 – Vertically integrated diatom (*P*, mmol C m⁻²) and copepod (*Z*, mmol C m⁻²) biomass on the 1st Jan each year of the increased predation run

Carbon transfer

The amount of carbon transferred from diatoms to copepods was on average 20% higher than that of the base run (tab.6.9): 3,254 mmolC m⁻² yr⁻¹ (s.d. 244.7 mmolC m⁻² yr⁻¹; percentage variation from the mean = 7.5 %; tab.6.39). The carbon transferred annually from copepod to predators was almost one quarter more than in the base run (tab.6.9): 110.2 mmol C m⁻² yr⁻¹, of which 6.9 mmol C m⁻² yr⁻¹ (s.d. 1.9 mmolC m⁻² yr⁻¹; percentage variation from the mean = 28.4 %; tab.6.39) was transferred to the squid population and the remaining 103.3 mmol C m⁻² yr⁻¹ (s.d. 37.4 mmolC m⁻² yr⁻¹; percentage variation from the mean = 36.2%; tab.6.39) went to the basal predator population. Compared to the amount of carbon transferred from the copepod population to the higher trophic levels in base run (tab.6.9), the amount of carbon ingested was about two thirds less for squid and about 60% more for the basal predator. The average annual carbon transferred from squid to visual predator was about 20% lower than that in the base run (tab.6.9): 17.8 mmol C m⁻² yr⁻¹ (s.d. 0.7 mmol C m⁻² yr⁻¹; percentage variation from the mean = 3.7%; tab.6.39).

Year	PingZ mmolC m ⁻² yr ⁻¹	ZingS mmolC m ⁻² yr ⁻¹	Zprot_ingS mmolC m ⁻² yr ⁻¹	Zlip_ingS mmolC m ⁻² yr ⁻¹	ZingBP mmolC m ⁻² yr ⁻¹	SingPred mmolC m ⁻² yr ⁻¹
2020	3624.3	5.7	2.5	3.1	155.0	17.8
2021	3092.2	7.5	3.6	3.9	70.0	17.9
2022	3457.3	5.9	2.4	3.5	128.7	17.3
2023	2852.7	7.7	3.8	3.9	65.9	18.6
2024	3393.1	4.7	1.7	3.0	132.6	17.0
2025	3031.7	7.7	3.7	4.0	60.0	18.5
2026	3342.2	5.3	2.3	3.0	126.6	17.5
2027	3162.1	10.4	4.4	6.0	78.9	18.7
2028	3499.3	4.7	1.8	2.8	145.3	17.0
2029	3086.4	9.2	4.0	5.2	69.7	18.2
Ave	3254.1	6.9	3.0	3.8	103.3	17.8
s.d.	244.7	1.9	1.0	1.0	37.4	0.7
% var	7.5	28.4	32.4	26.6	36.2	3.7

Tab. 6.39 – Carbon transfer through the trophic chain. Where: PingZ = Carbon ingested annually by Z; ZingS = Carbon ingested annually by S; Zprot_ingS = Protein ingested annually by S; Zlip_ingS = Lipid ingested annually by S; ZingBP = Carbon ingested annually by BP; SingPred = Carbon ingested annually by VP.

6.3.3.5 Number of agents

The number of diatom agents varied between about 2,100-4,850 (fig.6.135), with the same trend observed in the base run (fig.6.43). The number of copepod agents varied from a minimum of about 400 to a maximum of about 2,300 (fig.6.136). The trend was quite different from that in the base run (fig.6.44). The yearly succession of copepod agents was less regular, and characterised by the presence of non-

overwintering agents during the winter, and a yearly oscillation in the number of over-wintering agents (fig.6.136). Squid agents in stages S1-S6 were always maintained to a number of 300 in the period between hatching and recruitment (fig.6.137).

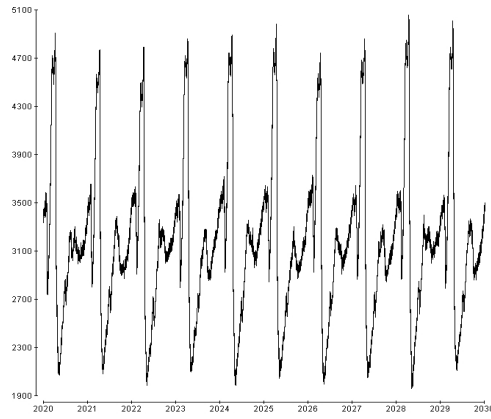


Fig 6.135 - Number of diatom agents

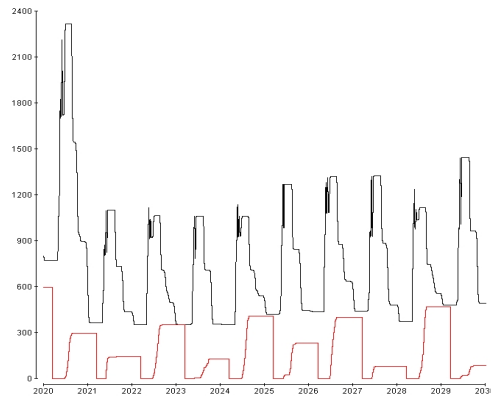


Fig 6.136 - Number of copepod agents

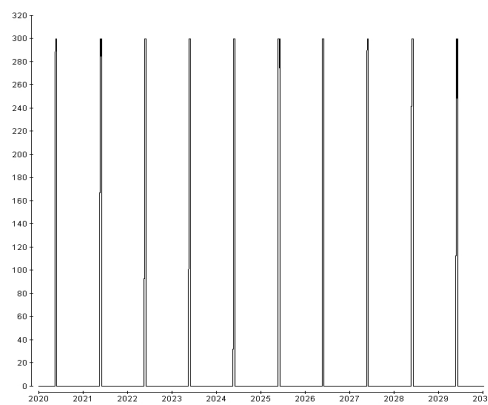


Fig 6.137 - Number of squid agents S1-S6

6.3.3.6 Physical environment

	Units	Year 16-25		
		Ave	s.d.	% var
MLD _{max}	m	157.8	2.5	1.6
T _{min} [0]	°C	14.4	0.01	0.1
T _{max} [0]	°C	29.2	0.1	0.3

Tab. 6.40 – Surface minimum and maximum average temperature and annual average maximum mixed layer depth, standard deviation and percentage variation from the average. Where:

MLD_{max}: Annual maximum mixed layer depth;

T_{min}[0] and T_{max}[0]: Annual minimum and maximum average surface temperature.

The physical environment was largely unchanged by the increase in visual predator abundance. The average annual maximum mixed layer depth (fig.6.138) was 157.8m (s.d. 2.5 m; percentage variation from the mean = 1.6 %; tab.6.40), which is not significantly different from the average annual maximum reached in the base run (tab.6.10) every year in mid-March. The average sea surface temperature varied from an annual minimum of 14.4°C (s.d. 0.01°C; percentage variation from the mean = 0.1 %; tab.6.40) in March to an annual maximum of 29.2 °C (s.d. 0.1°C; percentage variation from the mean = 0.3%; tab.6.40) in August (fig.6.139). It did not differ significantly from the base run (tab.6.10).

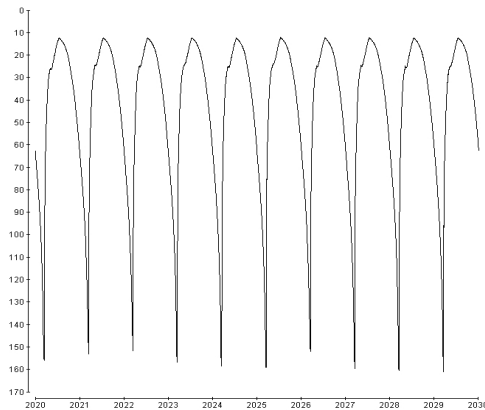


Fig 6.138 – Turbocline depth at 6 am (m)

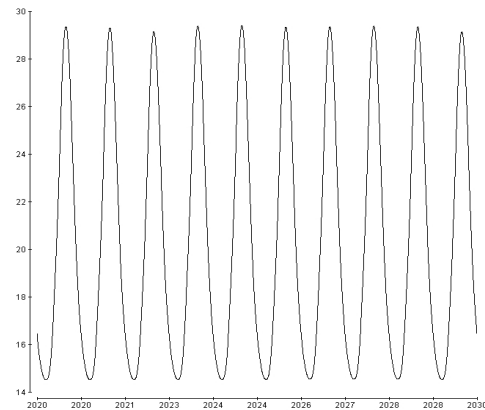


Fig 6.139 – Sea surface temperature (°C)

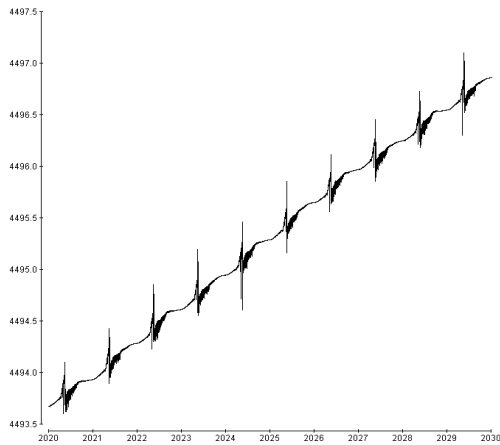
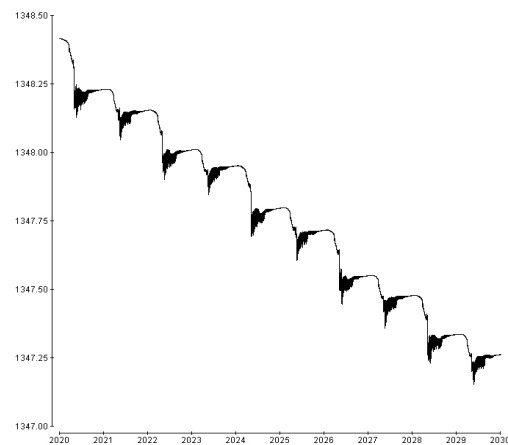
6.3.3.7 Chemical environment

	Units	Year 16-25		
		Ave	s.d.	% var
N [0]	mmol N m ⁻³	5.9	0.1	1.4
Si [0]	mmol Si m ⁻³	1.6	0.1	4.6

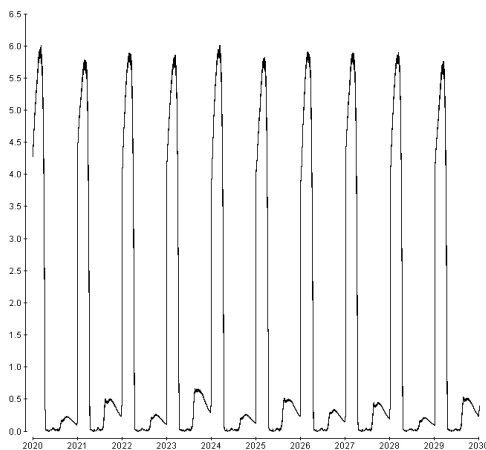
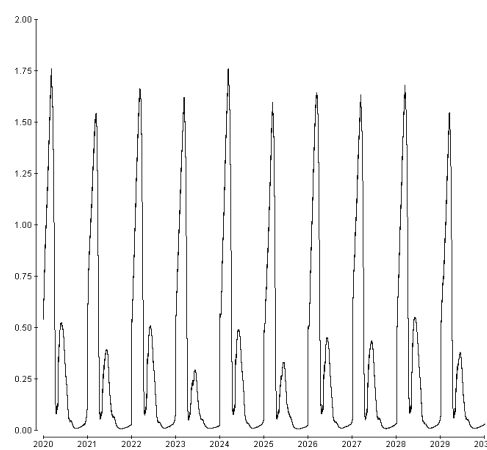
Tab. 6.41 – Surface nutrients average concentration, standard deviation and percentage variation from the average. Where: N[0]: Maximum dissolved N concentration at surface;

Si[0]: Maximum dissolved Si concentration at surface.

The total (dissolved + particulate) mesocosm nitrogen and silicate (fig.6.140-6.141) had a small drift as observed in the base run (fig.6.48-6.49). Both total mesocosm nitrogen and silicon concentrations were mostly unchanged from the base run. They drifted from about 4,493.7 to 4,497.0 mmol N m⁻² and from 1348.4 to 1347.3 mmol Si m⁻², respectively (fig.6.48-6.49 and fig.6.140-6.141).

Fig 6.140 – Total mesocosm nitrogen (mmol N m⁻²)Fig 6.141 – Total mesocosm silicon (mmol Si m⁻²)

Dissolved nitrogen and silicate (fig.6.142-6.143) reached an average maximum surface concentration respectively of 5.9 mmol N m⁻³ (s.d. 0.1 mmol N m⁻³; percentage variation from the average = 1.4%; tab.6.41) and 1.6 mmol Si m⁻³ (s.d. 0.1 mmol Si m⁻³; percentage variation from the average = 4.6%; tab.6.41). These average annual maximum surface concentrations were not significantly different from those in the base run (tab.6.11).

Fig 6.142 – Surf. dissolved nitrogen (mmol N m⁻³)Fig 6.143 – Surf. dissolved silicon (mmol Si m⁻³)

6.4 Sensitivity of recruitment to spawning

6.4.1 Variation in spawning stock (SS)

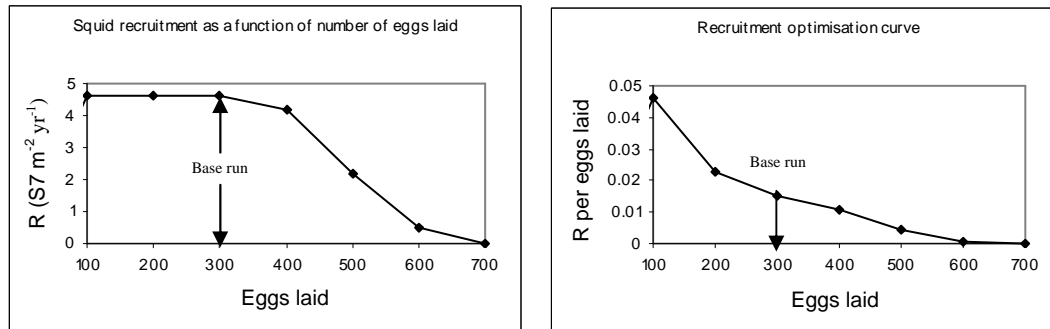


Fig. 6.144 – a) Number of recruits (ind $m^{-2} yr^{-1}$) and b) fraction of recruits per egg laid as a function of number of eggs laid (eggs $m^{-2} yr^{-1}$)

Annual squid recruitment decreased from 4.6 to 0 ind $m^{-2} yr^{-1}$ with increasing number of eggs being laid from 100 to 700 eggs $m^{-2} yr^{-1}$. Annual recruitment did not vary when 100 or 200 eggs were laid (fig.6.144a), and it decreased slightly when 300 and 400 eggs were laid. When 500 or more eggs were laid, annual recruitment decreased progressively, until no recruitment occurred when 700 eggs were laid (fig.6.144a). However, when considering the fraction of eggs laid that reaches the 8 mm in mantle length (recruits), it can be seen that it decreases progressively as more eggs are laid annually (6.144b).

6.4.1.1 Causes of mortality

When 100-400 eggs were laid, mortality was exclusively caused by predation, while, when more eggs were laid, it was caused by a combination of starvation and predation (tab.6.42).

Eggs laid	Sstarve	Sing	R
100	0.00	95.38	4.60
200	0.00	195.40	4.60
300	0.00	295.81	4.20
400	0.00	395.80	4.10
500	41.42	457.38	2.20
600	14.78	584.47	0.75
700	39.51	660.39	0.00

Tab.6.42 - Causes of squid mortality (ind $m^{-2} yr^{-1}$) and recruitment (ind $m^{-2} yr^{-1}$)

6.4.1.2 Food availability and ingestion

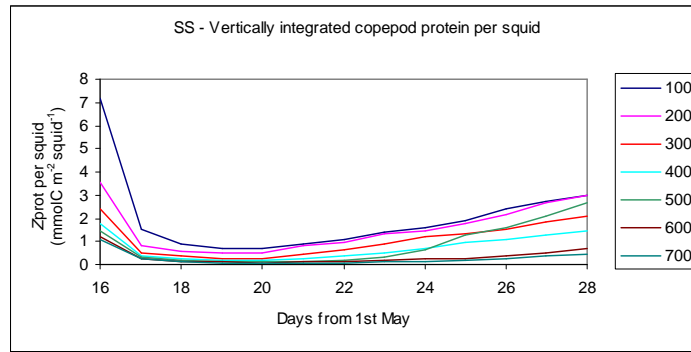


Fig. 6.145 – Vertically integrated protein availability per squid

When more eggs were laid, the limited food resources were smaller for each squid (fig.6.145). However, the amount of copepod protein ingested annually by the squid population increased with increasing the number of eggs, and stabilised when more than 400 eggs were laid annually (fig.6.146). Squid in stage S1 ingested more protein as more eggs were laid, but this trend was reversed for squid in stage S2 when more than 400 eggs were laid (fig.6.147).

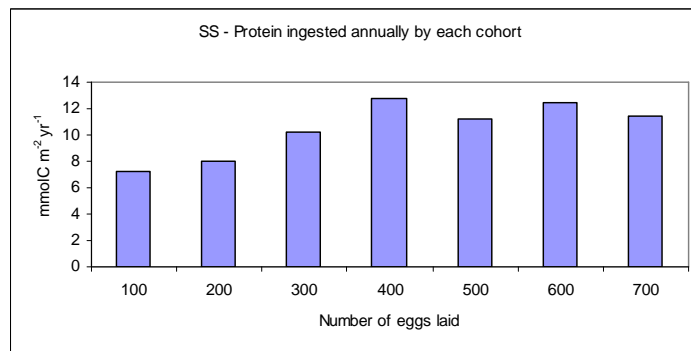


Fig. 6.146 – Annual ingestion of protein (mmol C m⁻² yr⁻¹) as function of number of eggs laid (eggs m⁻² yr⁻¹)

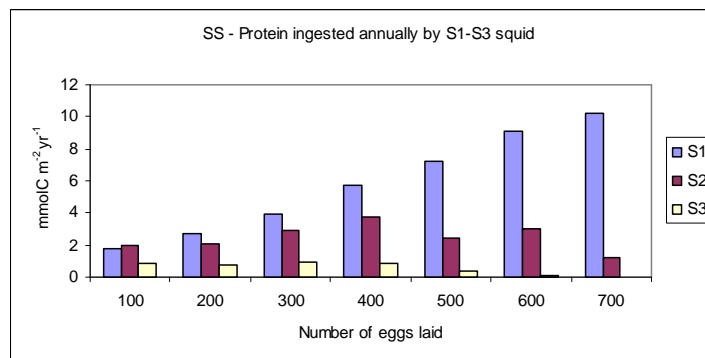


Fig. 6.147 – Annual ingestion of protein divided by stage S1 to S3 (mmol C m⁻² yr⁻¹) as function of number of eggs laid (eggs m⁻² yr⁻¹)

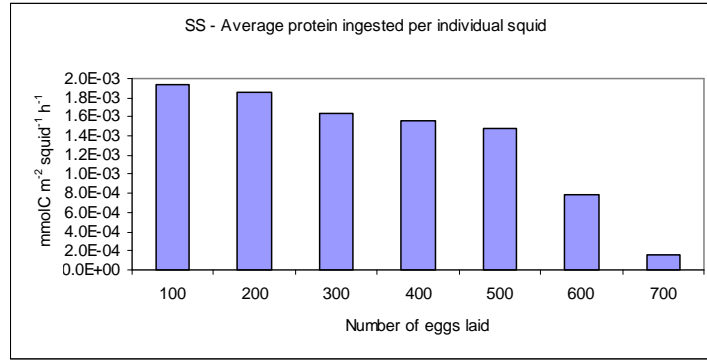


Fig. 6.148 – Annual recruitment (ind m⁻² yr⁻¹) as a function of number of eggs laid (eggs m⁻² yr⁻¹)

The average amount of protein ingested annually by individual squid decreased as the number of eggs laid increased (fig.6.148).

6.4.1.3 Time spent in each stage

The permanence time of squid in stages S1 and S2 increased with the number of eggs laid (tab.6.43). The only exception is the permanence in S2 when 700 eggs were laid, which is shorter due to premature extinction of the squid cohort (tab.6.43).

Eggs laid	S1	S2	S3	S4	S5	S6	R
100	5.54	10.08	8.35	6.06	5.92	6.60	4.60
200	6.38	10.96	8.29	6.71	6.67	6.94	4.60
300	6.38	11.40	7.42	6.08	6.02	7.13	4.20
400	6.40	12.94	8.77	8.25	9.00	9.79	4.10
500	11.40	14.00	5.85	5.15	5.29	6.13	2.20
600	10.38	21.27	11.94	10.69	9.65	8.27	0.75
700	13.40	11.94	-	-	-	-	0.00

Tab.6.43 – Duration (days) of each squid stage and annual recruitment (ind m⁻² yr⁻¹)

The time spent in stage S1 and S2 explained 99% of the recruitment variability (fig.6.149).

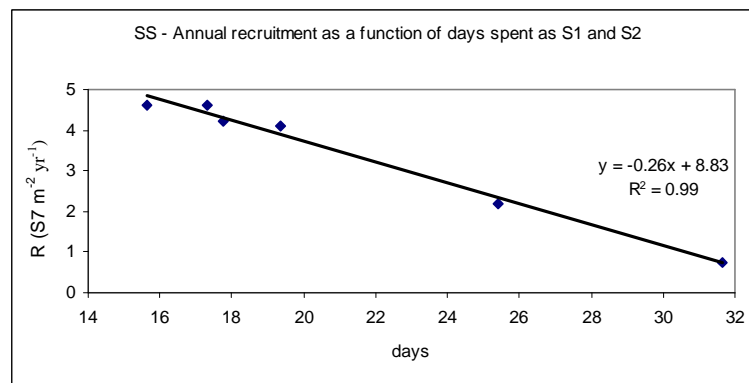


Fig. 6.149 – Correlation between recruitment and days spent as S1 and S2

6.4.2 Variation in squid spawning date

Spawning day since the 1 st Jan	Spawning date	R	S _{starve}	S _{ing}
88	29-Mar	0.0	32.7	267.3
92	02-Apr	1.8	29.8	268.4
96	06-Apr	7.0	0.1	292.8
100	10-Apr	4.2	0.00	295.8
104	14-Apr	4.9	0.00	295.0
108	18-Apr	6.1	0.3	293.6
112	22-Apr	4.1	12.0	283.9
116	26-Apr	3.7	34.1	262.2
120	30-Apr	4.1	6.7	289.2
124	04-May	1.7	52.3	246.1
128	08-May	0.6	92.1	207.2
132	12-May	5.8	97.0	197.2
136	16-May	3.0	153.3	143.8
140	20-May	0.5	165.0	134.4
144	24-May	0.0	190.5	109.4

Tab. 6.44 – Recruitment R ($S7\text{ m}^{-2}\text{ yr}^{-1}$) Causes of mortality: starvation, S_{starve} (ind $\text{m}^{-2}\text{ yr}^{-1}$) and predation, S_{ing} (ind $\text{m}^{-2}\text{ yr}^{-1}$) with different spawning dates.

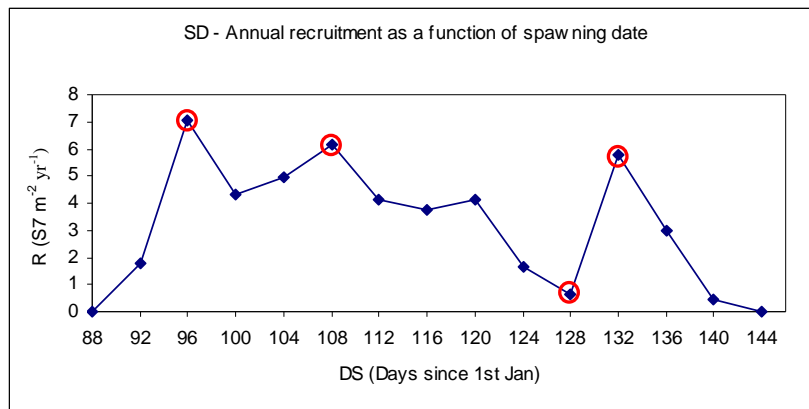


Fig.6.150 – Annual recruitment as a function of spawning date, DS. Red circles mark those spawning dates that have been analysed in detail.

Annual recruitment was sensitive to the date on which spawning occurred (fig. 6.150 and tab.6.44). No recruitment occurred when spawning occurred before day 88 (29th March) or after day 144 (24th May). In between these days, annual recruitment varied from a maximum of 7 squid $\text{m}^{-2}\text{ yr}^{-1}$ on day 96 (6th April) to a minimum of 0.6 squid $\text{m}^{-2}\text{ yr}^{-1}$ on day 128 (8th May). Annual recruitment was always above 4 squid $\text{m}^{-2}\text{ yr}^{-1}$ when spawning occurred between 96 (6th April) and 120 (30th April), after that date it dropped below 2 squid $\text{m}^{-2}\text{ yr}^{-1}$, with the exception of a sharp peak, in which the maximum recruitment of 5.8 squid $\text{m}^{-2}\text{ yr}^{-1}$ was reached on day 132 (12th May, fig. 6.150).

6.4.2.1 Causes of mortality

When spawning occurred between day 96 and 108, the number of squid annually lost due to starvation was negligible compared to that due to predation (tab.6.44). The stage-specific predation on squid was fiercer on smaller stages for all spawning dates (tab.6.45).

Spawning day	S1	S2	S3	S4	S5	S6
88	267.3	0.0	0.0	0.0	0.0	0.0
92	261.1	5.2	1.8	0.2	0.1	0.1
96	253.1	31.2	4.9	2.0	1.0	0.7
100	193.1	93.0	6.6	1.5	1.0	0.6
104	183.6	102.5	4.4	2.2	1.5	0.9
108	214.3	69.4	5.7	2.8	1.0	0.5
112	190.3	92.9	0.7	0.0	0.0	0.0
116	189.2	70.1	2.3	0.3	0.1	0.1
120	180.8	95.5	10.4	1.3	0.7	0.6
124	127.4	110.5	8.0	0.1	0.0	0.0
128	105.1	93.7	7.7	0.4	0.1	0.3
132	102.1	89.2	4.2	1.1	0.4	0.3
136	81.6	49.5	11.1	0.9	0.2	0.4
140	81.8	51.4	1.3	0.0	0.0	0.0
144	67.0	42.5	0.0	0.0	0.0	0.0

Tab.6.45 – Stage-specific predation (ind m⁻² yr⁻¹)

Spawning day	S1	S2	S3	S4	S5	S6
88	32.7	0.0	0.0	0.0	0.0	0.0
92	29.8	0.0	0.0	0.0	0.0	0.0
96	0.1	0.0	0.0	0.0	0.0	0.0
100	0.0	0.0	0.0	0.0	0.0	0.0
104	0.0	0.0	0.0	0.0	0.0	0.0
108	0.3	0.0	0.0	0.0	0.0	0.0
112	2.8	9.2	0.0	0.0	0.0	0.0
116	22.1	12.0	0.0	0.0	0.0	0.0
120	0.0	0.0	4.7	0.5	0.1	1.4
124	0.0	44.0	7.7	0.1	0.0	0.4
128	14.7	67.8	7.6	0.1	0.0	2.0
132	11.7	83.1	1.9	0.0	0.0	0.4
136	54.1	92.6	4.6	0.6	0.0	0.0
140	32.2	122.4	10.4	0.0	0.0	0.0
144	31.1	159.5	0.0	0.0	0.0	0.0

Tab.6.46 – Stage-specific mortality due to starvation (ind m⁻² yr⁻¹)

Mortality was caused by a mixture of starvation and mortality for squid spawned on day 88 and 92 and after day 112, and exclusively by predation for squid spawned between day 96 and 108 (fig.6.151). High mortality due to starvation occurred in S1 squid spawned on day 88 and 92 (tab.6.46). The highest mortality due to starvation occurred on S2 squid spawned between day 124 and 144, with higher loss due to starvation than predation for squid spawned from day 136 (tab.6.44).

In general, it can be seen that for squid spawned after day 112, there is a progressive shift of causes of mortality, with a higher proportion being lost due to starvation and a decrease of squid lost due to predation (fig.6.151).

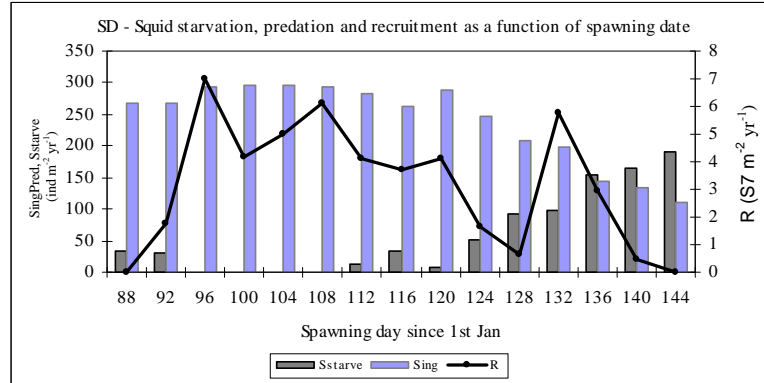


Fig. 6.151 – Annual squid starvation, S_{starve} , predation, $S_{ingPred}$ and recruitment, R , at different spawning dates

6.4.2.2 Causes of recruitment variability

The analysis of the causes of annual recruitment to spawning date will focus on the three spawning dates that exhibited annual recruitment higher than 5 squid $m^{-2} yr^{-1}$ (date 96, 108, 132) and the one with the lowest recruitment, 0.6 squid $m^{-2} yr^{-1}$ (date 128) between day 88 (29th March) and 144 (24th May, fig. 6.150).

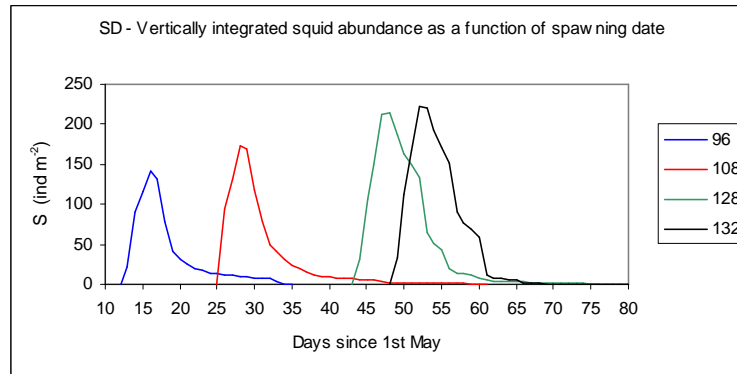


Fig. 6.152 – Daily vertically integrated abundance of squid, S , at 6 am spawned at different dates

Spawning at different dates caused the squid to hatch at different times of the year (fig.6.152) and to enter a virtual ecosystem with different food and predator concentrations (tab. 6.47).

	96	108	128	132
D_{hatch}	132	145	164	168
Date _{hatch}	13 th May	26 th May	14 th Jun	18 th Jun
Pred	2252.3	2065.3	1819.6	1771.7
Z _{prot_BP} squid	17.7	3.2	0.1	0.3
Z _{prot_S}	9.4	10.9	13.2	14.9
Z _{prot_BP}	67.1	26.5	22.0	24.0

Tab. 6.47 – D_{hatch} : Days since the 1st Jan, when squid hatching occurred; Date_{hatch}: Squid hatching date; Pred: vertically integrated visual predator concentration ($ind\ m^{-2}$); Z_{prot}: copepod protein biomass at the date of squid hatching ($mmol\ C\ m^{-2}$); Z_{prot_BP}squid and Z_{prot_BP}: maximum protein ingested by basal predator population during the period of squid permanence and annually ($mmol\ C\ m^{-2}\ yr^{-1}$); Z_{prot_S}: annual max protein ingested by squid ($mmol\ C\ m^{-2}\ yr^{-1}$) at different hatching dates

6.4.2.3 Predation

Squid that hatched earlier in the year entered a mesocosm in which predators were more abundant (fig.6.153), and were victim of higher predation mortality, especially for the smaller, more vulnerable stages (tab.6.45).

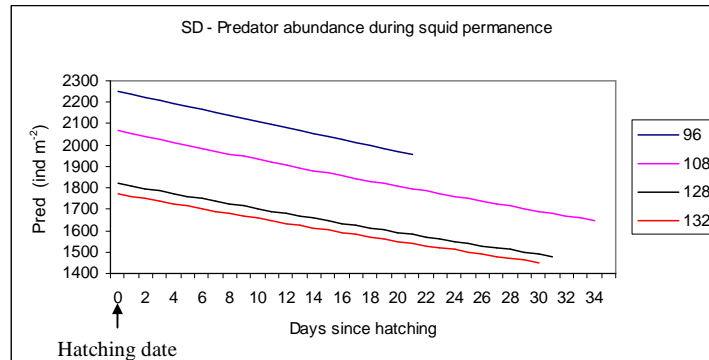


Fig. 6.153 – Predator abundance, Pred, during squid permanence in the mesocosm

This is clearly shown by a positive linear correlation between the number of squid in stages S1 being eaten and the predator concentration at the date of hatching (fig.6.154). As a consequence of this, the vertically integrated abundance of squid during the period of permanence in the mesocosm was different depending on the date of hatching (fig.6.155).

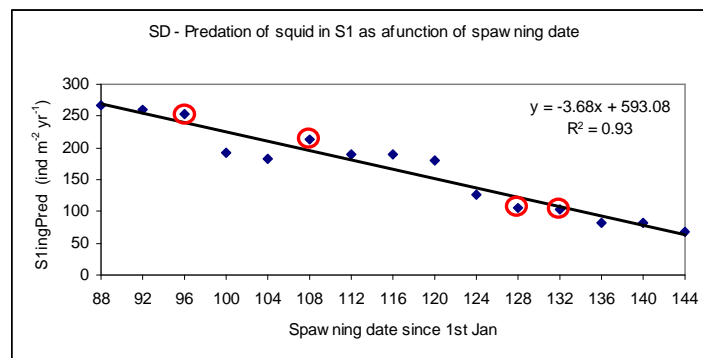


Fig. 6.154 – Correlation between stages S1 mortality due to predation and spawning date

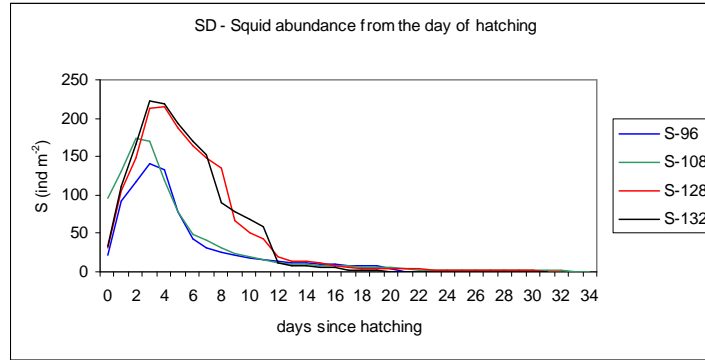


Fig.6.155 – Vertically integrated abundance of squid during their permanence in the mesocosm as function of their spawning day

The annual maximum vertically integrated squid abundance was lower for squid that were spawned earlier in the year, when predators were more abundant (fig.6.155).

6.4.2.4 Competition for food

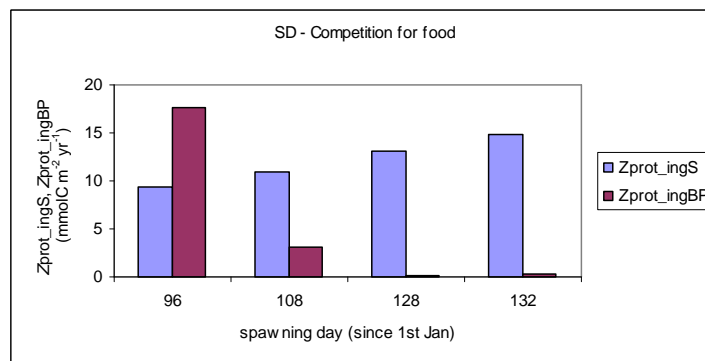


Fig. 6.156 – Amount of protein transferred to squid ($Z_{\text{prot_ingS}}$) and to basal predator ($Z_{\text{prot_ingBP}}$) during the period of squid permanence

The annual amount of protein ingested by the squid population increased with the time of squid spawning (fig.6.156). Squid cohorts, spawned earlier in the year, ingested less protein compared with those spawned later. On the other hand, the amount of protein ingested by the basal predator population greatly reduced with time (fig.6.156).

6.4.2.5 Food availability

The amount of food available was different depending on the date on which squid hatched (fig.6.157).

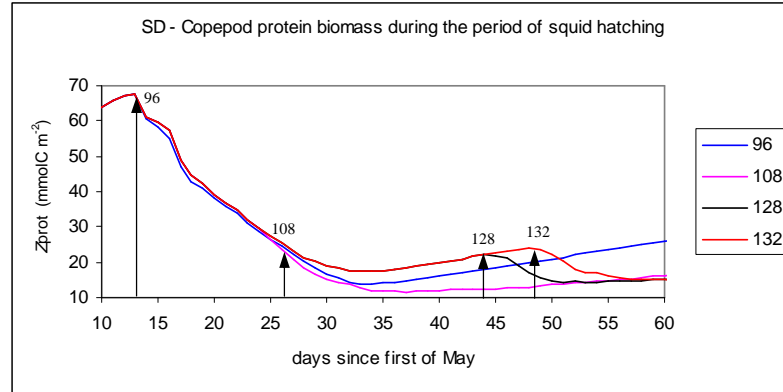


Fig.6.157 – Copepod protein biomass at different hatching dates (arrows and number show the hatching date of squid spawned on different days)

Squid that were spawned on day 96 (6th April), hatched very close to the annual maximum copepod protein biomass and had potentially much more food available than those that hatched later, when the copepod protein biomass was less than half (fig. 6.157 and tab.6.47). However the amount of protein ingested annually by squid spawned on day 96 was the lowest (fig.6.156 and tab.6.47).

6.4.2.6 Copepod protein availability

When comparing the vertically integrated copepod biomass available at squid hatching (fig.6.157) per individual squid during their permanence in the mesocosm, it can be seen that squid spawned on day 96, hatched in a mesocosm that offered much higher copepod protein biomass per squid (fig.6.158). In the first 10 days since hatching, squid that spawned on day 96 had at least double the amount of copepod protein biomass per squid. From four days after hatching, squid spawned on day 108 had the second most abundant copepod biomass per individual squid (fig.6.158). From day 6 to day 11, squid that were spawned on day 108 had about double the amount of copepod protein per squid than those that were spawned on days 128 and 132. Squid that were spawned on day 128 and 132 experienced a similar amount of copepod protein biomass per individual squid until 11 days from hatching (fig.6.158).

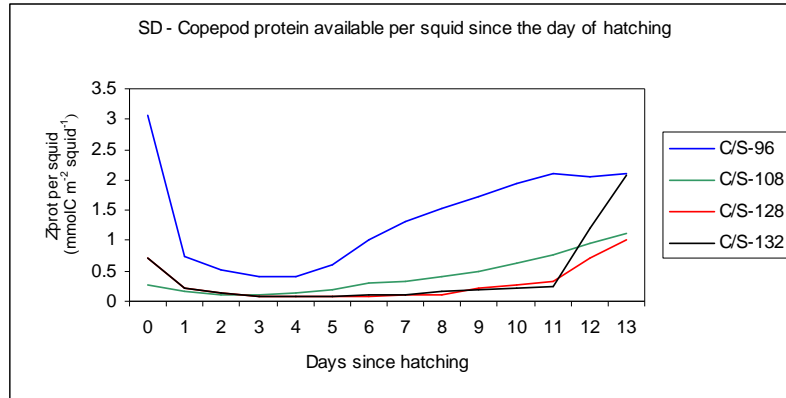


Fig.6.158 – Food availability per individual squid during the first two weeks since hatching

Twelve days after hatching, a large number of squid that spawned on day 132 died of starvation, and this caused an increase in food availability for the survived ones (fig.6.158). On the same date, a similar but milder phenomenon occurred also for squid spawned on day 128 (fig.6.158). After the second week since hatching, the biomass of copepod protein available to individual squid increased for all cohorts, especially those spawned on day 132 (fig.6.159).

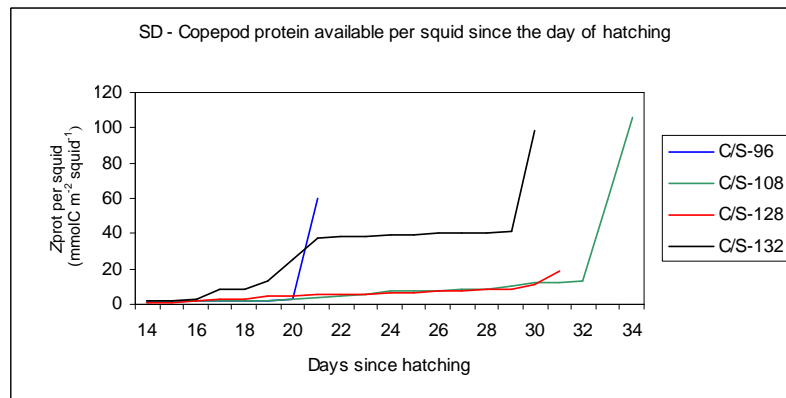


Fig.6.159 – Food availability per individual squid during after two weeks since hatching

6.4.2.7 Squid protein ingestion

	$Z_{prot_ingS} S^{-1} day^{-1}$
96	0.033
108	0.037
128	0.017
132	0.026

Tab.6.48 – $Z_{prot_ingS} S^{-1} day^{-1}$: average protein ingested per squid per day²

² This was calculated by dividing the population protein ingested each timestep by the number of squid in the population, to have the average protein ingested by individual squid each timestep,

As already said, the total amount of copepod protein ingested by the squid population increased depending on date of spawning (fig.6.156 and tab.6.47). However, when looking at the annual protein ingested by individual squid per day, it turns out that squid spawned on day 108 ingested the most protein per day, followed by those spawned on day 96, day 132 and 128 (tab.6.48).

The average squid protein content per individual squid is shown on fig.6.160.

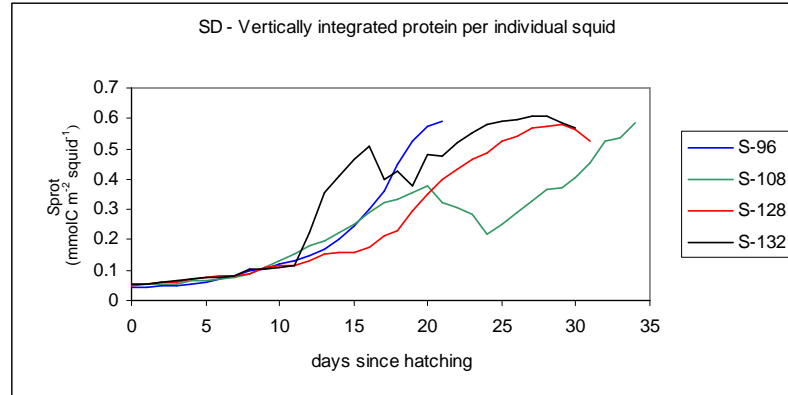


Fig.6.160 – Vertically integrated average protein content of individual squid

6.4.2.8 Prey composition

Spawning day	Z_{ingS}	Z_{prot_ingS}	Z_{prot}/Z
98	193243.9	9.4	4.88E-05
108	17797.6	10.9	6.13E-04
128	9617.4	13.2	1.37E-03
132	10202.2	14.9	1.46E-03

Tab.6.49 – Z_{ingS} : Annual number of copepods ingested by the squid population ($ind\ m^{-2}\ yr^{-1}$); Z_{prot_ingS} : Annual amount of protein ingested by the squid population ($mmolC\ m^{-2}\ yr^{-1}$); Z_{prot}/Z : Average protein per copepod ingested ($mmolC\ ind^{-1}$)

The annual amount of protein ingested by squid as a population was composed of many small copepods for squid spawned on day 96, and progressively by fewer larger copepods (tab.6.49).

6.4.2.9 Recruitment

Two weeks after hatching (day 14) squid recruitment started (fig.6.161). The first squid cohort to recruit was that spawned on day 132. Its recruitment lasted about 1 week and reached a maximum of $5.8\ squid\ m^{-2}\ yr^{-1}$ (fig.6.161 and tab.6.44). Squid

Z_{prot_S}/T_s . Adding all the Z_{prot_S}/T_s for the time of permanence of squid in the mesocosm, and finally dividing the result by the number of days spent in the mesocosm.

spawned on day 108, recruited from day 17 to 35 after hatching, with 6.1 squid recruited $\text{m}^{-2} \text{yr}^{-1}$ (fig.6.161 and tab.6.44). Squid, spawned on day 96, recruited in a short pulse from day 19 to 21, showing the highest recruitment: 7.0 squid $\text{m}^{-2} \text{yr}^{-1}$ (fig.6.161 and tab.6.44). Squid, spawned on day 128, were the last to recruit, from day 22 and 26, and with the lowest rate of success: 0.6 squid $\text{m}^{-2} \text{yr}^{-1}$ (fig.6.161 and tab.6.44).

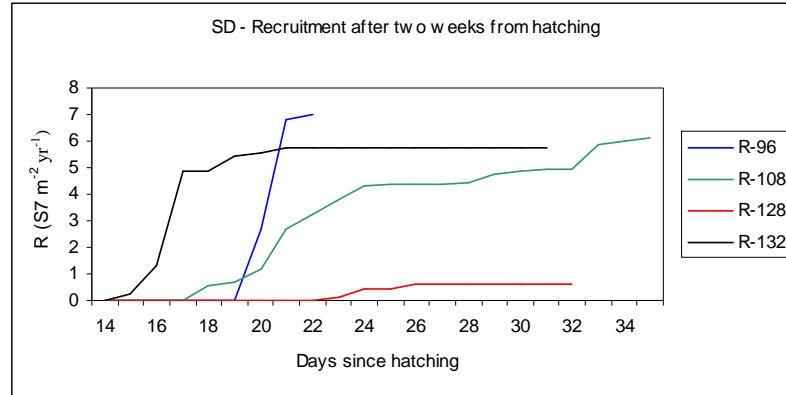


Fig.6.161 - Squid recruitment magnitude and duration. The lines end when there are no more squids

6.4.2.10 Squid audit trails

Fig.6.162-6.163 illustrate the life history of two squid that spawned on day 132. One recruited (id: 215787785), the other did not (id: 215787576). Fig.6.162a shows the growth of the two squids. The one that recruited reached the 8mm in mantle length, while the other nearly did it, but died before then. Fig.6.162b-e show how their carbon, protein, lipid pool and weight varied in time. Fig.6.162f shows that the recruiting squid ingested more protein than the non recruiting one over the period of permanence in the mesocosm. Fig.6.163 focused on the recruiting squid. As it grew bigger it migrated deeper during the day (fig.6.163a), keeping a depth, in which it would reduce the risk of predation (fig.6.163a). In the period between the 17th June and the 7th of July, it ate a maximum of 14 copepods per timestep (half-hour, fig. 6.163c). Respiration rate shows daily fluctuation due to metabolic, digestion and swimming costs (fig. 6.163d). The digestion of a full meal (gut fullness = 1) takes about 6 hours (fig. 6.163e). They fed at dusk and dawn (fig. 6.163f).

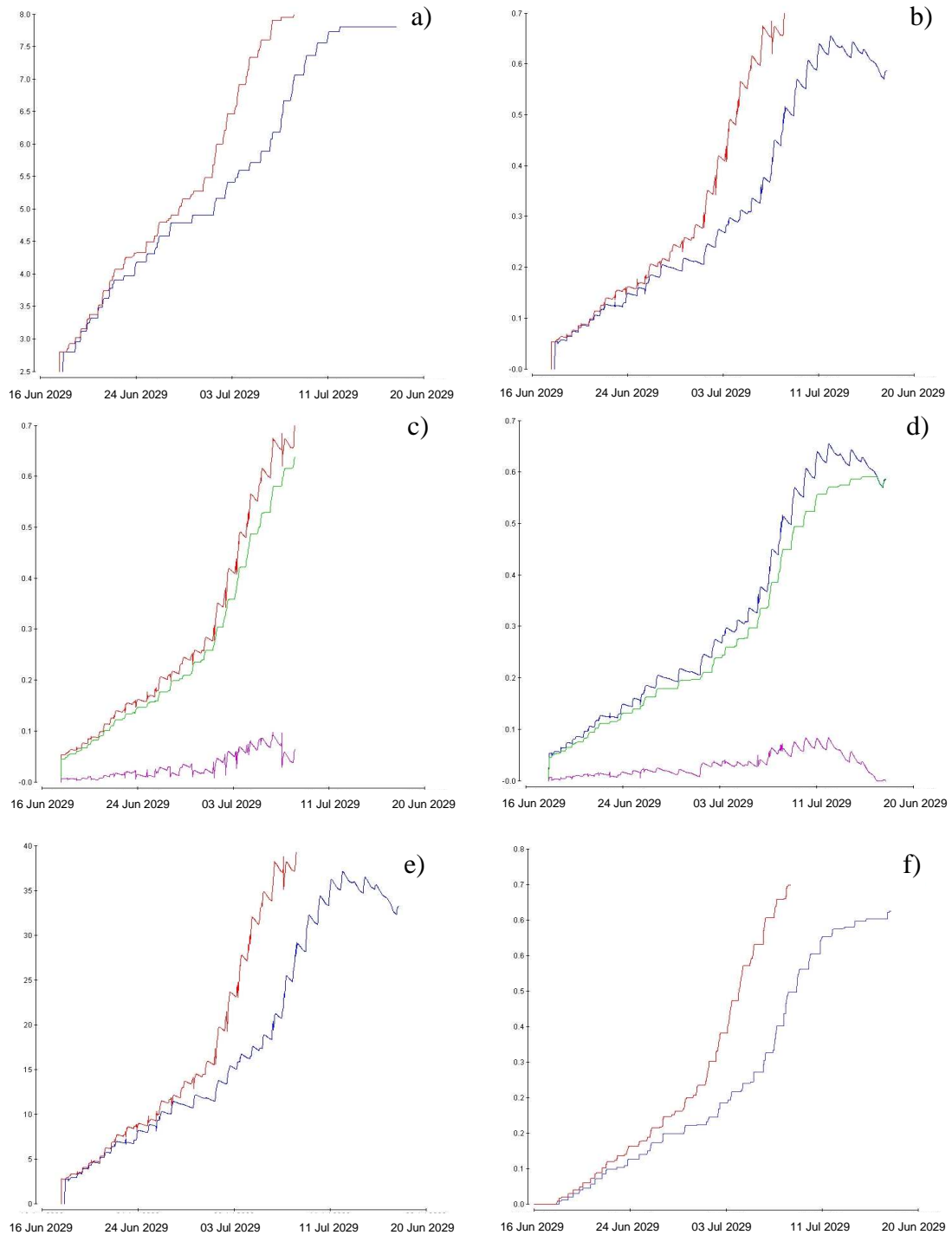


Fig.6.162 – Audit trails for one recruiting and one non recruiting squid. a) Mantle length (mm) for recruiting squid (red) and non recruiting squid (blue). b) Carbon pool (mmol C) for recruiting squid (red) and non recruiting squid (blue). c) Carbon (red), protein (green) and lipid (purple) pools for recruiting squid d) Carbon (blue), protein (green) and lipid (purple) pools for non recruiting squid. e) wet weight (mg) for recruiting squid (red) and non recruiting squid (blue). f) accumulated protein ingested (mmol C ts⁻¹) for recruiting squid (red) and non recruiting squid (blue).

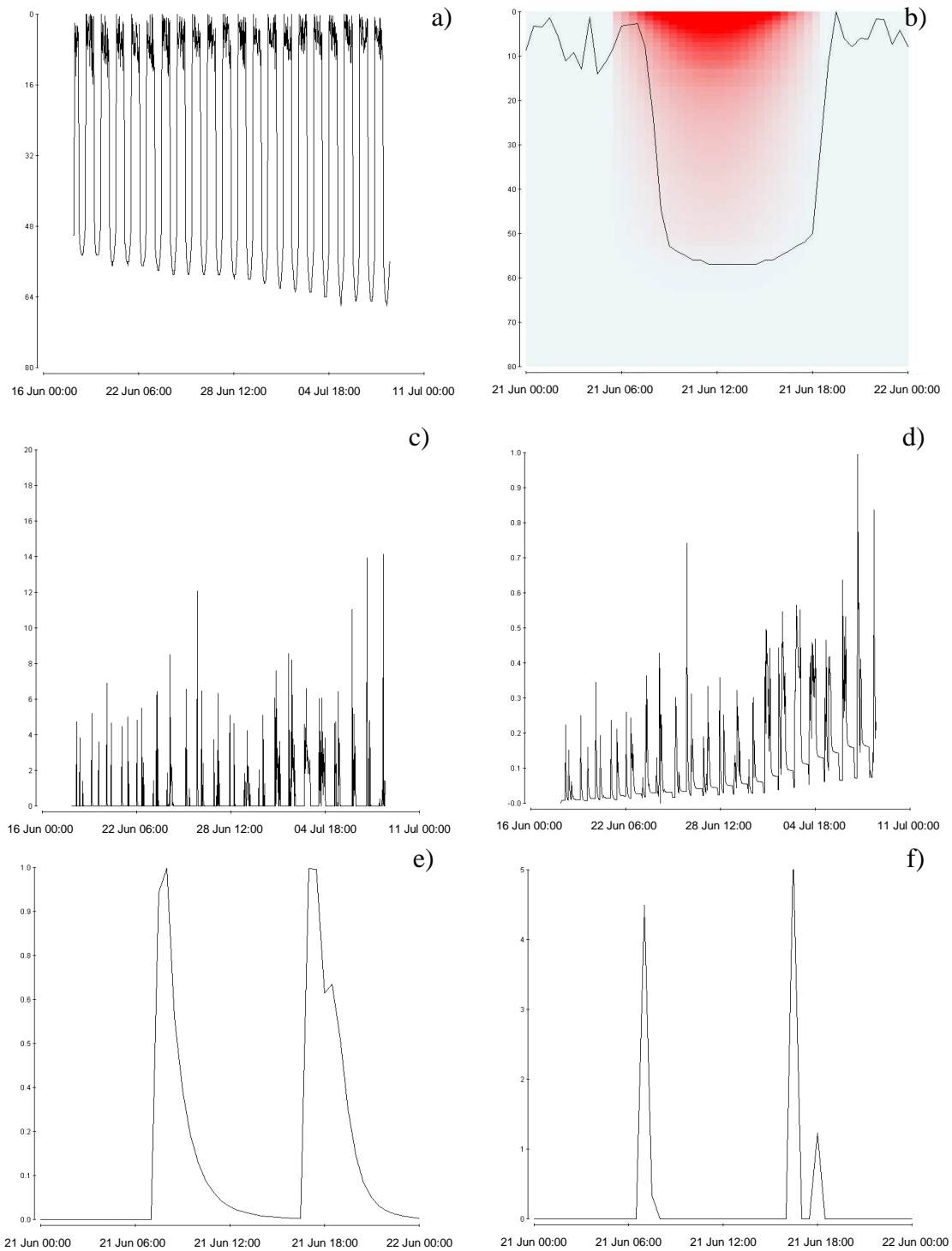


Fig.6.163 – Audit trails for the recruiting squid. a) depth (m) b) depth (m) and irradiance (Wm^{-2}) on the 21st June. c) ingested copepods ($ind\ ts^{-1}$). d) respiration rate ($mmolC\ h^{-1}$). e) gut fullness (wd) on the 21st June. f) ingested copepods ($ind\ ts^{-1}$) on the 21st June.

6.5 Preliminary results on the effect of temperature on recruitment

Ten jobs were run, all built on the base run. The temperature adjustment was varied from -5°C to $+5^{\circ}\text{C}$ in one-degree steps.

The vertically integrated concentration of diatom, copepod, squid, and annual recruitment are shown as they vary over time for one year (fig.6.164).

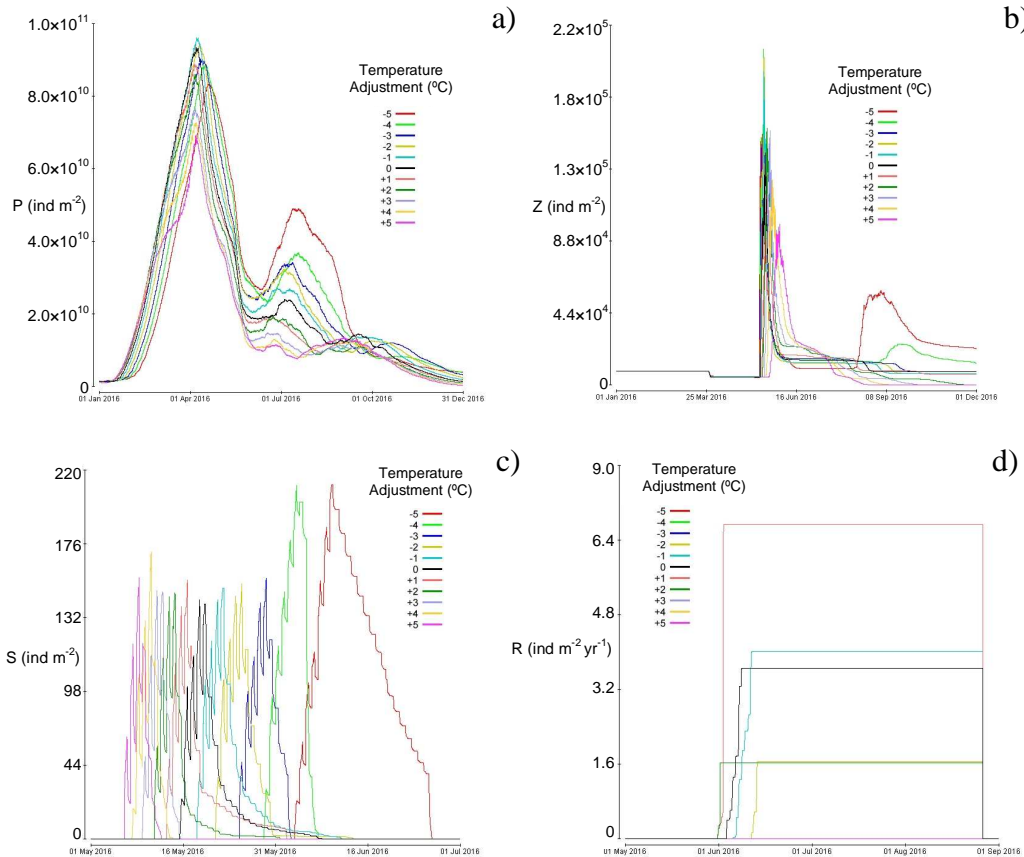


Fig.6.164 – Vertically integrated concentration (ind m^{-2}) a) P; b) Z; c) S (S1-S6); d) S in stage S7 (recruited)

The demography of all population responded to the changes in temperature, in particular, squid embryonic period, which is a function of the mean incubation temperature. This caused the timing of squid hatching to vary, affecting recruitment success.

CHAPTER 7 - DISCUSSION

7.1 Stability

The base experiment demonstrated that the virtual ecosystem created by using LERM-ES under the Lagrangian Ensemble metamodel is stable, in the sense that the inter-annual variability of the ecosystem emergent properties is a few percent of their multi-year average.

This has three important implications: 1) as stability determines the limits of predictability (Woods et al., 2005), LERM-ES can be used as a base for experiments to investigate the dynamics of planktonic ecosystems and fisheries recruitment; 2) results from the stability experiments provide more evidence that virtual ecosystems created using LERM-ES are globally stable; 3) it proves that when a third dynamic population is added to the food chain, the stability of LE simulations with an NPZD model is not lost. The stability experiments, in which the base run was repeated with four different P and Z initial concentrations, prove that the VEs created converge to a stable attractor within 15 years, independently of initial conditions, thereafter responding only to external forcing.

The convergence of the VEs to a stable attractor, independent of initial conditions, is illustrated by Poincaré maps, in which one emergent property of the VE is plotted against another on the same day of the year (28th May). All the versions of the base run (initialised with five different P and Z concentrations) showed that, once the ecosystems got on attractor, the inter-version noise is lower than the inter-annual noise. This is shown by 1) the reduced variability in both biomass and abundance of the VE populations in the last 10 years compared to the 25 years period (tab.6.2-6.3 and fig.6.1-6.12) and 2) results from a chi-squared test show that the error distribution was concentrated around the multi-year mean in the base run (on attractor) and could be represented by a Gaussian distribution (tab.6.4, fig.6.13-6.14). Once on attractor, the virtual ecosystems showed annual stable cycles in their emergent biological properties. On a specific date (28th May, a few days before squid recruitment occurs), the inter-annual variation in the plankton populations demography and biomass for all the five different versions varied by less than 15%

(below 3.7%, 8.6% and 11.3% for *P,Z,S* and 4.4%, 13.0% and 14.9% for *P,Z,S*) from the multi-year mean of the base run (tab.6.2-6.3).

This level of stability was illustrated by Poincaré maps plotting the daily value of the populations' abundance and biomass every day in the 10 analysed years (fig.6.20-6.21; 6.35-6.36).

The daily vertically integrated concentration and biomass of diatom and copepod showed remarkable stability, with very little inter-annual variation in magnitude and timing of their annual maxima (tab.6.5-6.8). The initial variability in the vertically integrated concentration of copepod versus squid was due to the steep change in copepod concentration, due to reproduction, at the time of squid hatching. However, the vertically integrated concentrations of the two populations converged on the 17th May (2 days after hatching) every year. The daily vertically integrated copepod and squid biomass during the period of squid permanence in the mesocosm showed the same trend in all analysed years, with some variation attributable to a combination of random displacement of particles above the turbocline and possibly to the encounter chance between copepod and squid migrating vertically through the mesocosm. However, more experiments, with increasing number of squid and copepod agents, are required to confidently test this assertion. Squid hatching date, depending on the mean incubation temperature of eggs, varied by less than one hour over the sample of 10 years. This low level of variability confirms the stability of the VE showing that, as the external forcing followed an annual stationary cycle, so did the biological properties of the VEs. The inter-annual variability from the multi-year mean in recruitment was only 12.2%, which is quite small compared to the inter-annual variation of recruitment in occurring naturally in squid populations, which are highly sensitive to environmental fluctuations (Sakurai *et al.*, 2000; Agnew *et al.*, 2000; Dawe *et al.*, 2000). This provides the basis for further investigation using real weather data to assess the effect of weather on recruitment variability (see 8.2.1).

7.1.1 Ergodicity

This set of experiments consists of a series of instances of the base run. An instance of a VE differs from another only in the random seed which determines the random displacement of plankters by turbulence. This random displacement of particles above the turbocline is the only stochastic process in LE modeling and it makes the particles follow different trajectories, and therefore their history of ambient environment and concentrations of prey and predators. This leads to intra-population variability of the biological properties of the individuals within a population. A test for ergodicity (Woods *et al.*, 2005) was carried out in order to 1) measure the demographic noise in the ecosystem by analysing the inter-instance variation for one year in an ensemble of independent runs, and comparing it with a timeseries of one instance of the virtual ecosystem, given the same degrees of freedom; 2) assess whether the emergent inter-annual variation in the biological properties of the VE is induced by the intra-population variability generated by turbulence, or rather by some artificial instability due to the modelling process. If the statistics of the timeseries of a single instance of VE and that of an ensemble of independent runs are not significantly different, then the system is ergodic. The inter-annual and inter-instance diatom, copepod and squid biomass averaged for each day of the year, show very little difference (tab.6.13a-b and fig.6.55a-6.57a), and are not significantly different from each other at the 4%, 97% and 20% respectively (tab.6.13c). The inter-annual and inter-instance variation from their mean for diatom and copepod biomass on the 28th May is not more than 5%, while for squid biomass it reaches a maximum of 20% (fig.6.55b-6.57b). This larger variability occurs during the periods of squid immigration and emigration and is due to the intra-population variability of the biological properties of individual squid, causing them to hatch and recruit at different times.

In the case of diatom and copepod abundance and biomass variations are not normally distributed around the inter-annual mean of the base run. They show a higher kurtosis, which is indicative of low variation from the inter-annual mean in the base run.

The populations deviate slightly from the ergodic ideal and the differences between ensemble and inter-annual statistics differ from a gaussian distribution (tab.6.14, fig.6.58-6.59). An earlier investigation of the ergodicity of a virtual plankton ecosystem created by the LE integration found a slightly non-ergodicity and explained it as a consequence of zooplankton inheritance of weight through lineages (Woods *et al.*, 2005). Understanding the reasons of this slight non-ergodicity in LERM-ES requires further investigation, at the individual level (audit trails).

7.1.2 Sensitivity

A series of numerical experiments was performed to investigate the effect of changes in the exogenous forcing on the VE dynamics, and in particular on squid recruitment (tab.6.15).

7.1.2.1 Variation in nutrients load

The ecosystem responded to a doubling of silicate in solution (from 0.6 to 1.2 mmol Si m⁻³ above the 1st January mixed layer depth, about 60 m) with an increase in diatom biomass. Although the mixed layer dissolved silicate concentration was doubled in year 2015, this was not maintained in successive years. In fact, during the period of adjustment of the ecosystem to the new attractor (2015-2020), the dissolved silicate concentration on the 1st January fell to the value of the attractor before the doubling occurred (0.6 mmol Si m⁻³). As a result, there was only a small increase in diatom biomass, which produced no significant difference in the demography and biomass of the upper trophic levels, and the multi-year average annual recruitment was not significantly different to that which occurred in the base run. The added silicate was lost below the annual maximum, and was never re-entrained above the mixed layer. The silicate is transferred below the permanent mixed layer by diatoms sinking out of the mixed layer. The silicon contained in their shells is eventually remineralised when they die, but the chemical is not re-entrained into the mixed layer. To address this, a chemical recycling adjustment was built

into the VEW, which keeps a track of all chemicals that are released (remineralised) from plankton, in each layer in the water column. The remineralised chemical below the permanent mixed layer is removed and transferred to the surface, where it gets homogenised by turbulence in the mixed layer. This was set to occur on the 1st January, where biological activity is at its lowest, and this adjustment has minimal impact on the ecosystem.

This correction assists in keeping the nutrient balance tight. However, it proved not to be sufficient for keeping the surface concentration of nutrients stable. Chemical recycling works when the annual maximum mixed layer depth does not vary inter-annually. However, if there is a sudden shallowing of the annual maximum mixed layer depth, then the chemical recycling does not succeed in transferring back to the surface the chemical lost in the previous year. The difference in annual maximum mixed layer depths in two successive years influences the amount of chemical available in the surface water (fig.6.80).

Another difficulty in controlling the chemical in solution, as in this experiment, arises from the fact that diatoms have a capacity for nutrient, which is model dependent. Exogenously providing extra chemical in solution can simply cause the diatoms to uptake more. As they reproduce they are effectively sequestering silicate from solution, adjusting to an attractor which is not the one expected. With the current way that chemical budgeting is handled by the VEW it is the ecosystem driving the chemical concentration and not vice versa.

Although nitrogen is more “mobile” than silicon, as it is transferred to the surface water by animal fertilisation, similar problems arose with doubling its dissolved concentration above the turbocline. This issue will be addressed in future work. One point to clarify is the small drift in the total mesocosm chemicals load of around 0.1% per annum, that occurs when running LERM-ES. The VEW attempts to automatically handle certain aspects of chemical budgeting. Particularly, when a model contains a rule for nutrient uptake, the VEW automatically handles the distribution of nutrient between different plankters, if their totalled requests exceeded the available nutrient. However, with many agents performing uptake and remineralisation, while agents represent a dynamic numbers of individuals, the job is

more complex. The small drift in total chemical is believed to be a bug in the VEW, when handling this automatic budgeting.

7.1.2.2 Variation in top predators abundance

Increasing the inter-population competition for food (basal predator)

Doubling the vertically integrated concentration of basal predators competing with the squid for food caused a 22% reduction in the average annual squid recruitment (tab.6.5-6.27). This decrease in recruitment was a direct effect of food limitation. The copepod population was reduced in size and biomass, as a consequence of the increased predation pressure exerted by basal predators. Under these conditions, less copepods managed to over-winter, therefore reducing the biomass potential for the following season. As a consequence, 20% less carbon was transferred to the squid population (tab.6.9-6.31). This reduction in food availability caused some squid to die of starvation, as they could not feed enough to fuel their metabolism. However, the vast majority of squid were victim of higher predation rates. This was a direct effect of the reduced food availability on growth rate, which, being less than optimal, made squid more vulnerable to predation.

Increasing predation pressure (visual predator)

Squid mortality due to predation was the most significant factor affecting annual recruitment. Doubling the vertically integrated visual predator concentration led to an almost 60% reduction in squid annual recruitment (tab.6.5-6.34). This was caused by a direct effect of predation on the squid population (tab.6.35), especially the more abundant and slower swimming newly hatched squid in stage S1, which increased by 30% (tab.6.36). As a result of increase predation on the squid, predation pressure on copepods was more relaxed (tab.6.6-6.35). Compared with the base run, copepods ingested 20% more carbon from the diatoms, which allowed the non-overwintering cohort to build-up enough lipids reserve to survive the winter.

This cohort of winter survivors constituted an extra portion of reproducing copepods in the following year, which means extra food for the squid (tab.6.9-6.39). The annual cycle of copepod agents, especially those overwintering, was less regular compared to the base run and this might have contributed to the increased level of noise in recruitment (fig.6.44-6.136). Also the diatom autumn bloom showed yearly fluctuations, suggesting that this non-overwintering cohort grazes on the autumn diatom population. This causes the diatom and copepod biomass on the 1st of January to fluctuate from year to year (fig.6.133-6.134). The percentage variation from the multiyear average for diatom and copepod biomass on the 1st of January increased from 4.5 to 10.3% and from 5.8 to 12.1% respectively (tab.6.38). The maintenance of a stable number of agents seems to affect the stability of the ecosystem. Another factor which could be responsible for this increase in inter-annual noise could be that the increase in predator concentration might have pushed the VE attractor close to a regime shift situation. However, in order to test this conjecture, it would be necessary to run a set of numerical experiments in which the number of predators in the mesocosm is progressively increased over a wide range of concentrations (see section 8.2.2).

7.1.2.3 Variation in spawning stock

Number of eggs laid

Competition for food between members of the same population was a significant factor affecting the magnitude of recruitment, through a strong density-dependent effect. Results from the sensitivity of recruitment to the magnitude of spawning (i.e. number of eggs laid) showed that increasing the number of eggs being laid annually above the carrying capacity of the system leads to significant reduction of recruitment (fig.6.144a). The carrying capacity of the VE could sustain the growth of between 400 and 500 eggs laid $\text{m}^{-2} \text{yr}^{-1}$, before the density-dependent effect becomes a limiting factor to annual recruitment (see section 7.2.2). Below this level annual recruitment decreased slightly, but when 500 or more eggs were injected into

the mesocosm, it caused a significant reduction in annual recruitment. Results from this set of experiments suggest that a strong density-dependent mechanism controls squid recruitment (see section 7.2.2).

Spawning time

Results from the experiments investigating the sensitivity of recruitment to timing between squid hatching and copepod biomass annual maximum suggest this is an important factor affecting squid recruitment, as suggested by Cushing's match-mismatch hypothesis (Cushing, 1972, 1990). There is an optimal period for spawning, judged by recruitment success (fig.6.150), between the 2nd April and the 20th May (tab.6.44). Changes in squid spawning date relative to the annual productive cycle of the ecosystem caused the newly hatched squid to enter a mesocosm, whose biological properties (i.e. food abundance and composition, predators abundance, etc.) were different, causing variation in predation pressure and squid growth rate. For squid spawned after the 22nd April, there is a progressive shift of causes of mortality, with a higher proportion being lost due to starvation and a decrease of squid lost due to predation (tab.6.44).

7.1.2.4 The effect of temperature on recruitment

The final stage of the project was involved with trying to design a set of numerical experiments for testing the sensitivity of recruitment to ambient temperature. This is not an easy task as it sounds. In the current state of the VEW, any physical variable of the mesocosm (i.e. mixed layer depth, temperature, etc.) emerges from the simulation and cannot be set by users. A solution to this problem was to allow adjustment of the temperature purely for the biological rules. The effect is that the temperature that emerges from the physics is adjusted by a constant value when used by the plankton primitive equations. Time did not allow a thorough analysis of the VEs, however results show that variation in temperature had a significant effect on the biological properties of diatom, copepod and squid population (fig.6.164), in

particular in the timing and magnitude of diatom blooms (earlier but smaller spring bloom and much smaller autumn bloom at higher temperature, fig.6.164a), timing and magnitude of copepod reproductions (earlier and larger at lower temperatures, with double reproduction when temperature adjustment was -4 or -5°C , fig.6.164b), squid hatching date (about one month delay between 5°C and -5°C , fig.6.164c) and recruitment (recruitment occurred only for temperature adjustments between -2°C and 2°C , fig.6.164d). The timing of recruitment varied as a function of temperature, with squid recruiting earlier at higher temperatures, as observed in several squid species (*Loligo forbesi*, Forsythe and Hanlon, 1989; *Todarodes pacificus*, Sakurai *et al.*, 1996; *Loligo gahi*, Hatfield, 2000). The reasons for such differences can be established through a careful analysis of the VEs.

7.2 Causes of recruitment variability

Analysis of the virtual ecosystems has shown that squid recruitment is determined by a combination of factors: competition for food, both within members of different populations (inter-population competition, i.e. squid and basal predator populations) and members of the same squid population (intra-population competition), predator pressure, food availability and feeding success. Changes in the magnitude of each of these factors caused recruitment to vary.

7.2.1 Competition

Squid mortality was caused by a mixture of starvation and predation. Mortality due to starvation occurred only when food availability became limiting, causing a decrease in annual recruitment. This occurred as a consequence of increased competition for food either at an intra-population (more squid competing for limited food) or inter-population (more basal predators) level. This concurs with speculation that stocks of squid have increased due to relaxed competition for food (Caddy and Rodhouse, 1998), however the suggested hypotheses cannot be validated due to the lack of field data quantifying the extent of ecosystem trophic

interactions (Shepherd and Cushing, 1980; Caddy and Rodhouse, 1998; Arkhipkin and Middleton, 2002).

7.2.1.1 Intra-population competition for food

As already said, competition for food between members of the same population was a significant factor affecting the magnitude of recruitment. Annual recruitment as a function of egg production showed a typical Ricker's domed shape (Ricker, 1954): it increased with egg production up to a point, the carrying capacity of the system, beyond which density-dependent processes are so strong that they over-compensate for changes in biomass, so that increased eggs production leads to decreased recruitment (fig.6.144, Shepherd, 1982). This phenomenon has been observed in nature for *Loligo pealei* (Rosenberg *et al.*, 1996) and *Loligo gahi* (Agnew *et al.*, 2000). Agnew *et al.*, 2000 suggested that this was caused by a density-dependent effect, but could only hypothesize that this could be due either to cannibalism or competition for food. Rodhouse (2001) suggested that the proposed density-dependent mechanism must presumably be different from cannibalism, as in squid such as *Loligo gahi*, the parent stock dies soon after spawning and is therefore not present to cannibalise the next generation when it starts to grow.

Results from the sensitivity of recruitment as a function of eggs production suggest that this density-dependent effect could be caused by intra-population competition for food. When the magnitude of spawning exceeds the carrying capacity of the system, then mortality increases mainly due to predation and to a much lower extent to starvation, leading to lower survival rates and recruitment (tab.6.42). On a population level, the annual amount of protein ingested increased with the number of eggs laid (fig.6.146), especially in the newly hatched paralarvae (fig.6.147), however this was shared between more squid, making it increasingly insufficient for rapid growth and survival. The average amount of protein ingested per squid per unit time decreased with increasing squid competing for the limited food (fig.6.145 and 6.148), causing them to grow slower and making them more vulnerable to predation. This emergent mechanism by which the interaction between density-dependent larval growth and predation during the critical period results in density-

dependent larval survival as been previously suggested to be an important factor in shaping recruitment of fish populations (Ricker and Foerster, 1948; Shepherd and Cushing, 1980; Cushing and Horwood, 1994).

7.2.1.2 Inter-population competition

Results from the model have shown that competition for food occurring within members of different populations is another significant factor affecting annual recruitment success (tab.6.5-6.27). As for intra-population competition, abundance of competitor populations affected squid mortality indirectly mainly through predation mortality caused by a Ricker-Foerster (1948) type effect (tab.6.28): lower abundance of food per squid causes a less than optimal growth, therefore exposing them to predation for longer. Some studies have pointed out the importance of inter-population competition on the abundance and recruitment of squid in different areas of the world (Caddy and Rodhouse, 1998; Arkhipkin and Middleton, 2002).

It has been suggested that the increased cephalopods landings observed over the last 30 years, in particular in areas where cephalopods and finfish have been both fished intensively (e.g. Mediterranean Sea, NW Pacific and East-central Atlantic), may be due to a reduction in competition for food (Caddy and Rodhouse, 1998). This could be due to the typically shorter life spans and faster growth rates and therefore increased spawning potential of cephalopods under intensive fishing compared with finfish populations (Caddy and Rodhouse, 1998). Possible competitive interactions between *Illex argentinus* and *Loligo gahi* have been reported in the Falklands Islands waters (Arkhipkin and Middleton, 2002). Analysis of the fisheries statistics for these two squid populations between 1987 and 1999 found a strong negative correlation between their abundance. The authors suggested that *Illex argentinus* affected *Loligo gahi* populations either due to competition of limited food resources or direct predation, however they were unable to discriminate between the two proposed mechanisms (Arkhipkin and Middleton, 2002).

7.2.2 Predation

Results from the numerical experiments presented suggest that predation is the most important cause of squid mortality during the post-hatching critical period. Doubling the predator abundance in the virtual mesocosm led to an almost 60% reduction in squid annual recruitment. The effect of predation on squid recruitment depends on the abundance of the predator, but also on the growth rate of the squid. Larger squid are better swimmers, and therefore more capable of escaping predators' attack, than small ones. As already observed in the competition experiments, squid that grows slowly spends more time in a set stage, on which swimming speed depends, and is more liable to predation than another squid that takes less time to get into the successive stage. In the double silicate run, the strong ingestion of S1 squid in year 16 was effectively beneficial as it reduced competition for food for the ones that survived. The higher survival rate of S1 squid in year 15 caused a density-dependent decrease in available food for individual squid, with a consequent slower growth rate and therefore a bigger exposure to predation, as suggested for fish populations (Ricker and Foerster, 1948; Shepherd and Cushing, 1980).

Several studies suggest that stocks of squid are sensitive to predation pressure (Caddy and Rodhouse, 1998; Arkhipkin and Middleton, 2002), however the lack of rigorous enough data to allow quantitative analysis of the significance of cephalopods (or other prey) in the diets of predatory fishes, and even the most comprehensive studies are not predictive because findings relate only to the time-period of each study (Boyle and Rodhouse, 2005).

7.2.3 Ingestion and prey composition

Prey composition was an important factor affecting recruitment. When squid hatched on different dates, as a consequence of different spawning dates, the composition of their prey field was different. Squid, that hatched just after copepod recruitment (spawning on day 96), were in an environment in which copepods were more abundant, but still in their naupliar or early copepodite stages (tab.6.49). On

the other hand, those that hatched about one month after copepod reproduction (spawning on day 132) entered an environment in which their prey was composed of fewer but larger and more nutritious copepods. The resultant annual recruitment in both years was high.

A similar phenomenon emerged in the double silicate experiment. Year 16 exhibited the highest annual recruitment. During that year, the number of copepod ingested was not significantly higher than in other years, but they got the most carbon out of them. Conversely, in year 15, squid consumed the highest number of copepods, but got much lower carbon out of them, compared to year 16, and they exhibited half the recruitment that occurred in year 16. Also in this case, the prey composition was different. Year 16 was characterised by an initial copepod population including copepods that survived the winter feeding on the diatom winter population. As the squid growing season starts they have a chance to feed on larger, more carbon rich copepods. Results from this set of experiments confirms that a balance between the quality of food, intended as the nutritional value of an individual prey, and its abundance, is an important factor affecting recruitment, as suggested by Cushing's match-mismatch.

7.3 Cushing's match-mismatch

The numerical experiments investigating the sensitivity of recruitment to squid spawning date support Cushing's match-mismatch suggesting there is an optimal period for spawning, judged by recruitment success. For these virtual ecosystems, squid recruited when spawning occurred between the 2nd April and the 20th May. This optimal spawning period is consistent with the observed spawning period (April to November) for *Loligo opalescens* in Monterey Bay (Hixon, 1983), which is located at latitude (37°N) close to that of the Azores site (41°N), where the virtual mesocosm was anchored. The end of the optimal spawning period predicted occurs at the end of May, which is earlier than that observed in Monterey Bay. This may be due to the fact that LERM-ES represents a simple trophic chain, in which phytoplankton is represented only by one diatom population. The productivity of

the ecosystem may therefore be temporally limited to the period in which diatom dominate the surface waters (Weeks *et al.*, 1993).

The results of the numerical experiments suggest that the timing of spawning, together with variations in the productive cycle, due to changes in nutrients, predator and competitors abundance, are important factor affecting recruitment success, as suggested by Cushing's match mismatch.

Annual recruitment was a product of the interactions between these inter-related factors. The availability of food at the time of hatching was one important factor affecting recruitment but not the only one: recruitment was determined by a combination of food availability and composition, predation, inter and intra-populations competition, and speed of growth.

In particular, it emerged that predation mortality was the single most important cause of mortality, especially for newly hatched squid (tab.6.45), as suggested by Hjort's critical period hypothesis (Hjort, 1914). This resulted directly by the effect of increased predation or indirectly through density-dependent survival (Ricker and Foerster, 1948; Shepherd and Cushing, 1980).

The advantage of hatching in a period of high food abundance could be balanced out by increased competition and predation, as in the case of squid spawned on day 96. Squid that hatched on day 96 entered an environment in which the amount of food available was more than double compared to any other squid spawned later in the year (fig.6.157), however, due to much higher competition for food (fig.6.154) and predator pressure (fig.6.154), recruitment was only slightly higher than those spawned on day 108 or 132 (tab.6.44).

In general, it can be seen that for squid spawned after day 112, there is a progressive shift of causes of mortality, with a higher proportion being lost due to starvation and a decrease of squid lost due to predation (tab.6.44).

Newly hatched squid paralarvae are capable of ingesting prey of their own size (Boletzky, 1974), so, contrary to what happens with fish, there was no limitation on the size (stage) of copepods the squid could feed on. However, for other species in which ingestion of prey is limited to a smaller range of prey sizes (or stages), excluding the unsuitable prey from the predator diet would be a simple exercise.

This would probably lead to a further restriction of the spawning time window for successful recruitment. This exercise could be addressed in future work investigating the recruitment of different species. Under the current model specification, preference in the copepods stages, which the squid feeds on, emerges from a balance of prey nutritional value, intended as protein contained (i.e. stage and size) and their swimming speed compared to that of the prey, which determines the ability of squid to catch their prey.

7.4 Verification

The main obstacle to model verification is the absence of reliable field data, especially for fine-grained processes which are difficult to observe, such as predator-prey interactions and density-dependent mechanisms. This is a serious problem, as it makes it possible to determine whether the emergent phenomena in the VE, such as the emergent density-dependent survival (Ricker and Foerster, 1948; Shepherd and Cushing, 1980), resemble what happens in reality. Previous work, trying to explain the causes of recruitment variability as a consequence of density-dependent survival of larval fish encountered similar problems and advocated the need to retrieve enough field data to validate the model (Shepherd and Cushing, 1980; Caddy and Rodhouse, 1998; Boyle and Rodhouse, 2005). Shepherd and Cushing (1980) suggested this could be achieved by tracking simultaneously patches of larvae and their predators to assess their growth and mortality, and investigate possible correlations between the two. This is not an easy task. A possible alternative could be to set up large mesocosms, which would facilitate the observations of predator-prey interactions. Until these type of field observations are unavailable, the proposed mechanisms responsible for recruitment variation remain interesting speculations.

Direct comparison between recruitment and fisheries data, where available and complete, is certainly possible. Currently the VEs, produced by the numerical experiments presented, were generated in a 1D environment, which is driven by

climatology rather than real weather. At this stage, any comparison of the emergent annual recruitment with fisheries data would be premature.

However some emergent properties of the virtual ecosystems generated using LERM-ES which match observations are now described.

7.4.1 The formation of deep chlorophyll maximum

LERM-ES reproduced the formation of the DCM in depth range and sinking speed (fig.6.54) comparable with several studies done in the Azores region (tab.7.1).

Fasham *et al.* (1985) measured the depth of the DCM south of the Azores in late April and May 1981. It consisted of slow growing phytoplankton and was about 100m deep in late May. During the period of this study, the DCM depth increased by 7-8m in 20 days following the increasing depth of the 1% light level and the nutricline.

A series of oceanographic cruises (Sea Rover surveys 1984-1986) recorded *in situ* chlorophyll-a concentrations, and the local environment. Strass and Woods (1991) used the Sea Rover dataset to investigate the new production during summer in the North Atlantic. In a site north of the Azores, the depth of the DCM was 50-70m in late June. The authors reported a progressive sinking of the DCM at a rate (almost 10m per month), consistent to that measured by Fasham *et al.* (1985). The rate of DCM sinking was correlated to the nutricline sinking rate.

Source	Location	Time	DCM depth range (m)
LERM-ES	41°N 27°W	April-May May-June June-July July-Aug Aug-Sep	30-70 40-80 50-90 55-95 55-100
Fasham <i>et al.</i> 1985	South of Azores	April-May 1981	~ 60-110 April ~70-120 May
Strass and Woods, 1991	North Atlantic	Apr-May 1985 Jun-Jul 1986 Aug-Sep 1984	At latitude 40°N 20-50 50-70 50-100

Tab.7.1 – Comparison of DCM depths predicted by LERM-ES with observations near the Azores

7.4.2 Observations of squid physiology and behaviour

The emergent physiological properties and behaviour of the simulated squid paralarvae is comparable to observations, as shown in the audit trail describing their life histories. The simulated squid vertical migration was comparable with in situ observations in Monterey Bay on the distribution of *L. opalescens* paralarvae: they perform diel migration and are vertically distributed above 80m (Okutani and McGowan, 1969; Zeidberg and Hamner, 2002). As they grow larger, they move deeper in the water column (Cargnelli *et al.*, 1999). Digestion rate is also comparable to laboratory observations: complete digestion of a meal takes about 6 hours for *L. opalescens* (Karpov and Caillet, 1978) and 4-6 hours for *L. vulgaris* (Bidder, 1950). The growth rates for the squid considered, varied between 5.2 and 6 mm per month, which is comparable with observations of squid growth rate ranging between 1.1 and 5.6 mm per month during the first three months post-hatching (Hanlon *et al.*, 1979).

CHAPTER 8 - CONCLUSIONS AND FUTURE WORK

8.1 Conclusions

8.1.1 LERM

The investigation reported here represents a proof of concept that LERM run under the Lagrangian Ensemble metamodel makes it possible to create a virtual ecosystem in which fisheries recruitment can be predicted and is fit for purpose to test Cushing's match-mismatch and other theories of fisheries recruitment.

The creation of LERM models was the result of substantial work in extracting from the literature biological equations derived from laboratory experiments and in translating these into phenotypic rules that are appropriate for coding in a model that obeys the LE metamodel. This provides a sound basis for the biology used in LERM-ES, from which all the reported results were obtained.

The major strength of the method used lies in the fact that it provides a logical framework for explaining emergent properties, such as recruitment, in terms of emergent ecological processes, all of which ultimately rest on phenotypic equations derived from reproducible laboratory experiments, as proposed by Woods (2003).

Cushing realized that the timing of eggs hatching and the abundance of food available during the critical period of first feeding was an important factor in determining hatchling survival, but could not discriminate whether this effect was caused by larval mortality due to starvation or to predation (Cushing, 1966). The same is true for other studies (Arkhipin and Middleton, 1996; Caddy and Rodhouse 1998; Agnew et al. 2000).

The reported numerical experiments provides more evidence to the Cushing's match-mismatch hypothesis that the timing between hatching of eggs and the peak in food abundance is indeed one important factor affecting recruitment. Annual recruitment emerged from a combination of food availability and composition, inter and intra-populations competition, speed of squid growth and predation. Results also support the Hjort's critical period thesis (Hjort, 1914) that recruitment is primarily determined by predation mortality during the early larval stages, the duration of which depends on growth rate and thus food availability. In particular, it provides more evidence to the hypothesis that density-dependent growth interacts with predation to produce density-

dependent survival: when competition for a limited food resource is high, larvae grow slowly and are vulnerable to predation for longer (Ricker and Foerster, 1948; Cushing and Shepherd, 1980). The demonstration was based on a simple representation of squid recruitment at the Azores. The method proved successful provided a plausible description of the mechanisms involved in determining squid annual recruitment, however it needs to be refined before it can be used operationally as a contribution to fisheries management. Experiments were set in a simplified scenario, in which the dispersal of squid paralarvae by currents was not considered and the ecosystem was driven by a stationary annual climatology.

In order to provide credibility to the model predictions and the mechanisms proposed, these have to be validated against field observations, which are difficult to obtain (Shepherd and Cushing, 1980; Caddy and Rodhouse, 1998; Boyle and Rodhouse, 2005). However, LERM-ES could provide a useful tool for planning which field data would be most effective for verifying LERM-ES.

LERMS-ES provides a base for further scientific investigations. The current biological equations can be further enriched with the introduction of new ones to target new problems (e.g. LERM-PS is currently being used as the base model by the Bermuda Institute of Ocean Sciences for simulating the Bermuda Atlantic Time-Series plankton community, BATS, and by the Plymouth Marine Laboratory to test hypothesis about the competition between population of *Calanus finmarchicus* and *Calanus helgolandicus*). This is an easy task thanks to the user-friendliness provided by the VEW.

8.1.2 The VEW

The third version of the VEW (Hinsley, 2005) was the first that could be considered fit for purpose in terms of creating simulations; previous versions inevitably required edits to be made at a low-level to update, or maintain simulations, requiring considerable computing support, which was provided by Dr Hinsley. However, VEW 3.0 was still in the early stages of development at the outset of the LERM research. LERM provided an immediate application that the software could be specified towards. It also gave advantages to the creation of LERM models, since the development process of the VEW could specifically include the features required for building LERM.

However, such a bilateral process of development also raises significant challenges. Software development is a lengthy process, especially considering the complexity of the systems that the VEW aims to create. Testing, and debugging such a system is just as complex, and in some cases a particular software fix can render a number of experiments void, or at least difficult to defend in terms of scientific integrity, due to errors that may not have been in their nature, scientific. In this way, a significant contribution of time and effort from this research has been towards the specification and development of the Virtual Ecology Workbench and indeed to the future of this type of research. The most significant enhancements and corrections that were added to the VEW in order to create LERM are summarized in Appendix V.

8.2 FUTURE WORK

8.2.1 Using weather data provided by ERA-40

One of the major aims of this PhD was originally to investigate the effect of short-term fluctuations in weather on the success of fisheries recruitment. It is generally accepted that the weather is the main contribution for variance in recruitment (Hjort, 1914; Shepherd, 1990; Heath, 1992; Koslow, 1992). It has a profound effect on the dynamics of plankton ecosystem, affecting the timing of plankton blooms, which determines how much food is available to the fish hatchlings every year and also influences hatchlings' development and metabolic rates.

This would have been achieved by running a series of numerical experiments using the ERA-40 global dataset, which provides the synoptic state of the atmosphere every six hours from 1957 to 2001 with a 1×1 degree of resolution, including wind speed, cloud cover, surface solar radiation, surface sensible heat flux, surface latent heat flux and surface long wave radiation.

ERA-40 weather data was obtained and converted into a VEW complaint format in the beginning of the project. Unfortunately, the dataset provided by the British Atmospheric Data Centre was initially incomplete, with many thousands of erroneous entries. The dataset was finally obtained and converted at the end of 2006. However, the engineering work to install the ERA-40 dataset into VEW 3.1 was more complicated than anticipated, as it required modifications in the physics code. For example, on many occasions, terms

which should have caused a loss of heat from the ocean were found rather to contribute a sudden gain. As a result, it has not been possible so far to run simulations using the ERA-40 six-hourly data. The problems have been demonstrated, and work is ongoing to upgrade the VEW's physics to handle the data, but for this reason, a full evaluation of the effect of weather on squid recruitment is not yet attainable using the VEW.

8.2.2 Coupling LERM with a 3D circulation model

A highly desirable feature would be to couple LERM-ES with a 3D circulation model, in order to simulate larval dispersion from the spawning grounds. This is considered to be a very important factor affecting recruitment success in many fish populations. However this requires a considerable amount of programming and testing.

8.2.3 Sensitivity of recruitment to a wider range of variation in exogenous factors

The sensitivity of the VE and squid recruitment to variation in nutrients (silicate and nitrogen), basal predator and visual predator abundance will be tested over a wide range of values (12 per exogenous factor), in order to gain a better picture of the importance of each and to establish threshold values beyond which the VE may experience a regime shift.

8.2.4 Method for testing the effect of temperature on squid recruitment

Temperature is an emergent property of the simulation and is calculated in the physics code. In the current specification of the physics, an exogenous change of temperature is immediately overwritten by the calculated value. In the final stage of this project, to test the effect of temperature on the biology, a modification in the VEW was made to allow adjustment of the temperature purely for the biological rules: the temperature that emerges from the physics is adjusted by a constant value when used by the plankton primitive equations. Time did not allow a thorough analysis of this functionality, and in any case, this represents a first attempt to proxy the weather. Nevertheless, the effects of changing the temperature in this way were shown (fig.6.164).

8.2.5 Modification of chemical budgeting

Analysis of the virtual ecosystems generated during this project exposed a small drift in the total mesocosm nutrients loads. The problem is thought to be in some calculations performed in the VEW kernel, and further investigation is going to be performed to pinpoint the exact cause of such problem.

Another problem in the budgeting of chemicals was due to the chemical conservation rule, which brings to the surface water chemicals that have been lost below the depth of the permanent thermocline in the previous year. The re-injection date was chosen to be the 1st January, as it is a biologically quiet period of the year. The problem occurred when the depth of the current year was shallower than in the previous. A solution to this problem would be to re-inject the chemicals in the current year just after the mixed layer has reached its annual maximum in the current year.

8.2.6 Lunar phase

Many marine animals are known to release their larvae to the environment during determined periods of the year, when conditions are favorable. Various studies suggest that the rhythm of release is periodic at short timescales and often coinciding with lunar cycles (Robertson, 1992; Robertson *et al.*, 1999; Smith and Suthers, 2000; Smith and Sinerchia, 2004). This increases the chances of larval survival as it involves reduced risk of predation and tidal transport to recruitment grounds. Future work will be devoted to add lunar phase to the astronomic component used to calculate solar irradiance.

8.2.7 VEW performance

The VEW addresses the difficulty in creating LE-based models with considerable success. However, a further factor to consider is the performance of simulations. The models in this thesis take between an hour (LERM-PS), and three hours (LERM-ES) per year of simulation time, to execute, when running on standard desktop computers, with a modest number of agents (around 20,000). It would be desirable to run the simulations with many more agents to achieve more statistically significant results. However, this has not yet been attempted, partly due to the increase time taken to run the simulations,

and partly due to computational memory cost. The VEW has not yet been optimised for performance, and runs only on a single processor. Parallelisation work on the VEW is currently being undertaken by Dr. Hinsley.

8.2.8 Analysis of all dates of the timing of spawning experiment

Due to time limitation the analysis of the causes of variability in squid recruitment as a consequence of timing of spawning was limited to the spawning dates that exhibited the highest recruitment and very low recruitment. In depth analysis will be performed at the end of the PhD.

8.2.9 Passage from food chain to food web

Future work will include extra populations in LERM. This will include a flagellate population, to study the passage from new to regenerated production, and altering the size of the existing copepod model to simulated micro-zooplankton.

8.2.10 Copepod

At the moment a set fraction of copepods enters and exit over-wintering on a set date, following the specifications of Carlotti and Wolf, 1998. To increase the realism of the model it would be desirable to achieve emergent over-wintering, by including environmental cues (e.g. temperature, day length, etc) to trigger the start and end of over-wintering.

8.2.11 Squid

Squid somatic growth is linear, however for predation sake, in the current implementation of the VEW, it has to be considered staged, as a predator can feed only on stages of prey, rather than individual preys. Future work could address this problem by allowing direct particle to particle interaction, taking into account the instantaneous size of squid, rather than a discretised stage value. Another possible improvement derives from the fact that, in the current version of LERM-ES, squid are assumed to be neutrally buoyant, while in reality they need to swim to maintain their position. This could be modified by including an additional respiration cost.

8.2.12 Changing geographical location

The model has so far been run only at the Azores location. Experiments at different latitudes, such as along the trans-Atlantic line where the annual surface heat budget is in balance, are required in order to test the robustness of the model. Another good candidate for this experiment would be a location close to the Falklands, where squid fisheries are of prime importance, and a large amount of fisheries data are available for verification of the model predictions.

8.2.13 Other fisheries recruitment theories

The model is ideally suited to test the squid specific Forsythe hypothesis, which explains that, due to the dramatic effect of small differences in temperature on the rate of growth during the exponential phase, in places where there is considerable seasonal increase in temperature, later hatching individuals can easily overtake those hatched earlier in the season by the time sexual maturity is reached (Forsythe, 1993).

In future experiments, this hypothesis will be tested comparing the relative growth rate of the two hatched cohorts, one occurring in spring and the other in autumn, which are subject to different ambient temperature.

REFERENCES

- Agnew DJ; S Hill; JR Beddington, 2000. Predicting the recruitment strength of an annual squid stock: *Loligo gahi* around the Falkland Islands. *Canadian Journal of Fisheries and Aquatic Sciences* 57: 2479-2487.
- Agnew DJ; JR Beddington; SL Hill, 2002. The potential use of environmental information to manage squid stocks. *Canadian Journal of Fisheries and Aquatic Sciences* 59: 1851-1857.
- Amaratunga T; JF Caddy, 1983. The role of cephalopods in the marine ecosystem. Advances in assessment of world cephalopod resources. *FAO Fisheries Technical Paper* 231: pp.379-415.
- Anderson TR, 2005. Plankton Functional Type Modelling: Running Before We Can Walk? *Journal of Plankton Research* 27(11): 1073-1081.
- Anderson, TR; P Pondaven, 2003. Non-redfield carbon and nitrogen cycling in the Sargasso Sea: pelagic imbalances and export flux. *Deep-sea research. Part I, Oceanographic research papers* 50(5): 573-591.
- Anderson TR; DO Hessen; JJ Elser; J Urabe, 2005. Metabolic stoichiometry and the fate of excess carbon and nutrients in consumers. *The American Naturalist* 165: 1-15.
- Arkhipkin AI; DAJ Middleton, 2002. Inverse patterns in abundance of *Illex argentinus* and *Loligo gahi* in Falkland waters: possible interspecific competition between squid? *Fisheries Research* 59: 181-196.
- Arkhipkin AI; DAJ Middleton, 2003. In-Situ Monitoring of The Duration of Embryonic Development In The Squid *Loligo gahi* (Cephalopoda: Loliginidae) On The Falkland Shelf. *Journal of Molluscan Studies* 69(2): 123-133.
- Baeg GH; Y Sakurai; K Shimazaki, 1993. Maturation processes in female *Loligo bleekeri* Keferstein (Mollusca: Cephalopoda). *The Veliger*. Vol. 36(3), pp. 228-235.
- Bakun A; J Csirke, 1998. Chapter 6 - Environmental processes and recruitment variability. pp. 105-124. In: P.G. Rodehouse, E.G. Dawe, and R.K. O'Dor (eds.). *Squid Recruitment dynamics: influences on variability within the genus Illex as a model, the commercial Illex. Species and Influences on Variability*. *FAO Fisheries Technical Paper* 376.

Båmstedt U, 1986. Chemical composition and energy content. In: Corner, E.D.S., O'Hara, S.C.M. (Eds.), *The Biological Chemistry of Marine Copepods*. Oxford Univ. Press, Oxford, pp. 1–58.

Baretta-Bekker JG; JW Baretta; W Ebenhoeh, 1997. Microbial dynamics in the marine ecosystem model ERSEM II with decoupled carbon assimilation and nutrient uptake. *Journal of sea research* 38(3-4): 195-211.

Baron PJ, 2000. Estimation of the embryonic development length of *Loligo gahi* under a wide range of incubation temperatures and its application as a predictor of hatching recruitment. In: *Cephalopod Biomass and Production*. CIAC-2000 International Symposium. Abstracts, 17. University of Aberdeen, Aberdeen.

Baron PJ, 2001. First description and survey of the egg masses of *Loligo gahi* (D'Orbigny, 1835) and *Loligo sanpaulensis* (Brackoniecki, 1984) from coastal waters of the Patagonia. *Journal of Shellfish Research*, Vol. 20: pp. 289–295.

Baron PJ, 2003. The paralarvae of two South American sympatric squid: *Loligo gahi* and *Loligo sanpaulensis*. *Journal of Plankton Research*, Vol. 25(11): pp. 1347-1358.

Beddington JR; AA Rosenberg; JA Crombie; GP Kirkwood, 1990. Stock Assessment and the Provision of Management Advice for the Short Fin Squid Fishery in Falkland Islands Waters. *Fisheries Research* 8: 351–365.

Berges JA; PG Falkowski, 1998. Physiological stress and cell death in marine phytoplankton: Induction of proteases in response to nitrogen or light limitation. *Limnology and oceanography* 43(1): 129-135.

Beverton RJH; SJ Holt, 1957. On the dynamics of exploited fish populations. UK Ministry of Agriculture and Fisheries. *Fisheries Investigations*. (ser 2). 9: 533 pp.

Bidder AM, 1950. The Digestive Mechanism of the European Squids *Loligo vulgaris*, *Loligo forbesii*, *alloteuthis media* and *Alloteuthis subulata*. *Quarterly Journal of Microscopical Science*, Vol S3(91), pp. 1-43.

Boletzky SV, 1974a. Cephalopod rearing in aquaria. *Vie Milieu (A)*. Vol. 24(2A): pp. 309-340.

Boletzky SV, 1974b. The 'larvae' of Cephalopoda: a review. *Thalassia Jugoslavica*. Vol.10: pp.45-76.

Boucaud-Camou E; R Boucher-Rodoni, 1983. Feeding and digestion in cephalopods. Chapter 3 In: Saleuddin ASM, Wilbur KM (eds) *The Mollusca*, Vol. 5: Physiology, part 2. Academic Press, New York.

Bouchaud O; R Galois, 1990. Utilisation of egg-yolk lipids during the embryonic development of *Sepia officinalis* in relation to temperature of the water. *Comparative biochemistry and physiology. B. Comparative biochemistry*. Vol. 97(3): pp. 611-615.

Boucher-Rodoni R, 1973. Vitesse de digestion d'*Octopus cyanea*. (Cephalopoda: Octopoda). *Marine Biology*, Vol. 18: 237–242.

Boucher-Rodoni R, 1975. Vitesse de digestion chez les céphalopodes *Eledone cirrhosa* (Lamarck) et *Illex illecebrosus* (Lesueur). *Les Cahiers de Biologie Marine* 16: 159-175.

Boucher-Rodoni R; K Mangold, 1977. Experimental study of digestion in *Octopus vulgaris* (Cephalopoda, Octopoda). *Journal of Zoology (London)*. Vol. 183: pp. 505-515.

Boucher-Rodoni R; E Boucaud-Camou; K Mangold, 1987. Feeding and digestion. In: Boyle PR (Ed.) *Cephalopod life cycles Vol. II: Comparative reviews*. London, Academic Press.

Boyle PR; P Rodhouse, 2005. *Cephalopods: Ecology and Fisheries*, Blackwell, Oxford. 452 pp.

Brzezinski MA, 1985. The Si:C:N ratio of marine diatoms: Interspecific variability and the effect of some environmental variables. *Journal of phycology* 21(3): 347-357.

Caddy JF; PG Rodhouse, 1998. Cephalopod and groundfish landings: evidence for ecological change in global fisheries? *Reviews in Fish Biology and Fisheries* 8: 431–444.

Caparroy P; F Carlotti, 1996. A model for *Acartia tonsa*. Effect of turbulence and consequences for the related physiological processes. *Journal Plankton Research* 18(11): 2139-2177.

Cargnelli LM; Griesbach SJ; McBride C; Zetlin CA; WW Morse, 1999. Essential Fish Habitat Source Document: Longfin Inshore Squid, *Loligo pealeii*, Life History and Habitat Characteristics. NOAA Technical memorandum NMFS-NE-146.

Carlotti F; KU Wolf, 1998. A Lagrangian ensemble model of *Calanus finmarchicus* coupled with a 1-D ecosystem model. *Fisheries Oceanography* 7(3-4): 191-204.

Chen DS; G Van Dykhuizen; J Hodge; WF Gilly, 1996. Ontogeny of copepod predation in juvenile squid – *Loligo opalescens*. Biological Bulletin. Vol.190: 69-81.

Choe S, 1966. On the growth, feeding rates and the efficiency of food conversion for cuttlefishes and squids. Korean Journal Zoology. Vol.9(2): 12-20.

Clarke MR, 1996. Cephalopods as prey. III. Cetaceans. Philosophical Transactions of the Royal Society of London B 351: 1053-1065.

Craig S; PR Boyle; KD Black; J Overnell, 2000. Closing the life cycle and developmental plasticity in squid. In: Cephalopod Biomass and Production. CIAC-2000 International Symposium. Abstracts, 18. University of Aberdeen, Aberdeen.

Cushing DH, 1966. Biological and hydrographic changes in British seas during the last thirty years. Biological Reviews 41: 221–258.

Cushing DH, 1971. The dependence of recruitment on parent stock in different groups of fishes. Journal du Conseil International Pour l'Exploration de la Mer 33: 340–362.

Cushing DH, 1972. The production cycle and the numbers of marine fish. Symposia of the Zoological Society of London 29: 213–232.

Cushing DH, 1975, Marine ecology and fisheries, Cambridge University Press, London (UK). 292 pp.

Cushing DH, 1982. Climate and Fisheries. London, New York: Academic Press. 373 pp.

Cushing DH, 1990. Plankton production and year-class strength in fish populations: an update of the match/mismatch hypothesis. Advances in Marine Biology 26: 249-293.

Cushing DH, 1996. Towards a science of recruitment in fish populations. Ecology Institute, Oldendorf/Luhe. 175 pp.

Cushing DH; JW Horwood, 1994. The growth and death of fish larvae. Journal of Plankton Research, 16: 291-300.

Dawe EG; EB Colbourne; KF Drinkwater, 2000. Environmental effects on recruitment of short-finned squid (*Illex illecebrosus*). ICES journal of marine science 57(4): 1002-1013.

Doney SC, 1999. Major challenges confronting marine biogeochemical modeling. *Global Biogeochemical Cycles* 13: 705-714.

Droop MR, 1973. Some thoughts on nutrient limitation in algae. *Journal of phycology* 9: 264-272.

Fänge R; D Grove, 1979. Fish Digestion. In *Fish physiology*. W. Hoare (Ed.). Academic Press, New York.

FAO, 1984. *FAO Species catalogue Vol.3. Cephalopods of the world*. FAO Fisheries Synopsis 125(3).

FAO, 1997. Review of the state of world aquaculture. *FAO Fisheries Circular No. 886, Rev.1*. Rome, Italy.

FAO, 1999. *The state of world fisheries and aquaculture 1998*. FAO, Rome, Italy.

FAO, 2000. *The state of world fisheries and aquaculture 2000*. FAO, Rome, Italy.

FAO, 2002. Report of the Reykjavík Conference on Responsible Fisheries in the Marine Ecosystem, Reykjavík, Iceland, October 2001. *FAO Fisheries Report*, 658. 128 pp.

FAO, 2003. *The ecosystem approach to fisheries*. FAO, Rome, Italy.

FAO, 2006. *The state of world fisheries and aquaculture 2000*. FAO, Rome, Italy.

Fasham MJR; T Platt; B Irwin; K Jones, 1985. Factors affecting the spatial pattern of the deep chlorophyll maximum in the region of the Azores front.

Fasham MJR, 1993. Modelling the marine biota. In Heimann M (ed) *The Global Carbon*. Springer-Verlag, Berlin. pp. 457-504.

Fasham, MJR; HW Ducklow; SM McKelvie, 1990. A nitrogen-based model of plankton dynamics in the oceanic mixed layer, *Journal of Marine Research* 48(3): 591-639.

Fields WG, 1965. The structure, development, food relations, reproduction and life history of the squid *Loligo opalescens* Berry. *California Department Fish and Game, Fisheries Bulletin*. Vol. 131: 1-108.

Fiksen O; F Carlotti, 1998. A model of optimal life history and diel vertical migration in *Calanus finmarchicus*, *Sarsia* 83(2): 129-147.

Flynn KJ; MJR Fasham; CR Hipkin, 1997. Modelling the interaction between ammonium and nitrate uptake in marine phytoplankton. Philosophical Transactions of the Royal Society of London (B) 352:1625-1645.

Flynn KJ, 2005. Castles built on sand: dysfunctionality in plankton models and the inadequacy of dialogue between biologists and modellers. Journal of Plankton Research 27(12): 1205-1210.

Forsythe JW; WF Van Heukelem, 1987. Growth. In: Boyle PR (Ed.) Cephalopod life cycles Vol. II: Comparative reviews. London, Academic Press.

Forsythe JW; RT Hanlon, 1989. Growth of the Eastern Atlantic squid, *Loligo forbesi* Steenstrup (Mollusca: Cephalopoda). Aquaculture and Fisheries Management 20: 1-14.

Forsythe JW, 1993. A working hypothesis of how seasonal temperature change may impact the field growth of young cephalopods. In Okutani, T; RK O'Dor; T Kubodera (Eds). Recent advances in cephalopods fisheries biology. Tokai University Press: Tokyo, Japan: 133-143.

Forsythe, JW; LS Walsh; PE Turk; PG Lee, 2001. Impact of temperature on juvenile growth and age at first egg-laying of the Pacific reef squid *Sepioteuthis lessoniana* reared in captivity. Marine Biology 138(1): 103-112.

Forsythe JW, 2004. Accounting for the effect of temperature on squid growth in nature: from hypothesis to practice. Marine and Freshwater Research. Vol. 55(4): 331-339.

Frost BW, 1972. Grazing control of phytoplankton stock in the open subarctic Pacific Ocean: A model assessing the role of mesozooplankton, particularly the large calanoid copepods *Neocalanus* spp. Marine Ecology Progress Series 39: 49-68.

Garcia SM and C Newton, 1995, Current situation, trends and prospects in world capture fisheries. In Pikitch E; D Hubert; M Sissenwine (eds), Global trends in fisheries management. American Fisheries Society Monograph Series. Bethesda, MD, 352pp.

Geider RJ; HL MacIntyre; TM Kana, 1996. A dynamic model of photoadaptation in phytoplankton. Limnology and oceanography 41(1): 1-15.

Geider RJ; HL MacIntyre; TM Kana, 1997. Dynamic model of phytoplankton growth and acclimation: Responses of the balanced growth rate and the chlorophyll a: Carbon ratio to light, nutrient-limitation and temperature. *Marine ecology progress series* 148(1-3): 187-200.

Geider RJ; HL MacIntyre; TM Kana, 1998. A dynamic regulatory model of phytoplanktonic acclimation to light, nutrients, and temperature. *Limnology and oceanography* 43(4): 679-694.

Giese AC, 1969. A new approach to the biochemical composition of the mollusk body. *Oceanography and Marine Biology Annual Reviews*. Vol. 7: 175-229.

Gilpin, LC; K Davidson; E Roberts, 2004. The influence of changes in nitrogen: silicon ratios on diatom growth dynamics. *Journal of sea research* 51(1): 21-35.

Grimm V; SF Railsback, 2005. *Individual-based modeling and ecology*. Princeton University Press, Princeton, New Jersey.

Grotius H, 1609. *Mare liberum*.

Guerra, A; F Rocha; AF Gonzalez; LF Bueckle, 2001. Embryonic Stages of the Patagonian Squid *Loligo gahi* (Mollusca: Cephalopoda). *Veliger* 44(2): 109-115.

Hanlon RT, 1990. Maintenance, rearing and culture of teuthoid and sepioid squids. In: Gilbert DL; WJ Adelman; JM Arnold (eds). *Squid experimental animals*. Plenum, New York, pp.35-62.

Hanlon RT; RF Hixon; WH Hulet; WT Yang, 1979. Rearing experiments in the California market squid *Loligo opalescens* Berry, 1911. *Veliger*, 21(4), 428-431.

Hanlon RT; MJ Smale; WHH Sauer, 2002. The mating system of the squid *Loligo vulgaris reynaudii* (Cephalopoda, Mollusca) off South Africa: Fighting, guarding, sneaking, mating and egg laying behavior. *Bulletin of Marine Science* 71(1) 331-345.

Harrison WG; LR Harris; BD Irwin, 1996. The kinetics of nitrogen utilization in the oceanic mixed layer: Nitrate and ammonium interactions at nanomolar concentrations. *Limnology and oceanography* 41(1): 16-32.

Hatfield EMC, 2000. Do some like it hot? Temperature as a possible determinant of variability in the growth of the Patagonian squid, *Loligo gahi* (Cephalopoda: Loliginidae). *Fisheries research* 47(1): 27-40.

Hatfield EMC; RT Hanlon; JW Forsythe; EPM Grist (2001). Laboratory testing of a growth hypothesis for juvenile squid *Loligo pealeii* (Cephalopoda: Loliginidae). Canadian journal of fisheries and aquatic sciences 58(5): 845-857.

Heath MR, 1992. Field investigations of the early life stages of marine fish. Advances in Marine Biology 28: 1-174.

Heath M; W Robertson; J Mardaljevic; WSG Gurney, 1997. Modelling the population dynamics of *Calanus* in the Fair Isle Current off northern Scotland. Journal of sea research 38(3-4): 381-412.

Hinsley WR, 2005. Planktonica: a system for doing biological oceanography by computer. PhD Thesis, Imperial College of London.

Hirtle RMW; ME Demont; RK O'Dor, 1981, Feeding, growth, and metabolic rates in captive short-finned squid, *Illex illecebrosus*, in relation to the natural population. Journal Shellfish Research 1: 187-192.

Hixon RF, 1983. *Loligo opalescens*. In In: Boyle PR (Ed.) Cephalopod life cycles Vol. I: Species accounts. London, Academic Press.

Hjort J, 1914. Fluctuations in the great fisheries of northern Europe viewed in the light of biological research. Rapports et Procès-Verbaux des Réunions. Conseil International pour l'Exploration de la Mer 20: 1-228.

Hjort J, 1926. Fluctuations in the year classes of important food fishes. Journal du Conseil International Pour l'Exploration de la Mer 1: 1-38.

Hood RR; VJ Coles; DG Capone, 2004. Modeling the distribution of *Trichodesmium* and nitrogen fixation in the Atlantic Ocean. Journal of Geophysical Research. C. Oceans 109(C6).

Huntley ME; W Nordhausen, 1995. Ammonium cycling by Antarctic zooplankton in winter. Marine Biology 121(3): 457-467.

Hurd DC; S Birdwhistell, 1983. On producing a more general model for biogenic silica dissolution. American Journal of Science 283: 1-28.

Hurley AC, 1976. Feeding behavior, food consumption, growth, and respiration of the squid *Loligo opalescens* raised in the laboratory. Fishery Bulletin 74(1): 176-182.

Ikeda T; JJ Torres; S Hernandez-Leon; SP Geider, 2000. Metabolism: 455-532. In Harris RP, Wiebe PH, Lenz J, Skjoldal HR and Huntley M [eds], ICES Zooplankton methodology manual. Academic Press, London.

Isemer HJ; L Hasse, 1987. The Bunker climate atlas of the North-Atlantic Ocean. Springer Verlag, Berlin.

Jackson, GD; JW Forsythe; RF Hixon; RT Hanlon, 1997. Age, growth, and maturation of *Lolliguncula brevis* (Cephalopoda: Loliginidae) in the northwestern Gulf of Mexico with a comparison of length-frequency versus statolith age analysis. Canadian Journal of Fisheries and Aquatic Sciences 54(12): 2907-2919.

Kamatani A, 1982. Dissolution rates of silica from diatoms decomposing at various temperatures. Marine Biology 68(1): 91-96.

Karpov KA; GM Caillet, 1978. Feeding dynamics of *Loligo opalescens*. Fish Bulletin 169: 45-185.

Kasugai T, 2001. Feeding behaviour of the Japanese pygmy cuttlefish *Idiosepius paradoxus* (Cephalopoda: Idiosepiidae) in captivity: evidence for external digestion? Journal of the Marine Biological Association of the United Kingdom 81(6): 979-981.

Kendall AW Jr; GJ Duker, 1998. The development of recruitment fisheries oceanography in the United States. Fisheries oceanography 7(2): 69-88.

Kjørboe T; P Tiselius, 1987. Gut clearance and pigment destruction in a herbivorous copepod, *Acartia tonsa*, and the determination of in situ grazing rates. Journal of Plankton Research 9: 525-534.

Kjørboe T; F Mohlenberg; K Hamburger, 1985. Bioenergetics of the planktonic copepod *Acartia tonsa*: relation between feeding, egg production and respiration, and composition of specific dynamic action. Marine Ecology Progress Series 26: 85-97.

Koueta N; E Boucaud-Camou (1999) Food intake and growth in reared early juvenile cuttlefish *Sepia officinalis*. Journal of Experimental Marine Biology and Ecology 240: 93-109.

Koueta N; E Boucaud-Camou, 2001. Basic growth relations in experimental rearing of early juvenile cuttlefish *Sepia officinalis* L. (Mollusca: Cephalopoda). *Journal of Experimental Marine Biology and Ecology* 265: 75-87.

Koslow JA, 1992. Fecundity and the stock - recruitment relationship. *Canadian Journal of Fisheries and Aquatic Sciences* 49: 210-217.

Kubodera, T. (eds), *Recent Advances in Cephalopod Fisheries Biology*. Tokai University Press, Tokyo, pp. 133-143.

Langdon C, 1993. The significance of respiration in production measurements based on oxygen. *ICES marine science symposia* 197: 69-78.

Laptikhovskiy VV, 1991. A mathematical model to study the duration of embryogenesis in cephalopods. *Biologicheskije Nauki* 3: 37-48.

LaRoe ET, 1971. The culture and maintenance of the loliginid squids *Sepioteuthis sepioidea* and *Doryteuthis plei*. *Marine Biology* 9: 9-25.

Lasker R, 1981. *Marine fish larvae. morphology, ecology, and relation to fisheries*. Washington. Washington Sea Grant Program. s. f. 131 p.

Lee PG, 1994. Nutrition of cephalopods: Fueling the system. *Marine behaviour and physiology* 25(1-3): 35-51.

Lenes JM; JJ Walsh; DB Otis; KL Carder, 2005. Iron fertilization of *Trichodesmium* off the west coast of Barbados: a one-dimensional numerical model. *Deep Sea Research (Part I, Oceanographic Research Papers)* 52(6): 1021-1041.

Mangold K; MR Clarke; CFE Roper, 1998. Class Cephalopoda. pp. 451-484 in Beesley PL, GJB Ross, Wells A (eds) *Mollusca: The Southern synthesis*. Fauna of Australia. Vol.5. CSIRO Publishing: Melbourne, Part A xvi 563 pp.

Mason F, 2002, The Newfoundland cod stock collapse: A review and analysis of social factors. *The Electronic Green journal* 17. URL:<http://egj.lib.uidaho.edu/egj17/mason1.html>

McConathy DA; RT Hanlon; RF Hixon, 1980. Chromatophore arrangements of hatchling loliginid squids (Cephalopoda, Myopsida). *Malacologia*, 19(2): 279-288.

Morejohn, GV; JT Harvey; LT Krasnow, 1978. The importance of *Loligo opalescens* in the food web of marine vertebrates in Monterey Bay. California. California Fish and Game Fish Bulletin 169: 67-98.

Moynihan M; AF Rodaniche, 1982. The Behavior and Natural History of the Caribbean Reef Squid *Sepioteuthis sepioidea*. Germany: Verlag Paul Parey.

Myers RA; NG Cadigan, 1993. Density-dependent juvenile mortality in marine demersal fish. Canadian journal of Aquatic Sciences 50: 1576-1590.

Neuert C, 1999. Die Dynamik räumlicher Strukturen in naturnahen Buchenwäldern Mitteleuropas. PhD dissertation. University of Marburg, Germany.

NOAA , 2002. World ocean atlas 2001. Volume 4: Nutrients. Levitus S (ed). National Oceanographic Data Center. Ocean Climate Laboratory. Silver Spring.

O'Dor, RK; K Mangold; R Boucher-Rodoni; MJ Wells; J Wells, 1984. Nutrient absorption, storage and remobilization in *Octopus vulgaris*. *Marine Behaviour and Physiology* 11(3): 239-258.

O'Dor, RK; MJ Wells, 1987. Energy and nutrient flow. In: Boyle PR (ed) *Cephalopod life cycles. II. Comparative reviews*. Academic Press Inc. Ltd., London pp. 109-134.

O'Dor RK; DM Webber, 1986. The constraints on cephalopods: Why squid aren't fish. *Canadian Journal of Zoology* 64(8): 1591-1605.

O'Dor RK; EA Foy; N Balch, 1986. The locomotion and energetics of hatchling squid, *Illex illecebrosus*. *American Malacological Bulletin*. 4(1): 55-60.

O'Dor RK, 2002. Telemetered Cephalopod energetics: swimming, soaring, and blimping. *Integrative and Comparative Biology* 43(5): 1065-1070.

Okutani, T; JA McGowan, 1969. Systematics, distribution, and abundance of the epipelagic squid (Cephalopoda, Decapoda) larvae of the California Current, April 1954-March 1957. Scripps Institution of Oceanography Technical Report 25(8).

Paasche E, 1973. Silicon and ecology of marine plankton diatoms. II. Silicate uptake kinetics in five diatoms species. *Marine Biology* 19: 262-269.

Paffenhöfer GA; SC Knowles, 1979. Ecological implications of faecal pellet size, production and consumption by copepods. *Journal of Marine Research* 37(1): 35-49.

Palmer C; P Sinclair, 1997. When the fish are gone: Ecological disaster and fishers in Northwest Newfoundland. Halifax, Nova Scotia, Canada: Fernwood Publishing.

Parry G, 1983. The influence of cost of growth on ectotherm metabolism. *Journal Theoretical Biology* 107: 453-477.

Parsons TR; Takahashi M and Hargrave B, 1984, *Biological oceanographic processes*. 3rd ed. Pergamon Press, Oxford. 330pp.

Rathjen WF; GL Voss, 1987. The cephalopod fisheries: a review. In: Boyle PR (ed) *Cephalopod life cycles. II. Comparative reviews*. Academic Press Inc. Ltd., London pp. 253-276.

Raven JA, 1980. Short- and long-distance transport of boric acid in plants. *New Phytology* 84: 231-249.

Ricker WE; Foerster RE, 1948. Computation of fish production. *Bulletin of the Bingham Oceanographic Collection* 11: 173-211.

Ricker WE, 1954. Stock and recruitment. *Journal of the Fisheries Research Board of Canada* 11: 114-128.

Robertson DR, 1992, Patterns of lunar settlement and early recruitment in Caribbean reef fishes at Panama. *Marine Biology* 114(4): 527-537.

Robertson DR; SE Swearer; K Kaufmann; EB Brothers, 1999. Settlement vs. environmental dynamics in a pelagic-spawning reef fish at Caribbean Panama. *Ecological Monographs* 69(2): 195-218.

Robin JP; V Denis, 1999. Squid stock fluctuations and water temperature: temporal analysis of English Channel Loliginidae. *The Journal of applied ecology* 36(1): 101-110.

Rodhouse PG, 2001. Managing and forecasting squid fisheries in variable environments, *Fisheries Research* 54: pp. 3-8.

Roper CFE; MJ Sweeney; CE Nauen, 1984. FAO species catalogue. Vol. 3. Cephalopods of the world. An annotated and illustrated catalogue of species of interest to fisheries. FAO fisheries synopsis FIR/S125.

Rosenberg A; P Mace; G Thompson; G Darcy; W Clark; J Collie; W Gabriel; A MacCall; RJ Methot; J Powers; V Restrepo; T Wainright; L Botsford; J Hoenig; K Stokes, 1996. Scientific review of definitions of overfishing in U.S. fishery management plan. NOAA Technical Memorandum. NSFS-F/SPO-17.

Sakurai Y; JR Bower; Y Nakamura; S Yamamoto; K Watanabe, 1996. Effect of temperature on development and survival of *Todarodes pacificus* paralarvae embryos and paralarvae. American Malacological Bulletin 13: 89–95.

Sakurai Y; H Kiyofuji; S Saitoh; T Goto; Y Hiyama, 2000. Changes in inferred spawning areas of *Todarodes pacificus* (Cephalopods: Ommastrephidae) due to changing environmental conditions. ICES journal of marine science 57(1): 24-30.

Segawa, S; WT Yang; HJ Marthy; RT Hanlon, 1988. Illustrated embryonic stages of the eastern *Loligo forbesi*. Veliger, 30: 230-243.

Shepherd JC; DH Cushing, 1980. A mechanism for density-dependent survival of larval fish as the basis of a stock-recruitment relationship. Journal du Conseil International Pour l'Exploration de la Mer 39: 160-167.

Shepherd JG, 1982. A versatile new stock recruitment relationship for fisheries and the construction of sustainable yield curves. Journal du Conseil International Pour l'Exploration de la Mer 40: 67-75.

Shepherd JG, 1990. Stability and the Objectives of Fisheries Management: the Scientific Background. Lowestoft Laboratory Leaflet No. 64.

Sinclair PR, 1992. Atlantic Canada's fishing communities: The impact of change. In Hay DA and GS Basran (Eds.). Rural sociology in Canada. Don Mills, Ontario, Canada: Oxford University Press.

Smale, M.J. 1996 Cephalopods as prey. IV. Fishes. Philosophical Transactions of the Royal Society of London. B 351, 1067-1081.

Smith KA; Suthers IM, 2000. Consistent timing of juvenile fish recruitment to seagrass beds within two Sydney estuaries. Marine and Freshwater Research 51(8): 765-776.

-
- Smith KA; M Sinerchia, 2004. Timing of recruitment events, residence periods and post-settlement growth of juvenile fish in a seagrass nursery area, South-Eastern Australia. *Environmental Biology of Fishes* 71(1), pp. 73-84.
- Solemdal P; M Sinclair, 1989. Johan Hjort – founder of modern Norwegian fishery research and pioneer in recruitment thinking. *Rapports et Procès-Verbaux des Réunions. Conseil International pour l'Exploration de la Mer* 191: 339-344.
- Steele DH; R Andersen; JM Green, 1992. The managed commercial annihilation of northern cod. *Newfoundland Studies*, 8(1):34-68.
- Strass VH; Woods JD. (1991). "New production in the summer revealed by the meridional slope of the deep chlorophyll maximum." *Deep-Sea Research (A Oceanographic Research Papers* 38(1A): 35-56.
- Strathmann RR, 1967. Estimating the organic carbon content of phytoplankton from cell volume or plasma volume. *Limnology and oceanography* 12(3): 411-418.
- Summers WC, 1983. *Loligo pealei*. In Boyle PR (ed). *Cephalopod life cycles*. Vol. 1: Species accounts. Academic press. London. pp. 115-142.
- Tang EPY; RH Peters, 1995. The allometry of algal respiration. *Journal of Plankton Research* 17(2): 303-315.
- Tett P; MR Droop, 1988. Cell quota models and planktonic primary production. In: Wimpenny JWT. *CRC Handbook of Laboratory Model Systems for Microbial Ecosystems*. Boca Raton, Florida. CRC Press 2: 177-233.
- Tidwell JH and GL Allen, 2001. Fish as food: aquaculture's contribution, *EMBO reports* 21(11): 958-963.
- Uye S, 1982. Length-weight relationships of important zooplankton from the inland Sea of Japan. *Journal of the Oceanographical Society of Japan* 38: 149-158.
- Uye S; K Kaname, 1994. Relations between fecal pellet volume and body size for major zooplankters of the Inland Sea of Japan. *Journal of Oceanography* 50(1): 43-49.
- van den Bosch F; W Gabriel, 1994. A model of growth and development in copepods. *Limnology and Oceanography* 39(7): 1528-1542.

-
- Vecchione M, 1981. Aspects of the early life history of *Loligo pealei* (Cephalopoda: Myopsida). *Journal of Shellfish Research* 1: 171-180.
- Vecchione M, 1987. Juvenile ecology. In: Boyle PR (ed) *Cephalopod life cycles. II. Comparative reviews.* Academic Press Inc. Ltd., London pp. 82.
- Vecchione M, 1999. Extraordinary abundance of squid paralarvae in the tropical eastern Pacific Ocean during El Nino of 1987. *Fishery Bulletin* 97(4): 1025-1030.
- Veldhuis MJW; GW Kraay; KR Timmermans, 2001. Cell death in phytoplankton: correlation between changes in membrane permeability, photosynthetic activity, pigmentation and growth. *European Journal of Phycology* 36: 167-177.
- Vidal J, 1980. Physioecology of zooplankton. II. Effects of phytoplankton concentration, temperature, and body size on the development and molting rates of *Calanus pacificus* and *Pseudocalanus* sp. *Marine Biology* 56(2): 135-146.
- Vidal EAG; FP DiMarco; JH Wormuth; PG Lee, 2002. Influence of temperature and food availability on survival, growth and yolk utilization in hatchling squid. *Bulletin of Marine Science*, 71(2): 915-931.
- Vojkovich M, 1998. The California fishery for market squid (*Loligo opalescens*). *California cooperative oceanic fisheries investigations, progress report* 39: 55-60.
- Vovk AN; LA Khvichiya, 1980. On feeding of long-finned squid (*Loligo pealei*) juveniles in Subareas 5 and 6. *Northwest Atlantic Fisheries Organization (NAFO). Sci. Coun. Res. Doc. 80/VI/50.* 9
- Vovk AN, 1985. Feeding spectrum of longfin squid (*Loligo pealei*) in the Northwest Atlantic and its position in the ecosystem. *Scientific council studies. Northwest Atlantic Fisheries Organization.* 8: 33-38.
- Wallace IC, RK O'Dor, T Amaratunga, 1981, Sequential observations on the digestive process in the squid, *Illex illecebrosus*. *NAFO Sci. Coun. Studies*, 1:65-69.
- Waluda, CM; PG Rodhouse; PN Trathan, 2002. Mesoscale oceanography of hatching grounds: Influences on recruitment variability in *Illex argentinus*. *Bulletin of Marine Science* 71(2): 1143.
- Waluda CM; Rodhouse PG, 2006. Remotely sensed mesoscale oceanography of the Central Eastern Pacific and recruitment variability in *Dosidicus gigas*. *Marine Ecology Progress Series* 310: 25-32.

Weeks, A; MH Conte; RP Harris; A Bedo; I Bellan; PH Burkill; ES Edwards; DS Harbour; H Kennedy; C Llewellyn; P Burkill; RFC Mantoura; CE Morales; AJ Pomroy; CCTurley, 1993. The physical and chemical environment and changes in community structure associated with bloom evolution: the JGOFS North Atlantic Bloom Experiment. *Deep-Sea Research II* 40: 347-368.

Wells MJ; A Clarke, 1996, Energetics: the costs of living and reproducing for an individual cephalopod. *Philosophical Transactions of the Royal Society of London B*, 351, 1083-1104.

Wheeler PA; SA Kokkinakis, 1990. Ammonium recycling limits nitrate use in the oceanic subarctic Pacific. *Limnology and oceanography* 35(6): 1267-1278.

Woods JD; R Onken, 1982. Diurnal variation and primary production in the ocean – preliminary results of a Lagrangian Ensemble model, *Journal of Plankton Research* 4: 735-756.

Woods JD; W Barkmann, 1986. The influence of solar heating on the upper ocean: I. The mixed layer. *Quarterly Journal of the Royal Meteorological Society*, 112(471): 1-27.

Woods JD; W Barkmann, 1993. Diatom demography in winter – simulated by the Lagrangian Ensemble method. *Fisheries Oceanography* 2(3-4): 202-222.

Woods JD; W Barkmann, 1994. Simulating plankton ecosystems by the Lagrangian Ensemble method. *Philosophical Transactions of the Royal Society of London. B* 343, 27-31.

Woods JD, 2003, Primitive equation modelling of plankton ecosystems. In: N. Pinardi and JD Woods (Eds), Chapter 18 in *Ocean modelling: conceptual basis and applications*. Berlin: Springer Verlag, pp. 472.

Woods JD, 2005. The Lagrangian Ensemble metamodel for simulating plankton ecosystems. *Progress in oceanography* 67(1-2): 84-159.

Woods JD; A Perilli; W Barkmann, 2005. Stability and predictability of a Virtual Plankton Ecosystem created with an individual-based model. *67(1-2): Progress in oceanography* 43-83.

Worms J, 1983. Aspects of the biology of *Loligo vulgaris* Lam. related reproduction. *Vie et milieu* 30(3-4): pp. 263-267.

Xavier JC; JP Croxall; PN Trathan; AG Wood, 2003. Feeding strategies and diets of breeding grey-headed and wandering albatrosses at South Georgia. *Marine biology* 143(2): 221-232.

Yang WT; RF Hixon; PE Turk; ME Krejci; WH Hulet; RT Hanlon, 1986. Growth, behavior, and sexual maturation of the market squid, *Loligo opalescens* cultured through the life cycle. Fishery Bulletin 84(4): 771-798.

Yim M, 1978. Developpement post-embryonnaire de la glande digestive de *Sepia officinalis* L. (Mollusque Cephalopode). These de Doctorat 3e cycle. Universite de Caen. pp.1-75.

Young, RE; RF Harman, 1988. "Larva," "paralarva" and "subadult" in cephalopod terminology. Malacologia 29: 201–207.

Zeidberg LD; WM Hamner, 2002. Distribution of squid paralarvae, *Loligo opalescens* (Cephalopoda: Myopsida), in the Southern California Bight in the three years following the 1997-1998 El Nino. Marine biology 141(1): pp. 111-122.

Zeidberg LD, 2003. The Early Life History and Fishery of the California Market Squid, *Loligo opalescens*. University of California, Los Angeles.

Zeidberg LD, 2004. Allometry measurements from in situ video recordings can determine the size and swimming speeds of juvenile and adult squid *Loligo opalescens* (Cephalopoda: Myopsida). Journal of Experimental Biology 207(24): pp. 4195-4203.

APPENDICES

“Testing theories on fisheries recruitment.”

APPENDIX I

DIATOM MODEL

APPENDIX I – DIATOM MODEL

I.1 STATE VARIABLES

$$\text{Eq.I.1 } A_{\text{pool}} = [A_{\text{pool}} + A_{\text{ing}} - (A_{\text{pool}} * R_N * T_{\text{function}} * Ts)] / Cd$$

$$\text{Eq.I.2 } N_{\text{pool}} = [N_{\text{pool}} + N_{\text{ing}} - (N_{\text{pool}} * R_N * T_{\text{function}} * Ts)] / Cd$$

$$\text{Eq.I.3 } Si_{\text{pool}} = [Si_{\text{pool}} + Si_{\text{ing}}] / Cd$$

$$\text{Eq.I.4 } C_{\text{pool}} = [C_{\text{pool}} + \{C_{\text{pool}} * [(Photo - (R_c * T_{\text{function}}) * Ts)]\}] / Cd$$

$$\text{Eq.I.5 } Chl_{\text{pool}} = \text{if } (\theta^N < \theta^N_{\text{max}})$$

$$Chl_{\text{pool}} + [(Rho_{\text{Chl}} * (A_{\text{ing}} + N_{\text{ing}}))] - [(R_{\text{chl}} * Chl_{\text{pool}} * T_{\text{function}} * Ts)]$$

Else

$$Chl_{\text{pool}} - \{Chl_{\text{pool}} - [(A_{\text{pool}} + N_{\text{pool}}) * \theta^N_{\text{max}}]\} \text{ Chlorophyll degrades if above}$$

the maximum threshold of Chl : N

A_{pool} = Ammonium pool (mmol N)

N_{pool} = Nitrate pool (mmol N)

Si_{pool} = Silicon pool (mmol Si)

C_{pool} = Carbon pool (mmol C)

Chl_{pool} = Chlorophyll a pool (mg Chl a)

$Ts = 0.5 \text{ h Timestep}^{-1}$

$Cd = \text{flag for cell division (reproduction occurs when } Cd = 2)$

I.2 EQUATIONS

I.2.1 MOTION

$$\text{Eq.I.6 } z = \text{If } (z < \text{MLD})$$

$$RND(\text{MLD}) + (v_s * Ts)$$

Else

$$z = z + (v_s * Ts)$$

$z = \text{depth (m)}$

I.2.2 PHOTO-ADAPTATION

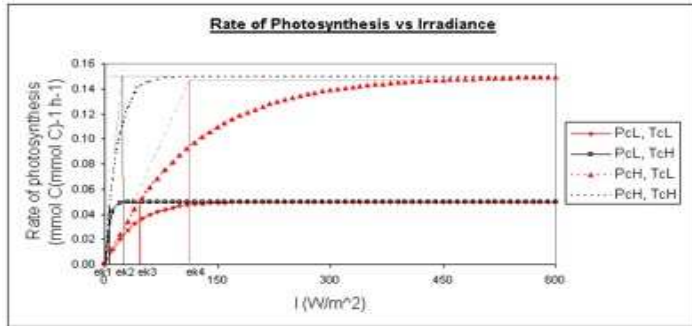


Fig.I.1 – Photosynthetic rate as a function of irradiance

Pc = max rate of photosynthesis
 PcL = 0.05 (mmol C / mmol C h))
 PcH = 0.15 (mmol C / (mmol C h))
 Tc = Chla : C ratio
 TcL = 0.1 (mg Chla / mmol C)
 TcH = 0.7 (mg Chla / mmol C)

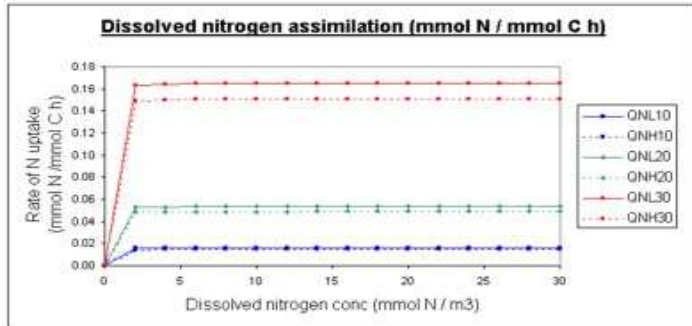


Fig.I.2 – Nitrogen uptake as a function of nitrogen concentration

Qn = N:C ratio (mmol N / mmol C)
 QnL = 0.05 (mmol N / mmol C)
 QnH = 0.15 (mmol N / mmol C)
 10,20,30 = Temperatures °(C)

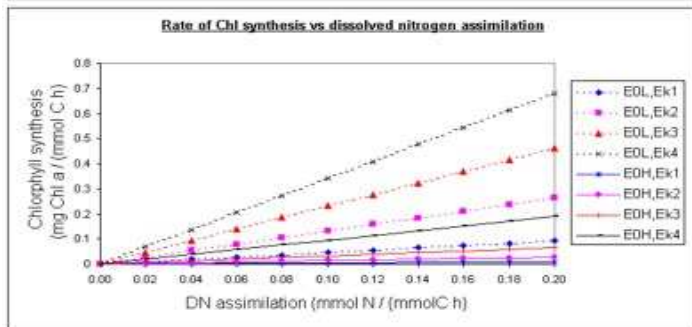


Fig.I.3 – Chlorophyll synthesis as a function of nitrogen uptake

E0 incident solar radiation
 E0L = 50 Wm⁻²
 E0H = 500 Wm⁻²
 Ek = light saturation parameter (irradiance at which the initial slope intercepts light saturated rate –Fig. I.1)

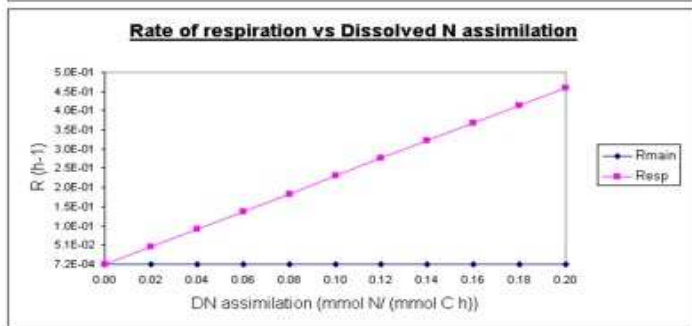


Fig.I.4 – Respiration cost as a function of nitrogen uptake

Rmain = maintenance respiration
 Resp = total respiration (Rmain + Rgrowth)

I.2.2.1 PHOTOSYNTHESISEq.I.7 if ($P_{\max}^C = 0$)

$$P_{phot}^C = 0$$

Else

$$P_{phot}^C = P_{\max}^C \{1 - \exp^{[-3600 \alpha^{Chl} \theta^C E_0] / P_{\max}^C}\}$$

Where:

 P_{\max}^C = maximum carbon specific rate of photosynthesis at ambient T(K) (h^{-1}) α^{Chl} = initial slope of photosynthetic light curve [$mmol\ C\ m^2\ (\mu E\ mg\ Chl\ a)^{-1}$] E_0 = incident scalar irradiance in the PAR part of the spectrum [$\mu E\ s^{-1}\ m^{-2}$] θ^C = Chl a:C ratio within the cell [$mg\ Chl\ a\ (mmol\ C)^{-1}$]

$$\theta^C = Chl_{pool} / C_{pool}$$

MAXIMUM RATE OF PHOTOSYNTHESIS

The maximum rate of photosynthesis is assumed to increase linearly with the cell nitrogen quota (Q_N)

Eq.I.8 $Q_N = N_{pool} / C_{pool}$

Eq.I.9 IF ($Q_{N,min} \leq Q_N \leq Q_{N,max}$)

$$P_{\max}^C = P_{ref}^C [(Q_N - Q_{N,min}) / (Q_{N,max} - Q_{N,min})] T_{function}$$

else if ($Q_N < Q_{N,min}$)

$$P_{\max}^C = 0$$

else if ($Q_N > Q_{N,max}$)

$$P_{\max}^C = P_{ref}^C T_{function}$$

Where:

 $Q_{N,min}$ = minimum nitrogen to carbon ratio [$0.034\ mmol\ N\ (mmol\ C)^{-1}$] $Q_{N,max}$ = maximum nitrogen to carbon ratio [$0.17\ mmol\ N\ (mmol\ C)^{-1}$] $T_{function}$ = defines the effect of temperature on metabolic rates (dimensionless):

Eq.I.10 $T_{function} = \exp \{A_E [(1/T) - (1/T_{ref})]\}$

Where:

 A_E = slope of the linear region of an Arrhenius plot [$-10000\ K$] T = ambient temperature (K) ; $T_{ref} = 293K$

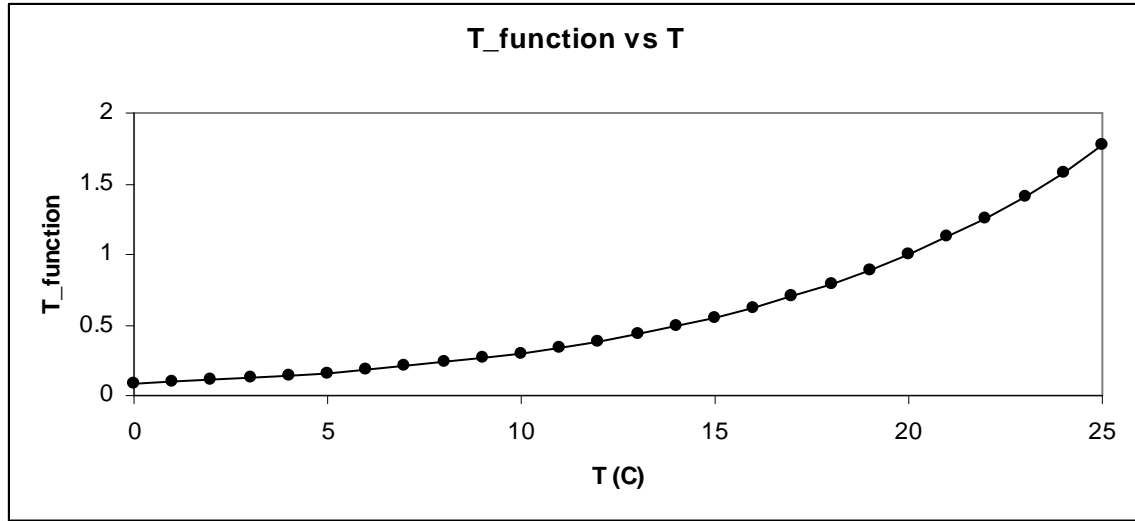


Fig.I.5 - The effect of temperature on metabolic rates

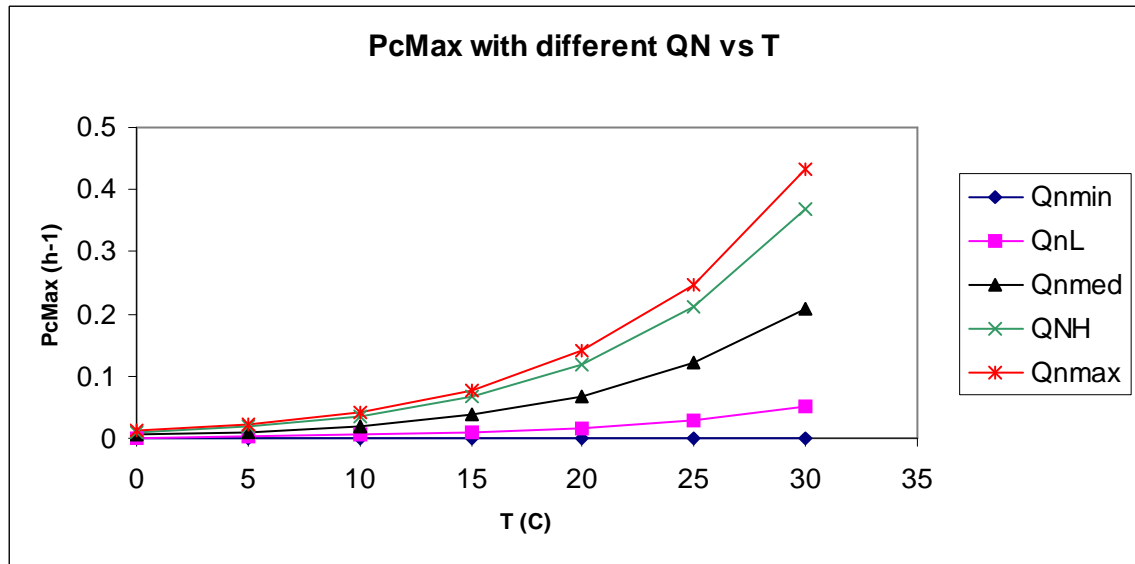


Fig.I.6 – The effect of internal N:C ratio and temperature on maximum photosynthetic rate.
 $Q_{nmin} = 0.034$, $Q_{nL} = 0.05$, $Q_{nmed} = 0.1$, $Q_{NH} = 0.15$, $Q_{nmax} = 0.17$

I.2.2.2 CHLOROPHYLL SYNTHESIS

ρ^{chl} = Chl *a* synthesis regulation index [$\mu\text{g Chl } a \text{ (mmol C)}^{-1}$]

θ^N = Chl *a*:N ratio [$\text{mg Chl } a \text{ (mmol N)}^{-1}$]:

Eq.I.11 $\theta^N = \text{Chl}_{pool} / N_{pool}$

Eq.I.12 IF ($E_0 > 0$)

$$\rho^{\text{Chl}} = \theta^{\text{N}}_{\text{max}} [P^{\text{C}}_{\text{phot}} / (3600 \alpha^{\text{Chl}} \theta^{\text{C}} E_0)]$$

Else

$$0$$

Where:

$\theta^{\text{N}}_{\text{max}}$ = maximum value for the (Chl *a*: N) ratio, θ^{N} [mg Chl *a* (mmol N)⁻¹]

$P^{\text{C}}_{\text{phot}}$ = carbon specific rate of photosynthesis (h^{-1})

α^{Chl} = initial slope of photosynthetic light curve [$\text{mmol C m}^2 (\mu\text{E mg Chl } a)^{-1}$]

θ^{C} =(Chl *a*:C) ratio within the cell [mg Chl *a* (mmol C)⁻¹]

E_0 = incident scalar irradiance in the PAR part of the spectrum [$\mu\text{E s}^{-1} \text{m}^{-2}$]

Considering that $1 \text{ W} = 4.6 \mu\text{E s}^{-1}$

And $E_0 (\mu\text{E s}^{-1} \text{m}^{-2}) = 4.6 \text{ Irradiance (Wm}^{-2}\text{)}$

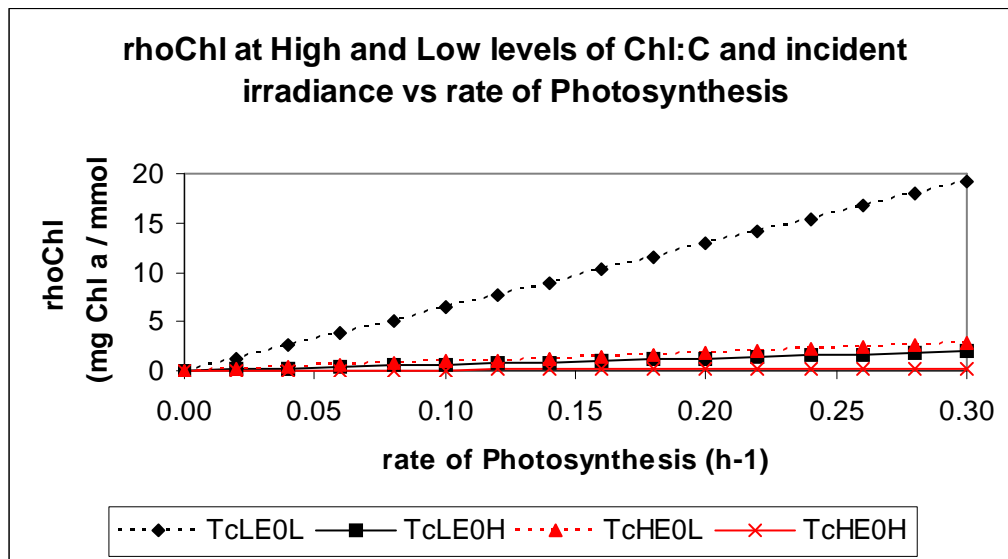


Fig.I.7 – Chlorophyll synthesis rate as a function of internal Chl:C ratio and irradiance
 $T_c = \text{Chl}_p : C_p$ $T_{cL} = 0.1$, $T_{cH} = 0.7$, $E_{0L} = 50 \text{ Wm}^{-2}$, $E_{0H} = 500 \text{ Wm}^{-2}$

I.2.2.3 NUTRIENTS UPTAKE

Specific rate of nutrient uptake is modelled using Droop dynamics (Droop, 1973), based on 3 experimentally verifiable postulates:

- uptake depends on the external substrate concentration
- growth depends on the internal substrate concentration

- in steady state system specific rate of uptake (in the absence of significant excretion) is necessarily the product of the specific growth rate and internal substrate concentration.

NITROGEN

Maximum rate of Nitrogen uptake, V_{max}^C (mmol N (mmolC h)⁻¹) :

Eq.I.13 IF ($Q_{N,min} \leq Q_N \leq Q_{N,max}$) $V_{max}^C = V_{ref}^C [(Q_{N,max} - Q_N)/(Q_{N,max} - Q_{N,min})]^n T_{function}$
 else if ($Q_N > Q_{N,max}$) $V_{max}^C = 0$
 else if ($Q_N < Q_{N,min}$) $V_{max}^C = V_{ref}^C T_{function}$

Where:

$Q_{N,min}$ = minimum nitrogen to carbon ratio [mmol N (mmol C)⁻¹]

$Q_{N,max}$ = maximum nitrogen to carbon ratio [mmol N (mmol C)⁻¹]

n = const. to define the rate of V_{max}^C decline with increasing Q_N (0.05)

$T_{function}$ = defines the effect of temperature on metabolic rates (dimensionless)

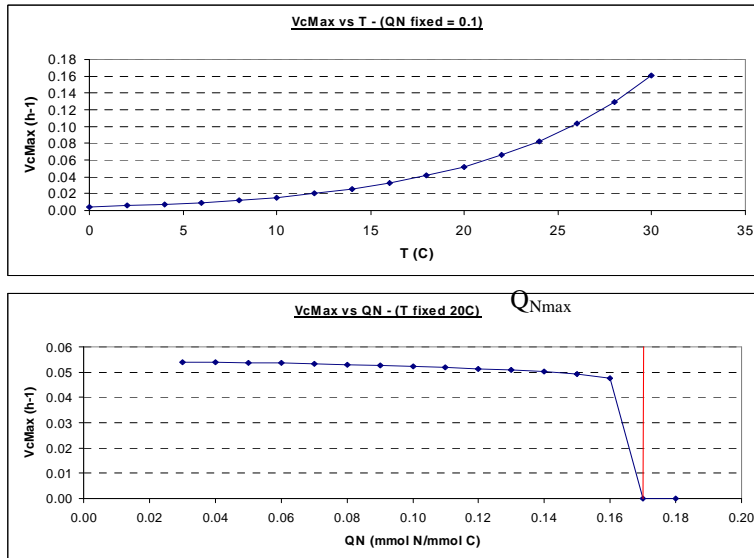


Fig.I.8 – Maximum rate of N uptake as a function of: a) temperature and b) N:C internal ratio

UPTAKE:

Eq.I.14 $V_N^C = V_{max}^C [N / (k_N + N)]$

SILICATE

Silicate uptake starts when C_{pool} has reached 90% of the C threshold for cell division (C_{Smin}).

$V_{silicate}^S$ dependent on Si:C ratio, Q_S

Brzezinski (1985) observed that Si:C ratios varied between 0.04-0.43, with the vast majority of species (27 in total) having ratios between 0.04-0.15.

Mean reported: 0.13 ± 0.04 (95% confidence).

Eq.I.15 If ($C_{pool} > C_{smin}$)

{ then if ($Q_S \leq Q_{Smin}$) $V_{max}^S = V_{ref}^S \cdot T_{function}$

else if ($Q_{Smin} < Q_S < Q_{Smax}$) $V_{max}^S = V_{ref}^S [(Q_{S,max} - Q_S) / (Q_{S,max} - Q_{S,min})]^n T_{function}$

else if ($Q_S \geq Q_{Smax}$) $V_{max}^S = 0$

}

Else $V_{max}^S = 0$

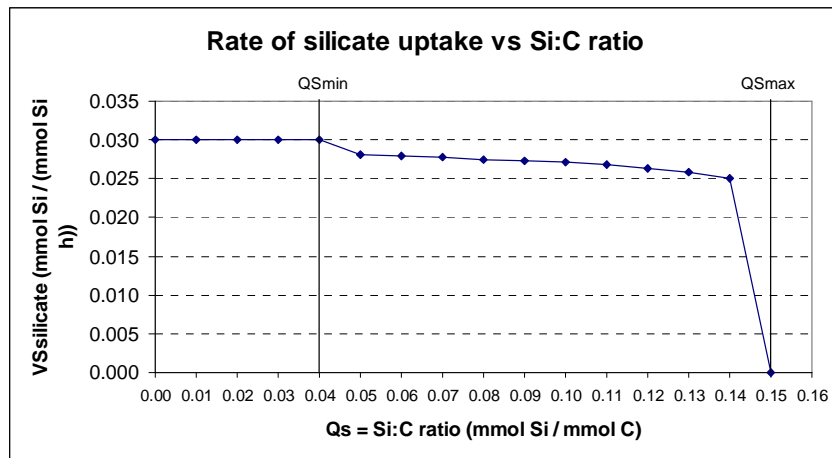


Fig.I.9 – Maximum rate of Si uptake as a function of Si:C internal ratio

$$\text{Eq.I.16} \quad V_{Si}^S = V_{max}^S [Si / (k_{Si} + Si)]$$

Where

k_S = half-saturation constant for silicate uptake (1 mmol Si)

Si = Silicate ambient concentration (mmol Si m^{-3})

 NUTRIENT UPTAKE CALLS (Specificity of chemical resolved)

$$\text{Eq.I.17} \quad \text{Nitrogen:} \quad \text{uptake} [(C_{\text{pool}} * V_N^C * T_s) \text{ from Nitrogen Conc}] \rightarrow N_{\text{ing}}$$

$$\text{Eq.I.18} \quad \text{Silicate:} \quad \text{uptake} [(Si_{\text{pool}} * V_{Si}^C * T_s) \text{ from SilicateConc}] \rightarrow Si_{\text{ing}}$$

N_{ing} and Si_{ing} return the amount of chemical uptaken during the previous timestep.

I.2.3 RESPIRATION

Geider 98 assumed that the maintenance metabolic rates $R_{\text{Cmaintenance}}$, describing C respiration; R_N describing remineralisation of N and R_{Chl} describing Chl degradation are equal:

$$\text{Eq.I.19} \quad [R_{\text{Cmaintenance}} = R_N = R_{\text{Chl}}] * T_{\text{function}}$$

R^C = Total C specific rate of respiration [h^{-1}]

$$\text{Eq.I.20} \quad R_C = [R_{\text{Cmaintenance}} * T_{\text{function}}] + R_{\text{growth}}^C$$

Where:

$R_{\text{Cmaintenance}}^C$ = Carbon specific rate of maintenance respiration

R_{growth}^C = Carbon specific rate of growth related respiration

$$\text{Eq.I.21} \quad R_{\text{growth}}^C = \zeta V_N^C$$

Where:

ζ = cost of biosynthesis [$\text{mmol C}(\text{mmol C})^{-1}$]

V_N^C = Carbon specific rate of DN uptake [$\text{mmol N}(\text{mmol C})^{-1} \text{h}^{-1}$]

I.2.4 CELL DIVISION

Silicon depletion in the water may limit diatom reproduction before nitrogen depletion.

$$\text{Eq.I.22} \quad \text{if } (C_p \geq C_{\text{rep}}) \text{ and } (S_p \geq S_{\text{rep}})$$

$$c_d = 2$$

else

$$c_d = 1$$

Where

c_d = flag for diatoms maturity [dimensionless]

C_{rep} = carbon content threshold for cell division (mmol C)

S_{rep} = silicon content threshold for cell division (mmol Si)

When $c_d = 2$, the number of cells in the subpopulation, c , are doubled.

Eq.I.23 If ($C_d = 2$) \rightarrow divide(2)

The daughters will have values for carbon, nitrogen, silicon and chlorophyll a which are half the value of their parents before division.

I.2.5 MORTALITY

Eq.I.24 If ($C_{pool} < C_{starve}$) \rightarrow Dead

Where

C_{starve} = carbon content threshold for energy starvation (mmol C)

I.2.6 REMINERALISATION

When Living:

Eq.I.25 Release $(A_{pool} + N_{pool}) * R_N * T_{function} * T_s$ to Ammonium_{conc}

When Dead:

Eq.I.26 $S_{remin} = S_{dissolution} * Q_{RemS} ^{(T - T_{Sref})/10}$

Eq.I.27 $N_{remin} = N_{dissolution} * Q_{RemN} ^{(T - T_{Nref})/10}$

I.3 PARAMETERS

Symbol	Name	Units	Value	Source
ζ	cost of biosynthesis	mmol C(mmol N) ⁻¹	2.3	Geider et al.,1997
v_s	sinking velocity	m h ⁻¹	0.04	Woods and Barkmann, 1993
$Q_{N,min}$	minimum nitrogen to carbon ratio	mmol N (mmol C) ⁻¹	0.034	Geider et al.,1998
$Q_{N,max}$	maximum nitrogen to carbon ratio	mmol N (mmol C) ⁻¹	0.17	Geider et al.,1998
A_E	slope of the linear region of Arrhenius plot	K	-10000	Geider et al.,1997
T_{ref}	Reference temperature	K	293	Geider et al.,1997
k_S	half-saturation constant for silicate uptake	mmol Si m ⁻³	1	Tett and Droop, 1988
$\theta^{N_{max}}$	Maximum Chl a:N ratio	mg Chl a(mmol N) ⁻¹	4.2	Geider et al.,1998
$Q_{S,min}$	minimum silicon:carbon quota	mmol Si (mmol C) ⁻¹	0.04	Brzezinski, 1985
$Q_{S,max}$	maximum silicon:carbon quota	mmol Si (mmol C) ⁻¹	0.15	Brzezinski, 1985
α^{Chl}	initial slope of photosynthetic light curve	mmol Cm ² (μE mg Chl a) ⁻¹	7.9×10 ⁻⁷	Geider et al.,1998
n	const. to define the rate of V_{max}^C decline with increasing Q_N	dimensionless	0.05	Partridge, pers. comm..
$R_{maintenance}^C$	Carbon specific rate of maintenance respiration	mmol C (mmol C) ⁻¹ h ⁻¹	2×10 ⁻³	Geider et al., 1996
R_N	Nitrogen specific rate of N remineralisation	mmol N (mmol N) ⁻¹ h ⁻¹	2×10 ⁻³	Geider et al., 1996 Geider et al., 1998
R_{Chl}	Chlorophyll specific rate of Chl degradation	mgChl (mg Chl) ⁻¹ h ⁻¹	2×10 ⁻³	Geider et al., 1996 Geider et al., 1998
K_{AR}	½ saturation constant for uptake of nitrate and ammonium	mmol N m ⁻³	1	Geider et al.,1998
P_{refC}	Maximum value of P_{photC} at temperature T_{ref}	mmol C(mmol C) ⁻¹ h ⁻¹	0.16	Geider et al.,1998
V_{refC}	Value of V_{maxC} at temperature T_{ref}	mmol N(mmol C) ⁻¹ h ⁻¹	0.026	Geider et al.,1998
V_{ref}^S	value of V_{max}^S at temperature T_{ref}	mmol Si(mmol Si) ⁻¹ h ⁻¹	0.03	Paasche, 1973
C_{rep}	carbon content threshold for cell division	mmol C	1.76×10 ⁻⁸	Strathmann, 1967
C_{starve}	carbon content threshold for starvation	mmol C	8.5×10 ⁻⁹	Assumed
S_{rep}	silicon content threshold for cell division	mmol Si	2.1×10 ⁻⁹	Derived from C_{rep} and Brzezinski, 1985 (Table 3)
C_{minS}	Minimum C content for Silicate uptake	mmol c	1.58×10 ⁻⁸	Assumed as 90% of C_{rep} , Brzezinski, 1985
$Si_{dissolution}$	Si specific dissolution rate of biogenic Si	mmol Si (mmolSi h) ⁻¹	8.3×10 ⁻⁴	Hurd and Birdwhistell, 1983
Q_{RemS}	factor by which Si dissolution increases with T (K)	wd	2.27	Kamatani, 1982
T_{SRef}	Reference T for Silicate dissolution	K	278	Hurd and Birdwhistell, 1983
$N_{dissolution}$	N specific dissolution rate of N	mmolN (mmolN h) ⁻¹	0.0042	Heath et al, 1997
Q_{RemN}	factor by which N dissolution increases with T (K)	wd	2.95	Heath et al, 1997
T_{NRef}	Reference T for Silicate remineralisation	K	283	Heath et al, 1997

Tab.I.1 – Diatom parameters

 ζ , Cost of biosynthesis (mmol C (mmol N)⁻¹)

The value of ζ in tab.3 (Geider et al, 1998, hereafter G98) is 2 gC gN⁻¹.

Conversion:

Molar mass of N = 14 gN /molN

Molar mass of C = 12 gC /mol C

Then is 2 gC gN⁻¹ = 2.3 mmol C mmolN⁻¹

 V_s , sinking rate (mh⁻¹)

Uses the WB value for constant sinking of diatoms (1 md⁻¹ → ~ 0.04 mh⁻¹)

 Q_{Nmin} and Q_{Nmax} , Min and max internal ratio between N and C (mmol N (mmol C)⁻¹)

The value of Q_{Nmin} and Q_{Nmax} in tab.3 (G98) for diatom species (*S. costatum* and *T. pseudonana*) were 0.04 and 0.2 gN (gC)⁻¹ respectively.

Molar mass of N = 14 gN/molN

Molar mass of C = 12 gC/mol C

Using the conversion above:

$$Q_{Nmin} = 0.04 \text{ gN (gC)}^{-1} * (12/14) \text{ mmolN/gN (mmolC/gC)}^{-1} = 0.034 \text{ mmolN (mmolC)}^{-1}$$

Similarly

$$Q_{Nmax} = 0.17 \text{ mmolN (mmolC)}^{-1}$$

 A_E , the initial slope of the linear region of the Arrhenius plot (K)

Geider *et al.*, 1997 (hereafter G97) used a value of -10⁴ K.

T_{ref} Reference temperature (K)

This parameter is not listed in G98. reported, after a personal communication with Geider, that T_{ref} = 293K.

K_s, half-saturation constant for silicate uptake (mmolSi m⁻³)

Value used in model by Tett and Droop (1998) pag 205 tab. 4, K_v = 1mmolN m⁻³

The same value is also used for K_{AR} (half-saturation constant for nitrate and ammonia uptake).

K_{AR}, half-saturation constant for uptake of nitrate and ammonium (mmolN m⁻³)

Value used in model by Tett and Droop (1998) pag 205 tab.4, K_v = 1mmolN m⁻³

Same value used by G98. Tab.3 K_{nit} = 1 mmolN m⁻³
(1 M = 1 mol l⁻¹ so 1 μM = 1 mmol m⁻³).

θ^N_{max}, Maximum Chl a:N ratio mg Chl a(mmol N)⁻¹

G98 Tab.3 give a value of 0.3 g Chl a (gN)⁻¹ for *S. costatum*.

Converting to mg Chl a (mmol N)⁻¹, using

Molar mass of N = 14 gN/molN → 14 E-3 gN / mmol N

then

$$0.3 [\text{g Chl a (gN)}^{-1}] * 14\text{E-3 gN (mmol N)}^{-1} * 1000 = 4.2 \text{ mg Chl a (mmolN)}^{-1}$$

Q_{Smin} and Q_{Smax} , Min and Max Silica to Carbon ratio $\text{mmol Si (mmolC)}^{-1}$

Brzezinski (1985) observed that Si:C ratio varied between 0.04 and 0.43, with the vast majority of diatom species having ratios between 0.04 and 0.15.

I decided to keep 0.04 mmolSi / mmolC as Q_{Smin} and 0.15 mmolSi / mmolC as Q_{Smax} .

 α^{Chl} , initial slope of photosynthetic light curve $\text{mmol Cm}^2 (\mu\text{E mg Chl a})^{-1}$

The averaged value of α^{Chl} for diatoms in Tab 2 of G97 = $0.95\text{E-}5 \text{ gC m}^2 (\text{gChl } \mu\text{mol photons})^{-1}$

1 mol of photons = 1 Einstein (E)

To convert into $\text{mmol Cm}^2 (\mu\text{E mg Chl a})^{-1}$

$$0.95 \text{ E-}5 \text{ gC m}^2 (\text{gChl } \mu\text{mol photons})^{-1} = 0.95\text{E-}8 \text{ gC m}^2 (\text{mgChl } \mu\text{E})^{-1}$$

$$= 0.95 \text{ E-}8 \text{ gC m}^2 (\text{mg Chl } \mu\text{E})^{-1} / [12\text{E-}3 \text{ gC mmolC}^{-1}] = 7.9 \text{ E-}7 \text{ Cm}^2 (\mu\text{E mg Chl a})^{-1}$$

 n const. to define the rate of V_{max}^C decline with increasing Q_N dimensionless

Value of n not present in Geider's articles. The value used 0.05 (w.d.) was derived from personal communication between Partridge and Geider.

 $R_{maintenance}^C$ Carbon specific rate of maintenance respiration $\text{mmol C (mmol C)}^{-1} \text{ h}^{-1}$

In G98 maintenance respiration rate for diatoms is 0 (tab.3).

Geider et al. 96: For diatoms, which typically have high light saturated growth rates, the respiration term in the model becomes significant only at extremely low irradiances.

Thus, the value of $R_{\text{maintenance}}^C$ is not critical.

They assumed a value of $0.05 \text{ mmolC (mmol C d)}^{-1} \rightarrow 2\text{E-3 h}^{-1}$

This value will be used also for the remineralisation of N and the degradation of Chl, which in Geider 98 are assumed to be equal and function of T.

So, $R_c = R_n = R_{chl} = 2\text{E-3} * T_{\text{function}}$ (effect of temperature on metabolic rates... see below in equations section).

K_{AR} , $1/2$ saturation constant for uptake of nitrate and ammonium, mmol N m^{-3}

G98 uses a value for $K_{\text{nit}} = 1 \mu\text{M} = 1 \text{ mmolN m}^{-3}$

**P_{ref}^C , Maximum carbon-specific rate of photosynthesis at temperature T_{ref}
 $\text{mmol C (mmol C)}^{-1} \text{ h}^{-1}$**

G98 : Maximum rate of carbon-specific rate of photosynthesis for diatoms varied between 3-5.1 gC (gC d)^{-1} experiments conducted at 293K. Average of 4 gC (gC d)^{-1}

$T_{\text{ref}} = 293\text{K}$ therefore we can neglect the effect of temperature function (eq.10 in G98).

Assuming Q_n (ratio between N content / C content , mmolN mmolC^{-1}) = 0.15

Then from eq 5

$$P_{\text{max}}^C = P_{\text{ref}}^C (\text{mmolC (mmolC h}^{-1}\text{)}) \left(\frac{0.15 - 0.034}{0.17 - 0.034} \right) = 0.85 P_{\text{ref}}^C / 24 (\text{h d}^{-1})$$

So $P_{\text{ref}}^C (\text{mmolC (mmolC h}^{-1}\text{)}) = 4 \text{ gC (gC d)}^{-1} * 0.85 / 24 (\text{h d}^{-1}) = 0.14 \text{ mmol C (mmol C h)}^{-1}$

V_{ref}^C , Value of V_{max}^C at temperature T_{ref} , $\text{mmol N (mmol C)}^{-1} \text{ h}^{-1}$

In table 3 G98 V_{\max}^C varied between 0.6 and 1 gN (gC d)⁻¹ average = 0.8 gN (gC d)⁻¹

As for P_{ref}^C , $T = T_{\text{ref}}$ so T effect can be neglected and $Q_N = 0.15 \text{ mmolN mmolC}^{-1}$

So from eq. 7

$$V_{\max}^C = V_{\text{ref}}^C [(0.17 - 0.15) / (0.17 - 0.034)]^n \text{ where } n = 0.05$$

$$V_{\max}^C = V_{\text{ref}}^C * 0.9$$

$$V_{\text{ref}}^C (\text{mmol N (mmolC h)}^{-1}) = [0.8 (\text{gN gC}^{-1} \text{d}^{-1}) * 12\text{E-3 gC (mmolC)}^{-1} * 0.9] / [14\text{E-3 gN (mmolN)}^{-1} * 24 \text{ h d}^{-1}] = 0.026 \text{ mmolN (mmolC h)}^{-1}$$

V_{ref}^S , value of V_{\max}^S at temperature T_{ref} , $\text{mmol Si (mmol Si)}^{-1} \text{ h}^{-1}$

This was calculated from lab experiments from Paasche 1973 averaging the maximum uptake rates of 5 diatom species (table1):

	Spp1	Spp2	Spp3	Spp4	Spp5
V_{\max}	0.095	0.073	2.15	26.6	4.09
Si_{cont}	5.4	1.81	145	240	550
V_{\max}^S	= 0.018	= 0.04	= 0.015	= 0.017	0.048

Tab.II.2 – Diatom maximum silicate uptake rate

Where

$V_{\max} \text{ pgSi (cell h)}^{-1}$ = Silicate maximum uptake rate

$\text{Si}_{\text{cont}} \text{ pgSi cell}^{-1}$ = Average Si content of cells

$V_{\max}^S \text{ h}^{-1}$ = Max Si-specific uptake rate = $V_{\max} / \text{Si}_{\text{cont}}$

So averaging the V_{\max}^S for the 5 diatom spp $V_{\max}^S = 0.03 \text{ h}^{-1}$

As all cultures were grown at $20^\circ\text{C} = 293\text{K} = T_{\text{ref}}$, then we can neglect the temperature effect and $V_{\text{ref}}^S = 0.03 \text{ mmol Si (mmolSi h)}^{-1}$.

C_{rep} , carbon content threshold for cell division, mmolC

Strathmann 1967 relates diatom volume, V (μm^3) to its C content, C (pgC) using:

$$\text{Log } C = -0.422 + 0.758 \log (V)$$

Assuming an ESD (equivalent spherical diameter) of $20 \mu\text{m}$, then $\text{Vol} (\mu\text{m}^3) = 4/3 \pi 10^3 = 4200 \mu\text{m}^3$

Then $\text{Log } C = 2.32 \rightarrow C = 210 \text{ pgC} \rightarrow 1.75 \text{ E-}8 \text{ mmolC}$

 C_{starve} , carbon content threshold for starvation, mmolC

Nutrients starvation was observed to be more severe than light starvation in diatoms (Berges and Falkowski, 1998). It was reported experimentally that, after 18 days of nutrients starvation at 18°C , F_v/F_m , a measure of fluorescence emissions, which provides an index of photosynthetic capability, dropped to ~ 0 . Field observations on phytoplankton from $40^\circ\text{N } 23^\circ\text{W}$ showed that once degradation of the photopigments, in particular chlorophyll, is initiated, it introduces the final stage of lysis, when cells disintegrate completely in less than a day (Veldhuis *et al.*, 2001).

I will assume that after a period of 18 days at 18°C of only maintenance respiration the diatom would have reached the threshold for lysis.

The value is $C_{starve} = 8.5 \times 10^{-9} \text{ mmol C}$.

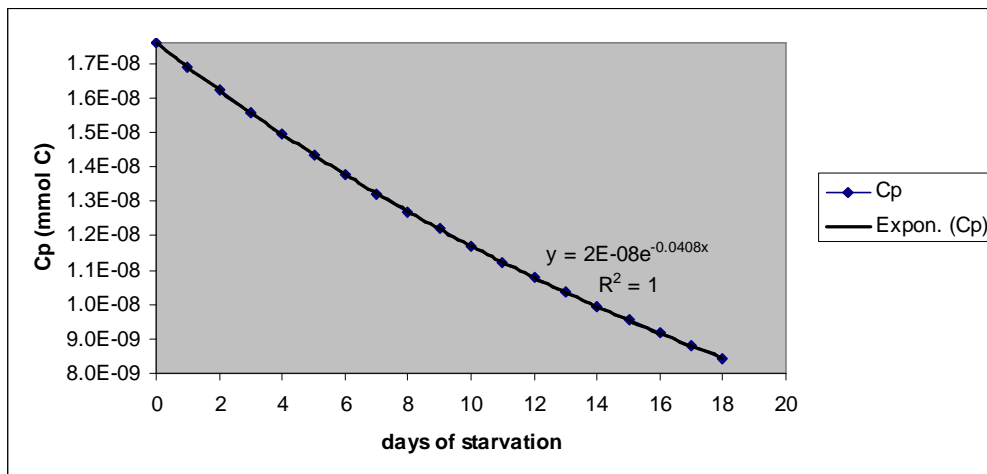


Fig.I.10 – Diatom carbon pool during starvation

S_{rep}, silicon content threshold for cell division, mmolSi

Estimated from C_{rep} and using an average Si:C ratio (0.12) of diatoms (tab 3 Brzezinski, 1985), then

$$S_{\text{rep}} = C_{\text{rep}} * 0.12 = 2.1 \text{ mmolSi}$$

C_{minS}, Minimum C content for Silicate uptake, mmol C

As diatoms rapidly uptake silicate when close to cell division (Brzezinski, 1985), It was assumed that the minimum C threshold for Si uptake would be 90% of C_{rep} = 1.6 E-8 mmolC.

“Testing theories on fisheries recruitment.”

APPENDIX II

COPEPOD MODEL

APPENDIX II – COPEPOD MODEL

The zooplankton species is based on *Calanus finmarchicus*. LERM assumes that all copepods are female. The phenotypic equations for behaviour and physiology were derived mainly from Carlotti and Wolf (1998). Each copepod features a pool for each of the chemicals present in diatoms. However copepods have no equations for handling silica and chlorophyll as they play no part in its physiology. Copepods reach the mature stage, after a fixed number of successive development stages (staged growth). Moulting from one stage to the next is triggered by size (i.e. protein pool).

The copepod physiological state is determined by ten biological state variables: carbon pool – including proteins (nitrogenous carbon, C_N), lipids (non-nitrogenous carbon, C_{NN}) and carapace (made of chitin, C_{shell}), nitrogen pool, gut content, gut fullness, gut volume, stage and age.

II.1 STATE VARIABLES

II.1.1 POOLS

Eq.II.1

$$C_N = C_N + ((1 - \text{gamma}) \times (1 - \text{alpha}) \times \text{Growth}_{\text{net}} \times \text{TimeStep})$$

Eq.II.2

$$C_{NN} = C_{NN} + (\text{If } \text{Growth}_{\text{net}} > 0 \text{ (gamma} \times (1 - \text{alpha}) \times \text{Growth}_{\text{net}} \times$$

TimeStep) Eq.II.3

$$C_{\text{shell}} = C_{\text{shell}} + ((\text{If } \text{Growth}_{\text{net}} > 0) \text{ then } (\text{Growth}_{\text{net}} \times \text{alpha} \times \text{TimeStep}) \text{ else } 0))$$

Eq.II.4

$$C_{\text{pool}} = C_N + C_{NN} + C_{\text{shell}}$$

Eq.II.5

$$C_{\text{pmax}} = \text{IF } (C_N > C_{\text{pmax}}) C_N \text{ else } C_{\text{pmax}}$$

Eq.II.6

$$N_{\text{pool}} = N_{\text{pool}} + N_{\text{ingested}} - (N_{\text{PelletLoss}} + N_{\text{Prot_excess}} + C_{\text{prot}})$$

Where:

C_N = Protein pool (nitrogenous carbon) (mmol C)

C_{NN} = Lipid pool (non-nitrogenous carbon) (mmol C)

C_{shell} = Carbon in shell (mmol C)

C_{pool} = Total C weight [(mmol C)

C_{pmax} = Maximum obtained protein pool (mmol C)

N_{pool} = Nitrogen pool (mmol N)

alpha = fraction of assimilated C allocated to carapace building (*wd*)

gamma = fraction of assimilated C allocated to fat storage (*wd*)

$N_{ingested}$ = Nitrogen ingested in current timestep (mmol N)

$N_{PelletLoss}$ = Nitrogen lost in faecal pellet (mmol N)

$N_{protExcess}$ = Excreted Nitrogen above Q_N (mmol N)

C_{prot} = Nitrogen excreted due to protein catabolism (mmol N)

II.1.2 STOICHIOMETRY

Assimilated carbon is dynamically allocated to lipids, proteins and carapace in different ratios depending on the life stage. The amount of ingested carbon allocated to lipid reserve per timestep depends on the development state they are in. The ratio of N:C for proteins is assumed to be constant¹. The total amount N is regulated by a minimum and maximum ratio of nitrogen:carbon, Q_N ²:

$$\text{Eq.II.7} \quad Q_N = N_{pool} / C_{pool}$$

a)	Units	Min	Max	Functions	Reference
C	mmol C	10^{-5}	Not fixed	State variable	Carlotti and Wolf, 1998
Protein	mmol C	4.75×10^{-6}	8.33×10^{-3}	State variable	Carlotti and Wolf, 1998
Lipid	mmol C	4.75×10^{-6}	Not fixed	State variable	Carlotti and Wolf, 1998
Shell	mmol C	5×10^{-7}	4.2×10^{-4}	State variable	Carlotti and Wolf, 1998
N	mmol N	1.2×10^{-6}	23% of C	State variable	Huntley and Nordhausen, 1995
b)					
N:C	mmol N : mmol C	0.12	0.23	Excretion	Huntley and Nordhausen, 1995

Tab. II.1 - Stage independent a) stoichiometry and b) cellular ratios of chemicals

¹ 0.27 mmolN:mmolC, according to Anderson *et al.*, 2005

² 0.12-0.23 mmolN:mmolC according to Huntley and Nordhausen, 1995

II.1.3 STAGES

Moulting

LERM-PS uses the Carlotti and Wolf (1998) model for copepod staged growth. An individual copepod can only be in one particular development stage at any time. As it grows and its protein pool reaches a threshold value, it moults and passes into the next stage.

Stage symbol	Stage name	Min C _N (mmol C)	Prosome length (mm)	Frontal Surface Area (mm ²)	Volume (mm ³)
N3	Nauplius III	1.00E-05	0.27	1.46E-04	1.00E-03
N4	Nauplius IV	1.70E-05	0.32	1.70E-04	1.64E-03
N5	Nauplius V	2.50E-05	0.36	1.94E-04	2.50E-03
N6	Nauplius VI	3.75E-05	0.41	2.22E-04	3.79E-03
C1	Copepodite I	6.25E-05	0.48	2.62E-04	6.42E-03
C2	Copepodite II	9.20E-05	0.55	2.97E-04	9.53E-03
C3	Copepodite III	2.10E-04	0.72	3.88E-04	2.22E-02
POW4	Pre-overwintering CIV	5.83E-04	1.00	5.42E-04	6.42E-02
POW5	Pre-overwintering CV	1.25E-03	1.29	6.95E-04	1.41E-01
OWD4	Overwintering descent CIV	5.83E-04	1.00	5.42E-04	6.42E-02
OWD5	Overwintering descent CV	1.25E-03	1.29	6.95E-04	1.41E-01
OW4	Overwintering CIV	5.83E-04	1.00	5.42E-04	6.42E-02
OW5	Overwintering CV	1.25E-03	1.29	6.95E-04	1.41E-01
OWA4	Overwintering ascent CIV	5.83E-04	1.00	5.42E-04	6.42E-02
OWA5	Overwintering ascent CV	1.25E-03	1.29	6.95E-04	1.41E-01
C4	Copepodite IV	5.83E-04	1.00	5.42E-04	6.42E-02
C4OW	Copepodite IV after OW	5.83E-04	1.00	5.42E-04	6.42E-02
C5	Copepodite V	1.25E-03	1.29	6.95E-04	1.41E-01
C6	Copepodite VI	3.33E-03	1.77	9.56E-04	3.87E-01
Adult	Adult	7.50E-03	2.31	1.25E-03	8.92E-01
Mature	Mature	8.33E-03	2.39	1.29E-03	1.0
Senescent	Senescent	8.33E-03	2.39	1.29E-03	1.0

Tab. II.2 - Copepod stages

II.1.4 COPEPOD SIZE

Prosome length, L (μm)

$$\text{Eq.II.8} \quad L = 10^{((\log_{10}(C_{\text{pmax}} \times C_{\text{conv1}}) + 8.37) / 3.07)} \quad (\text{Uye, 1982})$$

Copepod volume (m³)

Mauchline (1998) converted prosome length (μm) to body volume (mm³) using the following regression equation (r = 0.972):

$$\text{Log Body}_{\text{vol}} (\text{mm}^3) = 3.164 \log L(\mu\text{m}) - 10.690$$

This was rearranged to estimate Body_{vol} (m³) as:

$$\text{Eq.II.9} \quad \text{Body}_{\text{vol}} (\text{m}^3) = 10^{(3.164 \text{LOG}(L) - 10.69)} * 1 \times 10^{-9}$$

Surface area (cm²)

Using Vlymen's (1970) relationship between metasome length (~1/2 prosome length) and surface frontal area.

An adult copepod (2400 μm prosome length) has a metasome length of ~ 1.2 mm and, according to Vlymen's relationship, a surface frontal area of ~ 1.4 × 10⁻³ cm².

Assuming a linear relationship between length and surface area, then the conversion coefficient = 1.3 × 10⁻³ cm² / 2400 μm = ~ 5.4 × 10⁻⁷ cm² μm⁻¹

$$\text{Eq.II.10} \quad S = 5.4 \times 10^{-7} \text{ cm}^2 \mu\text{m}^{-1} * L (\mu\text{m})$$

II.2 EQUATIONS**II.2.1 ENERGETICS**

$$\text{Eq.II.11} \quad \text{Growth}_{\text{net}} = \text{growth} - \text{respiration}$$

Where

Growth_{net} = net growth rate (mmol C h⁻¹)

growth = assimilated carbon (mmol C h⁻¹)

respiration = respiration rate (mmol C h⁻¹)

When growth is negative lipids in the storage will be consumed preferentially.

II.2.2 RESPIRATION

The metabolic rate of an animal is defined with respect to its activities:

- Basal (or standard) metabolism is the oxygen (or carbon) consumption rate for maintaining bodily functions only
- Specific Dynamic action (SDA) is the catabolic cost associated with digestive processes (assimilation and gut clearance) and biomass formation. Strictly speaking is the catabolic cost of growth.
- Active metabolism is the oxygen consumption rate with activity at its maximal level (Ikeda, 1985)

$$\text{Eq.II.12} \quad \text{Respiration} = R_{\text{basal}} + R_{\text{sda}} + R_{\text{swim}}$$

Where

Respiration = total respiration rate (mmol C h⁻¹)

R_{basal} = basal respiration (mmol C h⁻¹)

R_{sda} = SDA (mmol C h⁻¹)

R_{swim} = Respiration due to swimming activity at velocity U (mmol C h⁻¹)

If overwintering: Fiksen and Carlotti (1996) assume that during over-wintering respiration is sustained exclusively by lipids catabolism. Respiratory losses are taken from C_{NN} . If C_{NN} empty, from C_N .

$$\text{Eq.II.13} \quad R_{ow} = R_{bas} \delta \quad \text{Fiksen and Carlotti (1996)}$$

Where:

R_{ow} = overwintering respiration rate (mmol C h^{-1})

δ = reduction of basic metabolism in a hibernating copepod (0.2)

When overwintering, the total respiration rate is:

$$\text{Eq.II.14} \quad \text{Respiration} = R_{ow}$$

Basal metabolism (mmol C h^{-1}) Carlotti and Wolf 1998

$$\text{Eq.II.15} \quad R_{bas} = r_{bas} (C_N)^{0.8} (QR_{10})^{(T - T_{ref})/10}$$

Where:

r_{bas} = basal metabolic coeff. Carlotti and Wolf (1998)

QR_{10} = Q_{10} basal metabolism (3.4)

T = ambient temperature ($^{\circ}\text{C}$)

T_{ref} = reference temperature (10°C)

Specific dynamic action

Associated with digestion and synthesis of new tissue.

The increased metabolism associated with SDA is largely related to biosynthesis and transport, while the energy cost of feeding, gut activity, amino-acids oxidation and urea excretion were minor contributors to the total SDA (Kiørboe *et al.*, 1985).

Kiørboe *et al.* (1985) found SDA to be proportional to the assimilation rate of organic matter:

$$\text{Eq.II.16} \quad R_{sda} = r_{sda} A_c$$

Where:

r_{sda} = SDA coefficient (0.17)

A_c = rate of C assimilation (mmol C h^{-1})

Catabolic cost of swimming (Caparroy and Carlotti,1996)

Catabolic cost of swimming activity at velocity U, $Z_{sw}(U)$ ($J s^{-1}$)

$$\text{Eq.II.17} \quad Z_{sw}(U) = \frac{P_{sw}(U)}{E_{mech} E_m}$$

Where:

U = swimming velocity ($cm s^{-1}$) $\rightarrow V_m$

E_{mech} = mechanical efficiency of swimming copepod (0.3)

E_m = muscular (metabolic) efficiency of copepod (0.25)

Power expenditure of swimming copepod at velocity U, $P_{sw}(U)$ ($J s^{-1}$)

$$\text{Eq.II.18} \quad P_{sw}(U) = \frac{k}{2} \rho^{(1-n)} L^{-n} U^{3-n} \mu^n S$$

Need to divide by $1000 \cdot 100 \cdot 100 = 10^7$ to match dimensions:

$$kg m^2 s^{-2} \cdot s^{-1} = g^{1-n} cm^{3n-3} \cdot cm^{-n} \cdot cm^{3-n} s^{n-3} \cdot g^n cm^{-n} s^{-n} \cdot cm^2$$

$$kg m^2 s^{-3} = g cm^2 s^{-3}$$

Where:

k = coefficient of empirical relationship between drag coefficient and Reynolds number (85.2)

ρ = seawater density ($1.024 g cm^{-3}$)

n = coefficient of empirical relationship between drag coefficient and Reynolds number (0.8)

L = prosome length (μm)

Body_{vol} = Body volume (m^3)

μ = seawater dynamic viscosity ($119 \times 10^{-4} g cm^{-1} s^{-1}$)

S = projected area of swimming copepod (cm^2)

Convert to oxygen consumption, with C_{cal} = oxycaloric coefficient ($20.3 kJ l O_2^{-1}$)

$$\text{Eq.II.19} \quad (3600 \times) O_{cons} (ml O_2 s^{-1}) = [Z_{sw}(U) \times 10^{-3} (kJ s^{-1}) / (C_{cal} / 1000) (kJ / l O_2)]$$

To convert respiration in O_2 to C use the conversion factor 0.536RQ (Parsons *et al.*,1984) where the respiratory quotient(RQ) varies depending on the metabolic substrate: 0.7 for lipids, 1.0 for carbohydrates and 0.84 for urea and 0.97 for ammonia (proteins).

Eq.II.20 (Ikeda *et al.*,2000)

$$O_{\text{cons}} [\text{ml O}_2 (\text{cell h})^{-1}] \times \text{RQ} \times 12/22.4 = \text{mg C} (\text{cell h})^{-1}$$

In this equation RQ is not considered as the substrate used in respiration is considered in the calculation of total respiration.

12/22.4 = is the weight (12g) of C in 1 mole of (22.4 l) of CO₂.

So depending on the substrate being respired C consumption will vary accordingly. Lipids are used preferentially (RQ = 0.7). The substrate used and therefore the rate of respiration varies as function of the state of the particle (i.e. starved individuals using carbohydrates for respiration, RQ shift from 0.7 to 1).

$$\text{Eq.II.21} \quad R_{\text{sw}} (\text{mg C} / \text{h}) = (O_{\text{cons}} \times 3600) \times (0.7) \times 0.536$$

II.2.3 CARBON ALLOCATION

The amount of lipids stored in the fat sac is function of the structural body mass. During copepodite stages (Structural weight 8.33×10^{-3} mmol C) assimilated matter can be allocated to storage (lipids) or growth (proteins). When a copepod reaches the threshold for reproduction, its structural mass does not change and the assimilated matter is allocated storage (Fiksen and Carlotti, 1996).

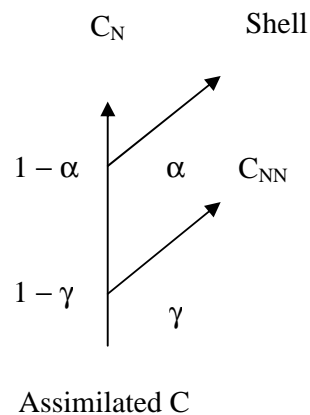


Fig. II.1 Dynamical allocation of assimilated C (Fiksen and Carlotti, 1996)

For stages N3 to C3 gamma = 0.5

For pre-overwintering stages gamma = 1

For all other stages gamma = 0.7

α = fraction of assimilated C allocated to carapace building (0.05)

II.2.4 INGESTION

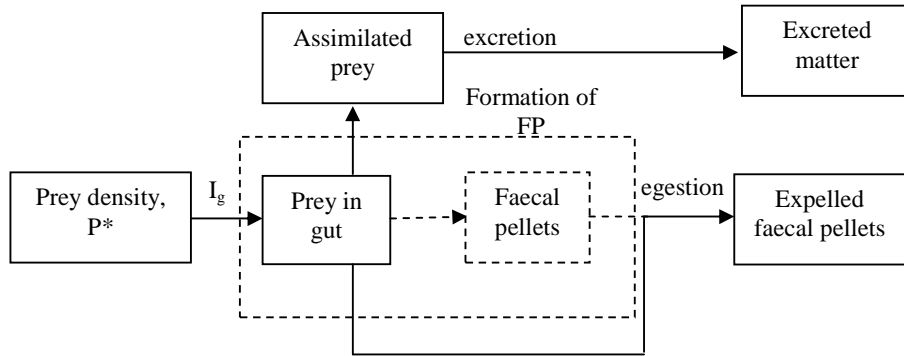


Fig.II.2 – Copepod ingestion, digestion, excretion and faecal pellets formation adapted from Caparroy and Carlotti, 1996

Maximum ingestion rate, I_{gmax} (cells s^{-1}):

Eq.II.22
$$I_{max} = ((0.67 * V_{gut}) - Gut_{content}) / V_{prey} * 1800$$

Where:

I_{max} = maximum ingestion rate (cells s^{-1})

0.67 : when the anterior 2/3 of the midgut are full, copepod stops feeding (Caparroy and Carlotti, 1996)

V_{gut} = midgut volume (cm^3)

$Gut_{content}$ = Volume of food in gut (cm^{-3})

V_{prey} = volume of a single prey cell ($cm^3 prey^{-1}$)

Ingestion rate, I_g (cells h^{-1}): Caparroy and Carlotti (1996)

Eq.II.23

IF ($I_g > I_{gmax}$)

$$I_g = I_{gmax}$$

ELSE

$I_g =$

IF ($P > P_{min}$)

$$\pi * r^2 * v * P * 10^{-6} * (1 - (Gut_{content} / 0.67 V_{gut})^2) * (1 - e^{-(1.7 \times 10^{-8} * P)})$$

else 0

Where:

I_g = stage specific ingestion rate ($\text{mm}^3 \text{s}^{-1}$)

Filtration = $\pi * r^2 * v$

Assume $v = 1 \text{ cm s}^{-1}$

For *A.tonsa* (820 μm) $r = 0.025 \text{ cm}$ assume double for *C.finmarchicus* (2400 μm)

$r / 2400 = 0.025 / 820$

Eq.II.24 $r = (0.07/2400) * PL = 2.9 \times 10^{-5} (\text{cm } \mu\text{m}^{-1}) * PL (\mu\text{m})$

So $r = 0.07 \text{ cm}$ for an adult copepod and $F = 0.015 \text{ cm}^3 \text{ s}^{-1}$

Assume linear relationship between r and PL .

Where:

F = Filtration rate ($3600 \times 10^{-9} \text{ m}^3 \text{ h}^{-1}$)

P^* = phytoplankton concentration available for grazing (cells m^{-3})

$P^* = P - P_{\min}$

P = phytoplankton concentration in current layer (cells m^{-3})

P_{\min} = minimum phytoplankton conc for grazing to occur ($10^5 \text{ cells m}^{-3}$)

z_1 and z_2 = initial and final depth of zooplankton particle within the current timestep

$|z_2 - z_1| = \text{timestep} |V_m|$

V_m = vertical migration rate (m h^{-1}) see below.

II.2.5 PELLETT VOLUME, PV (cm^3)

A pellet is expelled when the volume of non-assimilated prey reaches a threshold of pellet volume, PV_{egest} (cm^3) (Caparroy and Carlotti, 1996).

The volume of a pellet, PV (μm^3) is expressed as a function of prosome length using Uye and Kaname, 1994:

$\log PV ((\mu\text{m}^3)) = 2.474 \log PL (\text{mm}) + 5.226$

Eq.II.25 $PV (\text{cm}^3) = [10^{(2.474 \log (PL \times 10^{-3}) + 5.226)}] \times 10^{-12}$

PL is multiplied by 10^{-3} to pass from μm to mm

PV is multiplied by 10^{-12} to convert from μm^3 to cm^3

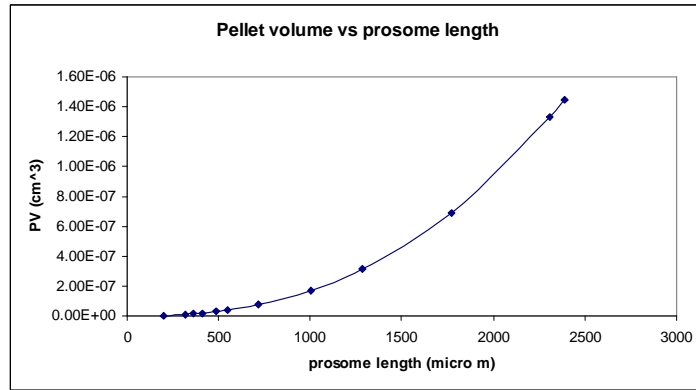


Fig.II.3 – Pellet volume as function of copepod prosome length

II.2.6 PELLETS SINKING RATE, SR (m h⁻¹)

Using the equation of Paffenhofers and Kwnoles (1979) obtained from Stoke’s law:

$$\text{Log SR (m d}^{-1}\text{)} = 0.698 \text{ log PV (}\mu\text{m}^3\text{)} - 2.030$$

Eq.II.26 $\text{SR (m h}^{-1}\text{)} = 10 ^ [0.698 \text{ log (PV} \times 10^{12}\text{)} - 2.030] / 24$

PV is multiplied by 10¹² to convert from cm³ to μm³

And SR divided by 24 to pass from m d⁻¹ to m h⁻¹.

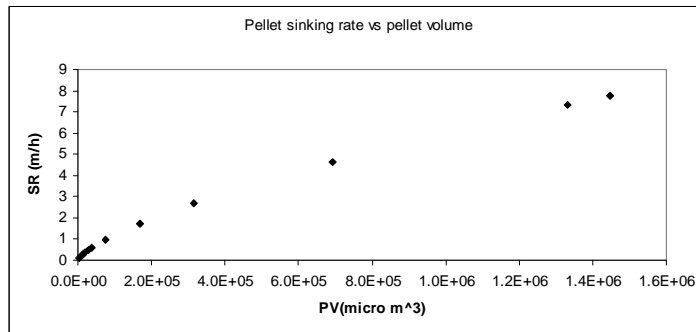


Fig.II.4 – Pellet sinking speed as function of its volume

II.2.7 CORPSES SINKING RATE

Gross and Raymont (1942) reported sinking rates up to 2.4mm s⁻¹ for female *Calanus finmarchicus*.

This is ~ 100m/h. I will assume a linear relationship surface area and sinking rate.

II.2.8 COPEPOD GUT VOLUME, V_{gut} (cm^3)

Max ingestion rates for adult female *Calanus pacificus* feeding on 4 size classes of diatoms are shown in tab.II.3 (Frost 1972).

	Diameter (μm)	Max ingested cells
<i>Thalassiosira fluviatilis</i>	11	12,000
<i>Coscinodiscus angatii</i>	35	1,200
<i>Coscinodiscus eccentricus</i>	75	600
<i>Centric spp.</i>	87	300

Tab.II.3 - *Calanus pacificus* maximum ingestion rate as function of diatom size

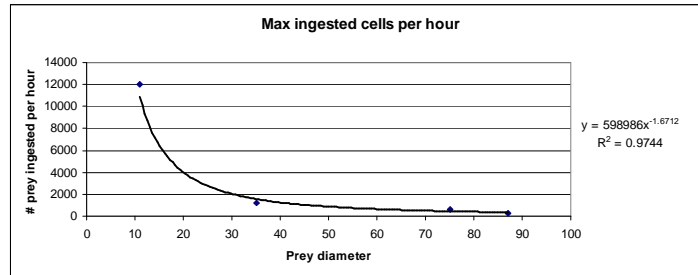


Fig.II.5 – Copepod maximum ingestion rate as a function of diatom size

Therefore, maximum ingestion rate for a diatom of 20 μm diameter is ~ 4000 cells per hour.

The volume of a diatom is $4.2 \times 10^{-9} cm^3 \rightarrow$ therefore $1.7 \times 10^{-5} cm^3$ is the maximum volume of prey to fill the midgut (2/3 of gut volume. Caparroy and Carlotti, 1996).

So of an adult copepod (length = 2400 μm) $V_{gut} = 1.7 \times 10^{-5} cm^3 / 0.67 = 2.5 \times 10^{-5} cm^3$

I will assume a linear relationship between length and gut volume.

$$vol_param = (2.5 \times 10^{-5} cm^3 / 2400 \mu m) = \sim 1 \times 10^{-8} cm^3 \mu m^{-1}$$

$$Eq.II.27 \quad V_{gut} (cm^3) = vol_param (cm^3 \mu m^{-1}) * L (\mu m)$$

II.2.9 GUT PASSAGE TIME (Caparroy and Carlotti, 1996)

$$Eq.II.28 \quad Gut_f = (Gut_{content} / 0.67 * V_{gut})^2$$

Where:

Gut_f = Gut fullness index (1: full; 0 : empty)

$Gut_{content}$ = volume of food in gut (cm^3)

V_{gut} = gut volume (cm^3)

$$\text{Eq.II.29} \quad \text{Gut}_{\text{content}} = \text{Gut}_{\text{content}} + \text{Prey}_{\text{vol}} - ((A + E) * \text{Timestep})$$

$$\text{Eq.II.30} \quad \text{Prey}_{\text{vol}} = X_1 * V_{\text{prey}}$$

$$\text{Eq.II.31} \quad A = Kc \times \text{Gut}_{\text{clear}}$$

$$\text{Eq.II.32} \quad E = (1 - Kc) \times \text{Gut}_{\text{clear}}$$

Where:

Prey_{vol} = Volume of food ingested (cm^3)

X_1 = ingested diatoms in last timestep (# prey)

V_{prey} = volume of individual diatom (cm^3)

A = volume of food digested in 1 hour (cm^3)

E = volume of food egestion rate (cm^3)

GUT PASSAGE TIME, Gut_{time} (h): (function of gut content) (Slagstad and Tande, 1981; Caparroy and Carlotti, 1996)

$$\text{Eq.II.33} \quad \text{Gut}_{\text{time}} = \frac{t_{\text{min}} \cdot t_{\text{max}}}{\left(\frac{X_1 \cdot V_{\text{prey}}}{V_{\text{gut}}} (t_{\text{max}} - t_{\text{min}}) \right) + t_{\text{min}}}$$

Where:

t_{min} = minimum gut passage time (2100 s \rightarrow 0.58 h)

t_{max} = maximum gut passage time (3900 s \rightarrow 1.08 h)

In the midgut of a copepod two main processes occur simultaneously on the ingested prey: ASSIMILATION and gut transit.

It has been observed an increase in gut passage time after 70-80% of the initial gut content has been released (Kiørboe and Tiselius, 1987).

GUT CLEARANCE RATE, $\text{Gut}_{\text{clear}}$ ($\text{cm}^3 \text{h}^{-1}$): Caparroy and Carlotti, 1996

$$\text{Eq.II.34} \quad \text{Gut}_{\text{clear}} = \text{Gut}_{\text{content}} / \text{Gut}_{\text{time}}$$

II.2.10 ASSIMILATION

Assuming the same assimilation efficiency for nitrogen and carbon.

Assimilated C available for growth and reproduction, A_C (mmol C h^{-1}):

Assimilated N, A_N (mmol N h^{-1}) (Caparroy and Carlotti, 1996)

$$\text{Eq.II.35} \quad A_C = k * \text{Carbon}_{\text{ingested}}$$

$$\text{Eq.II.36} \quad A_N = k * \text{Nitrogen}_{\text{ingested}}$$

Where:

A_C = C assimilation rate (mmol C h^{-1}); k = assimilation efficiency

$$\text{Eq.II.37} \quad k = 1 - e^{-a \text{ Gut}_{\text{time}}}$$

Where:

a = digestion rate of the prey ($4.4 \times 10^{-4} \text{ s}^{-1}$)

$$a = 3600 \times 4.4 \times 10^{-4} = 1.584 \text{ h}^{-1}$$

$$\text{if } \text{Gut}_{\text{time}} = 0.58 \text{ h} \quad k = 0.60$$

$$\text{if } \text{Gut}_{\text{time}} = 1.08 \text{ h} \quad k = 0.82$$

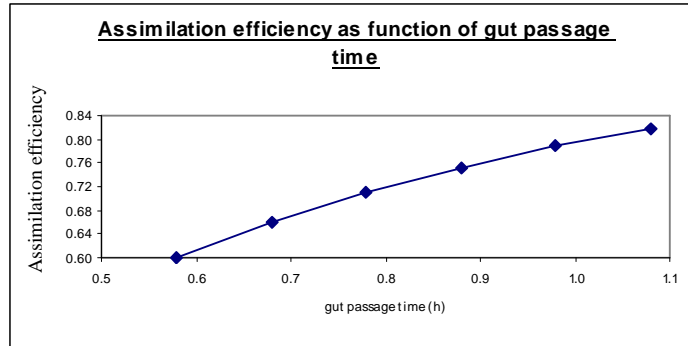


Fig.II.6 – Assimilation efficiency as function of gut passage time

II.2.11 EGESTION

Nitrogen that is not assimilated is egested in faeces:

$$\text{Eq.II.38} \quad E_N = (1-k) \cdot N_{\text{ingested}}$$

E_N = nitrogen added to faecal pellet (mmol N h^{-1})

Silicate is assumed to be completely removed before ingestion, therefore the S_p will always be empty.

II.2.12 EXCRETION

Lipids are assumed to be nitrogen free (Carlotti and Wolf, 1998), thus nitrogen is excreted when lipids are built and the total N:C ratio changes depending on the ratio between C_N and C_{NN} .

$$\text{Eq.II.39} \quad C = N_{\text{protexcess}} + C_{\text{prot}}$$

Where:

C = excretion rate (mmol N ts^{-1})

$N_{\text{protexcess}}$ is the nitrogen over the maximum N:C ratio, Q_{nmax} .

C_{prot} is the nitrogen released, when protein are catabolised (protein and nitrogen are linked by a fixed ratio, Q_{nprot})

II.2.13 MOVEMENT

An animal is assumed to be able to maintain neutral buoyancy with no energy expenditure.

Eq.II.40

Vertical migration, V_m (m h⁻¹)

if (Status = 40 or 50) → Overwintering

$V_m = 0$

else

$V_m = k_v V_{max} W_z$

Where:

k_v determines the direction of migration (dimensionless) ; $V_{max} = 45 \text{ mh}^{-1}$;

W_z introduces the effect of T and size on swimming velocity (dimensionless):

$W_z = (0.3 + (0.7 * (T/T_{ref})))(S/S_{max})$ adapted from Woods and Barkmann, 1994

Where:

T = ambient temp. (°C); T_{ref} = reference temp. (10°C); G = weight of each particle (mmol C); G_{max} = max weight of each particle (8.33×10^{-3} mmol C); S = surface area of individual (cm²) and S_{max} = Surface area of an adult copepod (1.4×10^{-3} cm²).

II.2.13.1 Over-wintering descent

When the depth of an animal ready to enter its dormant phase is below the daily maximum MLD, then it starts descending with a velocity V_{owD} to an overwintering depth of 450 m.

$$\text{Eq.II.41} \quad V_{owD} = \frac{Body_{vol}}{\nu} \times 3600$$

Where:

V_{owD} = Velocity of overwintering descent (mh⁻¹)

Body_{vol} = Volume of bug (m³)

ν = coefficient of kinematic viscosity ($10^{-6} \text{ m}^{-2} \text{ s}^{-1}$)

II.2.13.2 Over-wintering ascent

When either I_t or the MLD_{max} is reached, motion goes back to normal.

II.2.13.3 Day time

At daytime, Zooplankton keep to a depth, at which irradiance is relatively low such that the risk of being predated is reduced. In the WB model this depth is referred to as Target Isolume, I_t . However, if starved, they take the risk and stay at a higher depth, balancing the higher risk of being eaten by the higher concentration of food available.

$$\text{Eq.II.42} \quad I_t = I_r (2 - Gut_f) \quad (\text{Woods and Barkmann, 1994})$$

I_t , Size specific target isolume $[Wm^{-2}]$

Gut_f , the rate of change in satiation, (0 = starved, 1 = satiated)

This only gives a target isolume, I_t , independent of the size of the particle. The visibility of an individual is determined by the amount of light its body reflects. In the enhanced version of the WB, this equation should take into account the effect of size and be substituted by:

$$\text{Eq.II.43} \quad I_t = I_r (2 - Gut_f) (S_{max} / S)$$

I_t (Wm^{-2}) depends on the size of a particle and varies between:

1 Wm^{-2} and 2 Wm^{-2} for adults

77.5 Wm^{-2} and 145 Wm^{-2} for nauplii

Direction of migration

k_v is determined in base of the value of k_{calc} , i.e.:

$$\text{Eq.II.44} \quad K_{calc} = 0.4 (I - I_t)$$

$k_{calc} < 0$	$k_v = -1$	full speed upwards migration
$k_{calc} > 1$	$k_v = 1$	full speed downwards migration
$0 < k_{calc} < 1$	$k_v = k_{calc}$	slower downwards migration

In WB, no mechanism for slow upwards migration:

This was achieved by modifying the intervals for k_{calc}

$k_{\text{calc}} < -1$	$k_v = -1$	full speed upwards migration
$k_{\text{calc}} > 1$	$k_v = 1$	full speed downwards migration
$-1 < k_{\text{calc}} < 1$	then $k_v = k_{\text{calc}}$	slower migration

This method provides a slowing down mechanism, which is dependent on the light intensity offset from I_t , and solves the over-shooting problem affecting WB.

II.2.13.4 Night-time foraging

Eq.II.45 Woods and Barkmann, 1994

if within the ML ($z \leq \text{MLD}$)

$$V_m = 0$$

else

$$K_{\text{ncalc}2} = 0.4 (2 - \text{Gut}_f)$$

$$K_v =$$

If ($D_{\text{local}} < D_{\text{local previous}}$) then $-(\text{direction}[1] * K_{\text{ncalc}2})$
 else $\text{direction}[1] * K_{\text{ncalc}2}$

Direction = if ($k_{\text{vnight}} > 0$) then 1 else -1

Therefore, at night zooplankton below MLD migrate downwards if they are becoming hungrier and the local density of phytoplankton is high, otherwise they migrate upwards.

$k_{\text{calc}2}$ varies between -0.8 and -0.4 depending on how gut fullness

Direction = direction in current timestep (+ve: down; -ve: up)

Direction[1] = direction in previous timestep (+ve: down; -ve: up)

D_{local} = food concentration in current timestep

$D_{\text{local}}[1]$ = food concentration in previous timestep

II.2.14 REPRODUCTION

From Carlotti and Wolf, 1998.

When $C_N \geq G_{\text{max}}$ the particle has reached sexual maturity and A_r starts ticking.

A_r = time since maturity was reached

G_{max} = protein threshold for reproduction (8.33 E-3 mmol C)

When $A_r \geq A_{\text{rep}}$ (20 days)

The stored carbon is used to produce eggs. Copepods are assumed to be able to produce a maximum of 800 nauplii each (Carlotti and Wolf, 1998).

Each nauplii has a set initial carbon pool (G_{\min}), which is composed in equal parts by lipids and proteins. Nitrogen to the nauplii has the same ratio Q_N of the parent. 90% of the offspring is assumed to die.

The weight of the parental particles is then reduced to G_{\max} after reproduction.

II.2.15 OVERWINTERING

Pre-overwintering

The entire assimilated matter fills the lipid reserve to a maximum value, which in Carlotti depends on stage.

Eq.II.46

if (day < 210)

$$\text{probOW} = 30$$

else

$$\text{probOW} = 50$$

If before the 1st August copepod have 30% chance of entering pre-overwintering, after that date the chances become 50%.

Overwintering

When the lipid reserve is full, particle swim down to a depth below 450 until next spring (day 95).

II.2.16 MORTALITY

Mortality due to starvation

Eq.II.47 If $C_N < C_{p\max} / 2 \rightarrow$ dead

If the protein pool falls below half of the maximum protein pool reached the copepod dies of starvation

Mortality due to senescence

Eq.II.48 Pchange (Dead, $1/(A_{r\max} - A_r)$)

Where:

A_{max} = max lifespan since maturity (960h); A_r = time elapsed since maturity (h).

An increasing proportion of the copepods in the agents change stage to dead as function of time since they reproduced.

II.2.17 REMINERALISATION

As a dead copepod or faecal pellet sinks through the mesocosm, it remineralises nitrogen as a function of its nitrogen content and ambient temperature:

$$\text{Eq.II.49} \quad R_{\text{NT}} = N_{\text{dissolution}} * Q_{\text{RemN}}^{(T - T_{\text{Nref}})/10}$$

Where:

R_{NT} = Nitrogen remineralisation rate (mmol N h^{-1})

$N_{\text{dissolution}}$ = N specific dissolution rate of N ($\text{mmol N mmolN}^{-1} \text{h}^{-1}$)

Q_{RemN} = factor by which N dissolution increases with T (K) (*wd*)

T = temperature ($^{\circ}\text{C}$)

T_{ref} = reference temperature ($^{\circ}\text{C}$)

II.3 - PARAMETERS

Parameter	Description	Value	Unit	Source
a	N specific digestion rate of the prey	1.584	h ⁻¹	Caparroy and Carlotti, 1996
A_rep	Age at fecundity	240	h	Woods and Barkmann, 1994
A_rmax	Maximum lifespan since reaching reproductive maturity	480	h	Woods and Barkmann, 1994
b	C specific digestion rate of the prey	1.584	h ⁻¹	Assumed as 'a'
C1_min	Threshold for entering C1 stage	6.25 x 10 ⁻⁵	mmolC	Carlotti and Wolf, 1998
C2_min	Threshold for entering C2 stage	9.15 x 10 ⁻⁵	mmolC	Carlotti and Wolf, 1998
C3_min	Threshold for entering C3 stage	2.1 x 10 ⁻⁴	mmolC	Carlotti and Wolf, 1998
C4_min	Threshold for entering C4 stage	5.8 x 10 ⁻⁴	mmolC	Carlotti and Wolf, 1998
C5_min	Threshold for entering C5 stage	1.25 x 10 ⁻³	mmolC	Carlotti and Wolf, 1998
C6_min	Threshold for entering C6 stage	3.33 x 10 ⁻³	mmolC	Carlotti and Wolf, 1998
C_Cal	Oxycaloric coefficient	20.3	kJ IO ₂ ⁻¹	Ikeda <i>et al.</i> , 2000
C_conv1	C conversion factor from mmol to microg	12000	µgC mmolC ⁻¹	calculated
delta	Reduction of basic metabolism in hibernating copepods	0.2	no unit	Carlotti and Wolf, 1998
E_m	Muscular efficiency of copepod	0.25	no unit	Caparroy and Carlotti, 1996
E_mech	Mechanical efficiency of swimming Copepod	0.3	no unit	Caparroy and Carlotti, 1996
G_max	Maximum C content of an individual	8.33 x 10 ⁻³	mmolC	Carlotti and Wolf, 1998
G_min	Weight of newly born nauplii	1.67 x 10 ⁻⁵	mmolC	Woods and Barkmann, 1994
k	Coefficient of empirical relationship between drag coefficient and Reynolds number	85.2	no unit	Caparroy and Carlotti, 1996
mi	Seawater dynamic viscosity	0.000119	gm ⁻¹ s ⁻¹	Caparroy and Carlotti, 1996
n	coefficient of empirical relationship between drag coefficient and Reynolds number	0.8	no unit	Caparroy and Carlotti, 1996
N4_min	Threshold for entering N4 stage	1.7 x 10 ⁻⁵	mmolC	Carlotti and Wolf, 1998
N5_min	Threshold for entering N5 stage	2.5 x 10 ⁻⁵	mmolC	Carlotti and Wolf, 1998
N6_min	Threshold for entering N6 stage	3.75 x 10 ⁻⁵	mmolC	Carlotti and Wolf, 1998
N_mp	Chances of naupliar mortality	0.9	no unit	Woods and Barkmann, 1994
OW_lipid	Lipid content needed to overwinter	8.33 x 10 ⁻³	mmolC	Carlotti and Wolf, 1998
PreOW4	Minimum C content to pre-overwinter	5.8 x 10 ⁻⁴	mmolC	Carlotti and Wolf, 1998
PreOW5	Minimum C content to overwinter as C5	3.33 x 10 ⁻³	mmolC	Carlotti and Wolf, 1998
Q_Nmax	Maximum N:C ratio	0.23	mmoNmmolC ⁻¹	Huntley and Nordhausen, 1995
QnProt	Fixed N:C ratio in proteins	0.27	mmoNmmolC ⁻¹	Anderson <i>et al.</i> , 2005
QR_10	Q_10 for basl metabolism	3.4	no unit	Carlotti and Wolf, 1998
r_bas	Basal metabolic coefficient	0.000417	h ⁻¹	Carlotti and Wolf, 1998
r_sda	Specific Dynamic Action coefficient	0.17	no unit	Kjørboe <i>et al.</i> , 1985
S_max	Max cross-sectional area	1.3 x 10 ⁻³	cm ²	Estimated from Caparroy and Carlotti, 1996
t_max	Maximum gut passage time	1.08	h	Caparroy and Carlotti, 1996
t_min	minimum gut passage time	0.58	h	Caparroy and Carlotti, 1996
T_ref	Reference temperature	10	C	Carlotti and Wolf, 1998
V_max	Maximum swimming velocity	45	mh ⁻¹	Woods and Barkmann, 1994
V_mconv1	Swimming velocity conversion factor: m/h to cm/s	0.0278	cm h m ⁻¹ s ⁻¹	calculated
Vol_conv1	Conversion coefficient mm ³ to m ³	1 x 10 ⁻⁹	m ³ mm ⁻³	calculated
vol_gut	midgut growth coefficient	0.01174	cm ³ mmolC ⁻¹	Estimated from Caparroy and Carlotti, 1996
vPrey	Fixed diatom volume	3.5 x 10 ⁻⁸	cm ³	Estimated from Menden-Deuer and Lessard, 2000
z_startOW	Depth at which sinking starts	50	m	assumed

Tab.II.4 – Copepod parameters

“Testing theories on fisheries recruitment.”

APPENDIX III

SQUID PARALARVAE MODEL

APPENDIX III - SQUID MODEL

FISHERIES

Genus *Loligo* represents one of the most important species in volume of commercial landings. The fishery for *Loligo opalescens* began with the Chinese in Monterey Bay, California in 1860. By the turn of the century Italian fishermen had assumed the leading role. After WWII there was resurgence in squid fishing. Since 1981 the fishery has really grown, as effort in Southern California has increased. Now Southern California, mostly areas around the Channel Islands, comprises 90% of the squid landings. The fishery in Monterey Bay occurs from April to November coinciding with the upwelling season. In Southern California landings begin in November and continue through April correlated with the greater mixing of winter storms. Since 1993 squid has been the biggest fishery in California with landings of 118,000 tons and \$41 million in 2000. The population fluctuates greatly with the El Niño. During these warm water, nutrient poor years landings can disappear entirely in certain areas. It is proliferating whereas slower growing teleosts stocks are declining (Caddy and Rodhouse, 1998).

DISTRIBUTION

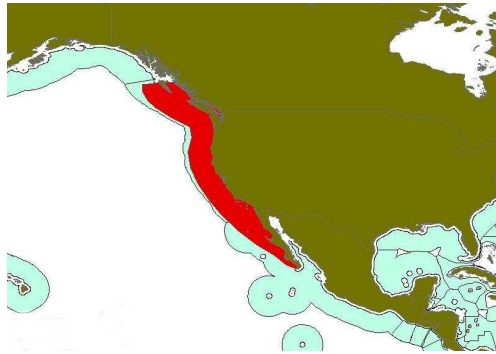


Fig.III.1 - *Loligo opalescens* distribution (FAO, 1984)

BIOLOGY

Young cephalopods in their first growth stage after hatching resemble miniature adults with most organs developed, but their planktonic mode of life differs from that of juveniles and adults (Baron, 2003). For this reasons they are different from others molluscs larvae and are referred to as paralarvae (Young and Harman, 1988).

III.1 STATE VARIABLES

Eq.III.1 The total carbon pool (mmol C):

$$\text{Carbon}_{\text{pool}} = \text{C}_{\text{Npool}} + \text{C}_{\text{NNpool}}$$

Eq.III.2 Lipid pool

$$\text{C}_{\text{NNpool}} = \text{C}_{\text{NNpool}} + (\text{Budg}_{\text{CNN}} - \text{Lip}_{\text{excess}})$$

Eq.III.3 Protein pool

$$\text{C}_{\text{N_Pool}} = \text{C}_{\text{N_Pool}} + \text{Budg}_{\text{CN}}$$

Eq.III.4 Nitrogen pool

$$\text{N}_{\text{pool}} = \text{N}_{\text{pool}} + \text{N}_{\text{ingested}} - [(\text{C} * \text{TimeStep}) + (\text{E}_{\text{protein}} * \text{Q}_{\text{Nprotein}})]$$

Eq.III.5 Dry weight

$$\text{DW} = \text{Carbon}_{\text{pool}} * \text{C}_{\text{conv}}$$

Eq.III.6 Wet Weight (Vidal *et al.*, 2002)

$$\text{WW} = (\text{DW} - 0.064) / 0.21$$

Eq.III.7 Mantle length (Hurley,1976)

$$\text{ML} = 10^{[(\log \text{DW} + 1.22)/2.37]}$$

Eq.III.8 Mantle width (Vecchione, 1981)

$$\text{MW (mm)} = 0.3768\text{ML (mm)} + 0.7842$$

Eq.III.9 Frontal surface area¹

$$\text{S (m}^2\text{)} = \pi * (\text{MW}/2)^2 * 10^{-6}$$

Where:

C_{NNpool} = Lipid pool (mmol C)

Budg_{CNN} = flux of body lipid (mmol C)

$\text{Lip}_{\text{excess}}$ = excess lipids (mmol C)

$\text{C}_{\text{N_Pool}}$ = Protein pool (mmol C)

Budg_{CN} = flux of body protein (mmol C)

N_{pool} = Nitrogen pool (mmol N)

$\text{N}_{\text{ingested}}$ = Nitrogen ingested during last timestep (mmol N)

C = Ammonium excretion rate (mmol N h⁻¹)

$\text{E}_{\text{protein}}$ = Protein not assimilated (mmol C)

¹ Frontal surface area (S) is assumed to be the area of the squid visible from above. This is assumed to be a circle, whose diameter is represented by MW. Frontal surface area is converted to m² (conversion factor 10⁻⁶ m² mm⁻²) for the calculation of visibility (irradiance is in Wm⁻²).

$Q_{N\text{protein}}$ = nitrogen:carbon ratio in protein (mmol N mmolC⁻¹)

Carbon_{pool} = Carbon pool (mmol C)

C_{conv} = mmol C to mg C conversion factor (12 mg C mmol C⁻¹)

ML = Mantle length (mm)

DW = Dry weight (mgC)

WW = Wet weight (mgC)

MW = Mantle width (mm)

S = Frontal surface area (m²)

III.2 SPAWNING

In Monterey Bay *Loligo opalescens* spawning occurs from April to November (Zeidberg and Hamner, 2002).

On the d₀: 10th April (day 100) eggs are laid at 50 m.

Inshore loliginid squid, such as *L. opalescens*, spawn elongated gelatinous egg capsules, which may contain from a few to over 100 eggs, depending on the species.

What is the critical size for squid recruitment?

Observations on laboratory reared *L. opalescens* revealed that squid mastery of copepod capture develops progressively, culminating by approximately 40 days post-hatching in adult-like prey capture behaviour and suggest that it is a skill that is acquired in an experience-dependent manner early in post-hatching life. (Chen *et al.*, 1996). *L. opalescens* absolute attack speed increases in proportion to ML (Chen *et al.*, 1996). After 40 days a squid fed *ad libitum* reaches a ML of about 8 mm, ML_{max}, this is around the same time when *L. opalescens* switches from a diet based on copepods to a diet composed on mysid and shrimp larvae up to 10 mm long (Yang *et al.*, 1983).

III.3 EMBRYOGENESIS

Duration

The duration of cephalopod embryogenesis depends mainly on egg size and ambient temperature (Laptikhovsky, 1991). In *L. opalescens* and *L. forbesi*, the period from the first paralarva hatching to the emergence of the last took 4-6 and 7 days, respectively (Yang *et al.*, 1986; Segawa *et al.*, 1988 From Arkhipkin and Middleton,

2003). Baron (2000) suggested taking into account daily accumulated temperature (DAT \equiv °C days) in the analysis of the duration of loliginid embryonic development. The intra-population variability in hatching date is modelled as a variation of the initial DAT and justified as a consequence of the variation in egg size.

For squid, the shortest embryonic period was observed for *L. pealeii* with small eggs developing in warm water (10 days at 23°C); the longest developmental period was recorded in the temperate *L. forbesi* with large eggs: 130 days at 8°C (Craig, Boyle, Black and Overnell, 2000). Baron (2000) incubated *L. gahi* eggs at temperatures varying between 4-23°C and found that full embryogenesis requires 600-850° DAT.

In LERM-ES eggs hatch when DAT is 600°DAT(DAT_{hatch}).

DAT is accumulated from the time eggs are laid (d_0) as follows:

$$\text{Eq.III.10} \quad \text{DAT} = \text{DAT} + (T/48)$$

Where:

T is temperature °C and 48 is the number of timesteps in a day.

When DAT exceeds DAT_{hatch}, the eggs will hatch.

Embryonic mortality

During embryogenesis eggs are not predated. Bat stars, *Asterina miniatus*, are the prevalent predators of *L. opalescens* eggs (Zeidberg, 2003). Fish do not eat them, although they nip at eggs not covered by the sheath. There is no brooding or parental care (Zeidberg, 2003).

III.4 HATCHING

III.4.1 Mantle length at hatching

The average size of *L. gahi* at hatching is inversely correlated with incubation temperature (Baron, 2003) by this regression equation ($r^2 = 0.83$, $n = 241$):

$$\text{Eq.III.11} \quad \text{MML} = -0.05 \times \text{MIT} + 3.54$$

Where:

MML = Mean Mantle Length (mm)

MIT = Mean Incubation Temperature (°C)

L. gahi, *L. opalescens*, *L. bleekeri* and *L. vulgaris* have similar egg length and mantle length (ML) at hatching due to their phylogenetic relationship (Baron, 2003).

Species	Egg length (mm)	ML at hatching (mm)
<i>Loligo gahi</i>	2.1-3.0 (1)	2.3-3.7 (6)
	2.5-3.2 (9)	2.6-3.1 (9)
<i>Loligo opalescens</i>	2.0-2.5 (2)	2.5-3.2 (7)
<i>Loligo bleekeri</i>	2.6-2.7 (3)	3.0-3.3 (3)
<i>Loligo vulgaris</i>	2.3-2.7 (4)	2.8-3.3 (8)
<i>Loligo sanpaulensis</i>	1.2-1.3 (1)	1.4-1.7 (6)
<i>Loligo pealei</i>	1.1-1.6 (5)	1.4-1.7 (7)

Tab.III.1- Egg diameter and mantle length at hatching for different squid species: (1) Baron, 2001; (2) Fields, 1965; (3) Baeg *et al.*, 1993; (4) Worms (1983); (5) Summers, 1983, (6) Baron, 2003; (7) McConathy *et al.*, 1980; (8) Hanlon *et al.*, 2002; (9) Guerra *et al.*, 2001

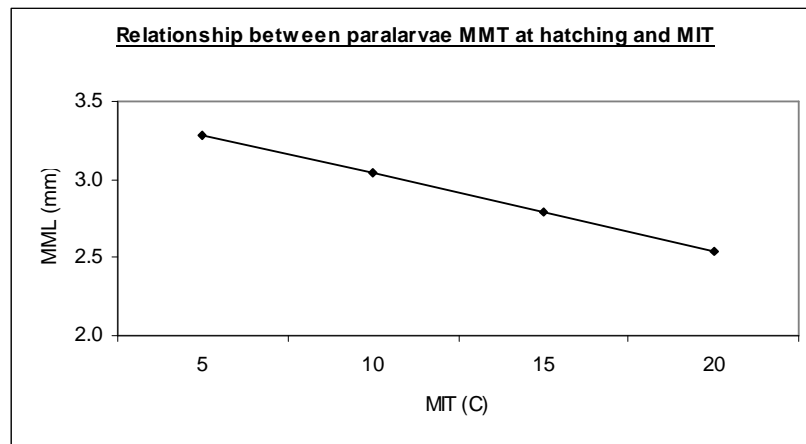


Fig.III.2 – Mantle length at hatching as a function of mean incubation temperature (Baron, 2003)

III.4.2 Mantle width

Mantle width (MW) was calculated using the relationship between ML and MW for *L. pealei* (comparable size with *L. opalescens*) reared in laboratory (Vecchione, 1981):

$$\text{Eq.III.12} \quad \text{MW (mm)} = 0.3768\text{ML (mm)} + 0.7842$$

III.4.3 Frontal surface area

Frontal surface area (S) is assumed to be the area of the squid visible from above. This is assumed to be a circle, whose diameter is represented by MW. Frontal surface area is converted to m^2 (conversion factor $10^{-6} \text{m}^2 \text{mm}^{-2}$) for the calculation of visibility (irradiance is in Wm^{-2}).

$$\text{Eq.III.13} \quad S (\text{m}^2) = \pi * (\text{MW}/2)^2 * 10^{-6}$$

III.4.4 Body weight at hatching

The wet weight of the newly hatched squid is function of its ML. It is calculated using the laboratory derived relationship for *Loligo opalescens* juveniles (Forsythe and Van Heukelem, 1987):

$$\text{Eq.III.14} \quad \text{WW}_{\text{hatch}} = 0.000194 \text{ ML}^{2.59}$$

Where:

WW_{hatch} = Wet weight (g)

ML = Mantle length (mm)

NB: In LERM weight is measured in mg. So, for a hatchling with mantle length of 2.8 mm would weight 2.8 mg WW.

DW (mg) is correlated to WW (mg) using the following lab derived correlation (Vidal *et al.*, 2002):

$$\text{Eq.III.15} \quad \text{DW} = 0.21 + (\text{WW}_{\text{hatch}} * 0.064)$$

III.4.5 Stoichiometry at hatching

Few animals are 18% WW protein, 79% moisture with just 3% left for all other biochemical compounds needed for life. In contrast to fishes, cephalopods contain 20% more protein, 80% less ash, 50-100% less lipid and 50-100% less carbohydrate. Lee (1994) reported lipid contents of cephalopods ranging between 0.34-3.4% WW. Assuming a body water percentage of 77.5% (75-80% Lee, 1994), the total lipids content is 15 %DW. LERM, therefore, assumes that the maximum body lipids is 15% DW. This is the same proportion of lipids found in the egg measured by Bouchaud and Galois (1990).

$$\text{Eq.III.16} \quad \text{C}_{\text{N_in}} = \text{DW} * \text{Prot}_{\text{in prop}} * \text{W}_{\text{conv}}$$

$$\text{Eq.III.17} \quad \text{C}_{\text{NN_in}} = \text{DW} * (1 - \text{Prot}_{\text{in prop}}) * \text{W}_{\text{conv}}$$

$$\text{Eq.III.18} \quad \text{Carbon}_{\text{pool_in}} = \text{C}_{\text{N_in}} + \text{C}_{\text{NN_in}}$$

$$\text{Eq.III.19} \quad \text{Nitrogen}_{\text{pool_in}} = \text{C}_{\text{N_in}} * \text{Q}_{\text{N_prot}}$$

Where:

$\text{C}_{\text{N_in}}$ = Initial protein pool (mmol C)

$\text{C}_{\text{NN_in}}$ = Initial lipid pool (mmol C)

Carbon_{pool_in} = Initial carbon pool (mmol C)

Nitrogen_{pool_in} = Initial nitrogen pool (mmol N)

Prot_{in_prop} = Max protein percentage of body weight (*wd*)

W_{conv} = mg C to mmol C conversion factor (mmol C mgC⁻¹)

Q_{N_prot} = Nitrogen percentage of protein weight (mmol N mmol C⁻¹)

III.4.6 Yolk reserve

Recent experiments conducted on *L. opalescens*, show that the weight and volume of yolk reserves in hatchlings vary with the temperature during embryogenesis. They observed that squid hatching at 12°C were larger, heavier and had more yolk than squid hatching at 16°C (Vidal *et al.*, 2002). This study showed that the yolk-weight to body-weight ratio at hatching was not significantly different the two temperature groups, indicating that the amount of yolk is proportional to body weight.

Egg yolk lipid level represents about 14% of the egg dry weight and seems to be independent of egg size (Bouchaud and Galois, 1990).

The yolk reserve at hatching is therefore assumed to be 15% of the WW_{hatch} and is converted into energy content (Cal). The caloric value of *L. opalescens* yolk is 1.71 cal mg⁻¹ (Giese, 1969):

$$\text{Eq.III.20} \quad \text{Yolk}_{\text{lipids}} = \text{WW}_{\text{hatch}} * \text{Yolk}_{\text{lipids_ratio}} * \text{Yolk_E}_{\text{conv}}$$

Where:

Yolk_{lipids} = Energy in yolk (cal)

Yolk_{lipids_ratio} = Yolk weight as percentage of WW (mg)

Yolk_{E_conv} = Yolk energetic value (cal mg⁻¹)

III.5 PARALARVAL STAGE

At this point, paralarvae have hatched with variable sizes and variable yolk reserves. Hatchlings' lipid content varies with incubation temperature and is link to their size.

III.5.1 MOTION

III.5.1.1 Swimming speed

The stage-specific maximum swimming speed for squid migration was estimated using the *in-situ* derived regression (Zeidberg, 2004):

$$\text{Eq. III.21} \quad V = 0.005 \text{ ML.}$$

Where:

V = maximum migration speed (mh^{-1})

ML = mantle length (mm)

So the maximum migration speed for a squid in stage 6 is 135 mh^{-1} .

Max swimming migration speed is a function of T and size on surface area:

$$\text{Eq. III.22} \quad W_z = [0.3 + (0.7 * T/T_{\text{ref}})] (S/S_{\text{max}})$$

Where :

W_z = effect of temperature and size on swimming speed (wd)

T = ambient temperature ($^{\circ}\text{C}$)

T_{ref} = reference temperature (10°C)

S = frontal surface area (m^2)

S_{max} = frontal surface area for a S6 squid (m^2)

III.5.1.2 Diel migration

In situ observations in Monterey Bay on the distribution of *L. opalescens* paralarvae revealed that diel migration starts immediately after hatching (Zeidberg and Hamner, 2002). Paralarvae are vertically distributed above 80m, with the maximum concentration occurring at 15 m during the night and 30 m during the day (Okutani and McGowan, 1969; Zeidberg and Hamner, 2002).

Hatchlings of *L. pealeii* are also found in surface waters day and night. They move deeper in the water column as they grow larger (Cargnelli *et al.*, 1999).

Diel migration is modelled using target isolumes, as for copepods (chapter 4). During the day a squid keeps to a depth at which irradiance is low enough to reduce the risk of being eaten². This depth is a function of squid visibility. Squid visibility is determined by its size and ambient irradiance:

² In situ observations in Monterey Bay on the distribution of *L. opalescens* paralarvae revealed that diel migration starts immediately after hatching (Zeidberg and Hamner, 2002). Paralarvae are vertically

Eq.III.23
$$I_t = I_{t_ref} * (S_{max} / S)$$

Where :

I_t = target isolume (Wm^{-2})

I_{t_ref} = reference target isolume (Wm^{-2})

S = frontal surface area (m^2)

S_{max} = frontal surface area for a S6 squid (m^2)

At dusk (irradiance $< 100 Wm^{-2}$) squid ascends the water column swimming at its routine speed. At dawn (irradiance $> 100 Wm^{-2}$) squid descends the water column chasing its target isolume.

III.5.1.3 Foraging

Not much is known about the foraging strategies in squids. The only observations relate to the Caribbean squid *Sepioteuthis sepioidea* (Moynihan and Rodaniche, 1982).

This species mostly rests during the day. Near dusk, the shoaling squid move to shallow water and slowly split up into progressively smaller groups until they are alone throughout the night. They forage and feed until dawn, when they aggregate into shoals.

Prey attack is elicited by visual stimuli (Boletzky, 1974). The impossibility of implementing lunar phase in the current version of VEW meant that during night-time squid are unable to detect the prey and feed. Predator-prey encounters can therefore only occur during the day as they both migrate in the virtual mesocosm in search of their target isolume.

III.5.1.4 Corpses and pellets sinking rate

Dead squid are assumed to sink at $20 mh^{-1}$. Squid pellets sink at $10 mh^{-1}$.

III.5.2 INGESTION

Mortality at first feeding, or “critical-period theory”, has received much attention in the study of young fishes (Lasker, 1981). Vecchione (1981) proposed based on field

distributed above 80m, with the maximum concentration occurring at 15 m during the night and 30 m during the day (Okutani and McGowan, 1969; Zeidberg and Hamner, 2002).

sampling that the critical period is important also for some species of cephalopods. The relationship between successful first feeding and yolk absorption seems to be a critical stage at which variable or high natural mortality occurs.

Exogenous and endogenous feeding overlaps until the yolk sac is completely absorbed (Vidal *et al.* 2002).

III.5.2.1 Endogenous feeding

All energetic costs (respiration, cal h^{-1}) are covered by the energy provided by the yolk, until its complete exhaustion. If the yolk energy is not sufficient to cover the costs, then the surplus costs (R_{surplus}) are covered by lipids, preferentially, or proteins.

Eq.III.25 $\text{Yolk}_{\text{lipids}} =$ if (the energy in the yolk is sufficient to fuel energetic costs)

$$\text{Yolk}_{\text{lipids}} - \text{respiration}$$

else 0

Eq.III.26 $R_{\text{surplus}} =$ if (the energy in the yolk is sufficient to fuel energetic costs)

$$0$$

else respiration – $\text{Yolk}_{\text{lipids}}$

Where:

$\text{Yolk}_{\text{lipids}} =$ Energy in yolk (cal)

respiration = energy consumption rate (cal h^{-1})

$R_{\text{surplus}} =$ energetic consumption rate not covered by the energy in yolk ($\text{cal mg}^{-1}\text{h}^{-1}$)#

III.5.2.2 Exogenous feeding

Some cephalopods hatch as miniature replicas of the adult and feed in a similar way. La Roe (1971) reported that the squid, even newly hatched fry, were extremely selective in their choice of foods; they would attack and eat only live, actively moving animals of a limited size range. They would not eat dead, inactive, drifting or benthic organisms.

Hunting efficiency

Observations on laboratory reared *L. opalescens* revealed that squid mastery of copepod capture develops progressively, culminating by approximately 40 days post-hatching in adult-like prey capture behaviour and suggest that it is a skill that is

acquired in an experience-dependent manner early in post-hatching life. (Chen *et al.*, 1996). Absolute attack speed increases in proportion to ML (Chen *et al.*, 1996). After 40 days a squid fed *ad libitum* reaches a ML of about 8 mm, ML_{\max} .

$$\text{Eq.III.27} \quad \text{Hunt}_{\text{eff}} = \text{ML} / \text{ML}_{\max}$$

Where:

Hunt_{eff} = hunting efficiency index (*wd*)

ML = mantle length (mm)

ML_{\max} = maximum mantle length (mm)

Ingestion rate

Squid high activity and rapid growth needs a large amount of food and high feeding and digestion efficiency. However, it is impossible to overfeed them (Boucher-Rodoni *et al.*, 1987). The cue to stop feeding when satiated is given by the pressure of food on the stomach walls of an animal. This sends a signal to the hypothalamus announcing that the gut is full. So maximum ingestion rate is modelled as a function of the gut volume that can be filled (i.e. maximum ingestion rate is zero if the gut is already full). For the squid *Illex illecebrosus* ingestion of a meal required 5-15 minutes (Wallace *et al.*, 1981), so we can safely assume that within a timestep (30 minutes), a squid can potentially fill its gut, so:

$$\text{Eq.III.28} \quad I_{\text{Max}} = [(1 - \text{Gut}_f) * V_{\text{gut}}] / 1800$$

Where:

I_{max} = maximum ingestion rate ($\text{mm}^3 \text{s}^{-1}$)

Gut_f = gut fullness index (*wd*) 0: empty gut; 1: full gut

V_{gut} = gut volume (mm^3)

Squid ingestion of copepods had to be implemented in different way compared to copepod ingestion on diatoms. While diatoms are assumed to have a fixed volume, so that the number of ingested diatoms correlates to the volume of food ingested, copepod volume varies with its development stage (a mature copepod has a body volume of 1mm^3 while a N3 nauplius has a volume of 0.001mm^3). In young cephalopods, as in most adults, attack is elicited by visual stimuli (Boucher-Rodoni *et al.*, 1987). The velocity of the prey is another factor affecting the efficiency of capture, in relation to the swiftness of the predator. Planktonic squid are only

successful in capturing relatively slow prey such as crustacean larvae and copepods (Boletzky, 1974a).

$$\text{Eq.III.29} \quad I_{gv} = \text{Min (between } I_{\max} \text{ and } I_{gv})$$

$$\text{IF } (P > P_{\min})$$

then

$$\begin{array}{c}
 \text{Predator feeding potential} \quad \text{Prey visibility} \quad \text{Prey escape ability} \\
 \underbrace{k_p * \text{Hunt}_{\text{eff}} * (1 - \text{Gut}_f)}_{\text{Stage specific prey volume encountered}} * \underbrace{(S_a / S_{a-\max}) * (\text{Irr} / \text{Irr}_{\text{ref}})}_{\text{Stage specific prey volume encountered}} * \underbrace{P_{\text{speed-max}} / P_{\text{speed}}}_{\text{Stage specific prey volume encountered}} * \\
 \underbrace{\{[(P - P_{\min}) * P_{\text{vol}}]^2 / \{[(P - P_{\min}) * P_{\text{vol}}] + (K_{iv} * P_{\text{vol}})\}\}}_{\text{Stage specific prey volume encountered}} \\
 \text{else 0}
 \end{array}
 \quad \left. \vphantom{\begin{array}{c} \text{Predator feeding potential} \\ \text{Prey visibility} \\ \text{Prey escape ability} \end{array}} \right\} z - z[1]$$

Where:

I_{gv} = stage specific ingestion rate ($\text{mm}^3 \text{s}^{-1}$)

k_p = predator hunting volume scan rate ($\text{m}^3 \text{s}^{-1}$)

Hunt_{eff} = hunting efficiency index (*wd*)

Gut_f = gut fullness index (*wd*) 0: empty gut; 1: full gut

S_a = copepod stage specific surface area (m^2)

$S_{a-\max}$ = maximum surface area for an adult copepod ($1.3 \times 10^{-7} \text{ m}^2$)

Irr = ambient irradiance (Wm^{-2})

Irr_{ref} = reference irradiance (Wm^{-2})

P_{speed} = stage specific maximum swimming speed (mh^{-1})

$P_{\text{speed-max}}$ = maximum swimming speed for an adult copepod (mh^{-1})

P = stage specific ambient prey concentration (prey m^{-3})

P_{\min} = stage specific minimum ambient prey concentration (prey m^{-3})

P_{vol} = stage specific prey volume (mm^3)

K_{iv} = half-saturation constant (prey m^{-3})

z = current depth (m)

$z[1]$ = depth in previous timestep (m)

The total potential volume that could be ingested by a squid is:

$$\text{Eq.III.30} \quad \text{Tot}I_{gv} = \text{varietysum } (I_{gv})$$

Where:

$\text{Tot}I_{gv}$ = total potential volume that could be ingested ($\text{mm}^3 \text{s}^{-1}$)

Varietysum = sum of the potential volume that can be ingested for each prey stage

Eq.III.31 ratioIng =

$$\begin{aligned} & \text{if } (\text{TotI}_{\text{gv}} > \text{I}_{\text{max}}) \\ & \quad \text{then } (\text{I}_{\text{max}} / \text{TotI}_{\text{gv}}) \\ & \quad \text{else } 1 \end{aligned}$$

Where:

ratioIng = is the ratio between maximum volume that can be ingested and the potential volume that is available for ingestion

In the case that maximum the potential volume that is available for ingestion is bigger volume that can be ingested, then the request is scaled down to avoid overfeeding.

Eq.III.32 $\text{I}_{\text{gv}2} = (\text{I}_{\text{gv}} / \text{P}_{\text{vol}}) * \text{ratioIng}$

Where:

$\text{I}_{\text{gv}2}$ = stage specific effective ingestion rate ($\text{mm}^3 \text{ s}^{-1}$)

Then an ingestion request is done for each prey stage depending on $\text{I}_{\text{gv}2}$, P and P_{min} :

Eq.III.33 ingest (P, P_{min} , $\text{I}_{\text{gv}2}$)

III.5.3 DIGESTION

The total time necessary to digest a meal varies from one species of cephalopods to the other, and within the same species it is highly influenced by temperature (Boucher-Rodoni, 1975). For octopus *Eledone cirrhosa*, digestion lasted 15 hours at 20°C, 20 hours at 15°C and 30 hours at 10°C (Boucher-Rodoni, 1973).

So I will assume that Q_{10} (the increase in digestion rate with a temperature increase of 10°C over the reference temperature) is 2.

Observations on the digestion rate of squid *Illex illecebrosus*, reared at 10°C, revealed that digestion rate was very high soon after feeding and then slows down gradually (Wallace *et al.*, 1981). The rate of food digested represents a fairly constant percentage of the quantity ingested and decreases with time after feeding (Boucher-Rodoni, 1975; Boucher-Rodoni and Mangold, 1977).

The percentage of digested food as function of time since ingestion is modelled using the laboratory derived regression (Wallace *et al.*, 1981):

Eq.III.34 $\text{Log}_{10} \% \text{ food digested} = 1.64 - 0.032 \text{ Last}_{\text{feed_time}}$

.Where:

% food digested (0-100)

Last_{feed_time} = hours since last ingestion (h)

The percentage of food in the gut that gets digested, Dig_{perc} is therefore:

$$\text{Eq.III.35} \quad \text{Dig}_{\text{perc}} = \underbrace{\{10^{\wedge} [(1.64 - (0.032 * \text{Last}_{\text{feed_time}})]\}}_{\text{Effect of time since last feeding}} * \underbrace{Q_{10}^{\wedge} [(T - T_{\text{ref}}) / T_{\text{ref}}] }_{\text{Temperature effect}} / 100$$

Where:

Dig_{perc} = ratio of digested food in gut (0-1)

Last_{feed_time} = hours since last ingestion (h)

Q₁₀ = index describing the increase in digestion rate for a 10°C increase in temperature from the reference temperature (*wd*)

T = ambient temperature (°C)

T_{ref} = reference temperature (10°C)

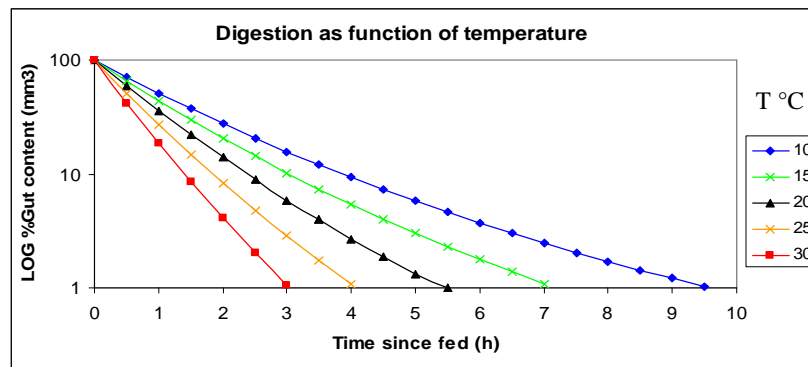


Fig.III.3 – Digestion rate as a function of temperature and time since feeding

Fig III.3 shows the duration of digestion of a meal at different temperatures using the above equation.

This compares well with laboratory observations. Complete digestion of a meal at 18°C takes about 6 hours for *L. opalescens* (Karpov and Caillet, 1978) and 4-6 hours for *L. vulgaris* (Bidder, 1950).

The volume of food digested in a timestep:

$$\text{Eq.III.36} \quad \text{Processed} = \text{Gut}_{\text{content}} * \text{Dig}_{\text{perc}}$$

Where:

Processed = The volume of food digested in a timestep (mm³)

Gut_{content} = Gut content at the end of the timestep (mm³)

III.5.4 Assimilation

Squid assimilation efficiency for proteins is very high, 81-92% (Lee, 1994; Wells and Clarke, 1996). However they have a problem with lipids. When they are given a fatty diet, a large part of it (45-70% according to Wells and Clarke, 1996) passes through the digestive tract and floats as faeces (O’Dor and Wells, 1987). Squid are assumed to assimilate 85% of the digested proteins and 50% of the digested lipids.

$$\text{Eq.III.37} \quad Q_{\text{lip}} = (C_{\text{NN_pool}} * C_{\text{conv}}) / \text{DW}$$

$$\text{Eq.III.38} \quad A_{\text{protein}} = [(\text{Gut}_{\text{protein}} + C_{\text{N_ing}}) * \text{Dig}_{\text{perc}}] * A_{\text{eff_prot}}$$

$$\text{Eq.III.39} \quad A_{\text{lipid}} = \text{if } [(Q_{\text{lip_max}} - Q_{\text{lip}}) * \text{DW}] > \{[(\text{Gut}_{\text{lipid}} + C_{\text{NN_ing}}) * \text{Dig}_{\text{perc}}] * A_{\text{eff_lip}}\} \\ \text{else} \\ [(\text{Gut}_{\text{lipid}} + C_{\text{NN_ing}}) * \text{Dig}_{\text{perc}}] * A_{\text{eff_lip}} \\ [(Q_{\text{lip_max}} - Q_{\text{lip}}) * \text{DW}]$$

Where:

Q_{lip} = Lipid to dry weight ratio

$Q_{\text{lip_max}}$ = Maximum lipid to dry weight ratio

$C_{\text{NN_pool}}$ = Lipid pool (mmol C)

DW = Dry weight (mg C)

C_{conv} = mmol C to mg C conversion factor

$A_{\text{protein}}, A_{\text{lipid}}$ = Protein and lipid assimilated in last timestep (mmol C)

$\text{Gut}_{\text{protein}}, \text{Gut}_{\text{lipid}}$ = Protein and lipid in gut (mmol C)

$C_{\text{N_ing}}, C_{\text{NN_ing}}$ = Protein and lipid ingested during last timestep (mmol C)

$A_{\text{eff_prot}}, A_{\text{eff_lip}}$ = Protein and lipid assimilation efficiency (*wd*)

III.5.5 EGESTION

The proportion of digested protein and lipid that is not assimilated is egested as a faecal pellet (O’Dor and Wells, 1987). Nitrogen is egested in pellets as a fixed ratio of protein egested ($Q_{\text{Nprot}} : 0.15 \text{ mmol N mmolC}^{-1}$).

$$\text{Eq.III.41} \quad E_{\text{protein}} = [(\text{Gut}_{\text{protein}} + C_{\text{N_ing}}) * \text{Dig}_{\text{perc}}] * (1 - A_{\text{eff_prot}})$$

$$\text{Eq.III.42} \quad E_{\text{lipid}} = [(\text{Gut}_{\text{lipid}} + C_{\text{NN_ing}}) * \text{Dig}_{\text{perc}}] * (1 - A_{\text{eff_lip}})$$

$$\text{Eq.III.43} \quad E_{\text{N}} = (E_{\text{protein}} * Q_{\text{Nprot}})$$

Where:

$E_{\text{protein}}, E_{\text{lipid}}$ = Protein and lipid not assimilated (mmol C)

G_{protein} , G_{lipid} = Protein and lipid in gut (mmol C)

C_{N_ing} , C_{NN_ing} = Protein and lipid ingested during last timestep (mmol C)

$A_{\text{eff_prot}}$, $A_{\text{eff_lip}}$ = Protein and lipid assimilation efficiency (*wd*)

III.5.6 EXCRETION

Due to the high content of protein compared to lipids, protein is used extensively for energy and the excretion of ammonia is 2-3 times higher than for fishes of similar body weight (Lee, 1994).

Ammonia excretion is a continuous linear process over short periods of time:

$$\text{Eq.III.44} \quad C = [\text{respiration} / (\text{En}_{\text{prot}} * C_{\text{conv}2})] * Q_{N_prot} * Q_{PL_used}$$

Where:

C = Ammonium excretion rate (mmol N h⁻¹)

respiration = total metabolic cost (cal h⁻¹)

En_{prot} = Energy content in squid protein (cal g C⁻¹)

$C_{\text{conv}2}$ = mmol C to g C conversion factor

Q_{N_prot} = N:C ratio in protein (mmol N mmol C⁻¹)

Q_{PL_used} = Proportion of protein-lipid used to fuel metabolism

$$\text{Eq.III.45} \quad \text{release} [(C * \text{Timestep}) + N_{\text{prot_excess}}]$$

$N_{\text{prot_excess}}$ = Body nitrogen above Q_{N_prot}

III.5.7 GUT PROCESSES

III.5.7.1 Gut volume

Experimental data on squid paralarvae meals showed it ranged from 5-15% DW meal/DW body (Boucher-Rodoni, 1975; Wallace O'Dor 1981, Hirtle *et al.*, 1981).

The stomach weight grows as function of body size (Hurley 1976).

So, squid gut volume, V_{gut} , is assumed to grow proportionally with mantle length:

$$\text{Eq.III.46} \quad V_{\text{gut}} = v_{\text{gut}} * ML$$

Where:

V_{gut} = gut volume (mm³)

v_{gut} = stomach volume coefficient (mm²)

ML = mantle length (mm)

A recently hatched squid (ML:3 mm, Carbon pool: 0.07 mmol C) has a gut volume of 0.6 mm³. It can potentially ingest about 90 C1 copepods (individual volume: 6.4×10⁻³ mm³; carbon content: 6.3×10⁻⁵ mmol C), therefore ingesting ~ 9.5% body weight.

III.5.7.2 Gut content

Gut content, $Gut_{content}$, represents the volume of food in the gut:

$$\text{Eq.III.47} \quad Gut_{contentTemp} = Gut_{content} + Prey_{vol}$$

$$\text{Eq.III.48} \quad Gut_{content} = Gut_{contentTemp} - Processed$$

Where:

$Gut_{contentTemp}$ = Gut content at the beginning of the timestep (mm³)

$Gut_{content}$ = Gut content at the end of the timestep (mm³)

$Prey_{volume}$ = volume of food ingested in last timestep (mm³)

Processed = volume of food digested in current timestep (mm³)

$$\text{Eq.III.49} \quad Prey_{vol} = \text{varietysum} (IngestedCells * P_{vol})$$

Where:

IngestedCells = number of stage-specific prey ingested in last timestep (#)

P_{vol} = stage-specific volume of prey (mm³)

III.5.8 RESPIRATION

Respiration is a heterogeneous process, whose separate components may vary independently (Wells and Clarke, 1996).

Cost associated with:

- maintenance (basal metabolism),
- new somatic tissues, feeding, digestion and assimilation (sda),
- movement.

$$\text{Eq.III.50} \quad \text{respiration} = R_{bas} + R_{sda} + R_{swim}$$

Where:

respiration = total metabolic cost (cal h⁻¹)

R_{bas} = basal metabolic rate (cal h⁻¹)

R_{sda} = specific dynamic action (cal h⁻¹)

R_{swim} = swimming cost (cal h⁻¹)

III.5.8.1 Basal respiration

The weight-specific temperature dependent basal metabolic cost for *L. opalescens*, R_{bas} (ml O₂ kg⁻¹h⁻¹) is $B(A)^T$ (O'Dor *et al.*, 1986). This was transformed into:

$$\text{Eq.III.51} \quad R_{bas} = \frac{WW * B A^T E_{conv}}{1 \times 10^6}$$

Where:

R_{bas} = basal metabolic cost (cal h⁻¹)

WW = Wet weight (mg)

B and A = respiration parameters (*wd*)

T = temperature (°C)

E_{conv} = mlO₂ to cal conversion factor (cal mlO₂⁻¹)

III.5.8.2 Specific Dynamic Action

The cost associated with SDA, R_{sda} , is proportional to the amount of assimilated carbon (protein and lipid) (Parry, 1983):

$$\text{Eq.III.52} \quad R_{sda} = \{r_{sda} [(A_{protein} * E_{nprotein} * C_{conv2}) + (A_{lipid} * E_{nlipid} * C_{conv2})]\} / \text{TimeStep}$$

Where :

r_{sda} = specific dynamic action coefficient (*wd*)

$A_{protein}, A_{lipid}$ = Protein and lipid assimilated in last timestep (mmol C)

$E_{nprotein}, E_{nlipid}$ = Energy content of squid protein and lipid (cal gC⁻¹)

C_{conv2} = gC to mmol C conversion factor (gC mmol C⁻¹)

TimeStep = timestep duration (h ts⁻¹)

III.5.8.3 Cost of swimming

Cost associated with swimming is estimated using the calculations for the locomotion energetic cost for hatchling squid, *Illex illecebrosus* (O'Dor *et al.*, 1986):

1. Calculate Re number as:

$$\text{Eq.III.53} \quad Re = (U * ML) / \nu$$

Where:

U = swimming velocity (ms⁻¹)

ML = mantle length (m)

ν = coefficient of kinematic viscosity ($10^{-6} \text{ m}^2 \text{ s}^{-1}$)

2. Calculate the drag coefficient (C_d):

$$\text{Eq. III.54} \quad C_d = 24 / \text{Re}^{0.7}$$

3. Calculate the drag force (D)[N \equiv kg m s⁻²]:

$$\text{Eq. III.55} \quad D = 0.5 C_d \rho S U^2$$

Where:

ρ = density of the water (kg m^{-3})

S = frontal surface area (m^2)

4. Calculate the Power consumption (P)[W \equiv kg m² s⁻³]:

$$\text{Eq. III.56} \quad P = D U$$

5. Convert P from W to cal d⁻¹ using the conversion 1 W = 20,635 cal d⁻¹ (O'Dor *et al.*, 1986):

$$\text{Eq. III.57} \quad R_{\text{swim}} = (P * E_{\text{conv}2}) / 24$$

Where:

R_{swim} = cost of swimming at speed U (cal h⁻¹)

$E_{\text{conv}2}$ = W to cal per day conversion factor (cal W⁻¹ d⁻¹)

III.5.9 ENERGETICS

The flux of body protein (Budg_{CN}) and lipid (Budg_{CNN}) results from the difference between energy gained for protein (A_{protein}) and lipid (A_{lipid}) assimilated and the total respiration cost (respiration):

$$\text{Eq. III.58} \quad \text{Budg}_{\text{CNN}} = A_{\text{lipid}} - \{[(\text{respiration} * \text{timestep}) + R_{\text{surplus}}] / (\text{En}_{\text{lipid}} * C_{\text{conv}2})\}$$

Where:

Budg_{CNN} = flux of body lipid (mmol C)

A_{lipid} = Lipid assimilated in last timestep (mmol C)

respiration = total metabolic cost (cal h⁻¹)

timestep = timestep length (0.5 h ts⁻¹)

R_{surplus} = Cost not covered by the yolk (mmol C)

En_{lipid} = Energy content of squid lipid (cal gC⁻¹)

$C_{\text{conv}2}$ = gC to mmol C conversion factor (gC mmol C⁻¹)

Body lipid to dry weight can never exceed its maximum observed ratio, Q_{lipMax} , so the excess lipids, $\text{Lip}_{\text{excess}}$, are egested as a faecal pellet (O'Dor and Wells, 1987):

$$\text{Eq.III.59 } \text{Lip}_{\text{excess}} = \text{if } \{[(C_{\text{NN_Pool}} + \text{Budg}_{\text{C}_{\text{NN}}}) * 12] / \text{DW}\} > Q_{\text{lipMax}} \\ \text{then } (\{[(C_{\text{NN_Pool}} + \text{Budg}_{\text{C}_{\text{NN}}}) * 12] / \text{DW}\} - Q_{\text{lipMax}}) * \text{DW} \quad \text{else } 0$$

$$\text{Eq.III.60 } \text{Budg}_{\text{CN}} = (\text{A}_{\text{protein}} - \{[(\text{respiration} * \text{timestep}) + \text{R}_{\text{surplus}}] / (\text{En}_{\text{protein}} * \\ C_{\text{conv2}})\}) * \\ \text{if } [(\text{Budg}_{\text{C}_{\text{NN}}} < 0) \text{ and } (|\text{Budg}_{\text{C}_{\text{NN}}}| > C_{\text{NNpool}})] \\ \text{then } 1 \quad \text{else } Q_{\text{PL_used}}$$

Where:

Budg_{CN} = flux of body protein (mmol C)

$\text{A}_{\text{protein}}$ = Protein assimilated (mmol C)

respiration = total metabolic cost (cal h^{-1})

timestep = timestep length (0.5 h ts^{-1})

$\text{R}_{\text{surplus}}$ = Cost not covered by the yolk (mmol C)

$\text{En}_{\text{protein}}$ = Energy content of squid protein (cal gC^{-1})

C_{conv2} = gC to mmol C conversion factor (gC mmol C^{-1})

$\text{Budg}_{\text{C}_{\text{NN}}}$ = flux of body lipid (mmol C)

C_{NNpool} = Lipid pool (mmol C)

$Q_{\text{PL_used}}$ = Proportion of protein-lipid used to fuel metabolism (*wd*)

III.5.10 STARVATION

A squid dies of starvation when its $\text{Carbon}_{\text{pool}}$ falls below $\frac{3}{4}$ of its maximum ever achieved $\text{Carbon}_{\text{pool}}$, C_{pmax} , or when it has been ingesting less than 10% of its $\text{Carbon}_{\text{pool}} \text{ day}^{-1}$ for more than three days (La Roe, 1971).

III.5.11 REMINERALISATION

As a dead squid or faecal pellet sinks through the mesocosm, it remineralises nitrogen as a function of its nitrogen content and ambient temperature:

$$\text{Eq.III.61 } \text{R}_{\text{NT}} = \text{N}_{\text{dissolution}} * \text{Q}_{\text{RemN}} \wedge ((T - T_{\text{Nref}}) / 10)$$

Where:

R_{NT} = Nitrogen remineralisation rate (mmol N h^{-1})

$\text{N}_{\text{dissolution}}$ = N specific dissolution rate of N ($\text{mmol N mmolN}^{-1} \text{ h}^{-1}$)

Q_{RemN} = factor by which N dissolution increases with T (K) (*wd*)

T = temperature ($^{\circ}\text{C}$) and T_{ref} = reference temperature ($^{\circ}\text{C}$)

III.6 LIST OF PARAMETERS

Parameter	Description	Value	Unit	Source
A	Basal respiration parameter2	1.0879	no unit	O'Dor <i>et al.</i> , 1986
Aeff_lip	Assimilation efficiency for lipid	0.5	no unit	
Aeff_prot	Assimilation efficiency for protein	0.85	no unit	
B	Basal respiration parameter1	123.7	no unit	O'Dor <i>et al.</i> , 1986
C_conv2	C_conv2	0.012	gC mmolC ⁻¹	calculated
DAT_hatch	DAT threshold for hatching	600	°C days	Baron, 2000
E_content	Energy contained in squid flesh	4000	J gC ⁻¹	
E_conv	Energy conversion	4.6	c(1 x 10 ⁻³) ⁻¹	
E_conv2	Conversion coefficient calories from power	20635	cal W ⁻¹ d ⁻¹	
E_conv2	Energy conversion	20635	Jg ⁻¹	
En_lip	Energy content of copepod lipid	9000	cal gC_NN ⁻¹	
En_prot	Energy content of copepod protein	5700	cal gC_N	
G_Conv	mmolC to microgC conversion factor	12000	µgC mmolC ⁻¹	calculated
G_max	Maximum weight	0.62	gC	
ML_max	Maximum ML	8	mm	
Protein_inProp	Protein proportion	0.85	no unit	
Q_lipMax	Maximum ratio of lipids to DW	0.15	no unit	Lee, 1994
Q_Nprot	N:C ratio in proteins	0.15	no unit	Lee, 1994
Q_PLused	Ratio of protein to lipid catabolism	0	no unit	
QR10	Increase of digestion with T	2	no unit	
R_N	R_N	0.0042	no unit	
r_sda	Cost of somatic growth parameter	0.2	no unit	Parry, 1983
S2_ML	Minimum ML for S2	3	mm	assumed
S3_ML	Minimum ML for S3	4	mm	assumed
S4_ML	Minimum ML for S4	5	mm	assumed
S5_ML	Minimum ML for S5	6	mm	assumed
S6_ML	Minimum ML for S6	7	mm	assumed
S7_ML	Minimum ML for S7	8	mm	assumed
S_max	Maximum frontal area	1.0 x 10 ⁻⁵	m ²	
S_maxIsolume	Ref max Sa for target isolume	5.0 x 10 ⁻⁶	m ²	
Spawning_date	Date of spawning	100	Days from 1 st Jan	
T_ref	Reference temperature	10	°C	
T_ref2	Reference temperature for digestion	20	°C	
v	Coefficient of kinematic viscosity	1.0 x 10 ⁻⁶	m ⁻² s ⁻¹	
v_gut	Stomach volume coefficient	0.2	mm ³	
V_max	Maximum swimming speed	135	mh ⁻¹	
Vis_IrradRef	Reference irradiance	1	no unit	assumed
W_conv	mgC to mmolC conversion factor	0.0833	mmolC mgC ⁻¹	calculated
Yolk_lipidsRatio	Ratio Yolk:Wet Weight	0.15	mmol	Bouchaud and Galois, 1990
YolkE_cont	Yolk energetic value	1.71	cal mgC ⁻¹	Giese, 1969
z_egg	Depth of egg mass	50	m	Zeidberg and Hamner, 2002

Tab.III.2 – Squid parameters

“Testing theories on fisheries recruitment.”

APPENDIX IV

TOP CLOSURE IN LERM-PS & ES

APPENDIX IV - TOP CLOSURE IN LERM

IV.1 LERM-PS

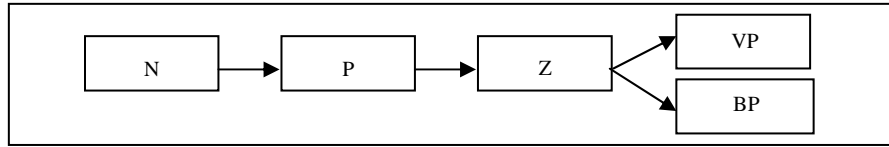


Fig.IV.1 – LERM-PS.N: nutrients , P: phytoplankton, Z: zooplankton, VP: visual predators, BP: background predators

IV.1.1 VISUAL PREDATORS IN LERM-PS

For the Azores scenario, LERM-PS visual top predators represent a population of squid *Loligo forbesii*. It is an abundant species at the Azores and it is known to graze on copepods during the early phase of its life.

IV.1.1.1 Exogenous equations (Top predator demography)

Exogenous equations defined in the scenario describe the demographic state of the predator population, in particular, its growth rate, its annual distribution and its vertical distribution.

Predator growth

Laboratory experiment on *Loligo forbesii* estimated daily growth rates of 7% of its mantle length (ML) in its first months of life (fig.IV.2). During this period squid feed on planktonic organisms, mainly copepods (Vovk 1972, Tibbetts, 1977). Juveniles 4 cm long switch to a diet made of euphausiids and arrow worms (Vovk and Khvichiya, 1980; Vovk, 1985). The maximum ML at which predator feeds on copepods is therefore assumed to be 40 mm. It takes about 100 days for a young squid, growing at a daily rate of 7% of its mantle length, to switch diet.

$$\text{Eq.IV.1} \quad S_t = \begin{cases} \text{If } (d_{\text{year}} \text{ is between } d_0 \text{ and } d_{\text{max}}) \\ \text{then } S_0 * [(p + 1)^{(d_{\text{year}} - d_0)}] \text{ else } 0 \end{cases}$$

S_t = Mantle length (mm)

S_0 = Mantle length at immigration (3 mm)

p = daily growth rate (7% ML)

d_0 = Day of top predator immigration (90 = 1st April)

d_{max} = Day of top predator emigration (221 = 10th August).

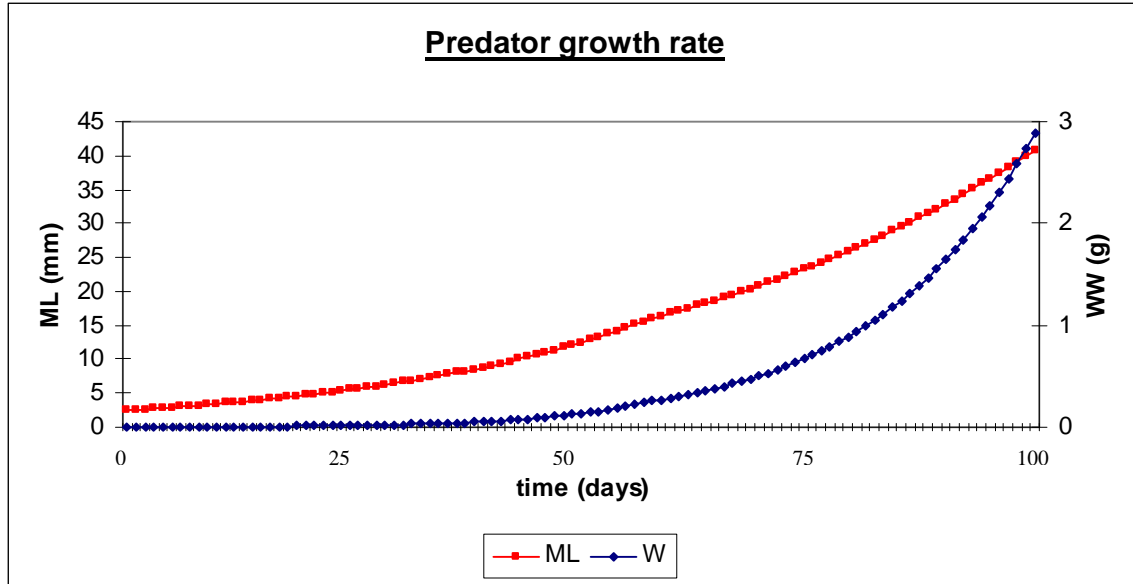


Fig.IV.2 – Predator growth rate expressed as mantle length and wet weight

Predator annual distribution

Squid eggs all hatch simultaneously on the 1st April, they feed on copepods until mid-July, before switching diet. The mortality rate of predator population is assumed to follow a negative exponential function of the time of the year. Every year the concentration of predators is set back to its initial value.

$$\text{Eq.IV.2} \quad N_t = \begin{cases} \text{If } (d_{\text{year}} \text{ is between } d_0 \text{ and } d_{\text{max}}) \\ \text{then } N_0 e^{-[(d_{\text{year}} - d_0)/d_{\text{star}}]} & \text{else } 0 \end{cases}$$

N_t = Top predator vertically integrated concentration (predators m⁻²)

N_0 = Top predator vertically integrated concentration at immigration (3000 predators m⁻²)

$d_{\text{star}} = d^* = \text{e-folding time (150)}$

Vertical distribution of predators

The concentration of visual top predators is assumed to be homogeneous in the top 100m. So there are 30 predators per m³ in the top 100 m.

IV.1.1.2 Endogenous equations

Ingestion

Visual top predators feed on all copepod stages, but overwintering, dead and pellets. The maximum rate of ingestion is modelled as the maximum daily percentage of body weight that can be consumed (Koueta and Boucaud-Camou, 2001). Maximum ingestion rate is therefore a function of the weight of the predator and the weight of the prey. Ingestion rate depends on the concentration and visibility of prey and ambient temperature. The visibility of the prey is determined by the ambient irradiance and the surface area of the prey (fig.IV.3). Ingestion rate can never exceed maximum ingestion rate.

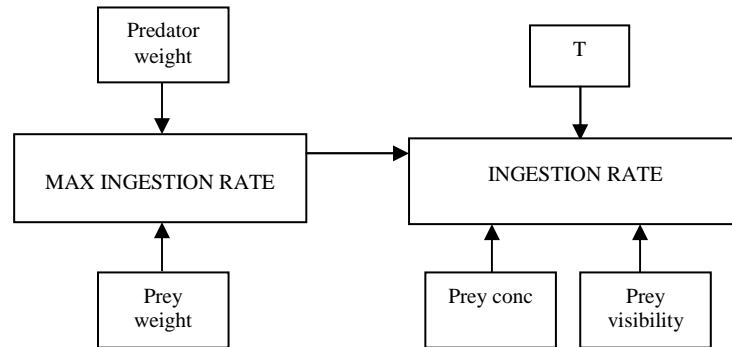


Fig.IV.3 – Predator ingestion rate, internal and external controlling factors

S_t is converted into predator weight, G (mmol C) using:

$$\text{Eq.IV.3} \quad G = [2.37 * \text{LOG}_{10}(S_t) - 1.22] / 12 \quad [\text{Hurley,1976}]$$

12 converts mg C into mmol C.

$$\text{Eq.IV.4} \quad W_{tg} = [0.3 + (0.7 * (T/T_{ref}))] * [\text{IF}(S_t < S_{max}) \\ \text{then } S_t / S_{max} \text{ else } 1]$$

Where:

W_{tg} = effect of temperature and size on swimming (wd)

T = ambient temperature ($^{\circ}\text{C}$)

T_{ref} = Reference temperature (10°C)

S_{max} = Maximum mantle length (15 mm)

Eq.IV.5 $I_{\max} = \{G * 0.6156 e^{-[0.0321*(d_{\text{year}} - d_0)]}\} / (86400 * P_{\text{size}})$

Where

G = predator weight (mmol C)

$0.6156 e^{-[0.0321*(d_{\text{year}} - d_0)]}$ (Koueta and Boucaud-Camou, 2001) determines the maximum percentage (expressed as 0-1) of predator carbon (G) that can be ingested per day by a predator as function of time since immigration ($d_{\text{year}} - d_0$) (fig.IV.4).

This is then divided by $86,400 \text{ s}^{-1}$ to convert daily maximum C ingestion to s^{-1} , and by P_{size} = the prey stage specific carbon content (mmolC prey^{-1}) to convert from mmolC s^{-1} to # prey s^{-1} (tab.IV.1).

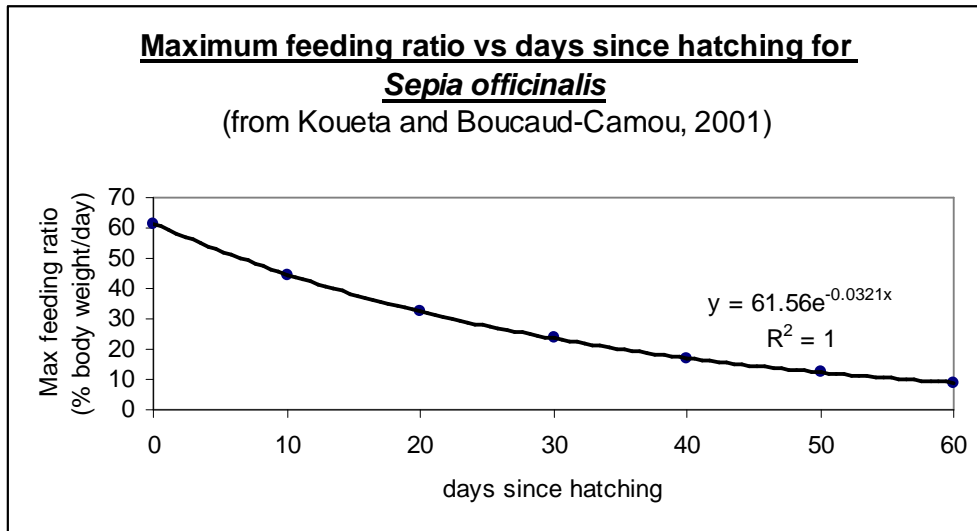


Fig.IV.4 – Top predator maximum ingestion rate

Eq.IV.6 $I_{g_v} =$
 Min (between I_{\max} and
 [IF ($P > P_{\min}$)
 then

$$W_{\text{tg}} * k_p * \underbrace{(S_a / S_{a-\max})}_{\text{Prey visibility}} * \underbrace{(I_{\text{rr}} / I_{\text{rr}_{\text{ref}}})}_{\text{Prey escape ability}} * \underbrace{(P_{\text{speed-max}} / P_{\text{speed}})}_{\text{Prey abundance}} * \{(P - P_{\min})^2 / [(P - P_{\min}) + K_{\text{iv}}]\}$$

 else 0
)

Where:

I_{gv} = stage specific ingestion rate (prey s^{-1})

W_{tg} = effect of temperature and size on swimming (wd)

K_p = predator hunting volume scan rate ($m^3 s^{-1}$)

S_a = Stage specific surface area (m^2 see table 1)

S_{a-max} = Maximum surface area for an adult copepod ($1.29 \times 10^{-7} m^2$)

Irr = ambient irradiance (Wm^{-2})

Irr_{ref} = reference irradiance (Wm^{-2})

P_{speed} = Stage specific maximum swimming speed (mh^{-1})

$P_{speed-max}$ = Maximum swimming speed for an adult copepod (mh^{-1})

P = Stage specific ambient prey concentration (prey m^{-3})

P_{min} = Stage specific minimum ambient prey concentration (prey m^{-3})

K_{iv} = Half-saturation constant (prey m^{-3})

Development stage	Stage description	K_p	P_{size} (mmol C)	P_{min} (prey m^{-3})	k_{iv} (prey m^{-3})	S_a m2	P_{speed} m/h
N3	Nauplius III	0.001	1.00E-05	1000	1E6	1.46E-08	5.09
N4	Nauplius IV	0.001	1.70E-05	1000	1E6	1.70E-08	5.93
N5	Nauplius V	0.001	2.50E-05	1000	1E6	1.94E-08	6.77
N6	Nauplius VI	0.001	3.75E-05	1000	1E6	2.22E-08	7.74
C1	Copepodite I	0.001	6.25E-05	1000	1E6	2.62E-08	9.14
C2	Copepodite II	0.001	9.20E-05	1000	1E6	2.97E-08	10.36
C3	Copepodite III	0.001	2.10E-04	1000	1E6	3.88E-08	13.53
POW4	Pre-overwintering CIV	0.001	5.83E-04	1000	1E6	5.42E-08	18.91
POW5	Pre-overwintering CV	0.001	1.25E-03	1000	1E6	6.95E-08	24.24
OWD4	Overwintering descent CIV	0.001	5.83E-04	1000	1E6	5.42E-08	18.91
OWD5	Overwintering descent CV	0.001	1.25E-03	1000	1E6	6.95E-08	24.24
OW4	Overwintering CIV	0	5.83E-04	1000	1E6	5.42E-08	0
OW5	Overwintering CV	0	1.25E-03	1000	1E6	6.95E-08	0
OWA4	Overwintering ascent CIV	0.001	5.83E-04	1000	1E6	5.42E-08	18.91
OWA5	Overwintering ascent CV	0.001	1.25E-03	1000	1E6	6.95E-08	24.24
C4	Copepodite IV	0.001	5.83E-04	1000	1E6	5.42E-08	18.91
C4OW	Copepodite IV after OW	0.001	5.83E-04	1000	1E6	5.42E-08	18.91
C5	Copepodite V	0.001	1.25E-03	1000	1E6	6.95E-08	24.24
C6	Copepodite VI	0.001	3.33E-03	1000	1E6	9.56E-08	33.35
Ad	Adult	0.001	7.50E-03	1000	1E6	1.25E-07	43.60
Ma	Mature	0.001	8.33E-03	1000	1E6	1.29E-07	45.00
Se	Senescent	0.001	8.33E-03	1000	1E6	1.29E-07	45.00

Tab.IV.1 – Visual top predator stage-specific prey parameters

Faecal pellets

A pellet, containing all the nitrogen and carbon ingested, is released every timestep. As it sinks at a constant speed of 10 m h^{-1} , it is remineralised by an implicit bacteria population. Pellets remineralization is modeled as in copepods (cfr.II.2.17).

IV.1.2 BACKGROUND TOP PREDATORS

IV.1.2.1 Exogenous equations (Top predator demography)

Background top predators are assumed to maintain a constant size (40 mm). They are present all year at a constant concentration (3000 m^{-2}), and they are homogeneously distributed in the top 100m. They feed on all copepod stages, but overwintering, corpses and pellets.

IV.1.2.2 Endogenous equations

The maximum rate of ingestion for background predators is based on the equation used for visual predators (Koueta and Boucaud-Camou, 2001). It is calculated as the maximum daily percentage of body weight that can be consumed. As the weight of the predator is kept constant, maximum ingestion rate depends on the weight of the prey. The bigger the prey the less can be ingested by the predator, and vice versa. Ingestion rate is function of the ambient concentration of prey and temperature (fig.IV.5). Ingestion rate can never exceed maximum ingestion rate.

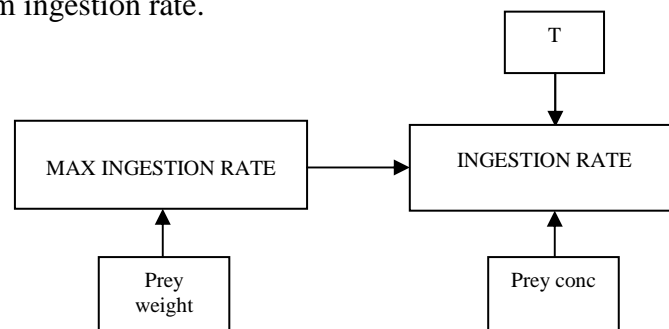


Fig.IV.5 – Predator ingestion rate, internal and external controlling factors

As the size of the predator is constant, maximum percentage of C that can be ingested is reduced to a constant, $I_{\text{max}40} = 6.5 \times 10^{-5} \text{ mmol C s}^{-1}$.

This is divided by P_{size} = the prey stage specific carbon content (mmolC prey⁻¹) to convert from mmolC s⁻¹ to # prey s⁻¹ (tab.2).

$$\text{Eq.IV.7} \quad I_{\text{max}} = I_{\text{max40}} / P_{\text{size}}$$

W_{tg} describes the effect of temperature solely on ingestion:

$$\text{Eq.IV.8} \quad W_{\text{tg}} = 0.3 + (0.7 * T/\text{Tref})$$

As ingestion is not visually elicited, the prey visibility component is not considered.

$$\text{Eq.IV.9} \quad I_{\text{g}_v} =$$

Min (between I_{max} and

[IF ($P > P_{\text{min}}$)

then

$W_{\text{tg}} * k_p * \{(P - P_{\text{min}})^2 / [(P - P_{\text{min}}) + K_{\text{iv}}]\}$

else 0)

Development stage	Stage description	Kp	P _{size} (mmol C)	P _{min} (prey m ⁻³)	k _{iv} (prey m ⁻³)
N3	Nauplius III	0.0001	1.00E-05	1000	1E6
N4	Nauplius IV	0.0001	1.70E-05	1000	1E6
N5	Nauplius V	0.0001	2.50E-05	1000	1E6
N6	Nauplius VI	0.0001	3.75E-05	1000	1E6
C1	Copepodite I	0.0001	6.25E-05	1000	1E6
C2	Copepodite II	0.0001	9.20E-05	1000	1E6
C3	Copepodite III	0.0001	2.10E-04	1000	1E6
POW4	Pre-overwintering CIV	0.0001	5.83E-04	1000	1E6
POW5	Pre-overwintering CV	0.0001	1.25E-03	1000	1E6
OWD4	Overwintering descent CIV	0.0001	5.83E-04	1000	1E6
OWD5	Overwintering descent CV	0.0001	1.25E-03	1000	1E6
OW4	Overwintering CIV	0.0001	5.83E-04	1000	1E6
OW5	Overwintering CV	0.0001	1.25E-03	1000	1E6
OWA4	Overwintering ascent CIV	0.0001	5.83E-04	1000	1E6
OWA5	Overwintering ascent CV	0.0001	1.25E-03	1000	1E6
C4	Copepodite IV	0.0001	5.83E-04	1000	1E6
C4OW	Copepodite IV after OW	0.0001	5.83E-04	1000	1E6
C5	Copepodite V	0.0001	1.25E-03	1000	1E6
C6	Copepodite VI	0.0001	3.33E-03	1000	1E6
Ad	Adult	0.0001	7.50E-03	1000	1E6
Ma	Mature	0.0001	8.33E-03	1000	1E6
Se	Senescent	0.0001	8.33E-03	1000	1E6

Table.IV.2 – Background top predator stage-specific prey parameters

Faecal pellets are produced, sink and get remineralised in exactly the same way as for visual top predators.

IV.2 LERM-ES

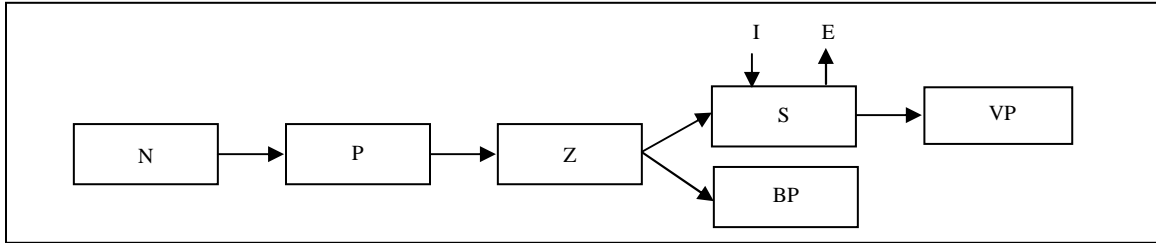


Fig.IV.6 – LERM-ES: N: Nutrients , P: Phytoplankton, Z: Zooplankton, S: Squid paralarvae, VP: visual predators, BP: background predators, I: immigrant squids; E: emigrant squids

IV.2.1 VISUAL PREDATORS IN LERM-ES

LERM-ES visual top predators represent a population of larger *Loligo forbesii*.

IV.2.1.1 Exogenous equations (Top predator demography)

Exogenous equations defined in the scenario describe the demographic state of the predator population, in particular, its growth rate, its annual distribution and its vertical distribution.

Predator growth

Laboratory experiment on *Loligo forbesii* estimated daily growth rates of about 2% in its mantle length (ML) after its first months of life.

$$\text{Eq.IV.10} \quad S_t = \begin{cases} \text{If } (d_{\text{year}} \text{ is between } d_0 \text{ and } d_{\text{max}}) \\ \text{then } S_0 * [(p + 1)^{(d_{\text{year}} - d_0)}] \\ \text{else } 0 \end{cases}$$

S_t = Mantle length (mm)

S_0 = Mantle length at immigration (15 mm)

p = daily growth rate (2% ML)

d_0 = Day of top predator immigration (90 = 1st April)

d_{max} = Day of top predator emigration (221 = 10th August).

Predator annual distribution

Squid eggs all hatch simultaneously on the 1st April, they feed on copepods until mid-July, before switching diet. The mortality rate of predator population is assumed to follow a negative exponential function of the time of the year. Every year the concentration of predators is set back to its initial value.

$$\text{Eq.IV.11} \quad N_t = \begin{cases} \text{If } (d_{\text{year}} \text{ is between } d_0 \text{ and } d_{\text{max}}) \\ \text{then } N_0 e^{-[(d_{\text{year}} - d_0)/d_{\text{star}}]} \\ \text{else } 0 \end{cases}$$

N_t = Top predator vertically integrated concentration (predators m^{-2})

N_0 = Top predator vertically integrated concentration at immigration (3000 predators m^{-2})

$d_{\text{star}} = d^* = \text{e-folding time (150)}$

Vertical distribution of predators

The concentration of visual top predators is assumed to be homogeneous in the top 100m. So there are 30 predators per m^3 in the top 100 m.

IV.2.1.2 Endogenous equations

Ingestion

Visual top predators feed on all squid stages, but recruited, dead and pellets. The maximum rate of ingestion is modelled as the maximum daily percentage of body weight that can be consumed (Koueta and Boucaud-Camou, 2001). Maximum ingestion rate is therefore a function of the weight of the predator and the weight of the prey. Ingestion rate depends on the concentration and visibility of prey, hunting efficiency and ambient temperature. The visibility of the prey is determined by the ambient irradiance and the surface area of the prey (fig.IV.7). The hunting efficiency of capture is modeled as the velocity of the prey (prey escape ability) in relation to the swiftness of the predator (Wtg). Hunting efficiency is modelled as function of the ratio of squid ML and the stage-specific squid maximum swimming speed (tab.IV.3).

Ingestion rate can never exceed maximum ingestion rate.

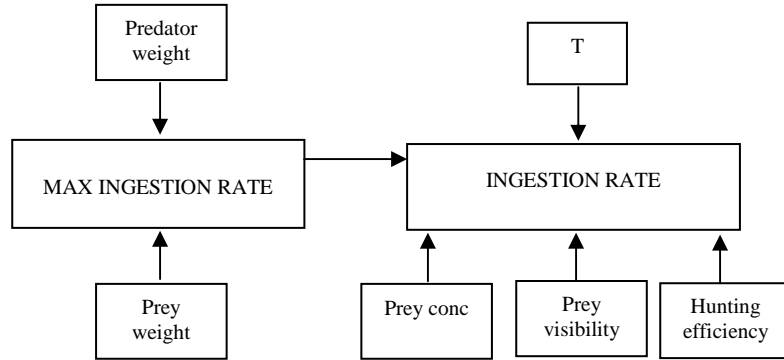


Fig.IV.7 – Predator ingestion rate, internal and external controlling factors

S_t is converted into predator weight, G (mmol C) using:

$$\text{Eq.IV.12} \quad G = [2.37 * \text{LOG}_{10}(S_t) - 1.22] / 12 \quad [\text{Hurley,1976}]$$

12 converts mg C into mmol C.

$$\text{Eq.IV.13} \quad W_{tg} = [0.3 + (0.7 * (T/T_{ref})] * [\text{IF}(S_t < S_{max}) \\ \text{then } S_t / S_{max} \text{ else } 1]$$

Where:

W_{tg} = effect of temperature and size on swimming (wd)

T = ambient temperature ($^{\circ}\text{C}$)

T_{ref} = Reference temperature (10°C)

S_{max} = Maximum mantle length (40 mm)

$$\text{Eq.IV.14} \quad I_{max} = \{G * 0.6156 e^{-[0.0321*(d_{year} - d_0)]}\} / (86400 * P_{size})$$

Where:

G = predator weight (mmol C)

$0.6156 e^{-[0.0321*(d_{year} - d_0)]}$ (Koueta and Boucaud-Camou, 2001) determines the maximum percentage (expressed as 0-1) of predator carbon (G) that can be ingested per day by a predator as function of time since immigration ($d_{year} - d_0$) (fig.IV.4).

This is then divided by $86,400 \text{ s h}^{-1}$ to convert daily maximum C ingestion to s^{-1} , and by P_{size} = the prey stage specific carbon content (mmolC prey $^{-1}$) to convert from mmolC s^{-1} to # prey s^{-1} (see tab.IV.3).

Eq.IV.15 $I_{gv} =$
 Min (between I_{max} and
 [IF ($P > P_{min}$)
 then

$$W_{tg} * k_p * \overbrace{(S_a / S_{a-max})}^{\text{Prey visibility}} * \overbrace{(Irr / Irr_{ref})}^{\text{Prey escape ability}} * \overbrace{(P_{speed-max} / P_{speed})}^{\text{Prey abundance}} * \{(P - P_{min})^2 / [(P - P_{min}) + K_{iv}]\}$$

 else 0)

Where:

I_{gv} = stage specific ingestion rate (prey s^{-1})

W_{tg} = effect of temperature and size on swimming (wd)

K_p = predator hunting volume scan rate ($\text{m}^3 \text{s}^{-1}$)

S_a = Stage specific surface area (m^2 see tab.IV.3)

S_{a-max} = Maximum surface area for a stage 6 squid ($1.29 \times 10^{-7} \text{ m}^2$)

Irr = ambient irradiance (Wm^{-2})

Irr_{ref} = reference irradiance (Wm^{-2})

P_{speed} = Stage specific maximum swimming speed (mh^{-1})

$P_{speed-max}$ = Maximum swimming speed for a S6 squid (mh^{-1})

P = Stage specific ambient prey concentration (prey m^{-3})

P_{min} = Stage specific minimum ambient prey concentration (prey m^{-3})

K_{iv} = Half-saturation constant (prey m^{-3})

Development stage	Stage description	K_p	P_{size} (mmol C)	P_{min} (prey m^{-3})	K_{iv} (prey m^{-3})	S_a m^2	P_{speed} m/h
S1	< 3 mm	0.001	1.00E-05	1-10	1E6	1.46E-08	5.09
S2	3-4 mm	0.001	1.70E-05	1-10	1E6	1.70E-08	5.93
S3	4-5 mm	0.001	2.50E-05	1-10	1E6	1.94E-08	6.77
S4	5-6 mm	0.001	3.75E-05	1-10	1E6	2.22E-08	7.74
S5	6-7 mm	0.001	6.25E-05	1-10	1E6	2.62E-08	9.14
S6	7-8 mm	0.001	9.20E-05	1-10	1E6	2.97E-08	10.36

Table.IV.3 – Visual top predator stage-specific prey parameters

Faecal pellets

A pellet, containing all the nitrogen and carbon ingested, is released every timestep. As it sinks at a constant speed of 10 mh^{-1} , it is remineralised by an implicit bacteria population. Pellets remineralization is modeled as in copepods (cfr.II.2.17).

IV.2.2 BACKGROUND TOP PREDATORS

Same as LERM-PS.

IV.3 PARTICLE MANAGEMENT

Both top predators are initialized in the existence stage, with a subpopulation of 30 individuals per particle. There is one particle per metre between 0-100 m, for a total of 100 particles. Particles in the existence stage are never split or merged. Faecal pellets, released as a new agent, are immediately merged with the other pellets in the same layer

“Testing theories on fisheries recruitment.”

APPENDIX V

CONTRIBUTIONS TO THE VIEW

APPENDIX V - Contributions to the Virtual Ecology Workbench

V.1 Inclusion and use of stages

One of the most fundamental enhancements of the VEW during the course of the project was the inclusion of stages. This had implications for the following issues.

V.1.1 Ingestion

Prior to LERM, the VEW had been specified towards modelling the WB model (Woods and Barkmann, 1986), which had two explicit populations: diatom and copepod. Members of the same species were all the same size, hence diatoms were considered of equal size to each other and it was not necessary for the copepods to make a choice between different types of food. LERM however models different sizes of predators and prey and it would be incorrect to use a “one rate fits all” approach to ingestion. Instead, an approach was required whereby a predator could choose to eat prey of different sizes but of the same species differently to each other. The further challenge was to limit the computational cost; while the most intuitive method could be to allow the predator to “interrogate” the properties of each prey and decide its ingestion rate accordingly, this type of one-to-one interaction would be prohibitively slow when considering many agents interacting.

A compromise was designed, which involved forcing each functional group to have one or more stages, and each plankton agent (that is, each member of a functional group), must be in one of those stages at any time. Ingestion was then redesigned so that instead of choosing just the species to ingest, ingestion could be targeted on a species and stage of prey.

V.1.2 Representing growth and changing behaviour

Two commands were added to the modelling language for the VEW, to handle transitions between different stages; the “change” command causes a change from one stage to another, whereas “pchange” allows a probabilistic change in stage. This allowed rules to be written where a plankter may grow and on reaching some criteria, change stage.

Considering also that in different stages of growth, a plankter may behave differently, (while still being the same species), the capability was added for functions to be switched on or off depending on the stage the plankter is currently in. Hence, a reproduction function can be set to occur only if a plankter is in a adult stage, or certain functions could be switch off for an over-wintering stage. Not only did this greatly enhance the capabilities of the VEW, but it also mimics approximately what happens in nature.

V.1.3 Reproduction, and generic creation

The function for creating offspring was then enhanced so that parents could create children with a different stage to themselves. It was also noted that this mechanism was equally applicable for creating pellets, which until then had required a separate special function in the VEW's modelling language. While a pellet is not a "stage" of its parent, it seemed more convenient to use a single "create" command, rather than separate functions for "create-offspring", and "create-pellet".

V.1.4 Other applications of stages.

Having designed stages and the accompanying support functions in a very generic way, a number of other modelling applications may make use of them. One such example was a conceptual study into modelling epidemiology (Cope, 2006). This study used stages to allow diatom to be classified as diseased, immune, or infectious. Although the work was entirely conceptual, it has shown that it is possible using stages to model plankton diseases, and to that end, future research is planned to attempt to model the spread of cholera.

V.2 Remineralisation over depth

Early versions of the VEW were tested with models that had a relatively slow sinking speed for dead diatoms and faecal pellets – considerably less than one metre per half-hour timestep, noting that the internal structure of the mesocosm in the VEW is stratified into one-metre layers. This sink rate was considerably smaller than in nature, which has pellets and dead diatoms commonly sinking at 10 metres

per hour. When adjusting this sink rate, it became clear that VEW only remineralised chemical at the instantaneous depths of detritus and pellets at the end of a timestep, and did not take account of the layers through which they had travelled. For a simulation where agents do not sink more than a layer in a timestep, this omission is harmless, but for simulations where agents sink faster than that (an adult copepod pellet can sink at a rate of about 10 mh^{-1} , Paffenhofer and Kwnoles, 1979), the results would be incorrect, showing striped bands of remineralised chemical (fig.V.1a).

As a result of this discovery, remineralisation was rewritten, assuming that plankton move from one depth to another between timesteps at constant speed, and apportioning the chemical remineralised to each layer between the starting and ending depth, depending upon the fraction of the timestep the plankter spent in it (fig.V.1b).

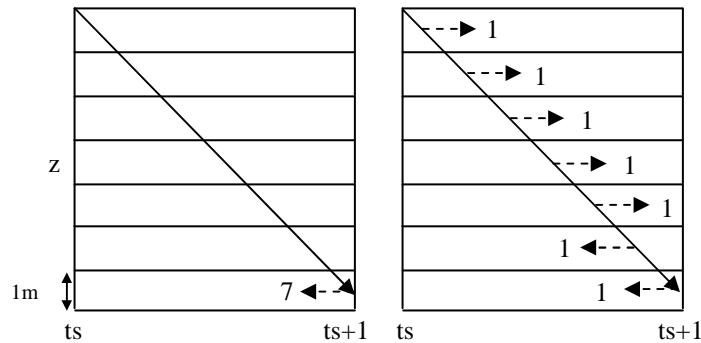


Fig.V.1 – Remineralisation before (a) and after (b) fix. The black line shows the trajectory of a sinking pellet. The dotted line shows the location and magnitude of chemical remineralisation.

V.3 Ingestion over depth

The VEW prior to the LERM research had assumed predators could move through a number of layers in one timestep, and so a system had been set up where predators would issue a “request for food” in each layer they visited, depending on the fraction of the timestep spent in each layer as they swam through their trajectory. What the VEW had not taken into account at that stage, was that the prey may also be swimming across multiple layers during a timestep. This was due to the fact that in the earlier versions of the VEW the diatom was the only prey and it sank slowly (less than a layer per timestep) through the mesocosm. In contrast, in LERM-ES

copepods and squid can swim through more than one metre layer per timestep (fig.V.2). The result of this lacking was that the chances of squid eating copepod were greatly reduced. Whether they got any food at all depended on the chance of the copepods “landing” in the locality of the squid at a timestep boundary (V.2b); if they started below the squid location, and swam above the vertical location squid (fig.V.2a), then despite the fact they must have swam through the predators, no predation would occur. It turned out that this was a source of considerable instability.

After demonstrating this erroneous behaviour, the ingestion code of the VEW was rewritten, and all agents were set to record in each layer the fraction of the timestep they spent in it (fig.V.2c). The ingestion routines would then compute the concentrations of the prey using these records, rather than just the final positions of the prey at the end of a timestep. This is particularly important when a predator movement is small compared to that of the prey (eg. when a squid is keeping position at a “safe” depth during the day, and copepods are migrating upwards after feeding in the deep chlorophyll maximum). As a result of this fix, inter-annual variability from the average in squid recruitment decreased from 34% to 12%.

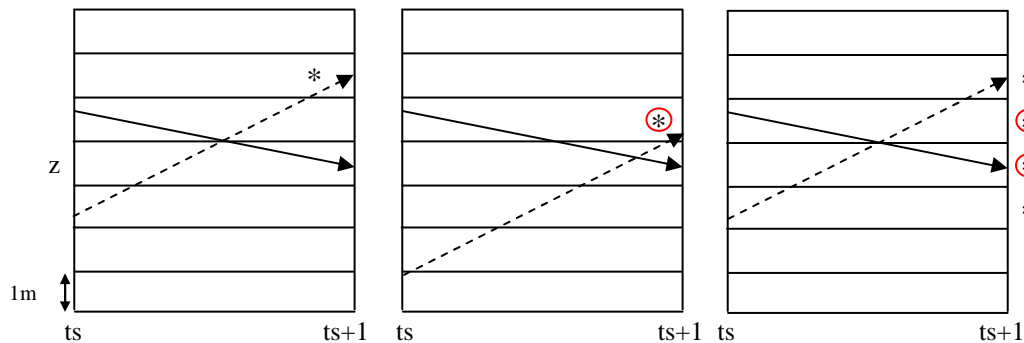


Fig.V.2 – Ingestion before (a,b) and after fix (c). Dotted line: movement of a prey, black line: movement of the predator. * marks where the prey can be ingested if a predator swims through that layer. \circledast shows where ingestion actually occurs in this example. a) No ingestion occurs. The prey is effectively swimming through the predator location safely. b) Ingestion occur, as the prey landed within the layers visited by the predator. c) prey gets predated in each layer the predator visited.

V.4 Ingestion in the mixed layer

However, having implemented this fix, while the simulations produced results with substantially lower noise, there was a considerable performance cost of keeping the records of all the locations plankton swam through and later calculating the number of individuals available for ingestion. A brief profiling exercise showed that the majority of this performance cost was spent dealing with agents above the turbocline; since all the agents are randomly placed as an approximation for turbulence, the number of crossovers between predators and prey may be extremely large here. Indeed, if total mixing occurs, then every predator above the turbocline should cross over with every prey.

This observation turns out to be very useful, because if we know every predator and prey should meet each other (which the assumptions of turbulence state they should), then the space above the turbocline can be treated as homogenous. Therefore, by creating, just for the purposes of ingestion, an artificial layer that tracks all the predators and prey above the turbocline, and handles them as if they were all interacting in the same layer, a crucial performance saving can be made.

V.5 The Virtual Ecology Workbench 3.1

In Spring 2007, work was finished on the first test versions of VEW 3.1, the next generation of the VEW software. This was an almost complete rewrite of the VEW, replacing interfaces that were found to be awkward and adding functionality that was always found to be lacking in the old. The LERM model was the single customer for these improvements, which took eight months to engineer. Many features were added to LERM's specification.

- Biological events – the introduction of a set of plankton of a given species and stage, at a specified moment in the simulation. Used for spawning events, or introduction of foreign organisms.
- Chemical recycling – a mathematical adjustment that can be made to recover chemical that is remineralised in the system below the annual maximum turbocline, and will never return to circulation.

- Logging of chemicals held internally by plankters of a given species and stage.
- Logging of ingestion – how many individuals of a given species and stage were ingested, and which predator (species and stage) ingested them.
- Physical events – while previous work (Woods *et al.*, 2005) had mentioned the need to adjust the oceanic heat loss, VEW 3.1 enabled this to be done at a user-interface level, and LERM was used to both demonstrate the instability, and test the correct adjustment for the Azores ecosystem.